

A11102 577663

REFERENCE

NBS
PUBLICATIONS

NAT'L INST OF STANDARDS & TECH R.I.C.



A11102577663

Ross, Howard D./An Investigation of horiz
QC100 .U56 NO.86-3450 1988 V19 C.1 NBS-P

86-3450

An Investigation of Horizontal Flow Boiling of Pure and Mixed Refrigerants

Howard D. Ross

U.S. DEPARTMENT OF COMMERCE
National Bureau of Standards
National Engineering Laboratory
Center for Building Technology
Building Equipment Division
Gaithersburg, MD 20899

August 1986

Issued November 1986

QC in part by:
100 Department of Energy
.U56 (Ridge National Laboratory)
86-3450 on, DC 20585
1986

NBSIR 86-3450

AN INVESTIGATION OF HORIZONTAL FLOW BOILING OF PURE AND MIXED REFRIGERANTS

Howard D. Ross

U.S. DEPARTMENT OF COMMERCE
National Bureau of Standards
National Engineering Laboratory
Center for Building Technology
Building Equipment Division
Gaithersburg, MD 20899

August 1986

Issued November 1986

Sponsored in part by:
U.S. Department of Energy
(via Oak Ridge National Laboratory)
Washington, DC 20585



U.S. DEPARTMENT OF COMMERCE, Malcolm Baldrige, *Secretary*
NATIONAL BUREAU OF STANDARDS, Ernest Ambler, *Director*

ABSTRACT

The research involved determining experimental heat transfer coefficients (HTC) and analyzing the predictive ability of available models for both pure and mixed R152a/R13B1 refrigerants. Over 1,000 data points were collected, covering a range of pressure, composition, quality, and heat and mass flux.

A current controversy regarding suppression of nucleate boiling was resolved in favor of traditional theory. A suppression criterion for pure refrigerants predicted quantitatively the quality at which suppression occurs. The method was extended to mixed refrigerants and partially verified.

Older pure fluid heat transfer correlations lacked general validity. The complete Chen correlation and many suggested variations were tested. The original correlation overestimates the nucleate boiling contribution. In the nucleate boiling regime, the method of Stephan and Abdelsalam (SA) was validated. In the evaporative regime, Bennett and Chen's (BC) Prandtl number correction predicted HTC's for pure refrigerants. The method incorporates the suppression criterion to determine when to invoke the Prandtl correction. It is better grounded in theory than recent regression-based correlations. The method predicted the values of this and other independent data well.

The circumferential variation in HTC is opposite for mixtures than observed for pure fluids, suggesting the existence of a circumferential gradient in concentration and interfacial temperature. The measured values in both the nucleate boiling and the evaporative regimes showed a degradation in heat transfer. In the nucleate boiling regime, mass transfer resistance caused the degradation. In the evaporative regime, the reduction may be due to mass transfer resistance suppressing nucleate boiling for the mixture but not for the pure component.

None of the mixtures' calculation methods achieved closure with measured values to the same degree as was achieved with pure fluids. Closure, however, was typical of the literature for mixtures. In the nucleate boiling regime, the method of Thome achieved the best agreement. It however predicted the opposite quality dependence. In the evaporative regime, the best fit was achieved by the evaporative portion of Chen's original equation which neglects any mixture effect and suggests the absence of nucleate boiling.

TABLE OF CONTENTS

	Page
ABSTRACT	iii
LIST OF TABLES	ix
LIST OF FIGURES	x
NOMENCLATURE	xiii
PREAMBLE	xv
1. BACKGROUND AND SCOPE	1
1.1 Introduction and Goals	1
1.2 Text Organization	2
1.3 Nomenclature	5
1.4 Test Fluids	5
1.5 General Description of Forced Convection Boiling (Flow Boiling) of Pure Fluids	6
1.6 The Differences Between Mixtures and Pure Fluids	9
1.7 Literature Review of Experiments of Annular Flow Boiling of Mixtures	12
2. PROPERTY DETERMINATION	21
2.1 Introduction	21
2.2 Thermodynamic Properties and the Equation of State ...	22
2.3 Transport Properties	26
2.4 The Effect of Non-Ideal Property Behavior on the Heat Transfer Coefficient	31
3. EXPERIMENTS	37
3.1 Introduction and Historical Review	37
3.2 General Description of Test Rigs Used in This Investigation	38
3.3 Testing Protocol	43
3.4 Measurement and Data Reduction Technique	44
3.5 Quality Assurance	61
3.6 Problems	68
3.7 Summary of Experimental Data	69
4. ON THE SUPPRESSION OF NUCLEATE BOILING	93
4.1 Background	93
4.1.1 Conventional Theory of Onset and Suppression of Nucleate Boiling	94
4.1.2 New Alternate Theory: Enhancement of Nucleate Boiling	98
4.1.3 Suppression of Boiling with Organic Fluids	99
4.1.4 Problem Resolution Methods	99
4.2 Summary of Visual Evidence	100

4.3	Summary and Analysis of Experimental Evidence: Dependence on Heat and Mass Flux	102
4.4	Summary of Experimental Evidence: Dependence of Heat Transfer Coefficient on Quality	104
4.5	Summary of Experimental Evidence: Effect of Pressure	105
4.6	Summary of Experimental Evidence: Presence of Hysteresis	106
4.7	Summary of Literature Review: Mixtures	106
4.8	Comparison of Experimental Results to Theory	108
4.8.1	Application of Conventional Theory to Refrigerants and Refrigerant Mixtures	108
4.8.2	Experimental Results: Pure Refrigerants	112
4.8.3	Experimental Results: Mixtures	116
4.9	Conclusions and Recommendations.....	118
5.	A FURTHER EXAMINATION OF THE DATA	141
5.1	Introduction	141
5.2	Circumferential Variation in Heat Transfer in Horizontal Flow Boiling	141
5.3	Effect of Equilibrium Quality on Mixture Heat Transfer	145
5.4	Departure from Nucleate Boiling (DNB) Events	147
5.5	Comparison Between Pure and Mixed Refrigerants	148
5.6	Pressure Drop in Horizontal Flow Boiling of Pure and Mixed Refrigerants	150
6.	PREDICTION OF PURE REFRIGERANT HEAT TRANSFER	161
6.1	Introduction	161
6.2	Correlation for Annular Flow Boiling	162
6.2.1	Miscellaneous Forms	165
6.2.2	The Original Chen Method	165
6.2.2.1	Closed Form Solution for Chen's Method	168
6.2.3	Comparing Chen's Method to Experimental Data: Literature Review	169
6.2.4	Modification to Nucleate Boiling Contribution in Chen's Method	170
6.2.5	Modification of Forced Convection Contribution	171
6.2.6	Modification of Suppression Factor	172
6.2.7	Other Modifications to Chen's Method	173
6.2.8	Application of Modification to Chen's Method ..	173
6.3	Experimental Results: Comparison to Measured Data ...	175
6.3.1	Comparison to Rig #1, R152a Data	176
6.3.2	Comparison to Rig #2, Preheat Data	177
6.3.3	Comparison to Rig #2, Test Section Data	178
6.4	Discussion of Findings	178
6.4.1	Nucleate Boiling Dominated Flow Situations	178

6.4.2	Forced Convection Dominated Flow Situations ...	181
6.4.3	A Complete Correlation	182
6.4.4	A Comparison with Other Data	185
6.5	Closing Remarks: Conclusions and Recommendations	186
7.	PREDICTION OF HEAT TRANSFER WITH MIXED REFRIGERANTS	205
7.1	Introduction	205
7.2	Pool Boiling of Mixtures	205
7.2.1	Modelling of Single Bubbles	205
7.2.2	Boiling of Mixtures versus Pure Fluids	207
7.2.3	Mixtures Correlations for Pool Boiling	208
7.3	Forced Convection/Evaporation of Mixtures	210
7.3.1	Analytic Modelling	210
7.3.2	Simplified Predictive Modelling for Forced Convective/Evaporation of Mixtures (Bell and Ghaly)	212
7.4	Complete Mixtures' Correlations	213
7.4.1	Modification to Bell and Ghaly to Include Nucleate Boiling	214
7.4.2	Modification to Bennett and Chen's Method to Include Mixture Effects	215
7.4.3	Other Modifications to Chen's Method to Include Mixture Effects	217
7.4.4	Other Correlations for Flow Boiling of Mixtures	218
7.4.5	Summary of Mixtures' Models	219
7.5	Comparison to Measured Data	220
7.5.1	Comparison to Preheat Data of Rig #2	220
7.5.2	Comparison to Rig #1 Data	221
7.5.3	Comparison to Rig #2: Test Section Data	223
7.6	Discussion of Findings	224
8.	CONCLUSIONS AND RECOMMENDATIONS FOR FURTHER RESEARCH	241
8.1	Summary of Findings and Contributions	241
8.2	Further Research Needs	246

APPENDICES

3A:	Experimental Data Collection	251
4A:	Alternate Suppression Criterion	289
4B:	Review of Correlations α/α_L with X_{tt}	291
4C:	Review of Visual Evidence: Review of Literature.....	295
4D:	Dependence on Heat and Mass Flux	301
4E:	Mixtures - Literature Review	309
6A:	Miscellaneous Heat Transfer Forms	317
6B:	Polley's Method	321
7A:	Development of COON (Mass Transfer Effect on Liquid Side) in Bennett and Chen's Method	323
7B:	Bennett and Chen's Inclusion of Sensible Heating of Liquid	327

7C: Microlayer Evaporation Models	329
7D: Further Comments on Shock's Analysis	333
7E: The Bell and Ghaly Model	335
REFERENCES	343

LIST OF TABLES

- 1-1: Flow Boiling Experiments with Pure Refrigerants: Literature Review
- 2-1: Comparison of Equation of State Values and Mole Fraction Weighting of Pure Components
- 3-1a: Hardware Differences Between Rig #1 and Rig #2
- 3-1b: Data Reduction Differences Between [Ra83] and This Thesis (Rig #1)
- 3-2: Effect of Pressure Taps on Heat Transfer Coefficient
- 5-1: Summary of Experimental Data
- 6-1: Some Simple Correlations for Flow Boiling of Pure Refrigerants
- 6-2: Simple Correlations for Average Heat Transfer of Flow Boiling Refrigerants
- 6-3: Comparison of Predictions to Data: Mass Fractional Deviation
- 6-4: Summary of Chen-Styled Methods
- 7-1: Pool Boiling Correction Factors for Binary Mixtures
- 7-2: Summary of Assumptions in Mixtures' Models
- 7-3: Comparison of Mixed Refrigerant Correlations and Experimental Data

LIST OF FIGURES

- 1-1: Regimes of Two Phase Flow (Reprinted from [La62]).
- 1-2: Temperature-Composition Diagrams for Test Fluids in Terms of weight and Molar Fractions.
- 1-3: Heat Balance on Control Volume in Annular Flow of Mixtures.
- 1-4: Effect of Oil on Heat Transfer Coefficients of Refrigerants.
- 2-1: Comparison of Transport Properties as Determined by Mole Fraction Weighting and Mixing Rules.
- 3-1: Typical Test Rig in the Literature.
- 3-2: Experimental Test Rig #1.
- 3-3: Experimental Test Rig #2
- 3-4: Thermocouple Lead Arrangement.
- 3-5: Thermocouple Mounting Scheme Including Electrical Isolation.
- 3-6: Wall and Instream Temperature Measurement.
- 3-7: The Simulation of Pressure Taps.
- 3-8: Calculated Pressure Drop via Martinelli-Nelson Method.
- 3-9: Effect of Instream Thermocouples on Single Phase Measurements.
- 3-10: Effect of Instream Thermocouples on Evaporative Heat Transfer Coefficient.
- 3-11: Sampling Technique to Determine Mixture Composition.
- 3-12a: Data Reduction Scheme for Pure Refrigerants.
- 3-12b: Data Reduction Scheme for Mixtures.
- 3-13: Condensation Curves for Various Compositions.
- 3-14: Typical Output from Test Run Data Reduction.
- 3-15: Comparison of Predicted to Measured Data for Single Phase Heat Transfer Coefficients.
- 3-16: Pressure Drop: Predicted versus Measured.

- 3-17: Effect of Preheat Flux on Test Section Wall Temperature Measurements.
- 3-18: Effect of Preheat Flux on Heat Transfer Coefficients for Mixtures.
- 4-1: Criterion for the Onset of Nucleate Boiling.
- 4-2: Flow Chart for Determining Suppression Heat Flux.
- 4-3: Effect of Pressure and Mass Flux on Suppression Heat Flux (R152a).
- 4-4: Calculated Suppression Heat Flux for Mixtures--Isolated Bubble Theory.
- 4-5: Calculated Suppression Heat Flux for Mixtures--Pool Boiling Theory.
- 4-6: Effect of Heat Flux on Pure R152a at Low Pressure.
- 4-7: Effect of Pressure on Pure R152a.
- 4-8: Effect of Heat Flux on Pure R13B1
- 4-9: Effect of Heat flux on Pure R152a and R152a/R13B1 Mixture: Preheat Data.
- 4-10: Effect of Heat Flux on Pure R13B1 and R152a/R13B1 Mixture: Preheat Data.
- 4-11: Effect of Heat Flux on Pure R152a--Test Section Data.
- 4-12: Effect of Mass Flux: Test Section Data.
- 4-13a: Effect of Step Change in Heat Flux: Pure Refrigerants.
- 4-13b: Effect of Step Change in Heat Flux: Mixtures.
- 4-14: Effect of Heat and Mass Flux on 0.662 wt. R13B1 Mixture.
- 4-15: Effect of Heat and Mass Flux on 0.706 wt. R13B1.
- 4-16: Effect of Heat and Mass Flux on 0.75 wt. R13B1.
- 4-17: Effect of Heat and Mass Flux on 0.833 wt. R13B1.
- 4-18: Rig #2 Test Section Data.
- 5-1: Variation in Measured Heat Transfer Coefficient.
- 5-2: Variation in Measured Heat Transfer Coefficient for Mixtures.

- 5-3: Effect of Composition on Top-Bottom Wall Temperature Difference.
- 5-4: Indications of Probable Film Boiling for Pure R13B1 and a Mixture.
- 5-5: Probable Film Boiling in the Data of [Mi81].
- 5-6: Comparison Between Mixtures and Pure Fluids in Evaporative Flow.
- 5-7: Comparison Between Predicted and Measured Pressure Drop for Mixtures.
- 6-1: Comparison of Shah's Method with Experimental Data.
- 6-2: Comparison of Empirical and Analytic Functions in Chen's Method.
- 6-3: Comparison of Chen-Styled Methods to Experiments.
- 6-4: Comparison of Forster-Zuber and Stephan-Abdelsalam Methods.
- 6-5: Comparison of Complete Correlation with Test Section Data.
- 6-6: Comparison of Complete Correlation with Selected Rig #1 Data
- 6-7: Comparison of Complete Correlation with Others' Data.
- 7-1: Isolated Bubble Growing in a Superheated Binary Liquid.
- 7-2: Pool Boiling Experiments of Happel and Stephan with Binary Mixtures.
- 7-3: Comparison of Mixture Correction Factors.
- 7-4: Comparison of Preheat Data to Pool Boiling Models.
- 7-5: Comparison of First Thermocouple Station Preheat Data to Pool Boiling Models.
- 7-6: Comparison of Rig #1 Data to Thome's and Bell and Ghaly's Methods.
- 7-7: Comparison of Measured Test Section Data to Evaporative Only Methods.
- 8-1: Proposed New Test Rig.
- 4C-1: Visualization Methods.
- 7C-1: Microlayer Evaporation Models.
- 7E-1: The Bell and Ghaly Method.

NOMENCLATURE

English

T	temperature
P	pressure
M	molecular weight
X	concentration of liquid
Y	concentration of vapor
R	gas constant
C_p	specific heat at constant pressure
q	heat flux
x	vapor quality
G	mass flux
\dot{m}	mass flow rate
V	velocity
h	enthalpy
Δh_v	latent heat of vaporization
s	entropy
L	length
E	energy
(TD)	as determined by a transducer
(GAUGE)	as determined by a gauge
A_c	cross sectional area
A_s	surface area
v	specific volume
z	distance
F	factor in Chen's method [Ch66]
S	factor in Chen's method [Ch66]
d*	break-off diameter [St80]

Greek

α	heat transfer coefficient
σ	surface tension
μ	viscosity
	kinematic viscosity
γ	conductivity
Δ	change in property
ϵ	eddy diffusivity or void fraction
ρ	density
ϕ_L^2	two phase multiplier [Ma48]
δ	thickness (length) of layer

Dimensionless Numbers

Re	Reynolds Numbers GD/μ
Pr	Prandtl Number $\mu C_p/\lambda$
Co	Convection Number
X_{tt}	Martinelli Parameter
L	Lewis Number a_T/a_D
Sc	Schmidt Number $\mu/\rho a_D$

Superscripts

-	molar value
*	vapor value in equilibrium with liquid

Subscripts

T	thermal
D	mass
SL	sensible heat, liquid
SV	sensible heat, vapor
G	gas
L	liquid
LO	liquid only
A	component A
B	component B
DEW	dew point
BUB	bubble point
LIN	as determined by a linear relation
O, TOT	overall, total
C	due to Chen
BC	due to Bennett and Chen
FC	forced convective
TPF	two phase, frictional component
i	component i
j	component j
r	reduced
c	critical
sat	saturation
in	inlet
out	outlet
f	fluid
sc	subcooled
w	wall
pr	preheat
a	acceleration component
nbc	nucleate boiling contribution
e	evaporative contribution
n	nucleate boiling relation used in Chen's method
pool	pool boiling
egb	equilibrium value
id	ideal value (mole fraction weighted)
v	vapor
act, meas	actual, measured value
20	two phase
m	mixture

PREAMBLE

This report is essentially the dissertation of Howard Ross which was submitted to the University of Maryland in partial fulfillment of his Ph.D. requirements. The following are the acknowledgments from that document.

Special thanks must go first to my advisor, Marino di Marzo, for his spirited and insightful advice in the preparation of this report. Also, deep gratitude is expressed to Reinhard Radermacher for his generous and patient counsel in the lab. Sponsors are usually noted in the cursory fashion. However, in this case, David Didion provided support on both a technical and personal level for which the author is grateful. Appreciation is given to Dave Ward for accommodating my unusual schedule and demands in operating the brine cooling system. Extra effort was required in typing this report. My special thanks go to Laurie Watkins for enduring the several drafts, and Gail Crum and Mary Baier for typing the final. I also thank everyone in the group at NBS, especially Mark McLinden, Graham Morrison, and Brian Weber for many fruitful technical discussions.

CHAPTER 1: BACKGROUND AND SCOPE

1.1 Introduction and Goals

The interest in two phase gas-liquid flow is increasing dramatically. In 1966, less than 60 papers were published; in each of the last three years (1982-84), more than 1000 papers have appeared in the technical literature. Surprisingly, however, the study of flow boiling of mixtures, a commonly occurring process, has received relatively little attention; a recent literature survey [St82] turned up only six papers. While in fact there may be twice that number, the availability of existing data and models is scarce. Of those studies many were with aqueous solutions, which due to certain properties of water, may be inapplicable for other fluids.

The boiling/evaporation of mixtures is a very common industrial application. In distilleries and in reboilers of which there are tens of thousands in use, the evaporation of a mixture is inherent in the process. More recently, the use of refrigerant mixtures as the working fluid in heat pumps and refrigerator/freezers has shown theoretical promise [St80, Sc85] which has been verified experimentally [Di84]. One of the serious barriers to the use of these refrigerant mixtures is the current lack of understanding of the heat transfer process in refrigeration equipment, specifically the impact of mixtures on the heat transfer coefficient and therefore the heat exchanger size in evaporators and condensers.

The principal goal of this study therefore is to experimentally determine heat transfer coefficients under a wide range of conditions, to assess and recommend models and correlations for their predictions, and to examine specific physical processes governing the heat transfer.

The need for such work has been expressed widely in the literature:

"No other tests [of the Chen correlation for fluids with $Pr > 1$] have been reported and this is a gap which should be filled". — recent flow-boiling review keynote paper at int'l Heat Transfer Conference [Bu82].

"It is clear that several possible methods are now available for convective vaporization. It is essential in order for them to be tested, the present lack of data for local convective heat transfer coefficients in multicomponent systems should be remedied". [Sa82].

"Further experiments with other mixtures are still necessary. Some of the assumptions [in the models] seem to be very far going and require further experimental scrutiny". — recent boiling of mixtures review keynote paper at Int'l Heat Transfer Conference [St82].

This study attempts to respond directly to these requests.

1.2 Text Organization

In the remainder of this chapter, background is given regarding the boiling/evaporation process in flow boiling, especially annular flow. The general complications introduced by the use of mixtures are also discussed.

In Chapter 2, a review of the physical property determination is given. The use of a special equation of state for determining thermodynamic properties is described. Transport property correlations for pure fluids and rules for determining these properties for mixtures are

given; these rules take into account the non-idealities of mixing. Non-ideal mixing properties are shown to reduce heat transfer coefficients, both in single and evaporative two phase flow.

In Chapter 3, the experimental test rigs used in the heat transfer coefficient investigation are described. Particular attention to potential errors is included, as well as the testing protocol and results of various quality assurance tests. A total of 1459 data points are collected in this effort; about 15% are not in the annular flow regime and are eliminated from further consideration.

Chapter 4 discusses a current controversy in the literature, the suppression of nucleate boiling. For many years, increased heat transfer at high vapor quality was attributed to the thinning of the liquid film and the acceleration of the vapor core. Recently a much different phenomena, an enhancement of nucleate boiling, has been suggested in this region. The literature is reviewed critically and new experimental data are analyzed in favor of traditional theory. A suppression criterion is applied and validated for pure fluids. Extensions to mixed fluids are hypothesized and partially validated.

In Chapter 5, the general results of the various experimental tests are further discussed. A circumferential variation in heat transfer coefficient was observed in horizontal flow boiling of mixtures as compared to pure fluids. A reason for the new variation is hypothesized. The effect of quality on the mixtures' heat transfer coefficient is

discussed. Finally, sudden departure from nucleate boiling (DNB) were observed in some of the data. The implication of DNB events for heat pumps are discussed.

Chapter 6 reviews the available models and correlations for predicting heat transfer coefficients with pure fluids. In particular, the Chen correlation [Ch66] is reviewed and analyzed, as it is the most widely recommended method in texts [Hs76, Co80] as well as within the nuclear industry in general [Tr78]. The method has been dismissed historically within the refrigeration industry because of its poor predictive ability with refrigerants. Recent modifications of the correlation and the application of the method to refrigerants are examined. It is shown that portions of the correlation may be used successfully with refrigerants. A new procedure, more analytical, based on recent correlations, is developed.

The modelling and correlations for pool and flow boiling of mixtures is the subject of Chapter 7. The available methods proposed for estimating heat transfer coefficients are reviewed critically and compared to the experimental data. None of the methods produced agreement with the data as closely as was achieved for pure fluids, however, closure was achieved to the same degree as is found currently in the mixtures' literature.

Conclusions and recommendations regarding flow boiling models for pure and mixed refrigerants are discussed in Chapter 8. It is likely

that these first studies of mixtures will lead to further experimental work. As such, several recommendations for test fluids, experimental apparatus and testing protocol are also made in Chapter 8.

1.3 Nomenclature

There has been a recent attempt at standardized nomenclature in two phase literature. As such, the author has used, wherever possible, the latest international convention. In particular, the following symbols should be noted:

α = heat transfer coefficient
 Δh_v = latent heat of vaporization
 a_T = thermal diffusivity
 a_D = mass diffusivity
 X = molar concentration
 x = vapor quality
 λ = thermal conductivity

The general nomenclature is given in the foreward to this report. When exceptions are made, the text will define the variable directly.

1.4 Test Fluids

The test fluids used in this investigation are pure R152a (CH_3CHF_2), pure R13B1 (CF_3Br) and mixtures of various compositions of these fluids. The two refrigerants are recommended as a mixture by their manufacturer for heat pump use due to their relatively wide difference in boiling point ($35^\circ\text{C}@4.7$ bar). In addition, the mixture can be used in existing machinery without major modification. Some tests have been performed with pure R22 (CClHF_2), a much more widely utilized refrigerant. The R22 was used to ensure the experimental testing rig was operating correctly.

1.5 General Description of Forced Convection Boiling (Flow Boiling) of Pure Fluids

Figure 1-1 [La62] shows the typical flow pattern development of a moving fluid being boiled and then evaporated. In most of the applications for refrigerants, the annular flow pattern (sections E and F) is the one of interest, as refrigerants commonly enter the evaporator at a vapor quality of about twenty percent and quickly develop into annular flow.

For low heat flux, the heat transfer coefficient changes along the length of the tube as follows: when the fluid is a single phase liquid (section A on Figure 1-1), the heat transfer coefficient is approximately constant; it changes only as the thermodynamic and transport properties of the liquid change with temperature. In Section B, sub-cooled boiling occurs, i.e., vapor forms at portions of the tube wall despite the fact that the bulk fluid temperature remains below the saturation temperature. In this flow section, the thermodynamic quality, x , defined as $(h - h_{Lsat})/\Delta h_v$ is still less than zero, and the heat transfer coefficient owing to developing turbulence increases linearly. When x equals zero (between Sections B and C), saturated nucleate boiling begins, and the value of h is relatively constant. At a quality of a few percent, an annular flow pattern forms (sections E and F). In annular flow with heat addition, the quality increases, stripping the thickness of the liquid layer. Vapor generation in this region is commonly considered to be by evaporation primarily at the liquid/vapor interface, rather than by nucleate boiling at the wall. If nucleate boiling is completely absent, "suppression of nucleate boiling" is said to have taken place. The suppression process is the subject of some

recent controversy discussed in a later chapter. Since the liquid film becomes thinner and thinner with increasing quality and since the vapor core velocity increases sharply, heat is conducted more readily through the liquid, and the heat transfer coefficient increases. At some point, the liquid film is entirely evaporated and dryout (also known as boiling crisis) occurs: since vapor is a much poorer thermal conductor than liquid, the heat transfer is suddenly and severely diminished. As the quality approaches one, single phase vapor flow occurs, and the heat transfer coefficient again is relatively constant, changing only as fluid properties change.

The heat transfer coefficient depends not only on quality, but on mass and heat flux. As in single phase flow, an increase in mass velocity causes an increase in turbulence and may cause a consequent increase in the heat transfer coefficient. It should also be noted that at higher mass flux the dependence on quality becomes much stronger.¹ For the case of increased heat flux, nucleate boiling at the wall may occur in more locations, increasing the heat transfer coefficient. For very high heat flux, no annular flow may be established and sudden reductions in h values may occur at low quality or even in the subcooled boiling regime. This phenomenon is known as a sudden departure from nucleate boiling and is caused by sudden flashing of vapor all along the tube wall (i.e., film boiling).

¹If the vapor generation process is dominated by nucleate boiling, then the heat transfer coefficients become nearly independent of mass flux. This is one way among several to examine the physical process occurring inside the tube.

As previously noted, this study concentrates on the annular flow region prior to dryout. Some other comments are also appropriate: Figure 1-1 shows the flow patterns in a vertically-oriented tube. In a horizontal tube, the liquid film can be considerably asymmetric due to gravity. The thick liquid film on the bottom of the tube tends to reduce the local α values considerably; however the liquid film on the top and sides is thinner in the horizontally-oriented tube, increasing the heat transfer coefficient. To the author's knowledge only one group used the same tube, fluid, and experimental apparatus to measure the heat transfer coefficient in both orientations: Lavin and Young showed that α horizontal was fifty percent larger typically than α vertical, when the heat transfer coefficients at a location were averaged all around the tube (α -avg equals [α -top plus α -bottom plus α -leftside plus α -rightside]/4), [La66]. Actual average values are difficult to obtain in this asymmetric case.

This simplistic explanation of the flow pattern and heat transfer regimes masks many of the complicating features of real annular flow boiling. First in any annular two phase flow, the vapor-liquid interface is wavy. Film thicknesses at a fixed spatial location may vary over time by a factor of twenty due to wave passage. The wave changes the turbulent structure of the film and may induce or retard nucleate boiling at the wall. The presence of nucleate boiling may, in turn, break-up the viscous sublayer in the liquid film. Information about the turbulence structure at the vapor-liquid interface is unavailable, though there are suggestions that the turbulence may be damped in this

region. The waves themselves are frequently sheared, and liquid droplets entrained in the vapor core. A large fraction of the total liquid flow may be entrained in this manner. Rates of entrainment and droplet deposition are, for the most part, poorly quantified. These rates in fact control film thicknesses and are the key to any eventual analytical model. Liquid film models derived from the momentum and energy equations have poorly predicted heat transfer rates [Co80]. The literature suggests the problem is due to interfacial turbulence damping, but recently it has been suggested that the root cause is poor understanding of entrainment [He84]. In any case, these multiple problems have made realistic analytical model development a rather distant hope.

1.6 The Differences Between Mixtures and Pure Fluids

In this section a review is presented of the additional characteristics which must be considered when a fluid is a non-azeotropic mixture. The review is not intended to be comprehensive, but stresses the most important features of non-azeotropic refrigerant mixtures as applied to flow boiling.

Figure 1-2 displays a temperature-composition phase diagram for the R13B1/R152a mixture used in this report. It is typical of many non-azeotropic mixtures. Examination of the figure reveals immediately the two most important mixture features:

1. The evaporation process is non-isothermal.

2. As the fluid begins to evaporate, vapor is formed preferentially of one component (the more volatile or "light" component).¹

The non-isothermal nature of the mixture is advantageous in terms of use in a counter-flow heat exchanger (a higher effectiveness is possible since a constant temperature difference can be maintained throughout the exchanger). On the other hand, the non-isothermal nature also causes only a portion of heat input to a flowing mixture to be used for vapor generation; the remainder is required to heat sensibly the liquid and vapor streams. Figure 1-3 shows a control volume for a flowing evaporating fluid (ignoring momentarily nucleate boiling). For vapor generation to occur, the vapor already formed must be further heated, and the liquid heated as well to remain in near-equilibrium at their interface (where the evaporation is taking place). From a heat balance on the control volume, over a distance dz :

$$q = q_{SL} + q_e + q_{SV} \quad (1-1)$$

or

$$dh = (1-x) C_{pL} dT_L + (\Delta h_v) dx + x C_{pV} dT_V$$

where x is the mean quality over the interval. In the case of pure fluids the first and third terms in the right side are equal to zero (neglecting the superheating requirements for the liquid and other

¹The term light component is a misnomer. In this study, R13B1 is more volatile but is the more dense of the two refrigerants.

non-equilibrium effects). In the case of mixtures, the sensible heating may represent more than 20% of the overall heating required.

The second feature shown on the previous page, the composition difference between vapor and liquid, reveals that physical properties, both thermodynamic and transport, vary substantially throughout the evaporation process even in the absence of pressure drop. For example, with pure fluids, one tends to think of liquid density as constant under these conditions. With mixtures however, with one component stripped preferentially away from the liquid layer during evaporation, the liquid density may vary by 50% or more, even without pressure drop from inlet to outlet of an evaporator tube. Other thermodynamic properties such as latent heat of vaporization also possess this complicating feature. Thus thermodynamic properties must be reevaluated continuously during the evaporation process.

A great difficulty appears with mixtures in that the addition of a second component into a pure fluid may have spectacular effects on surface tension or viscosity. Precise prediction of these properties is impossible in many cases. Surface tension directly affects the nature of nucleate boiling, yet may be impossible to even estimate since general mixing rules are unavailable.

In addition to the property complications, the vapor-liquid composition difference introduces mass transfer resistance. The interfacial composition is different from the bulk liquid and vapor streams. In

condensation various calculation methods have been developed to account for this problem, with rather extreme assumptions used in common practice. The addition of mass transfer resistance suggests that mass diffusivities should be known; yet these are rarely known for refrigerants. In turbulent flow one needs to estimate the eddy (mass) diffusivity, a process which itself is uncertain, and made even more complicated in the presence of nucleate boiling.

Given the above consideration along with those described earlier for pure fluids, it is easy to understand the current futility of analytically modeling the heat transfer process from first principles. Instead, the literature has proceeded with correlations or simple models which account for as many physical phenomena as their authors deemed possible. To the author's knowledge, no published verification of their proposed models has taken place prior to this report.

1.7 Literature Review of Experiments of Annular Flow Boiling of Mixtures

A number of texts provide a general review of annular flow boiling experiments for pure fluids [Co80, Hs76]. Table 1-1 lists experimental investigations with refrigerants. Very few experiments however have been conducted under similar conditions for mixtures. Some early experiments used calorimetric methods to determine overall heat transfer in reboilers [Bo51] or long steam heated evaporators [Mc42]. These experiments did not provide sufficient information for evaluation of local conditions or physical processes governing the heat transfer.

Shock investigated an ethanol-water mixture in a vertical tube [Sh73]. The inlet conditions were subcooled and the maximum outlet quality he tested was 0.16. This quality is less than the inlet to most heat pump evaporators. The flow patterns he investigated rarely included annular flow. The ethanol-water mixture has a very non-ideal (see Chapter 2) property behavior. The tube used in his experiments was specially plated with a thin nickel film, removing many cavity sizes and possible nucleation sites. His experiments therefore are not particularly relevant to this report. However, Shock performed very substantial analytic modelling in this effort, and several subsequent publications. These efforts will be referred to frequently throughout this report.

Toral modified the test loop used by Shock [To79]. A copper tube was vertically oriented, and the working fluid of ethanol-cyclohexane was selected due to its near-ideal property behavior. Wall thermocouples were spaced very closely so that the position of the onset of nucleate boiling could be located. They were however, mounted only on one side of the tube and symmetry assumed. He found a deterioration of heat transfer due to mass transfer resistance and that nucleate boiling was the dominant mechanism for his testing conditions. Maximum outlet quality was 0.30. He compared his experimental results to the Chen correlation; poor prediction was attributed to the poor prediction of nucleate boiling. Surprisingly, the correlation underpredicted the experimental results. This result, as will be shown in Chapter 7, is unusual since mass transfer resistance is not accounted by the

correlation. Like Shock, Toral performed substantial theoretical studies and they will be quoted frequently.

Bennett recently tested mixtures of ethylene-glycol and water, again in a vertical tube [Be80]. The test section was very short ($L/D \sim 3$) and inlet flows were in the two phase region, provided by preheaters. Only a single wall thermocouple was used in all the measurements, again with symmetry assumed. Several hundred data points were taken over a wide range of conditions. Bennett developed a modification to Chen's correlation to account for mixture effects. They predicted his data to a mean deviation of $\pm 15\%$.

Chaddock and Mathur investigated refrigerant-oil mixtures in a serpentine horizontal copper tube [Ma79]. The full quality range was covered. One potential complication with the study was the impact of oil on properties such as surface tension. The authors noted a dependence of the heat transfer coefficient on heat flux, indicating a nucleate boiling contribution (neglected in the authors' final correlation). Nucleate boiling behavior with refrigerant-oil mixtures defies current understanding [Bu79]; pool boiling experiments with these mixtures show rather erratic results (see Figure 1-4). In the study of Mathur and Chaddock, the addition of oil produced an increased heat transfer at low qualities and a decrease at high qualities, the latter due to the liquid composition being oil-rich.

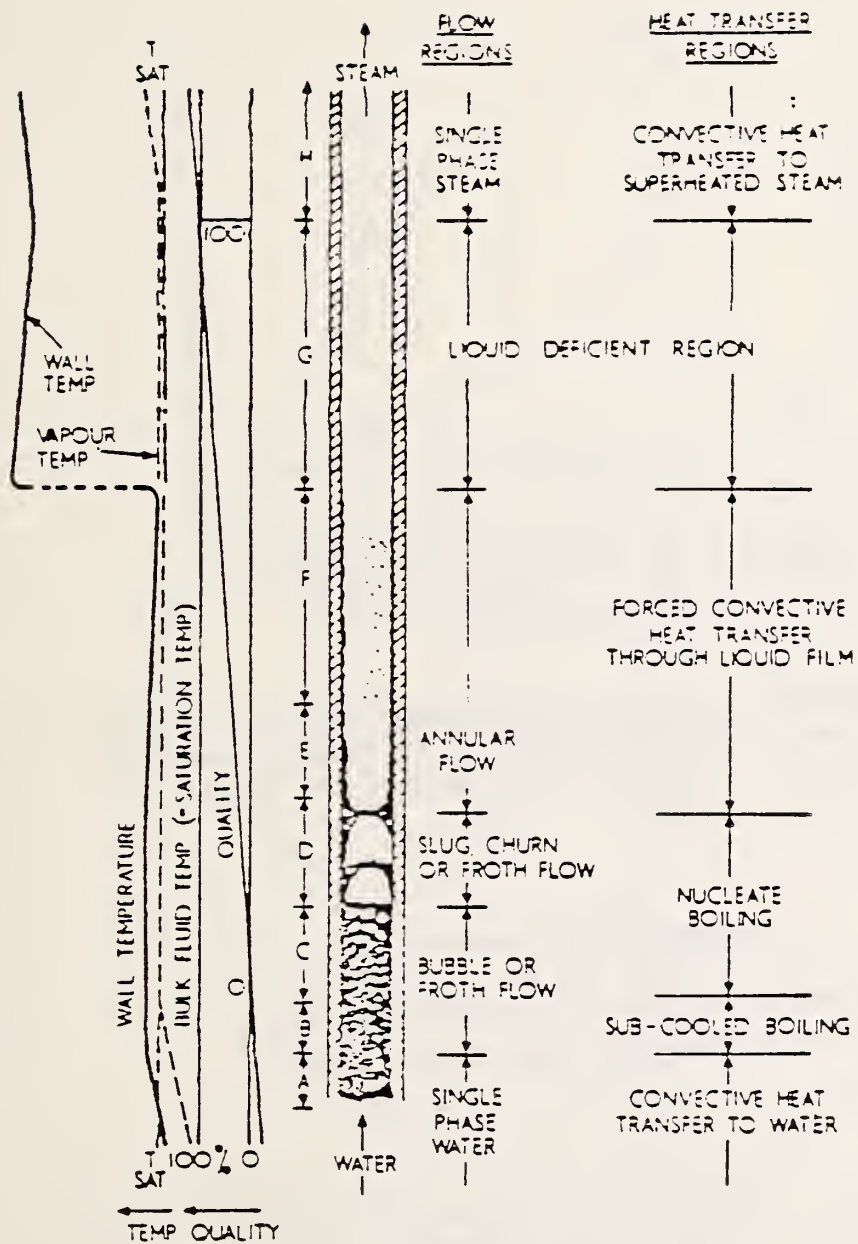
Mishra, et al., investigated mixtures of R12/R22 over a limited composition range in a horizontal stainless steel tube [Mi81, Va79]. Two phase inlet conditions were maintained by a preheater. No tests of pure R22 were conducted. The authors used pure fluid correlations and revised the exponents of the correlations to fit most of their experimental results to $\pm 25\%$.

Singal, et al., experimented with an R13/R12 mixture, again with a horizontal tube over a limited quality range [Si83]. The authors again correlated their results with a different pure fluid correlation. They concluded that the α was decreased for mixtures compared to pure R13 whenever the quality was less than 0.3, and that with a further increase in vapor quality an increased heat transfer coefficient was observed when mixtures were compared to pure R13.

Radermacher, Ross and Didion investigated a mixture of R152a/R13B1 selected for its wide range of boiling points [Ra83]. This work has been reanalyzed and is presented in detail as part of this report.

Table 1. Flow Boiling Experiments with Pure Refrigerants:
Literature Review

<u>Authors</u>	<u>Refrigerant</u>	<u>Ref.</u>
Bryan and Siegel	R11	Br55
Bryan and Quaint	R11	Br51
Baker et al.	R12	Ba53
Pierre	R12	Pi56
Worsoe-Schmidt	R12	Wo60
Altman, Norris, and Staub	R22	Al60
Sacks and Long	R11	Sa61
Gouse and Coumon	R113	Go65
Noerager and Chaddock	R12	Ch66
Gouse and Dickson	R113, R11	Go66
Lavin and Young	R12, R22	La66
Staub and Zuber	R22	St66
Chawla	R11	Ch67
Bandel and Schlunder	R12	Ba74
Anderson, Rich, and Geary	R22	An66
Jallouck	R11	Ja74
Uchida and Yamaguchi	R12	Uc66
Thorsen et al.	R113	Th70
Rhee and Young.	R12, R22	Rh74
Purciple et al.	R11, R12, R113	Pu72
Danilova	R11	Da69
Aljajarh and Duninil	R12, R22, R502, R13B1	Al77
Singal et al.	R13	Si83
Mishra et al.	R12	Mi81
Radermacher et al.	R22, R152a, R13B1	Ra83
Chaddock and Mathur	R22	Ch79



REGIMES OF TWO-PHASE FLOW

AERE-R 3962

FIGURE 1

Figure 1-1: Regimes of Two Phase Flow (Reprinted from (La62))

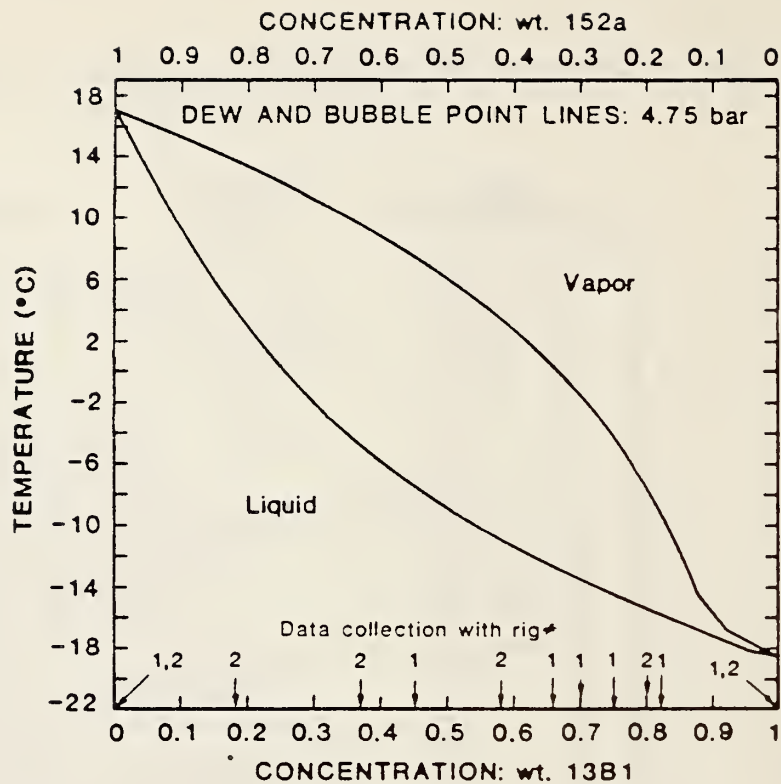
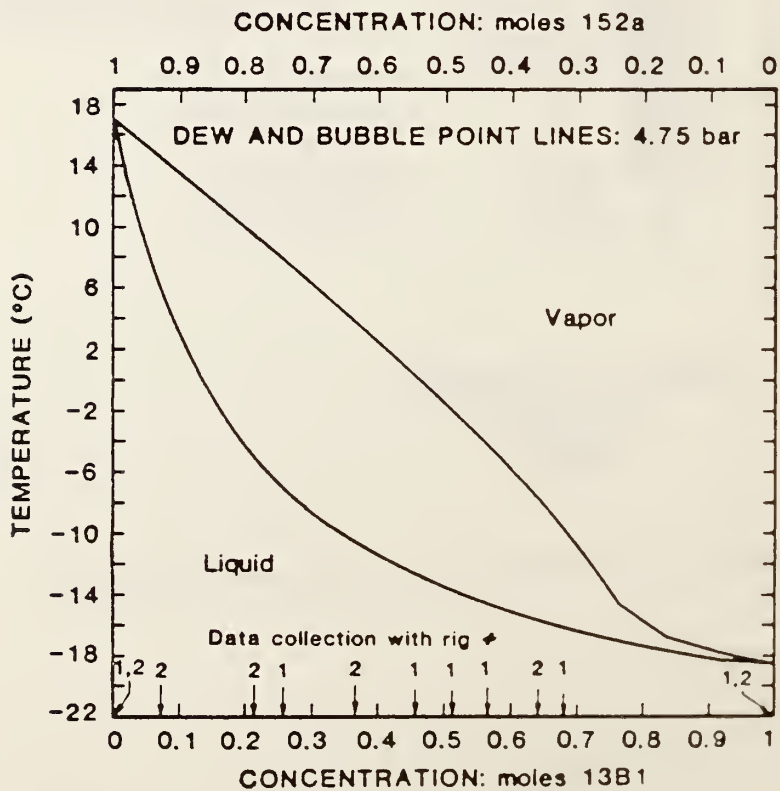


Figure 1-2: Temperature-Concentration Diagrams for Test Fluids in terms of Weight and Molar Fractions. Shown also are the feed concentrations used in the experiments



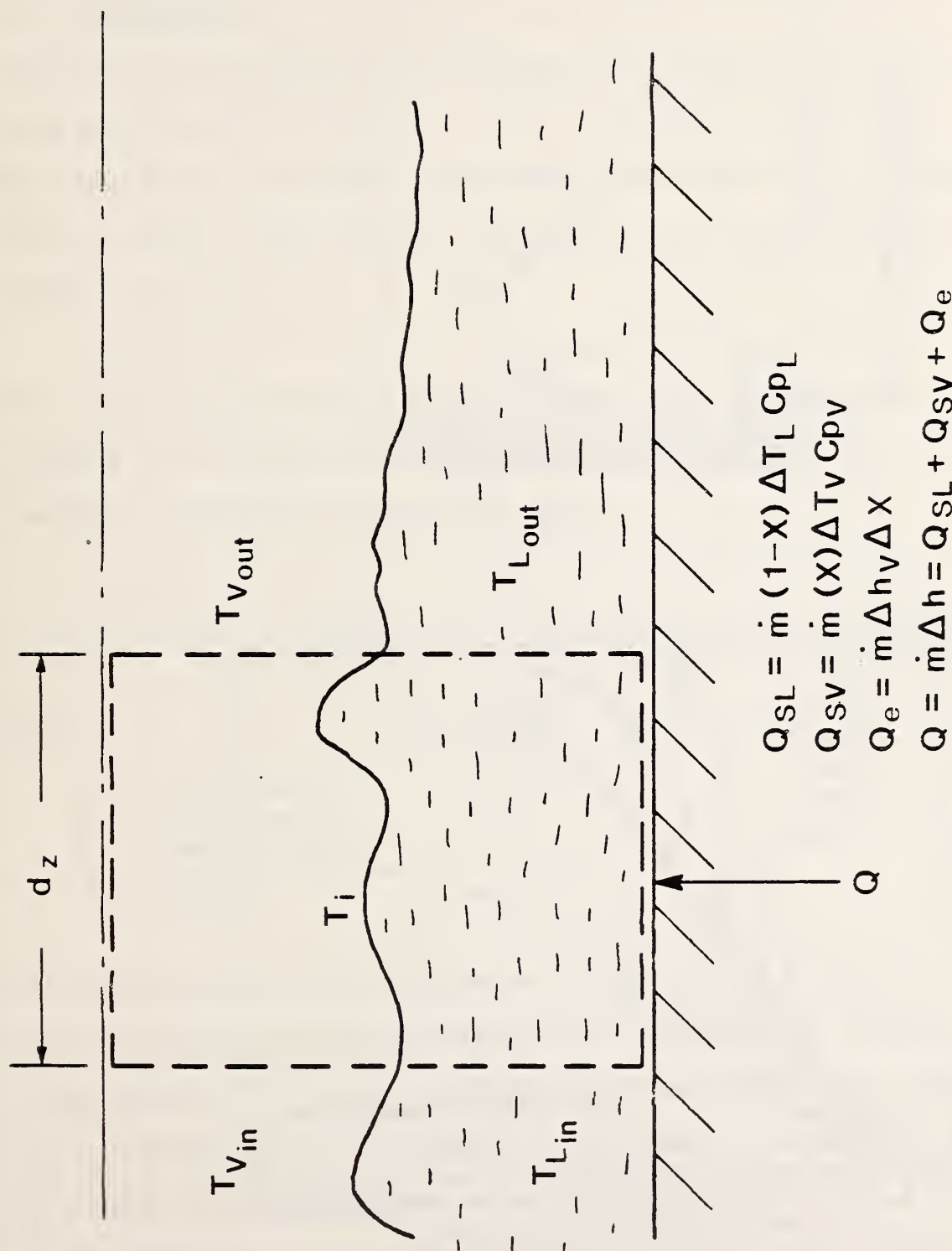


Figure 1-3; Heat Balance on Control Volume in Annular Flow Mixtures

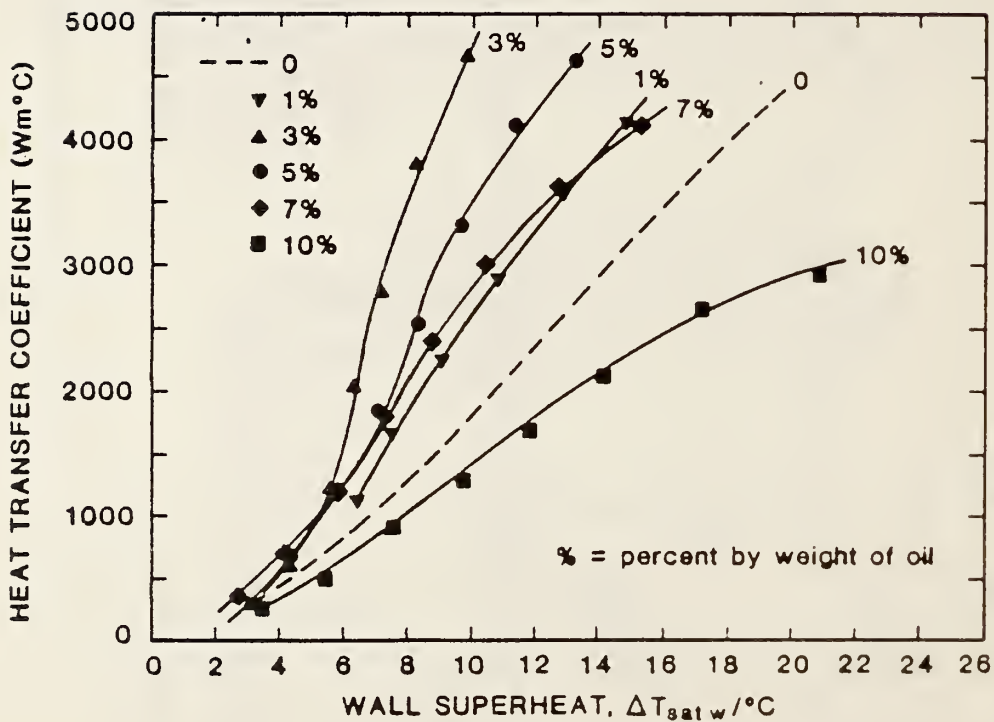
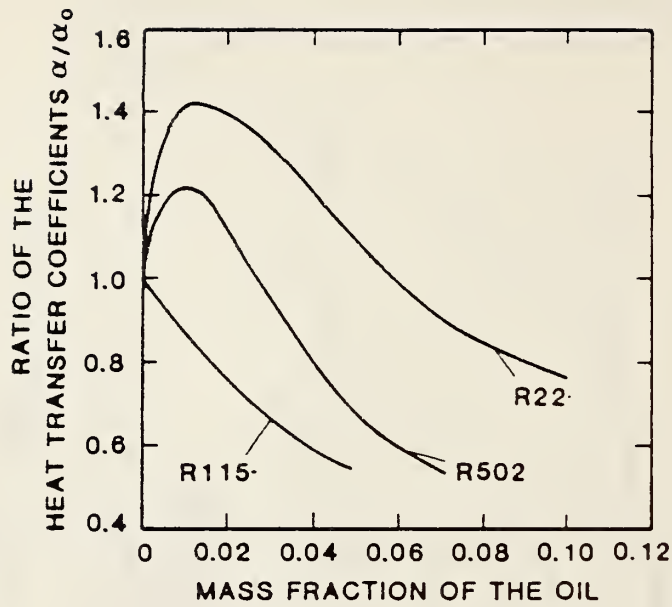


Figure 1-4: Effect of Oil on Heat Transfer Coefficients of Refrigerants. Small additions cause increase, however further additions cause decrease.

CHAPTER 2: PROPERTY DETERMINATION

2.1 Introduction

Determination of transport and thermodynamic properties for mixtures is much more difficult for mixtures than for pure fluids. This is due to more complicated theoretical considerations of molecular interactions as well as the very common lack of experimental data of the mixture's properties.

The most frequent method for estimating many of the properties of mixtures is to weight the mixture property by the mole fraction of the individual components comprising the mixture:

$$P_m = \bar{X}_A P_A + (1 - X_A)P_B \quad (2-1)$$

where

P = any property
X = mole fraction
A = component A
B = component B
M = mixture

This approach has several deficiencies. First of all, spectacular deviations from this presumed behavior have been observed. Examples include surface tension (e.g., ethanol water) and viscosity of liquids (e.g., water-N, N-dimethyl acetamide). Furthermore, a mixture may exist of a liquid at a pressure which is at or above the critical point of one of the components. In this region, specific heat and liquid viscosity are either undefined or infinite. Most engineering work is done away from the critical point; however, this point is exceeded with one of the

refrigerants of this report, R13B1, as it operates in a mixture in the condenser of real heat pumps.¹ Thus, the problem is not simply an academic one.

The refrigerant mixture of R152a and R13B1 presents a particular problem in that both molecules are polar (R13B1 is weakly polar; R152a strongly polar). Deviations from the ideal mixing rule of equation (2-1) can therefore be expected. Extensive P, T, v, X measurements of the mixture have been made by Morrison [Mo82]. However, no transport property measurements of the mixture have been found in the literature.

2.2 Thermodynamic Properties and the Equation of State

In order to determine the thermodynamic properties of a mixture, an equation of State (EOS) is required. The most commonly used one in industry is the Redlich-Kwong-Soave (R-K-S) equation:

$$\frac{Pv}{RT} = \frac{v}{v - b} - \frac{a}{(v + b) RT} \quad (2-1)$$

Mixing coefficients used in determining a and b can be estimated from the molecular structure of the components. The difficulty with the R-K-S equation is that it is not applicable to the liquid phase. In practice a library of liquid properties is used in conjunction with the R-K-S two phase and vapor phase predictions. Alternately, curvefit or semi empirical equations can be written for the liquid phase and pieced to

¹Measurements in this report were conducted below the critical point of either component.

the R-K-S model. Unfortunately, discontinuities appear in certain properties (e.g., C_{pL}) with this approach. Extrapolation near the critical point also produces significant error.

Morrison has applied the DeSantis equation of state to the R152a/R13B1 mixture. This EOS is continuous in both the liquid and vapor phases [Mo82]:

$$\frac{Pv}{RT} = \frac{1 + y + y^2 - y^3}{(1 - y)^3} - \frac{a}{(v + b)RT} \quad (2-2)$$

where

$$y = \frac{b}{4v}$$

The first term on the right hand side of equation (2-2) accounts for molecular repulsive forces and the second term accounts for attractive forces. As can be seen in the equation, the term b must have the units of molecular volume. It is a means of adjusting the closest approach distance between two molecules. As the temperature of a real fluid is raised, this distance becomes smaller (since molecular kinetic energy increases with increasing temperature). Thus, the variable b is a function of temperature. The term a accounts for the non-spherical nature of the forces between molecules because the refrigerants are polar. Again as temperature is raised, the directional attractions of the molecules are reduced, as well as the average attractive force. Thus, a has also a temperature dependence. Morrison determined

empirically the values of "a" and "b" from the pure R13B1 and R152a data sets published in in ASHRAE Tables of Refrigerants after these data sets checked with his own measurements.

In the case of mixtures, the terms "a" and "b" become:

$$\begin{aligned}
 a &= \sum_i \sum_j \bar{X}_i \bar{X}_j a_{ij} \\
 b &= \sum_i \sum_j \bar{X}_i \bar{X}_j b_{ij} \\
 a_{ij} &= (1 - f_{ij}) (a_i a_j)^{1/2} \\
 b_{ij} &= [(b_i^{1/3} + b_j^{1/3})/2]^3
 \end{aligned}$$

These account for molecular interaction between molecules of different components. The term, f_{ij} , is an empirically determined mixing coefficient which might account for both the non-spherical nature of the molecules and possible interactions such as hydrogen bonding.

The solution scheme, and actually the computer code, used in this report, is taken directly from Morrison [Mo84]. It requires an input pressure, temperature and overall composition and outputs enthalpy, entropy, specific volume, and composition of each of the phases as well as the overall mixture. Also output are molar quality and liquid and vapor specific heats.

The code requires several internal iterative loops. The form of equation (2-2) is fifth order and does not have an analytic solution.

In general, given T and X_i , one determines bubble and dew point pressures by iteration. If the given pressure is higher than P_{BUB} the mixture state is subcooled; if $P < P_{DEW}$, it is superheated vapor. In the two phase region, given T and P , one guesses \bar{X}_L , and determines by iteration P_{guess} . When the difference between P and P_{guess} is sufficiently small, the solution is considered closed. P_{guess} is itself the subject of certain conditions. For mixtures, the chemical potential of each component in each phase must be equal: this requirement determines the final pressure guess.

The computer code for the equation of state is not arranged to handle pure refrigerants easily. Furthermore, the data reduction time can be reduced substantially by using curvefits to the property table data.

These curvefits are:

$$(13B1) \quad 1/T = -.04 - .0004656 \ln(P/21867.08454) \quad T[^\circ K], P[\text{bar}]$$

$$(152a) \quad 1/T = .004039 - .0003809 \ln(P) \quad T[^\circ K], P[\text{bar}]$$

Most experimental tests with mixtures for this report were run at pressures between 4.4 and 5.0 bar. Table 2-1 displays the calculated densities for the liquid and vapor phases, as well as the latent heat of vaporization at a pressure of 4.75 bar. Values of the thermodynamic properties may vary by up to 15% from a mole fraction weighting of the pure components' values at the same pressure.

2.3 Transport Properties

The determination of various transport properties for mixtures is complicated by the requirement of using proper mixing rules. The mixing rules are taken inevitably from the widely referenced text by Reid, Prausnitz and Sherwood [Re79]. The mixing rules which they recommend, and which are used in this report, have not been verified experimentally for the particular R13B1/R152a combination.

Transport property data for the pure refrigerants are available from two sources: ASHRAE [As81] and HTFS [Ht83].¹

The ASHRAE tables are incomplete in their transport properties; the HTFS data only was used in this report. All correlation coefficients (R^2) were greater than 0.99 for the pure fluid curvefits.

(a) Thermal Conductivity (Liquid Phase)

The curvefit equation for the pure refrigerants was:

$$\lambda_L = A + BT_r + CT_r^2 + DT_r^3 \quad [10^{-3} \text{ w/M/k}]$$

	<u>A</u>	<u>B</u>	<u>C</u>	<u>D</u>	<u>T_{rmin}</u>	<u>T_{rmax}</u>
(13B1)	150.396	-77.341	-107.302	81.272	0.6	0.96
(152a)	244.932	-122.821	-177.969	133.061	0.6	0.88

¹The former has an error in R152a specific heat [Ra83, Mo84a] and the latter in latent heat [Mo84b].

Reference [Re79] recommends the following mixing rule, with a maximum error of 4%:

$$\lambda_m = [(1 + C)W_A - CW_A^2]\lambda_A + [(1 - C)W_B + CW_B^2]\lambda_B$$

where

λ = thermal conductivity

$C = 0.72$ (empirical constant)

W = weight fraction

Figure 2-1 shows the results of applying the mixing rule at various compositions. It can be seen that there is a substantial deviation from the ideal mixing rule of equation (2-1).

(b) Thermal Conductivity (Vapor Phase)

The vapor conductivity of each of the pure refrigerants was estimated from the HTFS data as:

$$\lambda_v = A + BT_r + CT_r^2 + DT_r^3 \quad [10^{-3} \text{ w/k}]$$

	<u>A</u>	<u>B</u>	<u>C</u>	<u>D</u>	<u>T_{rmin}</u>	<u>T_{rmix}</u>
(13B1)	-75.295	305.035	-396.984	183.196		
(152a)	-27.900	130.237	-177.807	101.216	0.6	0.88

The mixing rule in [Re79] (maximum error = 5%) which was selected was:

$$\lambda_m = \frac{\sum_{i=1}^2 \bar{Y}_i \lambda_i}{\sum_{j=1}^2 \bar{Y}_i A_{ij}}$$

where

$$A_{ij} = \frac{[1 + (\lambda_i/\lambda_j)^{1/2} (M_j/M_i)^{1/4}]^2}{[8(1 + (M_i/M_j))]^{1/2}}$$

\underline{M} = molecular weight

\underline{Y} = mole fraction of vapor

(c) Liquid Viscosity

The pure liquid viscosities were determined from:

$$\mu_{13B1} = 4935.37126 - 43.7022 T + 0.1379T^2 - 0.00015209T^3$$

$$T[^\circ K], \mu[10^{-6} \text{Pa-sec}] \quad 220 < T < 300$$

$$\mu_{152a} = A + BT_r + CT_r^2 + DT_r^3$$

$$A = 387.5886 \quad B = 1238.98 \quad C = 2864.765 \quad D = 1313.244$$

$$0.6 < T_r < 0.88$$

and the mixing rule used was (maximum error at $\pm 15\%$) described in terms of the kinematic viscosity:

$$\nu_m = \phi_A \nu_A^{K_A^*} + \phi_B \nu_B^{K_B^*}$$

where

ν \equiv kinematic viscosity (liquid) = μ/ρ

ϕ \equiv volume fraction

$$K_A^* \equiv 0.27 \ln \frac{\nu_B}{\nu_A} + (1.31 \ln \frac{\nu_B}{\nu_A})^{0.5}$$

(d) Vapor Viscosity

The pure component vapor viscosities were estimated from:

$$\mu_v = A + BT_r + CT_r^2 + DT_r^3 \quad [10^{-6} \text{Pa-sec}]$$

	<u>A</u>	<u>B</u>	<u>C</u>	<u>D</u>	<u>T_{rmin}</u>	<u>T_{rmax}</u>
(13B1)	-26.308	132.34	-166.51	81.7996	0.6	0.96
(152a)	-10.320	60.803	-74.075	38.667	0.6	0.88

The same mixing rule as used for vapor conductivity was used to determine vapor viscosity.

(e) Liquid Mass Diffusivity (Diffusion Coefficient)

No measurements of the liquid mass diffusion coefficient have been taken on any refrigerant pair. Furthermore, [Re79] makes no clear recommendation regarding this property, especially for polar mixtures.

Kandlikar et al. [Ka75] attempted to predict the mass diffusion coefficient for an R22/R12 mixture, using a formula suggested in [Re79]. The

method requires the mixture's liquid viscosity, an accurate equation of state, and generous assumptions regarding activity coefficients, ideal gas behavior, and interaction parameters. Their approach and result may be viewed as an order of magnitude approximation. For their mixture at 0°C and 0.6 mole R22,

$$a_D \simeq a_T/60$$

In turbulent flow, the following assumption is sometimes made for the eddy diffusivity:

$$\varepsilon_D = \varepsilon_T$$

Since the film flow is turbulent and since the presence of nucleate boiling may destroy the viscous sublayer, the actual diffusivity may be anywhere between these values (1 and 60).

In the models described in Chapter 7, a decision was made to assume parametric values of a_D to try to bound the results.

(f) Surface Tension

Surface tension of the pure components was estimated via the following relation:

$$\sigma = A + BT + CT^2 + DT^3 \qquad T[^\circ\text{K}], \tau[\text{mN-m}]$$

	<u>A</u>	<u>B</u>	<u>C</u>	<u>D</u>
(13B1)	37.969	-.01575	-6.73E-4	1142E-9
(152a)	52.828	-.12150	-2.10E-4	4349E-10

For the surface tension of the mixture, [Re79] provides little guidance.

Mole fraction weighting was assumed, regarding equation (2-1). Since the pure components are not particularly disparate, this assumption should lead to little error.

2.4 The Effect of Non-Ideal Property Behavior on the Heat Transfer Coefficient

Transport properties of mixtures are rarely determined by ideal mixing, i.e., simple mole weighting of the component properties. Mixtures tend to have higher liquid viscosities and lower liquid thermal conductivities than would be suggested by ideal mixing. The impact of these physical property tendencies are evaluated below.

In single phase heating, the following equation is widely accepted to be of sufficient accuracy for predicting heat transfer coefficients:

$$a_L = \frac{\lambda_L}{D} \frac{GD}{\mu}^{0.8} \frac{\mu_L C_{PL}}{\lambda_L}^{.4}$$

Consider first, α as calculated from ideal mixing

$$\alpha_{idL} = \frac{G^{0.8}}{D^{0.2}} C_{PidL}^{0.4} \lambda_{idL}^{0.6} \mu_{idL}^{-0.4} \quad (2-3)$$

and for a mixture using the appropriate mixing rules

$$a_m = \frac{G^{0.8}}{D^{0.2}} C_{p_{mL}}^{0.4} \lambda_{mL}^{0.6} \mu_{mL}^{-0.4} \quad (2-4)$$

Dividing (2-3) into (2-4)

$$\frac{a_{mL}}{a_{id}} = \frac{C_{p_{mL}}^{0.4}}{C_{p_{idL}}^{0.4}} \frac{\mu_{id}^{0.4}}{\mu_m^{0.4}} \frac{\lambda_m^{0.6}}{\lambda_{id}^{0.6}} \quad (2-5)$$

Now, it is known

$$\frac{C_{pm}}{C_{pid}} \approx 1, \frac{\mu_{id}}{\mu_m} < 1, \frac{\lambda_m}{\lambda_{id}} < 1 \text{ from mixing rules}$$

Therefore

$$\frac{a_{mL}}{a_{id}} < 1 \text{ always}$$

Thus, the mixture's single phase heat transfer coefficient should be less than that predicted by a mole fraction weighting of the pure fluid properties. The analysis can now be extended to forced convection evaporation flows.

For evaporating flows, the following correlation form appears often in the literature.

$$a_{2\phi} = a_L A(X_{tt})^{-B} \quad (2-6)$$

So, assuming ideal mixing rules

$$a_{id2\phi} = a_{idL} A X_{ttid}^{-B} \quad (2-7)$$

and for actual mixing

$$a_{id2\phi} = a_{idL} A X_{ttid}^{-B} \quad (2-8)$$

Dividing (2-7) into (2-8)

$$\frac{a_{m2\phi}}{a_{id2\phi}} = \frac{a_{mL}}{a_{idL}} \frac{X_{ttid}}{X_{ttm}} \quad (2-9)$$

Now,

$$X_{tt} = \left(\frac{1-x}{x} \right)^{0.9} \left(\frac{\rho_v}{\rho_L} \right)^{0.5} \left(\frac{\mu_L}{\mu_v} \right)^{0.1}$$

so,

$$\frac{X_{ttid}}{X_{ttm}} = \left(\frac{\rho_{Lm}}{\rho_{Lid}} \right)^{0.5} \left(\frac{\rho_{vid}}{\rho_{vm}} \right)^{0.5} \left(\frac{\mu_{Lid}}{\mu_{Lm}} \right)^{0.1} \left(\frac{\mu_{vm}}{\mu_{vid}} \right)^{0.1} \quad (2-10)$$

Substituting (2-10) and (2-5) into (2-9)

$$\frac{a_{m2\phi}}{a_{id2\phi}} = \left(\frac{C_{PLm}}{C_{PLid}} \right)^{0.4} \left(\frac{\mu_{Lid}}{\mu_m} \right)^{0.4} \left(\frac{\lambda_m}{\lambda_{id}} \right)^{0.4} \left(\frac{\rho_{Lm}}{\rho_{Lid}} \right)^{0.5B} \left(\frac{\rho_{vid}}{\rho_{vm}} \right)^{0.5B} \left(\frac{\mu_{Lid}}{\mu_{Lm}} \right)^{0.5B} \left(\frac{\mu_{vm}}{\mu_{vid}} \right)^{0.5B}$$

Grouping terms:

$$\frac{a_{m2\phi}}{a_{id2\phi}} = \left(\frac{C_{PLm}}{C_{PLid}} \right)^{0.4} \left(\frac{\lambda_{mL}}{\lambda_{idL}} \right)^{0.4} \left(\frac{\mu_{Lid}}{\mu_{Lm}} \right)^{0.4+.1B} \left(\frac{\mu_{vm}}{\mu_{vid}} \right)^{0.1B} \left(\frac{\rho_{Lm}}{\rho_{Lid}} \right)^{0.5B} \left(\frac{\rho_{vid}}{\rho_{vm}} \right)^{0.5B} \quad (2-11)$$

Away from the critical point the density ratios are ~ 1 and $\mu_{vm}/\mu_{vid} \sim 1$ for R152a/R13B1 so, $a_{m2\phi}/a_{id2\phi} < 1$ always. The evaporative heat transfer coefficient for the mixture is less than would be calculated from ideal property behavior.

Now, near the critical point, $\rho_{Lm}/\rho_{Lid} > 1$ and $\rho_{vm}/\rho_{vid} < 1$, and these tend to balance the other terms, so nothing definitive can be said. Furthermore near the critical point, estimation of transport properties is exceptionally difficult.

The exercise on the previous page, which to the author's knowledge, has not appeared in the literature, simply shows that even in the absence of the mass transfer resistance, assuming ideal mixing may lead to serious overestimation of heat transfer in both single and two phase mixtures.

DEW/BUBBLE LINES AT P = 175.00 KPA FOR R13P1 R152A
 LIQUID PROPERTIES EVALUATED AT (T_{BUB},X);
 VAPOR PROPERTIES EVALUATED AT (T_{BUB},YV)

X	YV	T _{BUB}	T _{DEW}	V _{LIS}	V _{LMF}	V _{VAP}	V _{VMF}	C _{PLIQ}	C _{PLMF}
(WT. FRAC)		(K)				(M ³ /KG)		(KJ/KG K)	
.000	.000	290.49	290.49	.0010888	.0010888	.06937	.06937	1.4653	1.4653
.020	.109	288.92	290.21	.0010755	.0010721	.06912	.06468	1.4407	1.4504
.040	.200	287.38	289.94	.0010625	.0010674	.06152	.06074	1.4168	1.4355
.060	.278	285.87	289.65	.0010496	.0010567	.05847	.05739	1.3935	1.4205
.080	.345	284.40	289.36	.0010369	.0010460	.05586	.05452	1.3710	1.4056
.100	.403	282.97	289.06	.0010245	.0010353	.05359	.05204	1.3491	1.3907
.120	.453	281.59	288.74	.0010122	.0010246	.05162	.04989	1.3279	1.3758
.140	.496	280.25	288.42	.0010002	.0010139	.04980	.04801	1.3073	1.3608
.160	.535	278.96	288.09	.0009883	.0010032	.04837	.04636	1.2874	1.3459
.180	.568	277.71	287.74	.0009767	.0009925	.04702	.04491	1.2680	1.3310
.200	.592	276.52	287.39	.0009652	.0009818	.04582	.04362	1.2493	1.3161
.220	.625	275.37	287.02	.0009539	.0009711	.04475	.04248	1.2311	1.3011
.240	.649	274.28	286.64	.0009428	.0009604	.04379	.04146	1.2134	1.2862
.260	.670	273.23	286.24	.0009319	.0009497	.04292	.04054	1.1962	1.2713
.280	.689	272.24	285.84	.0009211	.0009389	.04214	.03972	1.1795	1.2564
.300	.706	271.29	285.41	.0009104	.0009282	.04147	.03898	1.1632	1.2415
.320	.722	270.39	284.97	.0008999	.0009175	.04077	.03831	1.1474	1.2265
.340	.736	269.54	284.52	.0008896	.0009068	.04017	.03770	1.1320	1.2116
.360	.749	268.72	284.04	.0008794	.0008961	.03967	.03715	1.1169	1.1967
.380	.760	267.95	283.55	.0008692	.0008854	.03917	.03664	1.1022	1.1818
.400	.771	267.23	283.04	.0008592	.0008747	.03863	.03618	1.0878	1.1668
.420	.781	266.53	282.51	.0008493	.0008640	.03818	.03575	1.0737	1.1519
.440	.790	265.88	281.95	.0008395	.0008533	.03776	.03536	1.0599	1.1370
.460	.799	265.26	281.37	.0008297	.0008426	.03736	.03500	1.0464	1.1221
.480	.807	264.67	280.76	.0008201	.0008319	.03698	.03466	1.0331	1.1071
.500	.814	264.11	280.13	.0008105	.0008212	.03661	.03434	1.0200	1.0922
.520	.821	263.58	279.46	.0008009	.0008105	.03626	.03404	1.0071	1.0773
.540	.827	263.07	278.76	.0007914	.0007998	.03592	.03376	.9944	1.0624
.560	.834	262.59	278.03	.0007819	.0007891	.03559	.03350	.9819	1.0475
.580	.839	262.12	277.26	.0007724	.0007784	.03526	.03325	.9695	1.0325
.600	.845	261.68	276.44	.0007630	.0007677	.03494	.03300	.9573	1.0176
.620	.851	261.25	275.59	.0007536	.0007569	.03461	.03277	.9451	1.0027
.640	.856	260.84	274.68	.0007441	.0007462	.03429	.03254	.9331	.9878
.660	.861	260.44	273.73	.0007346	.0007355	.03396	.03231	.9212	.9728
.680	.866	260.05	272.71	.0007251	.0007248	.03362	.03209	.9094	.9579
.700	.871	259.66	271.64	.0007155	.0007141	.03327	.03187	.8976	.9430
.720	.877	259.29	270.49	.0007059	.0007034	.03292	.03165	.8858	.9281
.740	.882	258.92	269.28	.0006962	.0006927	.03255	.03142	.8741	.9131
.760	.887	258.55	267.99	.0006864	.0006820	.03216	.03119	.8625	.8982
.780	.893	258.19	266.61	.0006765	.0006713	.03175	.03094	.8508	.8833
.800	.899	257.82	265.16	.0006664	.0006606	.03133	.03069	.8391	.8684
.820	.905	257.46	263.64	.0006562	.0006499	.03088	.03042	.8274	.8535
.840	.912	257.11	262.08	.0006458	.0006392	.03041	.03013	.8156	.8385
.860	.919	256.77	260.52	.0006352	.0006285	.02992	.02982	.8039	.8236
.880	.927	256.37	259.05	.0006244	.0006178	.02943	.02948	.7920	.8087
.900	.936	255.92	257.75	.0006133	.0006071	.02894	.02911	.7801	.7938
.920	.945	255.48	256.68	.0006020	.0005964	.02845	.02869	.7681	.7788
.940	.956	255.35	255.65	.0005904	.0005857	.02796	.02822	.7560	.7639
.960	.969	255.05	255.25	.0005784	.0005749	.02746	.02762	.7438	.7490
.980	.983	254.80	254.85	.0005661	.0005642	.02697	.02706	.7315	.7341
1.000	1.000	254.62	254.62	.0005535	.0005535	.02633	.02434	.7191	.7191

Table 2-1: Comparison of EOS values and mole fraction weighting of pure components.

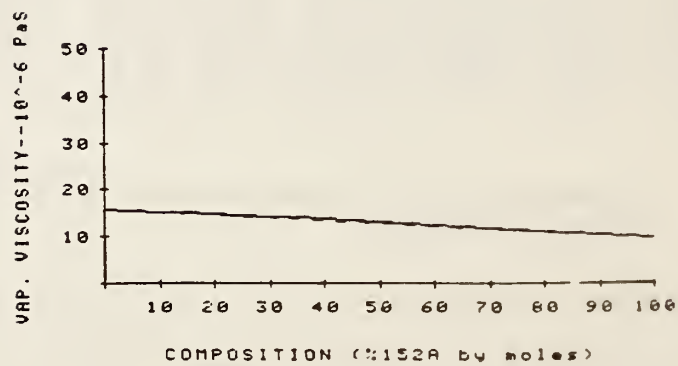
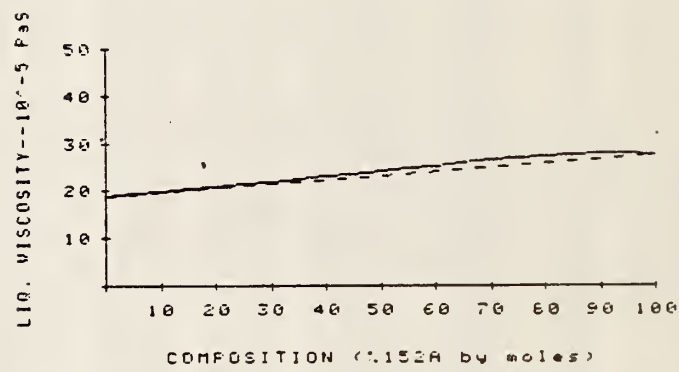
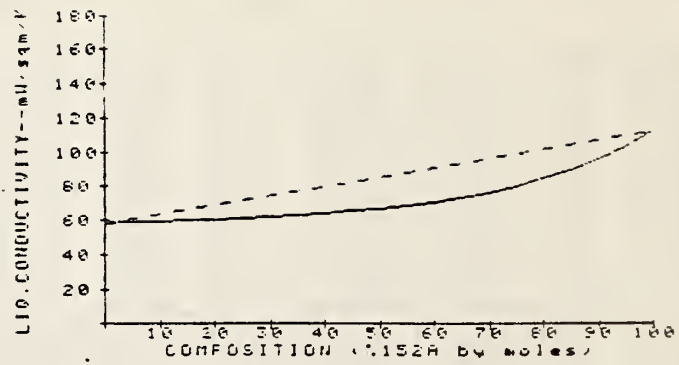


Figure 2-1: Comparison of Transport Properties as determined by mole fraction weighting and mixing rules

CHAPTER 3: EXPERIMENTS

3.1 Introduction and Historical Review

This chapter describes in detail the experimental apparatus, instrumentation, and data reduction methods used in this report. The remainder of this section reviews the types of experimental test rigs which have appeared in the literature. Sections 3.2 through 3.4 describe the detailed features of the test rigs. Section 3.5 displays the tests done to provide some assurance of the quality of the data. Problems which were encountered are discussed in Section 3.6. Finally a summary of the data is provided in Section 3.7.

Most experimental rigs described in the literature have been designed as shown in Figure 3-1. Fluid was circulated via a pump or compressor through a smooth heated circular tube where it was boiled/evaporated, and then reliquified in a condenser. Preheaters and afterheaters and sometimes pressurizers were employed to control entering or exiting conditions. Pressure taps were installed along the test section, and these pressure readings were used to determine the local saturation temperature of the moving fluid. Wall temperatures were determined by a series of thermocouples attached to the tube wall by solder [Ba53, Al60], spot weld [Ch79, Mi81], braze [Sa61] or mechanical clip [Di66, Ra83, Ab82]. The test section itself was electrically heated [Ch77, Ch66a, St66, Go65, Di66, Mi81] or heated isothermally by fast flowing water [Al60, An66] or by a condensing fluid surrounding the tube [Ba53]. In any case, the heat flux was considered well-known and the local heat transfer coefficient was then experimentally determined by the equation:

$$\alpha = \frac{\dot{q}/A_s}{T_w - T_f} \quad (3-1)$$

The test section in some investigations was made of glass so that visual observation of flow patterns could be made [St66, Di66]. However, the use of glass had a serious deficiency, forcing its eventual abandonment. A plating process was used to provide a continuous metal film on the inside of the glass test section. The metal film served as an excellent electrical resistance heater, however nonuniformities in its surface caused the surface roughness (despite attempts at milling smooth) to cavitate and swirl the flow and augment the heat transfer. The variable surface thickness also caused nonuniform heat generation. Most studies instead used thin wall metal tubes in which the temperature drop through the wall is quite small. 'Flow visualization' with metal tubes can be attempted through deduction, either from void fraction measurements, or from the appearance of large differences between top and bottom wall temperature measurements indicating stratified flow, [Cb66a].

3.2 General Description of Test Rigs Used In This Investigation

Through the course of this investigation, two experimental rigs were built and utilized.¹ Both employed a horizontal stainless steel tube (length 2.7 meters; inside diameter .9 cm; outside diameter .95 cm) which was electrically heated.

¹Preliminary results of tests conducted with Rig #1 have been published in [Ra83]. The author wishes to stress that the construction and original data collection described in [Ra83] was shared with his advisor for the experimental portion of the report. Since then, several improvements have been made independently in the data reduction techniques as well as analysis, interpretation and presentation.

Rig #1 is described in Figure 3-2. A semi-hermetic, oil free pump delivered subcooled liquid refrigerant to the test section. Heat was generated in the tube wall by applying a DC voltage difference along the tube. The test section itself was heavily insulated (approximately 15 cm radial thickness) to reduce heat gain from the surroundings; the minimal heat gain was accounted by calibration (described later). The vapor generated in the test section was reliquified in an oversized condenser/receiver. The pump then drew on the liquid reservoir in the condenser and the cycle completed. Inlet subcooling and flow rate were controlled by valves in the liquid line. Subcooling and pressure level could also be modified by altering the condenser temperature (by changing flowrate or supply temperature on the brine side of the condenser).

Thermocouple stations were located at axial positions shown in Figure 3-2b. At each station, thermocouples were clamped at 90° intervals around the outer tube circumference. Instream thermocouples were centered in the flow, extended and pointed upstream for a distance of at least 2 cm, at the single phase liquid inlet and two phase outlet. Pressures were also measured at these locations but not in the heated section. Fluid temperatures in the heated section were estimated from an assumed pressure drop distribution and thermodynamic equilibrium. Sight glasses located at the test section inlet and outlet allowed visual verification of the flow pattern. Flow rates were determined by means of a calibrated turbine meter in the subcooled liquid line.

One of the features of Rig #1 was the use of a uniform heat flux along a fixed tube length. With a given heat and mass flux and degree of inlet subcooling, the outlet quality is fixed at:

$$x_{out} = \frac{\Delta h_{act} - \Delta h_{sc}}{\Delta h_v} \quad (3-2)$$

where

$$\Delta h_{act} = \frac{\dot{q} D_o L}{\dot{m}} = \text{heat added to refrigerant by DC power supply}$$

$$\Delta h_{sc} = C_{PL} \Delta T_{sc} = C_{PL} (T_{bub} - T_{inlet}) = \text{heat needed to raise sub-cooled liquid to saturation or bubble point}$$

Generally, $\Delta h_v \gg \Delta h_{sc}$, i.e., the liquid is only slightly subcooled, so that:

$$x_{out} \cong \left(\frac{\dot{q}}{\dot{m} \Delta h_v} \right) D_o L \quad (3-3)$$

At a specified heat and mass flux, the outlet quality is then determined by the tube length. To reach high exit qualities with low heat flux a tube length of more than 20 meters is required in some cases. This length is impractical clearly for experimental purposes.

In order to obtain data over the full quality range at the required heat and mass fluxes and without using a tube length greater than 5 meters

(available space), a second experimental rig was constructed. It is displayed in Figure 3-3. The principal change is to employ two distinct heating sections, the first of which serves as a preheater. The tube itself was continuous, but heated separately by two independent DC power supplies. The first serving as a preheater provides partially evaporated fluid to the new shorter test section. The quality at the test section inlet is:

$$x_{in} = \frac{\Delta h_{pr} - \Delta h_{sc}}{\Delta h_v} \quad (3-4)$$

where

$$\Delta h_{pr} = \frac{q_{ph} D_o L_{ph}}{\dot{m}}$$

L_{pr} = length of preheat section

Upon entering the test section, the fluid is further evaporated by heat provided from a second power supply so that

$$x_{out} = x_{in} + \frac{\Delta h_{TS}}{\Delta h_v} \quad (3-5)$$

with

$$\Delta h_{TS} = \frac{\dot{q}_{TS} D_o L_{TS}}{\dot{m}}$$

L_{TS} = length of test section

By using a large, at times unrealistic, preheat flux, qualities at the test section inlet could be made greater than with Rig #1. In the test section itself, lower more realistic heat fluxes were used to further vaporize the fluid. The test section itself was .6 m in length, so that quality changes across the test section were relatively small. To 'build up' the entire quality range of interest, 20% to 90% vapor, several tests had to be run at a given mass flux. In each test, the amount of preheat was selected to provide a different inlet quality to the test section. While the use of a preheat section allowed the full quality range to be investigated, the time for data collection was increased greatly (factor 8) over that which would be necessary if a long uniformly heated tube was used. It also requires much stricter reproducibility of flow rates, heat fluxes and composition. Recommendations regarding improved experimental design are made at the end of this report.

While Rig #2 differed conceptually only in its use of a preheater, several changes were also made in the instrumentation and data reduction techniques. The following sections describe both rigs in great detail as such the discussion is somewhat fragmentary. A summary of their differences is provided in Table 3-1.

The sections are organized as follows:

3.3 Testing Protocol

3.4 Measurement and Data Reduction Technique

- (a) Wall temperature
- (b) Mass flow rate
- (c) Heat flux
- (d) Pressure
- (e) Instream temperature (inlet-outlet)
- (f) Data acquisition system
- (g) Sampling for composition
- (h) Calculated fluid temperature
- (i) Overall logic: data reduction scheme

3.5 Quality Assurance Tests

- (a) Single phase heating tests
- (b) Energy balance
- (c) Pressure drop: measured vs. predicted
- (d) Reproducibility
- (e) Effect of Preheater

3.3 Testing Protocol

With the uniformly heated test rig, Rig #1, a series of tests were performed at the following conditions:

COMPOSITION	$G = \dot{m}/A_c$ (kg/m ² /sec)	\dot{q}/A_{s2} (kw/m ²)	P (bar)
R152a	200-700	10-40	1.2-2.4 (a)
R13B1	400-1200	20-40	5.7-7
.833 wt R13B1	200-600	30-40	7-9
.750 wt R13B1	200-600	30-40	5.7-6.6
.706 wt R13B1	200-550	30-40	4-7
.662 wt R13B1	200-550	30-40	4-7
.454 wt R13B1	150-300	20-40	5-7
(a) isolated tests at higher pressure (5 bar)			

The selected mixture compositions span those recommended by the refrigerant supplier for use in heat pumps. Most of the mass fluxes were typical of those which might be employed in heat pumps. The heat

fluxes were representative of those found in evaporators in today's heat pumps. Rather than controlling pressure, outlet temperatures were controlled to be those typical in the desired application. Unfortunately, boiling phenomena is also a complicated function of pressure, so that a strict physical comparison and interpretation of the heat transfer coefficients between pure fluids and mixtures is complicated, if not impossible.

With the second rig, the following conditions were selected:

COMPOSITION	G (kg/m ² /sec)	\dot{q}_{ph}/A_c (kW/m ²)	\dot{q}_{ts}/A_c (kW/m ²)	P_{ts} bar
R152a	100-300	10-95	10-20	4.70-4.80 ^a
R13B1	200-500	10-50	10	4.70-4.80
.80 wt R13B1	200-500	10-70	10	4.70-4.80
.58 wt R13B1	200-500	10-70	20-30	4.70-4.80 ^a
.37 wt R13B1	100-400	10-80	10	4.70-4.80
.18 wt R13B1	100-300	10-90	10	4.70-4.80

a: isolated tests at other pressures

In all Rig #2 cases, pressure was controlled at a fixed level typical of that which might be found with mixtures in a heat pump. This experimental pressure was selected based on the range of condenser temperatures which could be provided by the brine system.

3.4. Measurement and Data Reduction Techniques

Heat transfer coefficients are calculated from:

$$\alpha = \frac{\dot{q}/A_s}{T_w - T_f} \quad (3-1)$$

The measurement of these and other critical variables are discussed in detail below.

3.4.a) Wall temperature, T_w

Wall temperature measurements were made with 0.25 mm thermocouples (T/C) which had been silver soldered and flattened to provide good thermal contact. Silver soldering was selected so that the T/C junction would survive dryout accidents. The T/C leads were arranged as shown in Figure 3-4 to reduce any 'fin' effect conduction gains. The T/C junction and wires were isolated electrically from the tube by a very thin layer of teflon tape ($< .01$ mm). Good thermal contact was maintained by clamping the thermocouple to the tube (see Figure 3-5). Inside wall temperatures were calculated from the measured outside temperatures by use of the steady-state radial, one dimensional (1 - D) conduction equation with uniform heat generation and assuming adiabatic conditions on the outside of the tube.

With Rig #1, wall temperature differences were in fact measured.

Specifically the difference between the instream outlet temperature and the local wall temperature were used; this temperature difference itself was referenced to a thermocouple submerged in a slush ice bath--see Figure 3-6. The use of temperature differences is generally considered more accurate than absolute temperature measurements. However, the

potential stability of the measured outlet temperature may be questioned. Entrained droplets strike and depart this instream thermocouple so that the T/C sees alternately vapor and droplet temperatures and may read something in between depending on its response time. In the case of pure fluids the measured outlet temperature was stable. This stability results from the fact that saturation temperatures change relatively little in the axial direction in the absence of pressure drop, no change would occur. Droplets and vapor tend to be near this saturation temperature. In the case of mixtures, however, entrained droplets may have a much different temperature since the bubble point temperature varies axially since evaporation is non-isothermal even in the absence of pressure drop. Thus, temperature fluctuations in outlet T/C measurements were greater for mixtures than for pure fluids, and wall temperature measurements which were referenced to the outlet T/C reflect these fluctuations.

One other potential difficulty with the Rig #1 wall temperatures is the analog-to-digital 'mV to °C' conversion. The usual industry technique is to utilize the curvefit formulas of NBS monograph 125 [NB]; the published errors in these formulae is $\pm 0.3^{\circ}\text{C}$. Near room temperature, where most of the Rig #1 data was taken, the error is in fact much smaller ($< 0.1^{\circ}\text{C}$). However, at colder conditions (-20°C), the error can in fact be 0.6°C .

Rig #2 employed a different measurement and data reduction technique for wall temperatures. Each wall thermocouple was referenced strictly to an electronic ice bath temperature (precision of electronic ice bath $\pm 0.02^{\circ}\text{C}$

typically, $\pm .05$ maximum). In this way, the wall temperatures were freed from instream fluctuations. Secondly, the use of an electronic ice bath reduced uncertainties regarding the quality of the slush ice bath. The use of more closely spaced test section thermocouple stations (see Figure 3-3b) provided redundancy to verify the goodness of the measured data. Finally, data was reduced with a more accurate curvefit to the 'mV to $^{\circ}\text{C}$ ' data of the NBS Monograph; the 4th order curvefit generated by the author has a maximum error of $\pm .01^{\circ}\text{C}$ over the 100°C temperature range of interest.

The higher precision of the data collected with Rig #2 was necessary because of the lower heat fluxes employed in the test section of Rig #2. The data of Rig #1 is still of satisfactory quality.

Corrections for heat gain from the room and for the teflon tape resistance and any contact resistances were made by the following procedure. Single phase liquid tests were run at high flow rate and zero heat input. Under these conditions, the fluid inlet-outlet temperatures rise was very small ($.2^{\circ}\text{C}$). If there was no heat gain from the room and if the T/C's were in perfect contact with the fluid, the wall T/C readings would match exactly the local fluid temperature. These single phase tests were run at various fluid temperatures covering the range used in later tests. The ΔT between the fluid and room ranged from 0 to 50°C). At the maximum ΔT between fluid and room a heat gain of about 200 w/m^2 was measured. This can be compared to the lowest heat flux employed of $10,000 \text{ w/m}^2$. Based on the measured ΔT of an actual boiling

test, this heat gain was subtracted away from the measured wall temperatures to give the value of T_w used in equation (3-1).

b) Mass flow rate

Though mass flow rate is not necessary to determine local α , it is required to calculate local equilibrium quality. In order to determine mass flow rate, a turbine meter was used in the subcooled liquid line about 50 diameters upstream of the test section. With Rig #1 the signal was sent to a pulse counter which took readings once per second. With the second rig, the signal was sent additionally to a counter integral to the data acquisition system. The two counters agreed to within 1% over the range of interest.

The turbine meter/pulse counters were calibrated with water at near room temperature (scale and electronic stopwatch technique). Temperature corrections were not made, as they are very minor ($\ll 1\%$) [Ma83]. The turbine meter response is also flat over a wide range of Reynolds numbers so that a viscosity correction was unnecessary. It was discovered from energy balance tests that near the upper end of its rated flow rate the spinning rate of the turbine meter was less than expected. Measurements in this flow rate range were avoided.

Calibration of the meter was made before the Rig #1 tests and before the Rig #2 tests (approximately 1 year apart). The change in calibration was less than 1%, the estimated accuracy of the measurement.

Finally with Rig #1, a rotameter was installed to provide visual confirmation of flow rate, as well as redundancy in measurement. It was removed from Rig #2 after it developed an internal leak which was difficult to repair.

c) Heat flux

Heat was generated by DC power supplies as noted previously:

- o Rig #1 and Preheat Section of Rig #2: Dynapower Corporation (0-60v, 0-300a)
- o Rig #2 Test Section: Rapid Electric Company (0-10v, 0-150a)

The DC power supplies were also checked for the addition of AC ripple current. Though the Dynapower Corporation claimed the ripple to be <5% at full load, its value was found to be 50% at part load. A bank of capacitors was used to reduce its ripple to the point that the AC contribution to the total heat flux was less than 1% [Ra83]. The integrity of the capacitors was checked throughout the measurement program. AC rippled with the Rapid Electric Company power supply was measured to be less than 1%.

Heat flux measurements (i.e., electrical input) were made with digital voltmeter integral to the data acquisition systems. Voltage drop across the test section and preheat section was measured at the busbars. Current was calculated by measuring the voltage drop across a calibrated resistor in series with the test section. Early in the testing program, the electrical resistance of the stainless steel tube was checked and its resistance determined to be linear with distance suggesting the

absence of local hot spots. The variation of electrical resistivity with temperature was calculated to be less than 1%, the estimated accuracy of the heat flux measurement [Ra83].

d) Local pressure

Local pressure values are needed to estimate the local fluid temperature of equation (3-1). In studies reported in the literature, it has been common to place pressure taps near thermocouple stations so that in the vicinity of the wall temperature measurements, one could calculate the local fluid saturation temperature. A decision was made to avoid this approach for the following reasons: (a) the stainless steel tube was thin and pressure taps might have intruded into the flow stream; (b) the only means to fix the pressure tap leads would be soldering; the solder would have provided a preferential electrical path (a local shunt) creating a local irregularity in heat flux; (c) pressure drops were relatively small, and errors would be small in estimating local pressure from overall measured values of pressure.

To the author's knowledge, no determination of the effect of pressure taps on measured heat transfer coefficients has appeared in the literature. As such, an experiment was devised to make such a determination. A test was run with refrigerant R22 as the evaporating fluid. Pressure was measured at the inlet and outlet, with boiling taking place very near the inlet. A linear pressure drop was assumed to occur between the location of $x = 0$ (saturation boiling point location) and the outlet. The test was repeated twice with the local α varying about 1%.

Following these tests, holes were drilled and hypodermic needles silver soldered in place about 5 cm downstream of each thermocouple station (see Figure 3-7); the opening at the needle top was sealed with epoxy. The needles served to simulate small pressure taps. The R22 test was then repeated with identical conditions and data reduction. The results of the comparison are shown in Table 3-2; in general the introduction of the pressure taps reduced the α by 10%. No change in pressure or heat flux was measured. The α result was surprising in that if any change occurred it was anticipated that an increased α would be observed due to increased nucleation at the tap locations or increased film turbulence due to tap intrusion. Instead, the reduction might be explained either by: the needles served as fins to add heat from the room, causing the wall thermocouples to read somewhat higher than anticipated; or the pressure tap intrusion, if it extended into the flow, increased the upstream film thickness slightly. The solder may also offer lower electrical resistance, so that the heat flux in the other parts of the tube might have been slightly raised. It is not clear which, if any, of these mechanisms caused the observed change, but the change is apparent. In any case, further tests were made without this type of experimental arrangement.

Figure 3-2b shows the means by which pressure was measured for Rig #1. At the outlet of the test section a tap was made through the busbar by spark erosion so that the hole would be exceptionally smooth. A calibrated pressure transducer and gauge were connected. At the test section inlet, a similar tap was made and a pressure gauge installed.

Inlet and outlet differential pressure was also measured both with a .139 bar (2 psi) pressure transducer [Sensotec] and a .6895 bar (10 psi) gauge. The absolute pressure devices were calibrated with a dead load tester; the size of the pressure gauges however prevented readings from being more precise than $\pm .0689$ bar (± 1 psi). The outlet pressure which was used in the data reduction was that of the pressure transducer accurate to .006895 bar ($\pm .1$ psi).

The .139 bar (2 psi) differential pressure transducer unfortunately had insufficient range. The .6895 bar (10 psi) differential pressure gauge had sufficient range but could be read to only .017 bar ($\pm .25$ psi) at $\Delta P > .139$ bar (2 psi). A decision was made in the original data reduction [Ra83] to use the differential pressure gauge results in all cases. The inlet pressure was then calculated as

$$P_{in} = P_{out}(TD) + \Delta P(GAUGE) \quad (3-6)$$

where the designations (TD) and (GAUGE) represent measurements by the transducer and gauge, respectively.

For Rig #2, pressures were measured as shown in Figure 3-3b. Pressure transducers were employed at the preheat inlet and test section outlet. Differential pressure transducers were used across the test section with a range = .139 bar (2 psi) and across the whole tube with a range = .345 bar (5 psi). While the pressure tap at the test section inlet may be questioned due to the R22 test results described above, care was

taken to reduce its potential impact. First, the hole was made by spark erosion so that there would be no intrusion into the flow. Secondly, the tap was located in the busbar so that there was no problem with electrical shunting. Thirdly, no thermocouple stations were placed in the immediate area of the pressure tap. For Rig #2, pressures were then obtained from

$$(\text{Preheat}) P_{in} = P_{out}(\text{TD}) + \Delta P_5(\text{TD}) \quad (3-7a)$$

$$(\text{Test Section}) P_{in} = P_{out}(\text{TD}) + \Delta P_2(\text{TD}) \quad (3-7b)$$

where $\Delta P_5(\text{TD})$ and $\Delta P_2(\text{TD})$ represent the measurements by the .345 bar (5 psi) and .139 bar (2 psi) differential pressure transducer.

The differential pressure transducers were calibrated in an upward and downward traverse bellowsmeter and a mercury manometer. Unfortunately, this could only be done at atmospheric pressure. Any errors which might develop by the use of the transducers at higher absolute pressure could not be quantified. Estimated accuracy is $\pm .005$ bar.

Given these overall pressure drops, local pressure values, i.e., the pressures at the thermocouple stations need still to be estimated. In [Ra83], the estimation was done by: (a) neglecting the single phase pressure drop in the region between the subcooled inlet and the saturated boiling point location (BPL), i.e., the position where $x = 0$; and (b) assuming a linear pressure drop between the BPL and the outlet.

The implications of the latter, more critical assumption can be examined by the following study.

Figure 3-8 displays the results of applying a widely recommended pressure drop correlation, that of Martinelli-Nelson modified by Chisholm [Ma48,Ch67a], to the typical flow conditions employed in Rig #2. The correlation requires a numerical integration, and steps of $\Delta x = 3\%$ in the preheat section and $\Delta x < 1\%$ in the test section were taken. The BPL was determined by an energy balance, and is denoted in the Figure by an arrow. The series of curves represent different levels of preheat flux, i.e., different overall Δx 's for a given flow rate. In all cases the test section flux was fixed at 10 kW/m^2 . It can be seen that as the change in quality between inlet and outlet increases, the preheat section pressure drop becomes sharply non-linear. However, in the test section, with the relatively small Δx , the pressure drop is nearly linear. These results imply that the assumption of a linear pressure drop in the test section for Rig #2 would be quite valid, but the same assumption in the preheat section at large Δx is somewhat questionable. The linear pressure drop assumption in [Ra83] then may be questionable since (1) flow rates were high increasing the non-linearity and (2) the distance between pressure taps was larger in Rig #1 than with Rig #2.

These errors are balanced by the neglect of single phase pressure drop and by the fact that at large flow rates x tended to be small with Rig #1.

In order to quantify these linear pressure drop errors a sensitivity analysis was run with varying pressure drops. The linear pressure drop assumption typically caused about a 5% error in α for Rig #1; errors could be as high as 15%. The error in preheat α of Rig #2 would be roughly 1/5 smaller, since the Rig #2 preheater is 20% shorter than the Rig #1 test section.

A few alternatives are available to the linear pressure drop assumption. The pressure drop correlation could be used to predict local pressure values. This procedure however requires numerical integration, increasing computation time dramatically in the case of mixtures where an iterative scheme is required because of the nature of the EOS code. It also requires normalization of the results to the measured pressure drops. A more convenient approach, and the one used in the final data reduction of Rig #1, was to weight the linear pressure drop assumption depending on the overall x :

$$\text{For } x_{\text{out}} < .4 \quad \Delta P = .85 \Delta P_{\text{LIN}} \quad 0 < x < x_{\text{out}}/2 \quad (3-8a)$$

$$= P_{\text{out}} - P_{x_{\text{out}}/2} \quad x_{\text{out}}/2 \leq x < x_{\text{out}}$$

$$.4 \leq x_{\text{out}} < 1 \quad \Delta P = .7 \Delta P_{\text{LIN}} \quad 0 < x < x_{\text{out}}/2 \quad (3-8b)$$

$$= P_{\text{out}} - P_{x_{\text{out}}/2} \quad x_{\text{out}}/2 \leq x < x_{\text{out}}$$

where ΔP_{LIN} = the pressure drop predicted by assuming a linear relation between BPL and the outlet

x_{out} = the outlet quality

$x_{\text{out}}/2$ = the outlet quality divided by 2.

The effect of this approach is to fit the curves on Figure 3-8 in a piecewise linear fashion.

While not exact, the pressure drop is corrected in the proper direction and reduces the overall error. The same approach was used in the pre-heat section of Rig #2; the direct linear pressure drop assumption was retained in the test section of Rig #2, since errors were negligible.

e) Instream Temperature (Inlet-Outlet)

With Rig #1, unshielded thermocouples were installed in the flow stream and supported by a brass collar (see Figure 3-6). The hole made by the thermocouple was sealed with epoxy. This technique provided an accurate measurement of the instream temperature however, the epoxy seal tended to fail over time, causing leaks and refrigerant loss (the latter being particularly critical with mixtures since one component is lost preferentially).

With Rig #2, shielded thermocouples were soft-soldered in place (see Figure 3-6b). These thermocouples eliminated the leak problem but provide poorer contact with the flow stream. They also tended to fail inexplicably, therefore neither approach was particularly advantageous.

An attempt was made to insert an instream T/C at the test section inlet. This thermocouple would have provided information about the true temperature rise across the test section. The thermocouple, unfortunately, affected both the single phase and two phase wall thermocouple readings.

Figure 3-9a shows the α calculated for single phase liquid heating R22 tests. The thermocouple was inserted into the flow stream near the tube bottom. As can be seen, a wide circumferential scatter is observed.

Figure 3-9b shows a similar test with the thermocouple removed. A series of tests were also conducted under flow boiling conditions.

Figure 3-10 shows the results of these tests with and without the thermocouple in place. Again, data scatter is reduced without the thermocouple. In order to preserve the purity of the wall temperature measurements, the Rig #2 tests were run without the instream thermocouple at the test section inlet.

This finding of the effect of instream thermocouples may be significant. The literature abounds with test rigs employing instream T/C's; it has been assumed often that the large turbulence in the flow is sufficient to overwhelm any disturbance introduced by the disturbance of the thermocouple. While this may be true with large tube diameters and smaller instream thermocouples, it was not the case here.

f) Data acquisition system

Data collection for both rigs involved the use of a Hewlett-Packard (HP) Series 80 computer connected to a data acquisition system (Rig #1: Fluke and Rig #2: HP 3497a). Automatic scanning of all thermocouples, pressure transducers and flow meters was done. Data was saved when steady-state was reached, i.e., when instream temperatures and pressures variation dissipated. This requirements was satisfied typically one hour after a change in mass or heat flux was made. With the second rig,

pressure control frequently added even more time between tests. With Rig #1, the result of 10 scans which took place at 1 minute intervals were stored. With Rig #2, seven to fifteen scans separated by 40 second intervals were stored. These results were later averaged, their standard deviation determined, and used in further data reduction.

g) Sampling

Mixture composition was determined by withdrawing a liquid sample, expanding it to a complete vapor state and analyzing the vapor sample by gas chromatography. Sample bottles are shown in Figure 3-11. The addition of a pressure gauge to the sample bottle helped determine if the sample had been completely vaporized in the expansion process (one could check the measured pressure at room temperature to see if the sample was well into the vapor region as predicted by the equation of state). However, sampling techniques associated in Rig #2 introduced unnecessary error. In what was thought an improvement, the sampling lines were purged of air before taking a final sample. This was accomplished as discussed in Figure 3-11; some vapor may have been trapped in the process. This vapor, preferentially of the more volatile component, may have caused variation in the results. Later sampling done without air purging proved very reproducible. Sampling errors on the order of 0.5% could have been avoided. On the other hand, the technique was able to show that virtually no air had dissolved in the refrigerant based on the GC analysis.

h) Calculated fluid temperatures

The only quantity missing in the determination of the α is the fluid temperature. This had to be estimated for reasons cited above.

For pure refrigerants the saturation temperature of each thermocouple station was calculated from property tables, given the local pressure as found by the procedures previously used. Sometimes researchers report their results based on $T_f = T_{\text{sat}}(P)$; other times it is based on $T_f = T_{\text{meas}} = T_{\text{bulk}}$. In this report, all values are reported on the basis of $T_f = T_{\text{sat}}(P)$.

For mixtures, the standard approach in the literature is to base T_f in equation (3-1) on T_{eqb} , the thermodynamic equilibrium temperature. The equilibrium temperature was calculated from the equation of state since at each thermocouple station, pressure, enthalpy and original overall composition are known.

i) Overall data reduction scheme

The above detailed discussion is necessarily fragmentary. Figure 3-12 is a flow chart of the data reduction scheme. As the figures are for the most part self-explanatory, only a few comments are provided here, principally on the mixtures' algorithms. All data reduction was performed on HP series 80 computers. The Equation of State (EOS) necessary for the mixture work, is fifth order in nature with several internal iterative loops. The code was developed, by the EOS author [Mo82],

and used here without change.¹ It requires as input T, P and overall molar composition (\bar{X}_0) and outputs overall \bar{h} , \bar{v} , \bar{s} , \bar{X} , \bar{Y} , \bar{C}_{PL} and \bar{C}_{Pv} on a molar basis. Runtime for the equation of state alone is 1-2 minutes on the HP Series 80 computer. As seen in Figure 3-12, two iterative loops involve the equation of state. The first is to determine the BPL; a bisection search method was used to determine a two phase quality very close to zero. Closure was reached typically in 6 iterations. The second iterative loop involved calculating the equilibrium temperature at each T/C station. There a secant method was used to reduce the number of iterations to 3-5.

Overall the program took 30-45 minutes to reduce the data from a single test, calculate the local α 's, and print the results in tabular and graphical form. By contrast, the data reduction for pure fluids took 5-10 minutes on the Series 80 computer, most of which was for printing time.

Typical outputs of each run are shown in Figure 3-14; a complete set is available upon request. Appendix 3A contains a summary of the measured results which can be used by other researchers.

¹The code results were compared by the author of this report with a separate code developed by [Mc85] with virtually identical results.

3.5 Quality Assurance

3.5.a) Single phase heating tests

In order to verify temperature measurements, several single phase liquid heating tests were made. The results of those with Rig #1 are shown on Figures 3-13a and 3-13b. The measured values have been compared with the well-known equation:¹

$$\alpha_L = .023 \frac{\lambda_L}{D} (\text{Re}_L)^{0.8} (\text{Pr}_L)^{0.4} \quad (3-9)$$

as well as the more accurate equation [Pe70]:

$$\alpha_L = \frac{(f/8) \text{Re}_L \text{Pr}_L}{k_1 + k_2 \text{Pr}_L (f/8)^{1/2} (\text{Pr}_L^{2/3} - 1)} \quad (3-10)$$

$$\begin{aligned} \text{with } f &= (1.85 \log_{10} \text{Re}_L - 1.64)^{-2} \\ k_1 &= 1 + 3.4f \\ k_2 &= 11.7 + 1.8 \text{Pr}_L^{1/3} \end{aligned}$$

All tests show good agreement. These tests were for Rig #1; a few tests with Rig #2 and R22 or R152a showed similar agreement.

b) Energy Balance

In order to assure that the instrumentation was behaving correctly, an energy balance was made between fluid temperature rise and energy input. Specifically, a comparison was made between

¹This equation has been credited variously in the literature to Dittus and Boelter, McAdams, Colburn, or Kraubold (F.R.G.). The author is not sure where credit belongs but will refer to it in this paper as Dittus-Boelter equation.

$$\Delta E_f = \dot{m} C_{pL} (T_{out} - T_{in}) = \text{energy gained by the fluid}$$

$$\Delta E = \dot{q} \pi D L = \text{electrical heat input}$$

The quantity $\left| \frac{\Delta E_f - \Delta E}{\Delta E} \right|$ was less than 7% with single phase heating R22 tests with Rig #1 and less than 5% with R22 and R152a tests with Rig #2. Energy balances quoted in the literature by other researchers are:

<u>REFERENCE</u>	<u>ENERGY BALANCE</u>
Al60	$\pm 5\%$
An67	$\pm 10\%$
Ch66a	$\pm 2\%^1$

In the process of these tests, the [As81] value for C_{pL} of R152a was shown to be in error by 15%. Independent work by [Mo85] later confirmed this finding.

c) Pressure drop

The most widely recommended two phase pressure drop correlation at low pressures is that of Martinelli-Nelson [Ma48], with various authors suggesting modifications [Ch67a, Hs76]. In their original development, Martinelli and coworkers used dimensional analysis and a large data base to predict isothermal two-component (e.g., air-water) pressure drop.

¹In [Ch66a], measured outlet T and calculated outlet T based on pressure measurements disagreed, however.

Later Martinelli and Nelson extended the approach to evaporating steam-water systems. Refrigerants were not included in the original Martinelli efforts. A literature search of the application of the technique to refrigerants revealed the following:

<u>REFERENCE</u>	<u>REF.</u>	<u>$(\Delta P - \Delta P_{exp}) / \Delta P_{exp}$</u>
An67	R11	+10-30%
Ch66a	R12	-30-50%
Si83	R12	+50/-20%
Ag82	R12	+/-25%
Al60	R22	0-20%
An67	R22	-20%

In horizontal evaporating flow, the pressure drop is composed of two terms,

$$\Delta P = \Delta P_f + \Delta P_a \quad (3-10)$$

where

ΔP_f = pressure drop due to friction

ΔP_a = pressure drop due to flow acceleration

Martinelli and coworkers developed an empirical procedure to predict the frictional pressure drop.

$$\Delta P_f = \Delta P_L \phi_L^2 \quad (3-11)$$

where

$$\phi_L^2 = 1 + \frac{C}{X_{tt}} + \frac{1}{X_{tt}^2} \quad (3-11a)$$

$$X_{tt} = \left(\frac{1-x}{x} \right)^{.9} \left(\frac{\rho_v}{\rho_L} \right)^{.5} \left(\frac{\mu_L}{\mu_v} \right)^{.1} \quad (3-11b)$$

ΔP_L = Pressure drop, as calculated for single phase liquid flow, for that portion of the flow which is liquid.

$$= \frac{f}{2} \frac{L}{D} \frac{G^2 (1-x)^2}{\rho_L} \quad (3-11c)$$

L = length of tube

and

$$C = \left(\frac{\rho_L}{\rho_v} \right)^{1/2} + \left(\frac{\rho_v}{\rho_L} \right)^{1/2} \quad \text{Chisholm [Ch65]}^1 \quad (3-11d)$$

The pressure drop due to acceleration can be derived from momentum considerations to yield

$$\Delta P_a = G \left(\frac{x^2 v_v}{\varepsilon} + \frac{(1-x)^2 v_L}{1-\varepsilon} \right) \quad (3-12)$$

¹ An alternate procedure which has been suggested is to calculate a 'property index' $(\mu_L/\mu_v) \cdot (\rho_v/\rho_L)$, for the fluid of interest. Then find the water pressure which gives the same value of the index and use the water/steam densities in (3-11d). For the refrigerants used here, very nearly the same results occur.

assuming a quality of zero at the inlet.

To apply equations (3-10), (3-11) and (3-12) correctly, a stepwise integration must be performed. This requirement derives from the fact that x changes as the flow proceeds downstream. The frictional pressure drop is a fairly strong function of quality (as was shown on Figure 3-8). At each step, the inlet, mean, and outlet qualities were calculated. Void fractions were estimated from Martinelli-Nelson [Ma48]. Equation (3-11) was applied at the mean quality equation (3-12) was applied at the step's outlet and inlet qualities, and the results subtracted:

$$\Delta Pa_j = \Delta Pa_{j\text{out}} - \Delta Pa_{j\text{in}} \quad (3-13)$$

The total pressure drop was the sum of the individual steps. The predicted results were compared with the pressure drop measurements of Rig #2 for all pure fluid tests. Figure 3-16 shows the results of a comparison between measurement and prediction. Results were considered quite satisfactory.

d) Preheater effect

A preheat section is commonly used to help set a desired quality of the fluid under investigation independent of the heat flux within the test section.

Consequently, in most cases the fluid experiences an abrupt change in heat flux upon leaving the preheater and entering the test section, which may affect the entrainment and therefore the wall temperature readings. The influence of sudden change in heat flux at wall thermocouples was tested at high flow rates, high qualities and low test section heat fluxes. For one set of experiments with pure R152a, no heat was supplied to the test section, while the heat flux of the preheater was changed between 30 kW/m^2 and 90 kW/m^2 . For a mass flow rate of about 400 kg/sqm/s , no significant change was found in readings of the test section wall temperatures. Nevertheless, all wall temperatures were an average of 0.25 K higher than the saturation temperature of the fluid calculated from the pressure drop; the value was the same for all thermocouples at a particular station. The data shown in figure 3-17 are for a thermocouple group which is 50 diameters downstream of the preheater. The fact that the wall temperatures are slightly higher than the saturation value, can be explained by the superheated liquid leaving the preheater, which is significantly but not completely cooled by further evaporation driven by both the existing superheat and the pressure drop.

The test with 75 kW/m^2 preheater heat flux was repeated with mass flow rates lower and higher than the one previously chosen. The deviation of the wall temperature readings becomes smaller with higher flow rates. This behavior might be expected because with increasing flow rates turbulence and the pressure drop increases causing higher evaporation

rates and a faster decrease of the superheat available in the liquid phase.

A second set of experiments was conducted with a 0.37 wt 13B1 mixture. A fixed heat flux in the test section and a fixed mass flow rate was maintained but heat flux was varied in the preheater. At the same time, the degree of subcooling of the fluid entering the preheater was changed. Therefore, when a large degree of subcooling was set, a large amount of preheat flux was required in order to obtain a given quality at the preheater outlet. Figure 3-18 shows the results of these tests. The heat transfer coefficient measured with the test section is obviously a function of the quality, but not of the amount of preheat used. Lower case letters in Figure 3-18 refer to tests where the liquid was subcooled by 5K, while the upper case letters refer to tests with a considerably more subcooled liquid (25°K) entering the preheater. The difference in preheat fluxes in order to obtain comparable qualities is between 10 to 20 kW/m² or 20 to 30 percent.

e) Reproducibility

Reproducibility of two phase flow results is rarely discussed in the literature. In the case of refrigerants, only two values could be found: $\pm 4\%$ [Sa61] and $\pm 10\%$ [Al60].

Some Rig #1 tests were repeated at various points in the day and sometimes from day to day. Agreement of Rig #1 heat transfer coefficients was within $\pm 2\%$ for tests done one day apart and $\pm 5\%$ for tests done one

week apart. Eighteen tests with pure R152a were repeated approximately 3 weeks apart for Rig #2. Preheat measured values were compared. In the original tests, test section heat fluxes were 10kW/m^2 ; in the later tests, the test section was set at 20kW/m^2 . Of the 54 data points, all agreed within 8%; most agreed much closer (about 4-5%). Most of the variation with Rig #2 was due to differences in mass flux. A few checks were made with mixtures, with similar findings.

3.6 Problems

Three problems occurred during the data collection with Rig #2. First, the measured and calculated temperatures at the outlet for one set of tests with R13B1 disagreed by about 1°K (at high flow rate, high quality). This set of data was not used in the further data analysis.¹

Second, the electrical isolation failed during some of the mixture tests at the top thermocouples in each of the preheat thermocouple stations. At the time, the preheat data was considered superfluous and repairs were not made in order to continue test section data collection. Later it was realized that the preheat data was a substantial resource. This data is included here by averaging only the side and bottom stations. The estimated effect of excluding the top station from the average is to increase the mixture's local α by 5%. The dependence of heat transfer on circumferential location is discussed in Chapter 5. The third problem was the failure of the electric icepoint reference for the last

¹With R13B1, the higher the flow rate and the quality, the greater the error.

series of tests, those with 0.58 wt 13B1. To bypass this problem, the data acquisition system was used directly with internal (software) temperature compensation. For the tests the uncertainty in temperature is $\pm 0.1^\circ\text{K}$, according to Hewlett Packard specifications. As such, test section heat fluxes were maintained at higher values for these tests to reduce the overall uncertainty in the heat transfer coefficient.

3.7 Summary of Experimental Data

A total of 1459 data points were collected with R152a/R13B1 in the following proportions: R152a:409, R13B1:170, Mixtures:880. The data are tabulated with relevant variables in Appendix 3A.

Approximately 20% of the data is not in the annular flow regime and is not included in further analysis.

The tested range of relevant variables includes:

Heat Flux: 10-95 kW/m²
Mass Flux: ~150-1200 kg/m²/sec
Composition: 0.0-1.0, several intermediate values
Pressure: 1.7-9.0 bar
Quality: 0.0-1.0
Martinelli Parameter ($1/X_{tt}$): 0.3-35
Subcooled Liquid Reynolds Number: 3000-50000
Prandtl Number: ~ 3-4

All parameters, except Prandtl Number, varied by nearly an order of magnitude. The data base then provides a strong basis for analysis of physical phenomena as well as the heat transfer coefficient.

Table 3-1a: Hardware Differences Between Rig #1 and Rig #2

	Rig #1	Rig #2
T_w	o ΔT between T_w and T_f	o individual T/C with redundant stations
$T_{reference}$	o slush ice bath	o electronic ice point
P_{out}	o P_{TD} and P_{GAUGE}	o same
P_{in}	o P_{GAUGE}	o P_{TD} and P_{GAUGE}
ΔP_{tot}	o ΔP (2 psi) and P_{GAUGE}	o ΔP (5 psi) ΔP (2 psi) and ΔP_{GAUGE}
Heat Flux	o uniform heat	o preheater and test section heater
T_f	o unshielded, inlet and outlet	o shielded, inlet and outlet
D.A.S.	o Fluke - HP85	o HP3497 - HP86B
Sampling Technique	o no air purge single bottles	o air purge, multiple samples, pressure gauge
Flow Metering	o Rotameter Turbine meter	o Turbine meter
Condenser	o Temp. controlled	o Temp. and flow controlled (via bypass) to give improved stability and pressure control

Table 3-1b: Data Reduction Differences Between [Ra83] and This Thesis
(Rig #1)

T_w	o NBS Monograph	o same
P_{local}	o linear pressure drop based on ΔP_{gauge}	o piecewise linear ΔP , based on calibrated ΔP_{TD} if within range, else ΔP_{GAUGE}
T_f	o linear between T_{out} (measured) and T_{BUB}	o equilibrium tempera- ture based on improved equation of state

Table 3-2: Effect of Pressure Taps on Heat Transfer Coefficient

Before (After)	Before (After)	Before (After)	Before (After) Taps
4096 (3546)	4636 (4346)	3665 (3069)	0.00 (0.00)
4494 (3830)	4687 (4511)	3654 (3404)	0.10 (0.10)
4278 (3574)	4380 (3915)	4233 (4062)	0.18 (0.18)
4221 (4068)	4448 (3393)	4096 (3620)	0.26 (0.26)
4488 (4040)	4352 (3393)	4091 (3416)	0.34 (0.34)
4584 (3438)	4233 (3359)	3807 (3126)	0.42 (0.42)
5402 (3801)	4454 (4079)	3989 (3938)	0.50 (0.50)
5504 (4698)	4749 (4516)	4153 (4034)	0.58 (0.57)
5379 (6656)	5612 (4182)	5033 (4925)	0.66 (0.65)

Refrigerant: R22

Mass flux: 228 kg/m²/sec

Heat flux: 29318 W/m²

TYPICAL TEST RIG

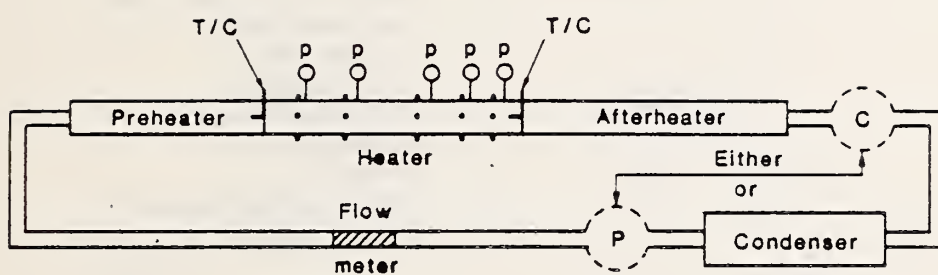
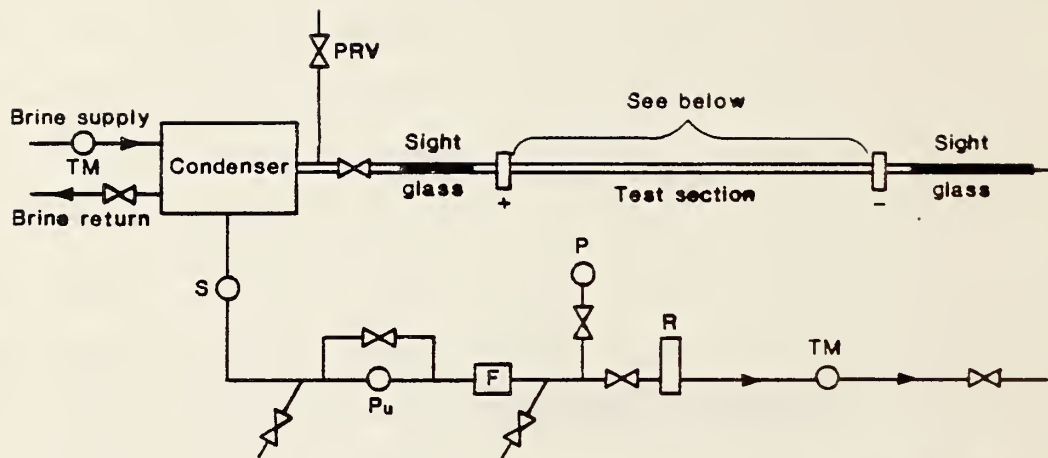


Figure 3-1: Typical Test Rig in the Literature: P= Pump;
C=Compressor; p=pressure tap and gauge



PRV-Pressure relief valve
 TM-Turbine meter
 R-Rotameter
 S-Sight glass
 P-Pressure gauge
 F-Filter/drier
 Pu-Pump
 ΔP -Differential pressure
 TD-Transducer

RIG #1

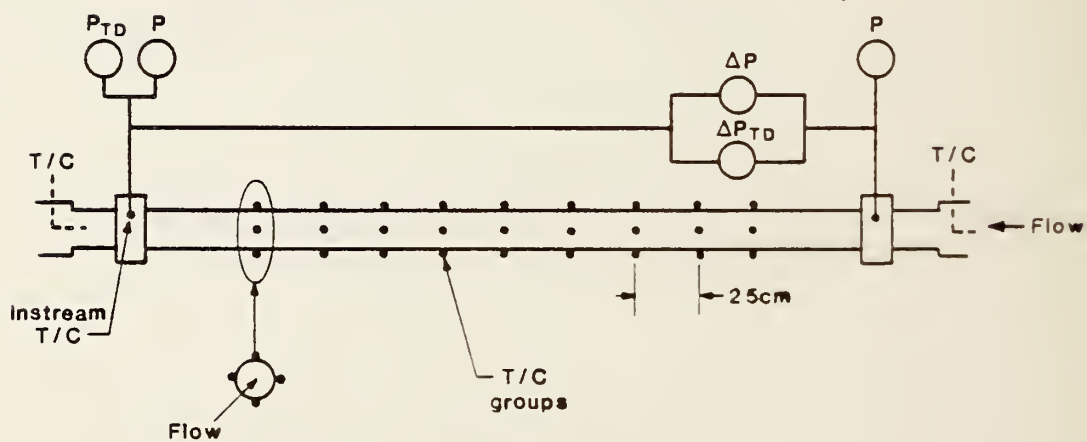
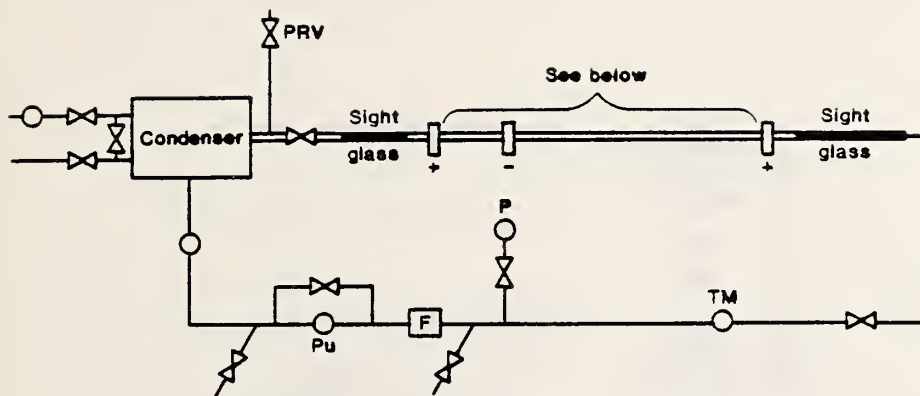


FIGURE TEST SECTION RIG #1

Figure 3-2: Experimental Test Rig #1: Uniform Heating. No Preheat Section.



RIG #2

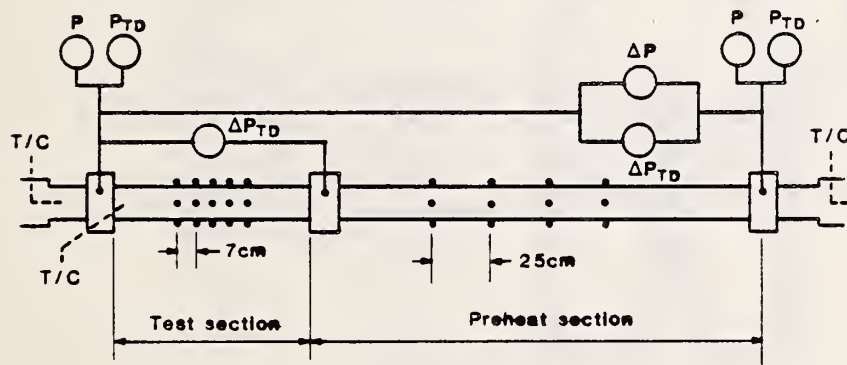


Figure 3-3: Experimental Test Rig #2: Preheat and Test Sections employed via separate DC power supplies.

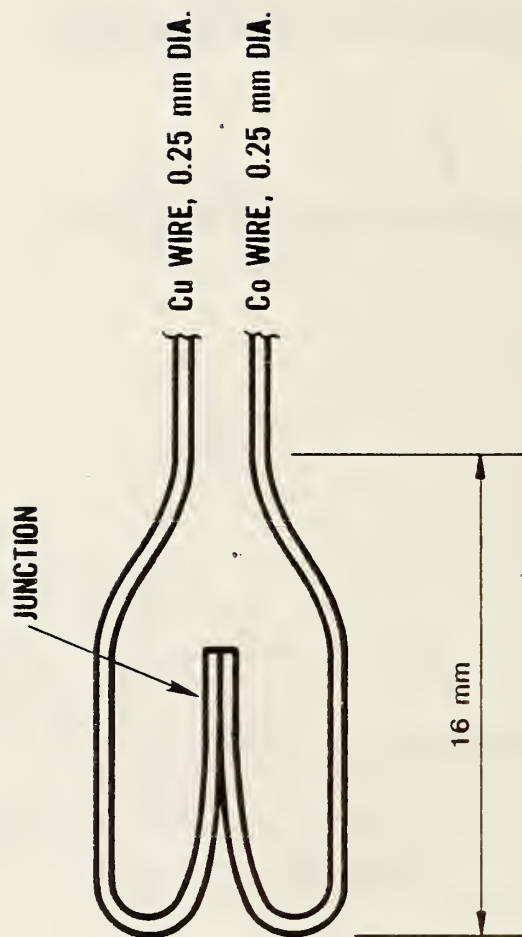


Figure 3-4: Thermocouple Lead Arrangement. Wires were bent to reduce conduction losses due to "fin" effect.

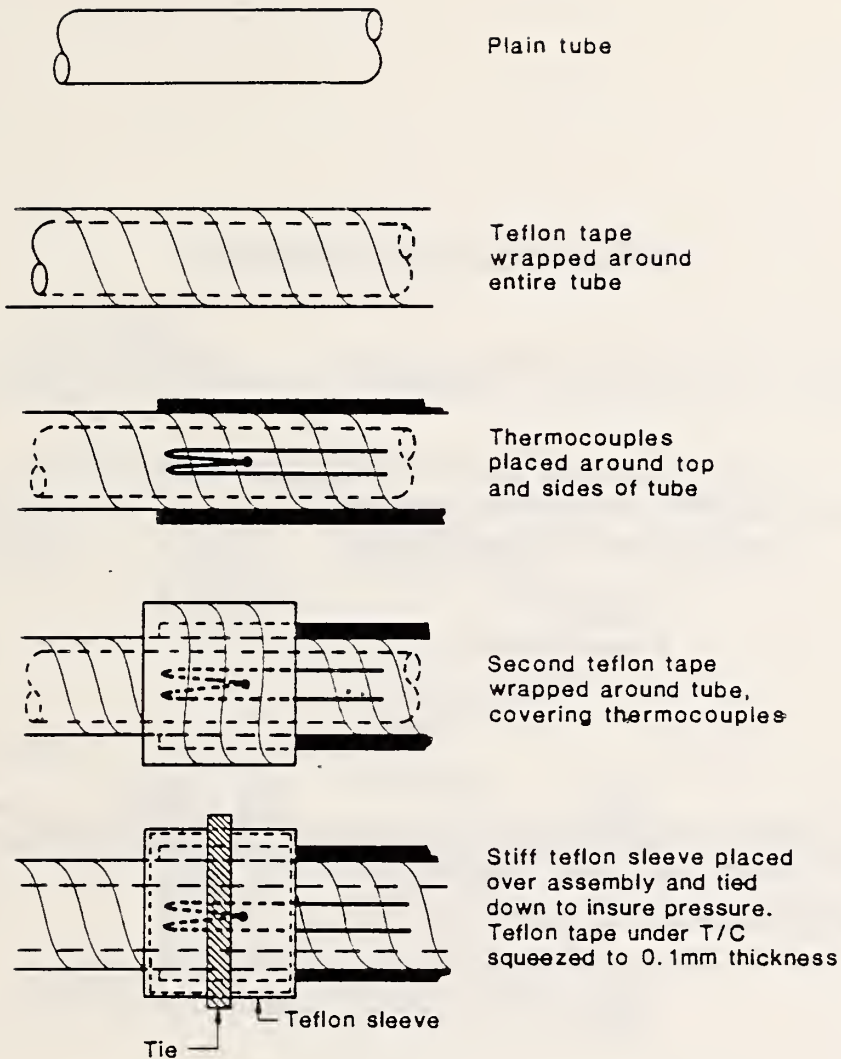


Figure 3-5: THERMOCOUPLE MOUNTING SCHEME INCLUDING ELECTRICAL ISOLATION

TEMPERATURE MEASUREMENT

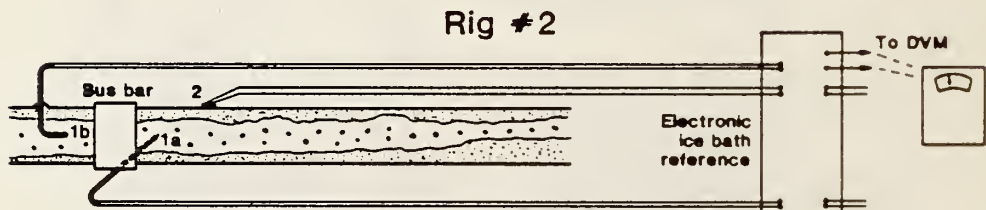
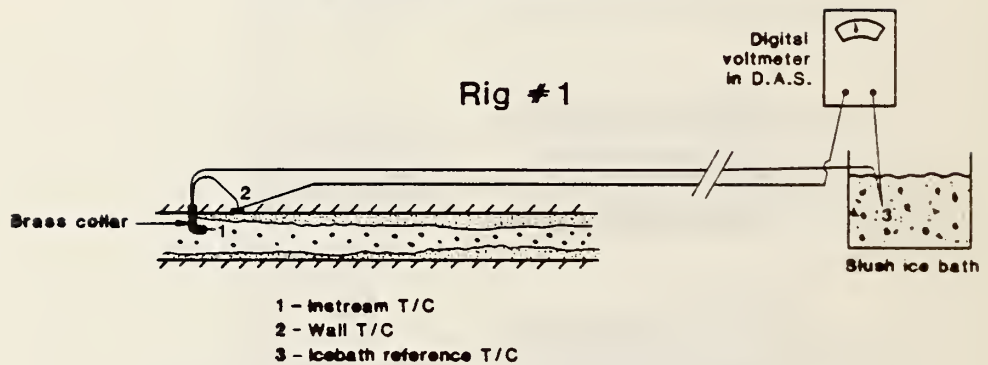


Figure 3-6: Wall and Instream Temperature Measurement: DVM= Digital Volt Meter; DAS: Data Acquisition System; Unshielded Thermocouples were used with Rig #1. Shielded thermocouples were used with Rig #2.

FIGURE SIMULATING PRESSURE TAPS

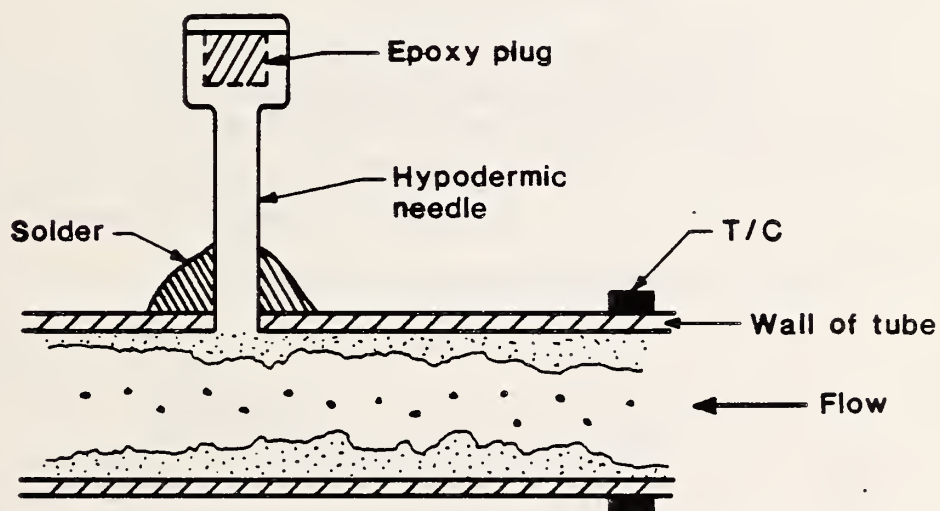


Figure 3-7: The Simulation of Pressure Taps: Taps mounted about 5 cm downstream of wall thermocouple measurement stations.

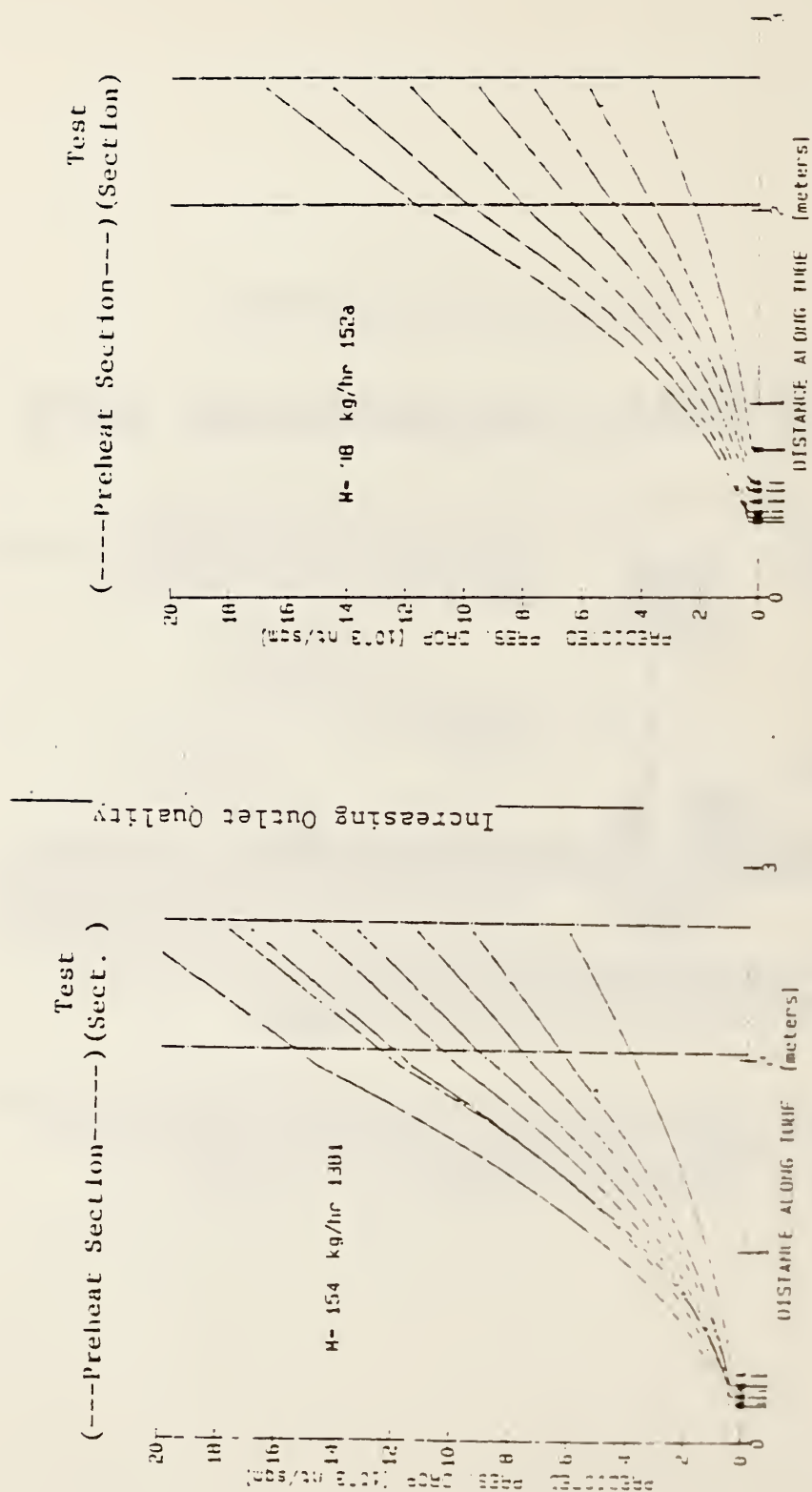


Figure 3.8: Calculated Pressure Drop via Martineau-Nelson Method. The various curves indicate different heat flux levels. The larger the preheat flux, the larger the outlet quality and pressure drop. The vertical arrows indicate the BPL at each preheat flux.

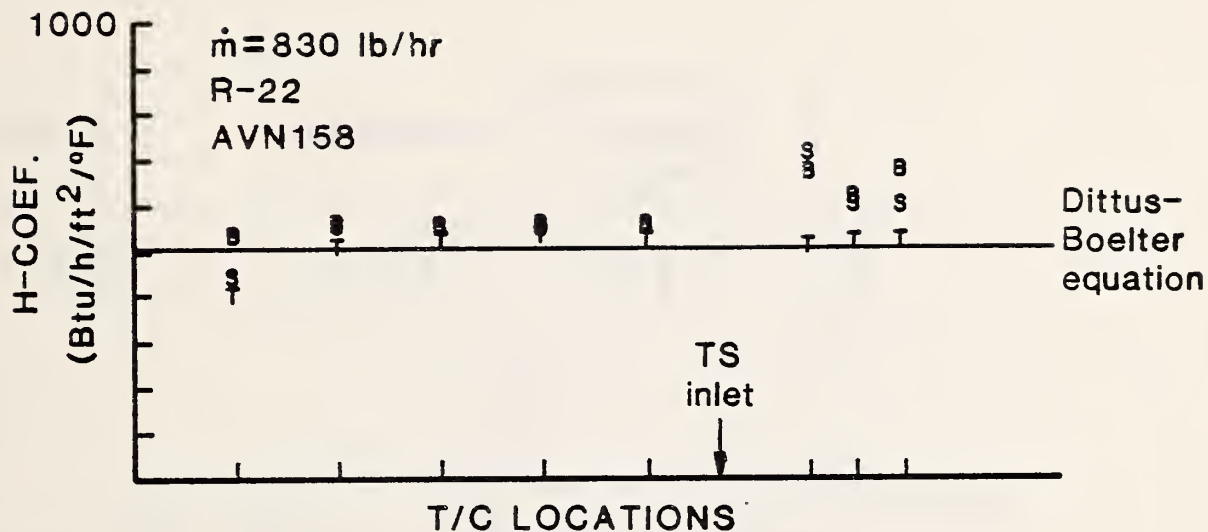
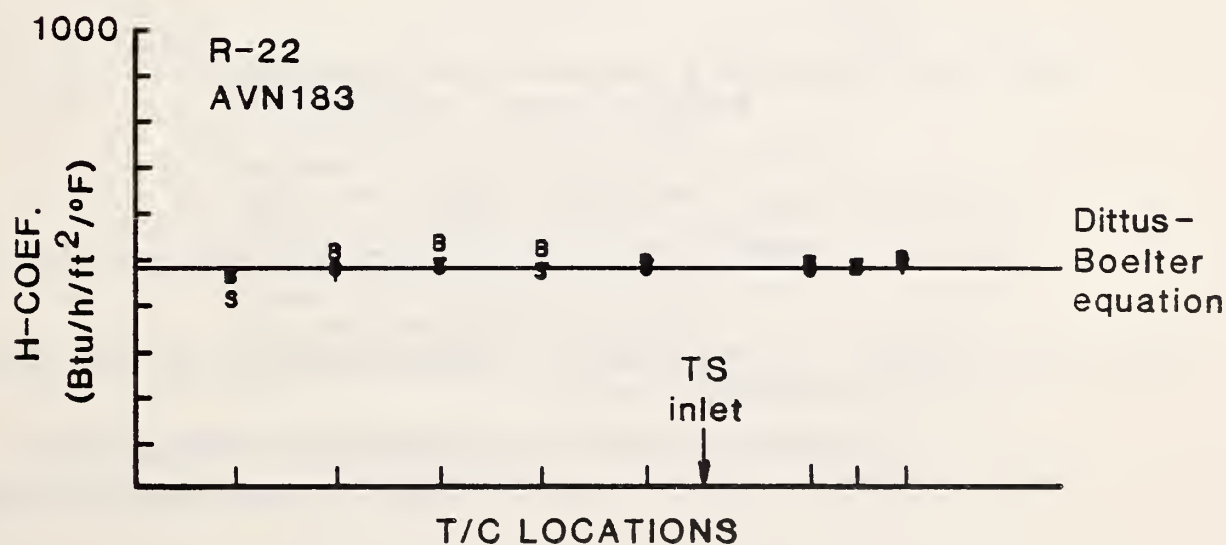


Figure 3-9: EFFECT OF INSTREAM THERMOCOUPLE:
Single phase (liquid) heating test with and without instream
thermocouple at test section inlet
(T-Top, B-Bottom, S-Sides)



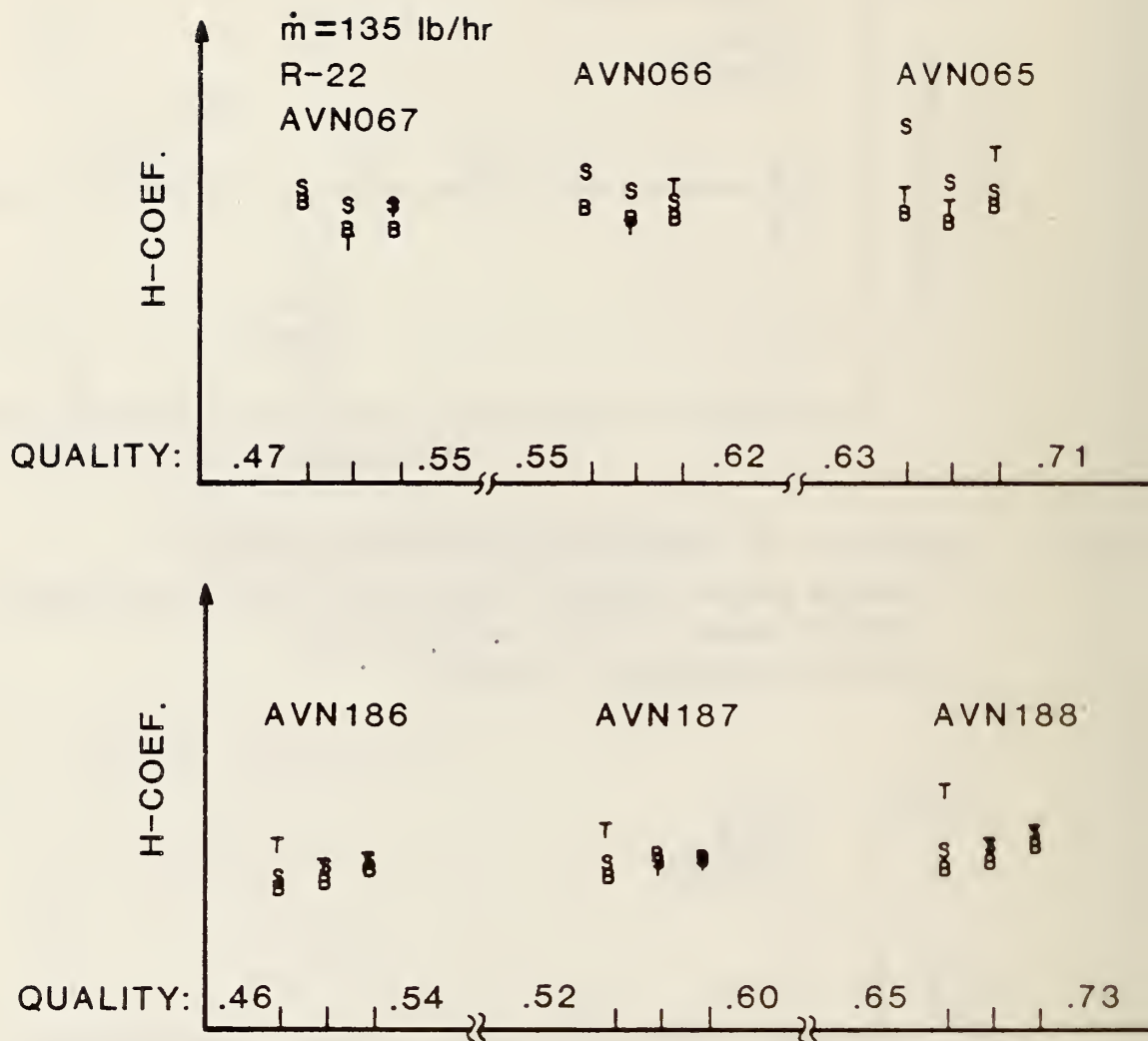
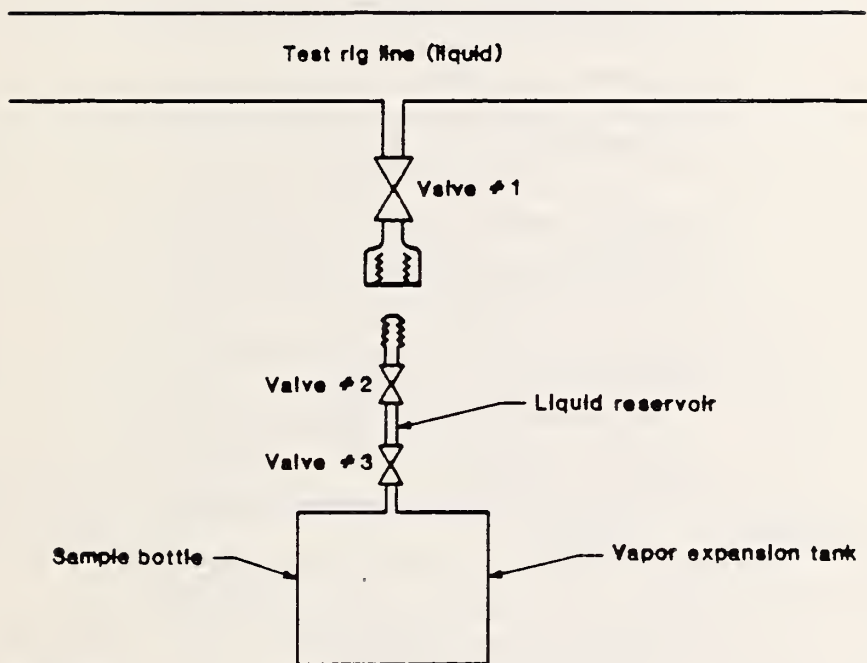


Figure 3-10: EFFECT OF INSTREAM THERMOCOUPLE ON EVAPORATIVE HT. TRANSFER COEFF.

Top set of curves: with instream thermocouple

Bottom set of curves: without instream thermocouples

SAMPLING TECHNIQUE



Procedure:

1. Evacuate sample bottle including vapor & liquid reservoirs; close valves
2. Attach bottle to test rig (all valves closed)
3. Open valves #1 & #2 to fill liquid section
4. Close valves #1 & #2; remove bottle from test rig
5. Open valve #3 to expand liquid into vapor
6. Bring bottle to gas chromatograph for analysis

Error: Between steps 2 and 3, valve #1 opened with bottle only loosely attached. Purges air between valves #1 and #2, but introduces vapor rather than liquid into this section.

Figure 3-11: Sampling Technique to determine mixture composition

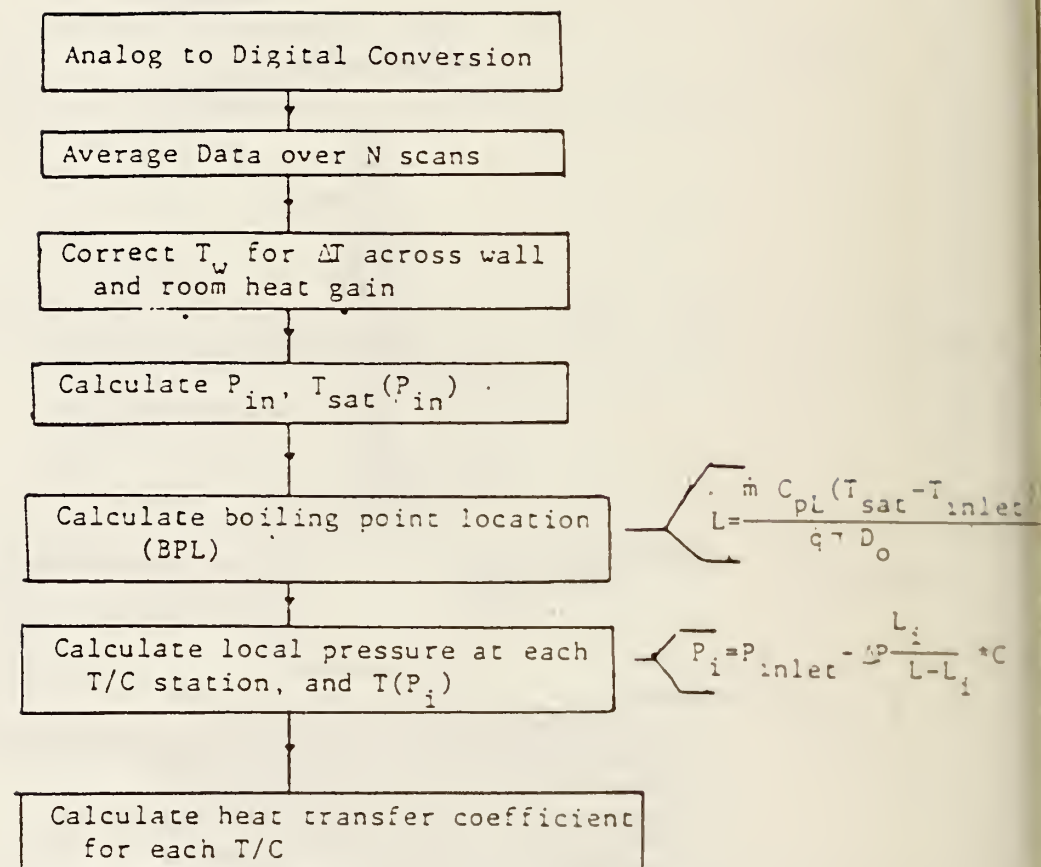


Figure 3-12a: Data Reduction Scheme for Pure Refrigerants

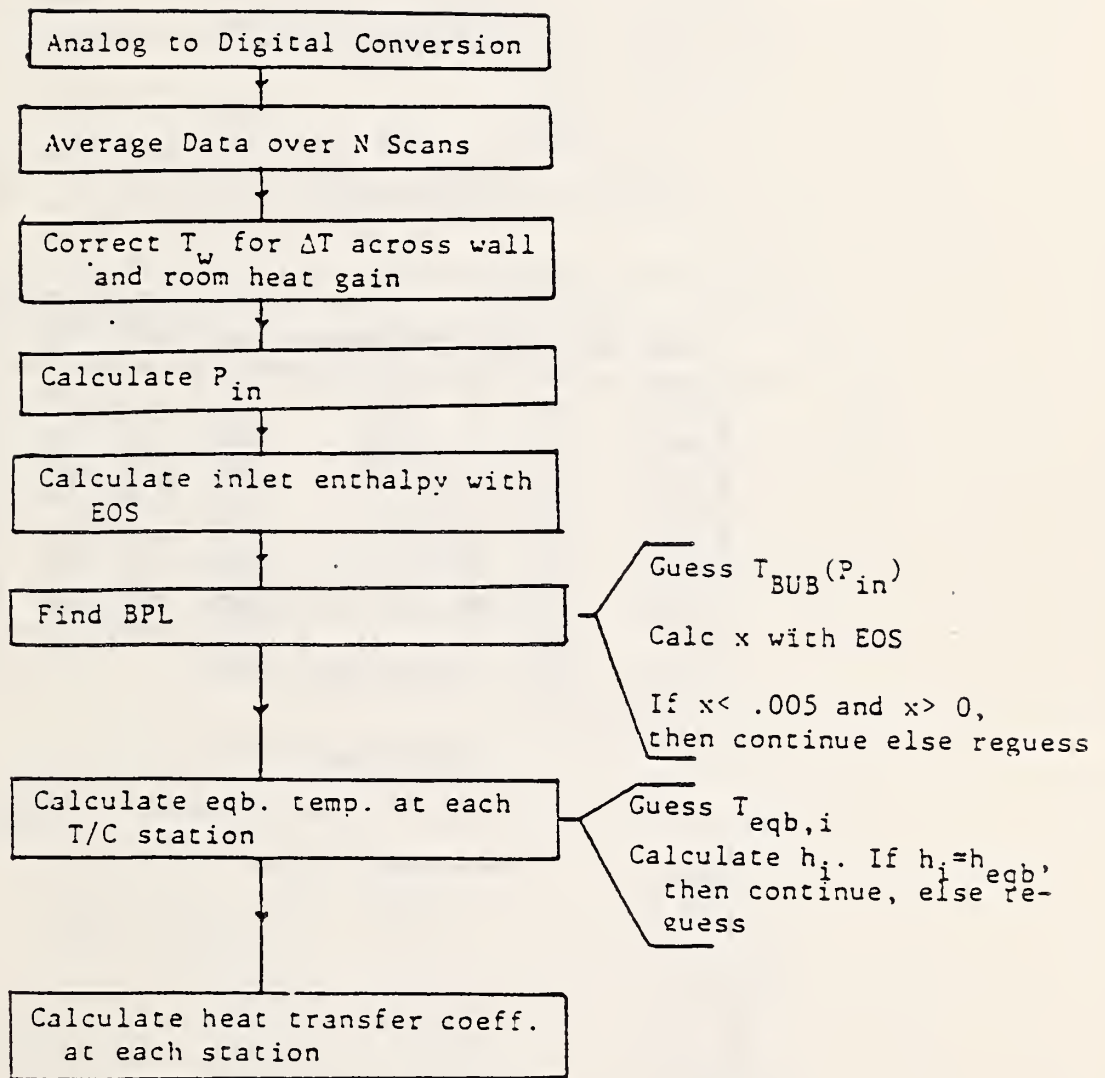


Figure 3-12b: Data Reduction Scheme for Mixtures

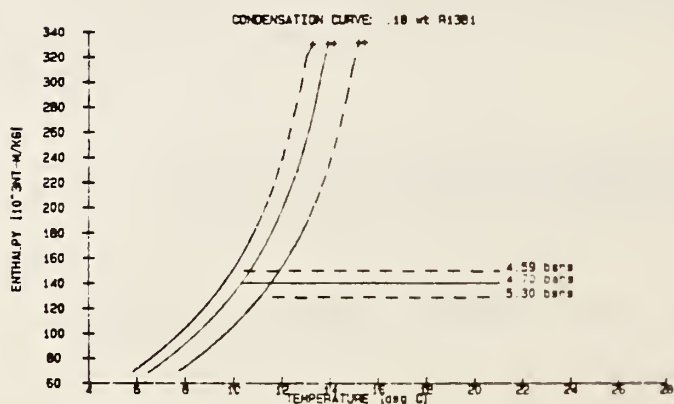
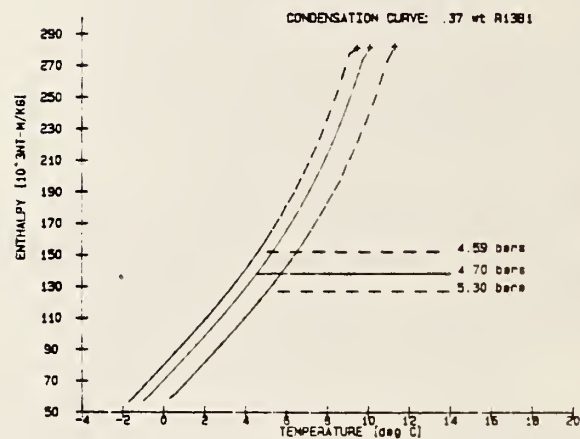
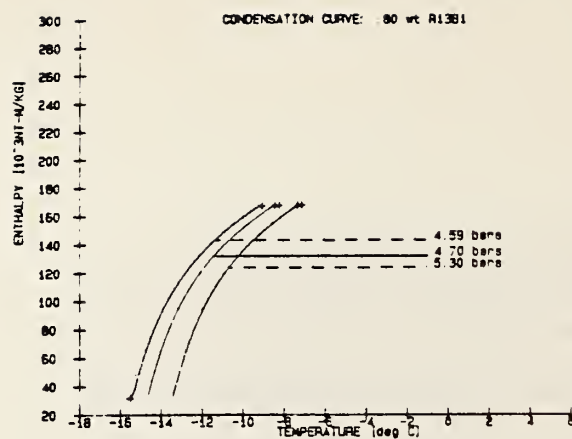


Figure 3-13: Condensation Curves (T vs. H) for Various Compositions. A poor guess of dH/dT may lead to divergence.

AVM403

REFRIG:MIXT. CONCENT(WT152a)= .630 FLOW:ANNULR 04:04:20:53:32

```
--in--!-----preheat-----!-----test-----!-----out-----
      20.4  20.1  18.8  10.2   9.9   9.9   9.8  10.0
-14.2  17.5  18.8  18.2   9.5   9.7   9.6   9.6   9.6   8.1   7.7  deg C
      17.6  17.9  17.8   9.5   9.6   9.5   9.5   9.4
      17.9  17.8  18.8   9.6   9.7   9.5   9.6   9.5
--in--!-----preheat-----!-----test-----!-----out-----
```

AuxT: 22.1 -21.7 -13.9 -12.3 8.0 -26.3 -7.9 deg C
 PRES: 4.77 .02 .05 4.70 5.08 4.84 .08 bars
 HEAT: 124.08 23.8 45.2 2.60 51708 6800
 FLOW: 67 144 80.4

```
*****
HEAT TRANSFER COEFFICIENT(w/sqm/K)                               Wt. 152a
TOP  LSIDE  BOTM  RSIDE  AVG  MassQuality  VapComp  LiqComp  Eqb.T
*****
3119  3805  3784  3676  3596          .35   .41   .75   3.83
3474  3811  4117  4142  3886          .48   .46   .79   5.22
4231  4442  4607  4223  4376          .59   .50   .82   6.51
2777  3841  3981  3813  3603          .70   .54   .85   7.52
3074  3566  3869  3566  3519          .71   .54   .85   7.54
3254  3820  3980  3829  3721          .71   .54   .85   7.56
3522  3746  3937  3788  3748          .71   .54   .85   7.58
3129  3853  4223  4038  3811          .71   .54   .85   7.60
TESTSEC AVG:          3680  ENERGY BALANCE:  1.1%  7.66
*****
```

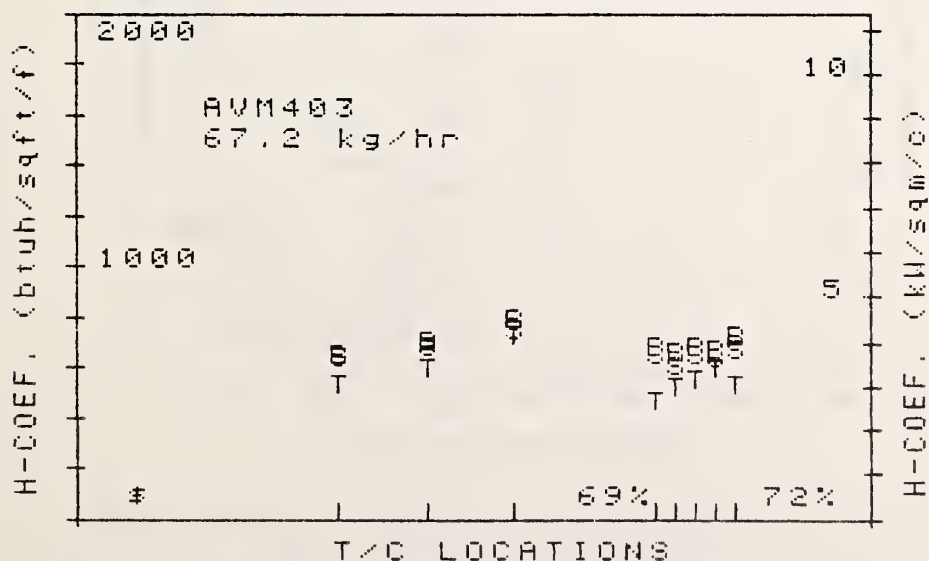


Figure 3-14: Typical Output from Test Run Data Reduction.
 T: Top; B: Bottom; S: Side average

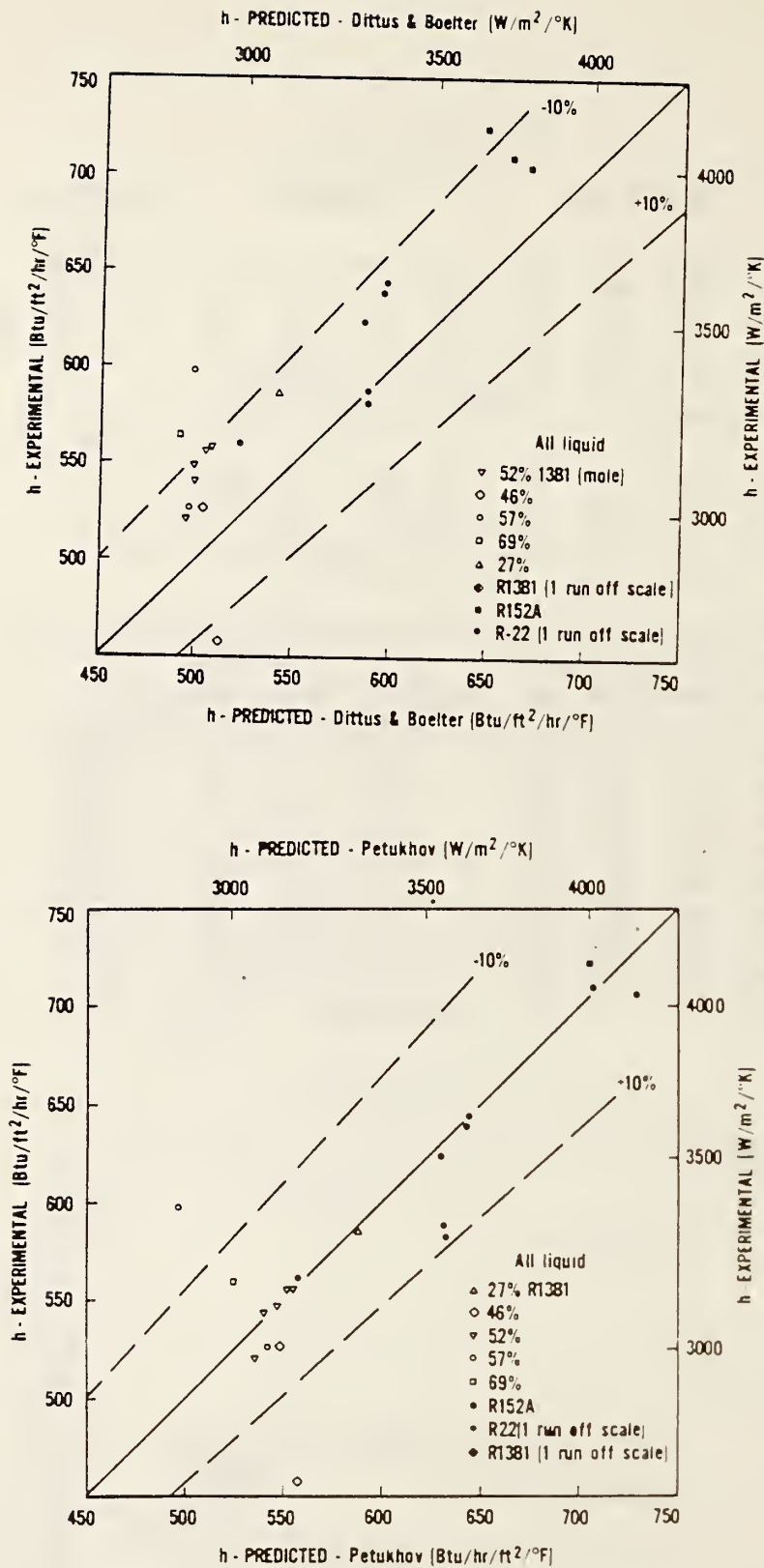


Figure 3-15: Comparison of Predicted to Measured Data for Single Phase Heating Tests

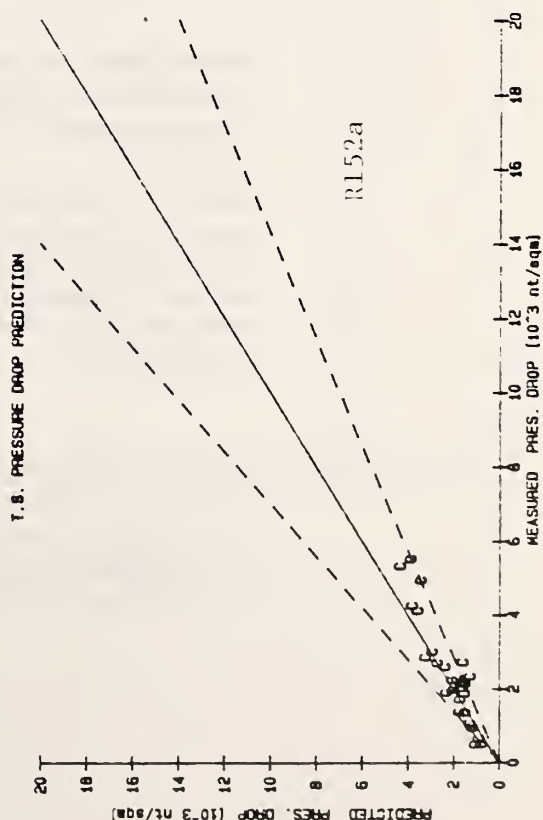
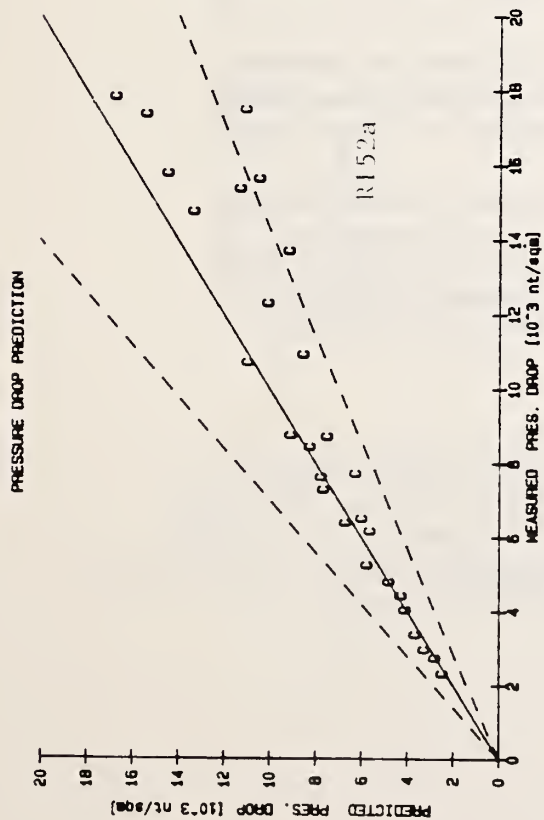
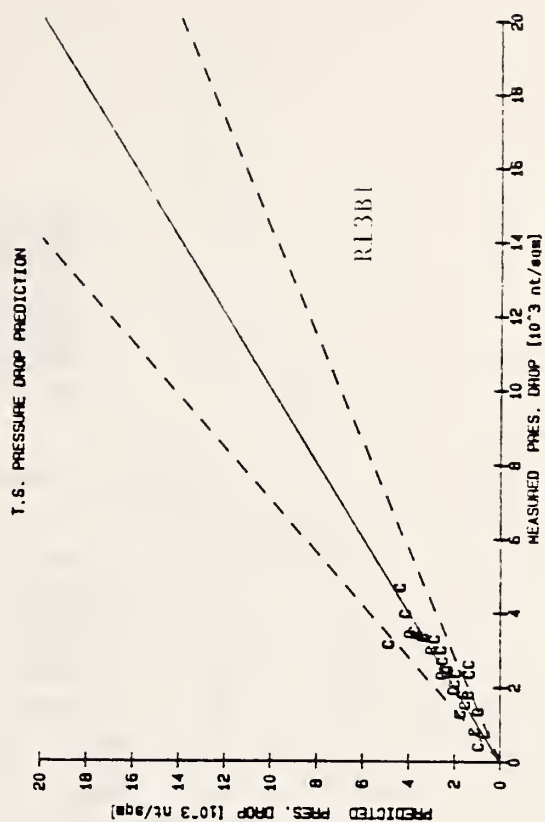
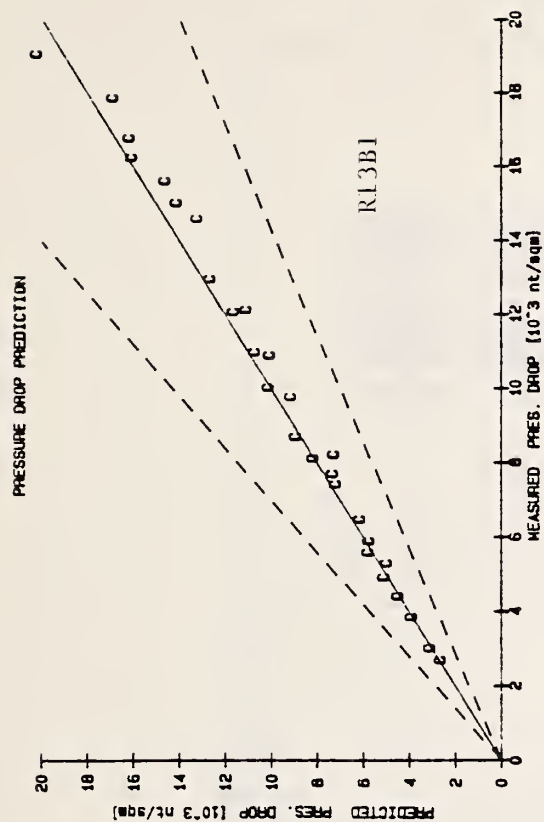
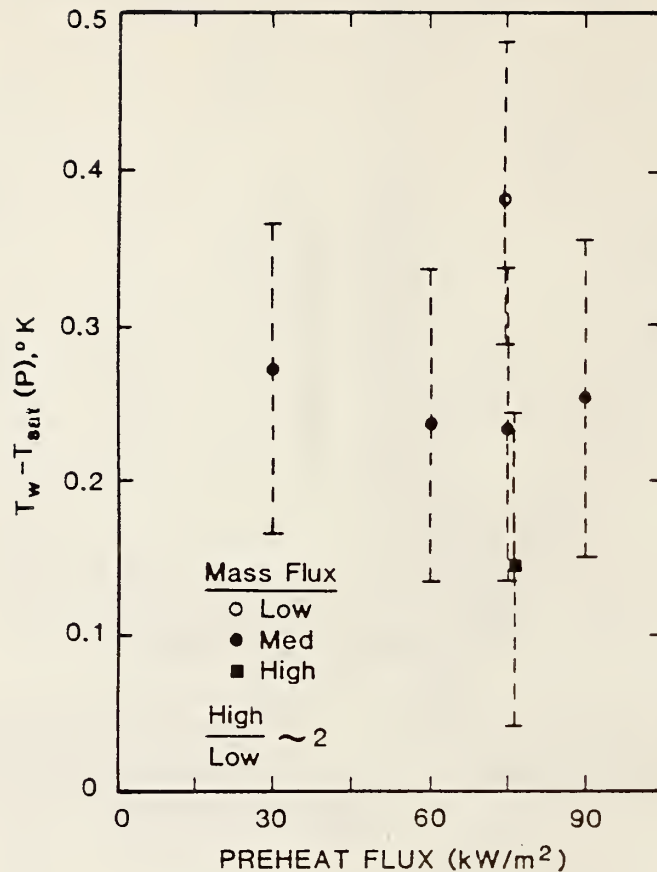


Figure 3-16: Pressure Drop: Predicted versus Measured



- Values shown are for T/C station 50 diameters downstream of preheat. No heat in test station. Top and bottom T/C agreed with each other within 0.1°C.
- Data at 15 kW/m² (preheat) showed distinct top/bottom difference even 50 diameters downstream. This is due to thicker liquid film at bottom. (Continued evaporation occurs due to pressure drop.) Thus flow patterns persist downstream.

Figure 3-17: Effect of Preheat Flux on Test Section Wall Temperature Measurements. The large error bars are due to the use of the DAS internal temperature compensator, rather than the normal ice point reference.

EFFECT OF PREHEAT FLUX: MIXTURES

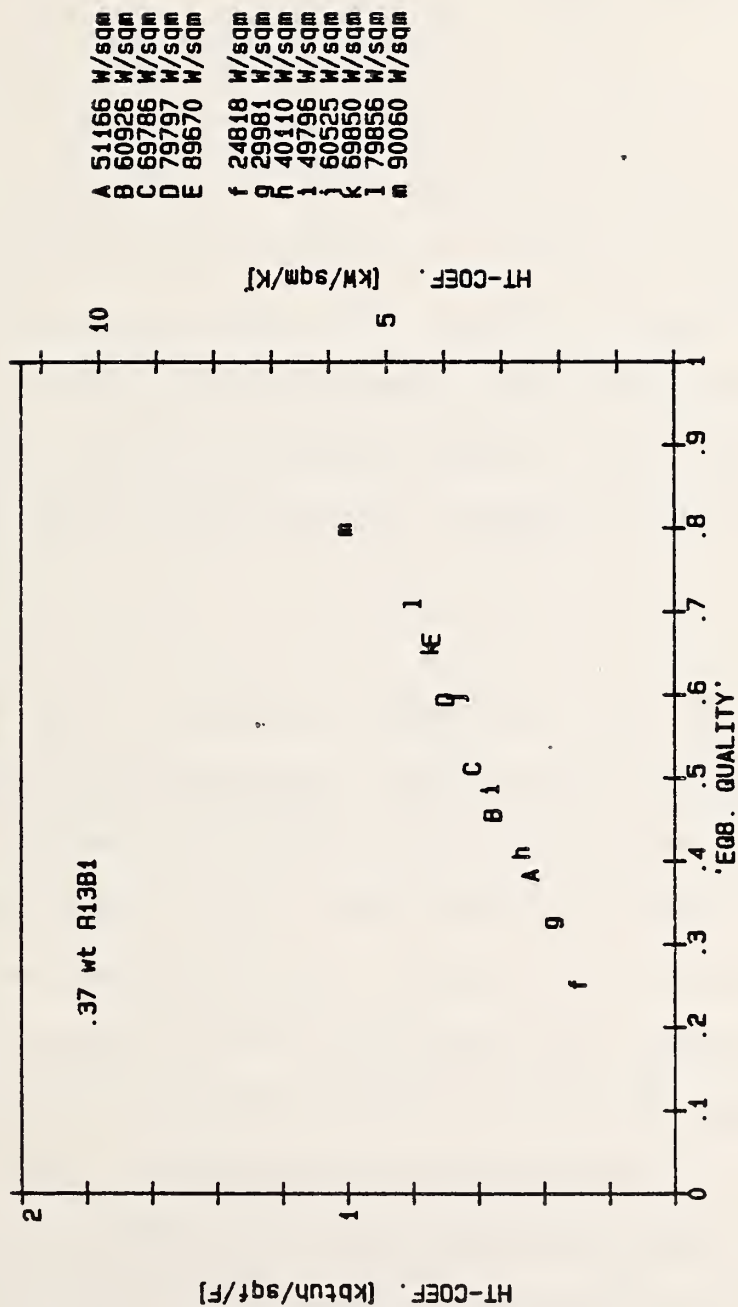


Figure 3-18: Effect of Preheat Flux on Heat Transfer Coefficients for Mixtures. No effect was seen.

CHAPTER 4: ON THE SUPPRESSION OF NUCLEATE BOILING

4.1 Background

The most common explanation of the physical mechanism of heat transfer in annular flow boiling is that of a superposition of a forced convection evaporative process and a nucleate boiling process. With increasing vapor quality the liquid film thins and the core vapor accelerates (as required by continuity). Heat transfer to the core is improved by this acceleration and the thinning of the liquid film also serves to lessen its conductive resistance. Heat transfer is thought to improve sufficiently and to occur with such rapidity that bubble growth disappears. At this point, the nucleate boiling process is said to be suppressed, and vapor generation is due strictly to evaporation from the vapor-liquid interface.

It is critical to know if nucleate boiling is suppressed. First, if the process becomes purely convective/evaporative, then the heat transfer coefficient should be independent of wall heat flux, and depend on flow and fluid parameters (e.g., mass flow rate, eddy diffusivity, Prandtl number), as in single phase shear-driven flow. In this case, the heat transfer process might be modelled strictly from single phase considerations. Also, correlations for annular film condensation might be applicable to the evaporative case, in the absence of nucleate boiling. If, on the other hand, nucleate boiling exists, from a sufficient number of sites then the liquid film viscous sublayer may be destroyed, and the fluid flow and heat transfer processes become more difficult to predict.

In the case of mixtures, chaotic concentration profiles may occur when nucleate boiling is not suppressed.

For heat transfer purposes, it is the boiling site density which is particularly important. The existence of an isolated, metastable bubble is not significant. Throughout this chapter, the former is of interest. However, as a starting point, the prediction of the existence of any individual bubbles is required.

4.1.1 Conventional Theory of Onset and Suppression of Nucleate Boiling

The onset and suppression of nucleate boiling are effectively the same problem, differing only in the direction from which the heat flux required to sustain nucleation/bubble growth is approached. Classical theory for the growth of a bubble begins with a force balance.

The maintenance of a spherical bubble requires, from a force balance, the liquid immediately surrounding the bubble to be superheated by an amount:

$$T_L - T_V = \frac{2\sigma}{r_c \frac{\partial P_{sat}}{\partial T}} \quad (4-1)$$

where r_c is the radius of the bubble. Upon applying the Clausius-Clapeyron relation and assuming the inside bubble temperature to be saturated, equation (4-1) becomes:

$$T_L - T_{sat} = \frac{2\sigma}{r_c} \frac{\Delta h_v}{T\Delta v_v} \quad (4-2)$$

The same criterion can be applied to a heated surface with a vapor bubble, assumed to be hemispherical, developing from a surface cavity of mouth radius, r_c . In the case of a heated surface, however, the liquid temperature surrounding the bubble will not be uniform generally, but instead diminish with distance from the heated surface. Also, the bubble shape will be approximately that of a truncated sphere with radius of curvature r_c , rather than completely spherical. Both of these effects were accounted by Hsu [Hs62], followed by others. First from pure geometrical considerations, the height, y_B , and radius of curvature, r_B , of a spherical truncated bubble are related to the mouth radius by:

$$y_B = (1 + \cos\theta)r_c = c_1 r_c \text{ and } r_B = \frac{1}{\sin\theta} r_c = c_2 r_c$$

so that equation (4-2) becomes:

$$T_L - T_{sat} = \frac{2\sigma}{(c_2/c_1)y_B} \frac{\Delta h_v}{T\Delta v_v} \quad (4-3)$$

Secondly, Hsu assumed bubble growth to be possible only if the liquid temperature at the bubble cap was superheated to satisfy (4-2). For a linear temperature field as might be reasonably approximated across a thin thermal boundary layer, the wall heat flux and temperature field are represented by:

$$q_w = \frac{\lambda_L}{\delta} (T_w - T_{sat}) \quad (4-4)$$

and

$$T(y) = T_w - \frac{T_w - T_{sat}}{\delta} y = T_w - \frac{q_w}{\lambda_L} y \quad 0 \leq y \leq \delta \quad (4-5)$$

where y is the distance from the wall and δ is the boundary layer thickness, the temperature at the edge of which the condition is assumed saturated.

Equations (4-3) and (4-5) may be plotted for a given heat flux and film thickness, as shown on Figure 4-1, and most importantly the range of cavity sizes which may be active (i.e., those from which ebullition is possible) can be determined. At cavities outside the range shown on Figure 4-1, the liquid is not sufficiently superheated for bubble growth to occur. A large superheat is necessary to activate the more numerous small cavities. The superheat may derive from either a large wall heat flux or a low liquid thermal conductivity (see equation 4-5). For large cavities the superheat requirement is small, but this superheat must be maintained far from the heated surface for the bubble to grow to its critical radius (hemispherical shape).

In the case of annular flow boiling, measured wall superheats have been sufficient seemingly to initiate bubble growth even when none has been observed [La62]. Collier and Pulling proposed to explain the apparent

contradiction by noting the sublayer thickness in turbulent films is smaller than for stagnant pools [Co64]. They assumed that owing to turbulence, the liquid outside the viscous sublayer was at or close to saturation. The temperature drop occurs then across only the small viscous sublayer, or:

$$q_w = \frac{K}{\delta_{vs}} (T_w - T_{sat}) \quad (4-6)$$

$$T(y) = T_w - \frac{q_w}{\lambda_L} y \quad 0 \leq y \leq \delta_{vs} \quad (4-7)$$

where δ_{vs} is the thickness of the viscous sublayer.

Collier and Pulling recommended using a dimensionless viscous sublayer thickness of $y^+ = 7$. In the single phase turbulent flow literature, the viscous sublayer thickness has been presented in values from $y^+ = 5$ to $y^+ = 10$. In fact turbulent eddies carrying cool fluid from the vapor-liquid interface may penetrate the sublayer down to $y^+ = 1$ [La62]. More relevantly, Bejan has studied analytically buckling and rolling of liquid layers in shear-driven flow (as occurs in annular flow boiling). He determined the value of $y^+ = 7.62$ as the viscous sublayer thickness which persists regardless of possible buckling or rolling [Be82].

Several years later, Collier suggested a modification to the viscous sublayer approach, relating the point of suppression to the Martinelli parameter, X_{tt} [Co80]. This parameter can be related however to the

viscous sublayer thickness, as both are subject to flow conditions. The viscous sublayer is a function of wall shear stress, which itself is a function of frictional pressure drop. Finally, Martinelli et al predicted frictional pressure drop for two phase flows through the parameter X_{tt} .¹

4.1.2 New Alternate Theory: Enhancement of Nucleate Boiling

Recently, the conventional explanation has been questioned initially by Mesler [Me76, Me77] and subsequently by Beattie et al [Be79, Be84].

Mesler has suggested that the heat transfer process, rather than becoming convective/evaporative at high quality, is due even in thin turbulent films to nucleate boiling. He has suggested that the high heat transfer rates experimentally measured with thin films (high compared to pools or thick films) is due to an enhancement of nucleate boiling with thin films. The high heat transfer rates seen with thin films are hypothesized to be due to evaporation of the thin liquid microlayer and rapid replenishment of the microlayer. The replenishment process with thin films is improved over usual pool boiling. With thin films, the bubble ruptures the film surface and vapor escapes through the top of the broken bubble, causing the liquid film to be reestablished quickly. An improved replenishment process which is related to film thickness might account for the observed improvement in heat transfer with increasing quality.

¹ Collier's recent suppression criterion is reviewed in Appendix 4-A, as are other proposed criterion.

4.1.3 Suppression of Boiling with Organic Fluids

A second issue was raised by Toral [To79], who suggested that complete suppression of nucleate boiling will not occur under common conditions in annular flow boiling of organic fluids. These fluids of which refrigerants are included, have a thermal conductivity much lower than water, and as such will tend to yield high wall superheats, sufficient for nucleation.

4.1.4 Problem Resolution Methods

The issues then are:

- (1) can the physical process by which vapor is generated be entirely evaporative, or is it best described by nucleate boiling theory?
- (2) is it possible for organic fluids, specifically refrigerants, with their relatively low thermal conductivity, to be vaporized by an entirely evaporative mechanism in annular flow?
- (3) can conventional suppression theory or various other suppression criteria be verified (and modified for mixtures) to quantify the point at which nucleate boiling is absent?
- (4) are there unique mechanisms which occur with nonazeotropic mixtures?

The following techniques might be employed to resolve the problem:

- A. Visual Evidence (e.g., vapor generation without bubble presence or bubble presence with thin films).
- B. Experimental Evidence
 - 1. Dependence of the heat transfer coefficient on heat fluxes and mass flux.
 - 2. Effect of pressure on heat transfer coefficient.
 - 3. Presence of hysteresis.
 - 4. Dependence of heat transfer coefficient on quality.
 - 5. Predictive ability of evaporative or pool boiling models to flow boiling data.

The following discussion critically analyzes the literature for pure and mixed fluids. Detailed reviews are available in Appendix 4C through 4F. New experimental evidence for single and binary refrigerants is presented. The new criterion for determining the suppression point for mixtures is hypothesized. The discussion will attempt to concentrate on refrigerants, but will cite several studies from other literature in response to the cautionary note and advice of Butterworth and Shock [Bu82]. It also serves as an interaction to the data base developed for this report, and as such several graphs are presented to display the data.

4.2 Summary of Visual Evidence

Several visualization studies of flow boiling of pure fluids have been done to determine flow pattern and bubble existence; the major studies

are discussed in detail in Appendix 4C. Most of the studies have been with water, but some with refrigerants. The studies employed transparent metal coating, heater strips on one side, or glass tubes. Often the surfaces had been milled smooth to ensure uniform heat generation, however, this process removes potential nucleation sites, preventing generalization of results. In one case an artificial nucleation site was added to the surface in order to witness boiling in a thin film flow. This study done by Mesler led him to formulate his alternate theory.

Nearly all visualization studies show some isolated bubbles within the liquid film, the number of sited bubbles diminishes with increasing quality. The authors attribute the continued vapor generation to evaporation from the vapor-liquid interface. It is possible however that ebullition continued in small cavities or that bubbles were so short lived as to escape notice even with high speed films or still photographs, thus visual evidence is not itself definitive.

The study by Hewitt et al [He84] showed activation of a site whenever heat transfer through the film was inhibited by wave passage, suggesting film thickness was an important though not solely definitive criterion. The Hewitt et al study also observed that vapor velocity had a strong influence on the observation of nucleation. The study of boiling from an artificial site did not have a higher vapor velocity and does not correspond directly to the physical case of turbulent flow boiling in tubes.

Many visualization studies used tubes which had been milled smooth or which were of materials without large cavity sizes; this could inhibit bubble growth. However, they suggest that vapor generation can take place in the absence of such cavity size availability, suggesting that a mechanism other than nucleate boiling is the cause of such vapor generation.

4.3 Summary and Analysis of Experimental Evidence: Dependence on Heat and Mass Flux

Appendix 4D describes in detail the studies which examined the dependence of the heat transfer coefficient on heat and mass flux. When no dependence on heat flux is observed ($\alpha \neq \alpha(q)$), nucleate boiling is considered suppressed, and $\alpha = \alpha(G)$. On the other hand, when nucleate boiling dominates, the heat transfer coefficient is a strong function of heat flux and a weak function of mass flux. Thus, the dependence of α on G or Q may define the dominant heat transfer mechanism, and if the heat transfer coefficient is independent of heat flux ($\alpha \neq \alpha(q)$), then the sole mechanism is usually considered evaporative.

A recent study by Aounallah et al [Ao82] showed clearly $\alpha \neq \alpha(q)$ for a range of qualities, heat and mass flux values. Care was taken in their experiment to ensure that measurements at the same spatial location were compared. In direct response, Beattie and Green [Be84] cited work by Bertoletti et al [Be64] with a similar experimental apparatus and also using water as the working fluid; the Bertoletti data showed a strong dependence on heat flux and was correlated well by a pool boiling correlation.

The results of Aounallah et al appear to contradict those cited by Beattie and Green (the Bertoletti et al experiments). However, the apparent discrepancy may be resolved by examining the test conditions used by the two groups. The latter, where nucleate boiling was observed to be dominant, involved higher pressures and heat fluxes where conventional theory suggests a small superheat requirement. The conventional theory therefore allows both experimental observations to be valid. The much higher heat fluxes employed by Bertoletti et al most likely produced a vapor generation process dominated by nucleate boiling.

In a separate publication, Beattie and Lawther [Be79] describe their own successful work in predicting pressure drop at high quality by theorizing the existence of attached bubbles within a liquid film. They point to their success as a proof of bubble existence.

The heat flux level of the Beattie and Lawther experiment was also very high, since their observations were made in a critical heat flux experiment. Here again, the existence of attached surface bubbles are entirely possible, and explained by the conventional theory.

Mesler has examined many studies of nucleate boiling in thin films, noting high heat transfer rates and a dependence on heat flux. However, the boiling studies cited by Mesler involved slow moving films. For example, the referenced Toda and Uchida study [To73] involved laminar or near laminar flows. The study by Fletcher et al (referenced by [Me77]) was designed specifically to avoid high vapor velocities, which Hewitt et al [He63] observed to be important in the suppression process. Thus the

referenced studies are not strictly comparable to the case of the turbulent flows associated with annular flow boiling.

4.4 Summary of Experimental Evidence: Dependence of Heat Transfer Coefficient on Quality

The inverse Martinelli parameter ($1/X_{tt}$) is sometimes referred to as a surrogate for quality. Because of its successful employment in pressure drop prediction, several authors have used it in heat transfer coefficient prediction. The idea was first advanced by Dengler and Addoms (Appendix 4D) based on their experimental observations [De56]. Mesler has reviewed the [De56] data, and upon careful examination, showed that the data is not closely correlated by the use of $1/X_{tt}$. He further attempts to show on theoretical grounds that the general approach of using $\alpha = \alpha_{LO} f(1/X_{tt})$ is inappropriate. However, these objections to the use of X_{tt} as a correlating parameter do not seem warranted. As shown in Appendix 4B, the Mesler analysis of $\alpha/\alpha_L = f(1/X_{tt})$ inadvertently neglects the fact that some parameters he considered constant do indeed vary.

The enhanced nucleate boiling theory cannot explain a phenomena observed in several experiments, that of a gradual reduction in heat transfer coefficient despite increasing quality. At times the measured reduction disappears as quality is further increased. Such behavior, originally attributed to an entrance length effect [Go66] has been seen at L/D ratios greater than 100, with pure refrigerants, water and with refrigerant mixtures [Ch67, Ma76, Ra83]. The experiments show in the nucleate

boiling dominated region, α decreases with increasing quality. Such observations are in sharp contradiction to the hypothesis of Mesler, which requires α to increase with reduced film thickness, i.e., an increased quality.

4.5 Summary of Experimental Evidence: Effect of Pressure

Pool boiling experimental heat transfer coefficients increase with increasing pressure. This often seen observation is accounted in equation (4-1) since $\partial P_{\text{sat}}/\partial T$ increases generally with pressure. Additionally, surface tension, at least for refrigerants, decreases with increasing temperature (related directly to saturation pressure). Both of these phenomena tend to reduce the superheat requirement so that more sites are activated for a given superheat as pressure is increased.

Conversely, in the case of forced convection/evaporation, the heat transfer coefficient may decrease with increasing pressure [De56]. The vapor density increases with pressure, so that at a given core vapor mass flux, the vapor velocity decreases. The reduced vapor velocity diminishes the level of shear at the liquid-vapor interface, inhibiting heat transfer through the liquid film. The correlating parameter, $1/X_{\text{tt}}$, decreases with increasing pressure so that again, the predicted α would decrease.

The opposite behavior associated with boiling vs. convection/evaporation might serve then as a line of demarcation between the two mechanisms.

The data of Toral with organic mixtures showed a proportional dependence

between α and pressure, even at 'high quality' ($x = .3$). This suggested the dominance of nucleate boiling in his experiments.

4.6 Summary of Experimental Evidence: Presence of Hysteresis

Hysteresis has been found sometimes in the pool boiling of pure fluids. Different superheat requirements were needed to initiate boiling when an experiment was conducted first with increasing and then with decreasing heat fluxes. Murphy and Bergles [Mu72] suggested that in subcooled flow boiling, high heat fluxes activated small cavities and bubbles from these cavities then migrated and activated large cavities. These large cavities remained active while the heat flux is reduced. On the upward heat flux traverse, the large cavities were considered fully wetted. It was noted that in subcooled flow boiling, a reduced hysteresis effect should be expected due to the steeper temperature profile; large cavities with trapped vapor may remain inactive due to the profile.

The presence of hysteresis then might confirm the presence of nucleate boiling. No parallel process occurs with convective evaporative flows.

4.7 Summary of Literature Review: Mixtures

The introduction of a second component has several consequences in the analysis of the onset and suppression of nucleate boiling, as described in detail in Appendix 4E.

First, the terms of the applicable equation (4-1) are changed in value. Surface tension may be drastically affected by even small additions of a

second component (e.g., figure 1-4 with refrigerant and oil). The theoretical value of dP_{sat}/dT is less for mixtures than for an equivalent pure fluid, suggesting an increased superheat requirement, however, the actual superheat requirement may be less than for either pure component, due to the change in surface tension.

Toral [To79] has attempted a theoretical study of the effect of turbulence damping near the liquid/vapor interface in thin film, shear-driven flow. He concludes that with organic fluids and organic fluid mixtures sufficient superheat will be available to initiate nucleation under common conditions of heat and mass flux. If turbulence damping exists, nucleation will be even more likely, as an additional resistance exists to transferring the heat away from the wall region. However, the boundary conditions used by Toral are flawed (see Appendix 4E). This conclusion may then be questioned, though not necessarily rejected with his problem being correctly reposed.

Thome and Shock recently reviewed the effect of composition on the ONB point and boiling site density [Th82]. While fewer sites are active with mixtures, the difference is not systematically related to $|\bar{Y} - \bar{X}|$, though mass diffusion is a likely contributor to change in boiling site density. In some onset of nucleate boiling studies, mass diffusion was seen as an important factor and in others, the ONB point was unaffected by composition.

To date, no one has analyzed, either theoretically or experimentally, the nature of the concentration profile in flow boiling with the presence of nucleate boiling, and the consequent mass transfer resistances in the liquid and vapor streams. With ebullition in flow boiling, the liquid surrounding the bubbles in the wall region will be depleted of the more volatile component. This will tend to increase the superheat requirement, i.e., make it easier to suppress bubble growth. However, at the same time, any resistance near the film interface (turbulence damping, both mass and thermal diffusion) will inhibit surface evaporation, so that more superheat might be available near the wall. A further complication is that the conductivity of the two fluids might be disparate, so that upon depletion of the more volatile component around a bubble, heat might be conducted more readily or with more difficulty through the viscous sublayer. The ultimate effect of these multiple competing processes has not been studied analytically for flow boiling.

4.8 Comparison of Experimental Results to Theory

4.8.1 Application of Conventional Theory to Pure Refrigerants and Refrigerant Mixtures

The Hsu/Collier and Pulling suppression criterion was applied to the two pure refrigerants used in this report. The pressure gradient, needed to determine the wall shear stress and subsequently the thickness of the viscous sublayer, was estimated using the Martinelli-Nelson/Chisholm correlation. Contact angle was assumed to be 35° , typical for refrigerants [St82]. A flow chart of the calculation is given in Figure 4-2.

Measured mass fluxes and pressures were used. Properties were estimated using the equations of Chapter 2. Assuming all cavities to be available, the criterion suggests a very small superheat requirement. Instead, a heat flux needed to activate a critical cavity size of 1.0 μm was calculated. Both Polley [Po82] and Stephan [St80] have offered this size as a rough guideline for refrigerants. Cavities of size greater than 1.0 μm were assumed to exist either in an insufficient number to affect the heat transfer, or to be fully wetted by refrigerant. This assumption then modifies the basic suppression criterion, so that a greater wall superheat is needed to initiate boiling than if all sizes were available in large numbers and were unwetted.

Three factors complicate the analysis, leading to substantial uncertainty. First, the estimate of the critical viscous sublayer thickness is not exact. It depends both on the determination of pressure drop and on a selected critical value (Collier and Pulling's $y^+ = 7$). Secondly, the selection of a critical cavity size may be in error. Collier has suggested 0.5 μm as a rough guideline for refrigerants [Co80]. This leads to a larger estimate of the suppression heat flux. Thirdly, vaporization may take place nearer the bubble base even in the absence of vaporization at the bubble cap. The required heat flux in this case would be less than as calculated. These complications lead to an estimated uncertainty of about $\pm 40\%$. Despite the large uncertainty, it will be shown that the criterion can be used with success.

Figure 4-3 displays sample results of the procedure, showing the effects of changes in pressure and mass flux. As pressure is lowered or as mass flux is raised, the criterion predicts a greater suppression heat flux. If the experimental heat flux was below the calculated 'suppression heat flux' value, the heat transfer coefficient should be independent of heat flux and instead depend proportionately on mass flux and quality. Conversely, if the criterion predicts sufficient heat flux, a dependence on heat flux should be observed.

A similar analysis can be applied to mixtures and was applied here to the R13B1/R152a mixture. The governing equation is effectively the same for mixtures, except as noted in Section 4.7. Properties such as $\Delta \bar{h}_v$ and $\Delta \bar{v}_v$ were evaluated at different compositions, so

$$\Delta \bar{h}_v \cong \bar{h}_v(\bar{Y}^*) - \bar{h}_1(\bar{X}_B)$$

$$\text{and } \Delta \bar{v}_v \cong \bar{v}_v(\bar{Y}^*) - \bar{v}_1(\bar{X}_B)$$

The suppression criterion was then applied, assuming the liquid layer was well-mixed, i.e., without any mass transfer resistance. It was therefore implicitly assumed that the turbulence in the liquid film supplied a sufficient concentration of the more volatile component to the bubble interface. This is a very conservative assumption for predicting suppression, since boiling site density is likely to be reduced by the mixture. The above treatment then considers the mixtures as an equivalent pure fluid. Two possible approaches to correct for mixture effects on boiling site density were also hypothesized. An exact solution is available in the literature for the growth rate of an isolated

spherical bubble located in a quiescent, uniformly superheated liquid. When the basic equations are solved, a reduction in bubble growth rate for a mixture over that of an equivalent pure fluid can be calculated. Chapter 7 discusses this problem in more detail; the reduction due to mass transfer resistance, is given in equation (7-0). When this factor, C_{bub} , is applied to the suppression criterion, the required heat flux to sustain ebullition is raised, typically by about 25% with $a_T/a_D = 5$ or 40-80% with $a_T/a_D = 60$ as shown in Figure 4-4. The concentrations shown are 'feed concentrations', i.e., the initial concentration of a sub-cooled liquid being evaporated/boiled. At the larger value of a_T/a_D , the mixture effect may be sufficient to increase the suppression heat flux above other pure components. The assumption with this approach is that mass diffusion is the sole reason for reducing boiling site density.

An alternate correction factor can be calculated from the literature on pool boiling of mixtures. As described in Chapter 7, equation (7-0) underpredicts the measured reduction in heat transfer coefficient for the pool boiling of mixtures. A variety of empirically based correction factors are available for predicting the reduction (Table 7-1). None of the methods of Table 7-1 has been tested for flow boiling of mixtures. However, the method of Stephan and Korner [St69] has been used widely with some success in pool boiling. When it is used, the increase in the suppression heat flux, Q_{sup} , may be sufficiently substantial to raise the suppression heat flux for mixtures above that of either pure component (figure 4-5).

4.8.2 Experimental Results: Pure Refrigerants

The first experimental results to be examined are those for pure R152a at low pressure; the tests were conducted with Rig #1. If measured data taken at the same mass flux and pressure but different heat flux levels yield identical heat transfer coefficients, then boiling is completely suppressed. Unfortunately, pressure was not held strictly constant with Rig #1; however in some cases, the pressure variation was small enough to allow such comparisons. The suppression point can also be inferred approximately by the dependence of da/dx on quality. When da/dx becomes strongly positive, forced convection/evaporation is dominant. Complete or near complete suppression should occur in this range. Figures 4-6a,b,c plot the effect of heat flux at constant flow rate. A strong heat flux dependence is observed at low qualities, but this effect is reduced with increasing quality. Shown also is the prediction of the suppression criterion for the heat flux level required to initiate boiling as a function of quality and the given flow rate. When the criterion states that boiling should be suppressed, the measured data are shown in upper case; lower case letters indicate the criterion predicts sufficient heat flux to sustain boiling of a $1\text{ }\mu\text{m}$ cavity.

The criterion predicts quantitatively the quality at which complete suppression occurs. Apparent discrepancies are seen in only two cases (runs OLDH201 and OLDH203) where the error is within the range of uncertainty in the method.

Both the figures and the criterion show that as mass flux is increased, suppression occurs at lower quality. A strong dependence on mass flux is observed suggesting a convective/evaporative process to be dominant.

Figure 4-7 shows the effect of pressure on the heat transfer coefficient. The experimental value is greater at high pressure initially, but the difference is reduced or disappears at high quality. These results indicate nucleate boiling, easier to achieve at high pressure, to be dominant at low quality. The boiling process then diminishes in favor of forced convection evaporation at high quality. The transition point is a function of heat flux: the lower the heat flux, the lower the quality at which nucleate boiling diminishes. The initial decrease of the heat transfer coefficient despite increasing quality has been observed by several other researchers [Ch67, Ch66a]. Mesler's proposed explanation of the heat transfer process cannot predict this observation; it in fact suggests the opposite behavior.

These results are consistent with the traditional theory. They suggest that nucleate boiling can be suppressed even at significant heat flux levels with relatively low conductive fluids such as refrigerants; however suppression becomes much more difficult as pressure is increased.

Similar Rig #1 tests were done with pure R13B1 at the high pressure level since the condenser could not be made colder to reduce pressure. The results on Figure 4-9 show little quality dependence and suggests

nucleate boiling domination. These results are consistent with the criterion.

All pure refrigerant tests with Rig #2 were done at a pressure around 4.75 bar (+.2/- .02 preheat, +/- .05 test section). Measurements were made in the preheat section where heat flux levels were varied over a wider range (10-95 kW/sqm R152a; 10-55 kW/sqm R13B1). Representative preheat data is shown on Figures 4-9 and 4-10. Here a clear dependence on heat flux is observed, indicating a strong nucleate boiling contribution.¹ The suppression criterion predicts that at this pressure level the actual heat fluxes were sufficient to initiate nucleate boiling. There is a very slight dependence on mass flux.

The test section data is for low heat flux but high vapor quality. The data is shown on Figures 4-11 and 4-12. Tests were done with R152a and 10 and 20 kW/sqm in the test section at three different mass fluxes. Figure 4-11a shows that only a weak dependence on heat flux occurs. The dependence on mass flux is seen clearly in Figure 4-12. The dependence on quality increases with increasing mass flux as was observed with Rig #1 and by others in the literature [An66]. These results suggest the dominant vapor generation mechanism is by evaporation, but that complete suppression may not be achieved. The criterion predicts sufficient heat flux to prevent complete suppression.

¹The only substantial contradiction to this trend is with heat flux above 50,000 w/m², which yielded lower heat transfer coefficient than expected. The high heat flux initiated a departure from nucleate boiling (DNB), with film boiling being the probable heat transfer regime. DNB events were observed with pure R13B1 in other tests around the same heat flux.

The test section data for R13B1 shows a dependence on mass flux at high quality, but not at low quality. Nucleate boiling dominates in the low quality region but the process is controlled by convection/evaporation at high quality. This conclusion is made tentatively however. The outlet temperature and pressure measurements for R13B1 tended to disagree (Chapter 3). Shown here are the results based on pressure measurements. The temperature based results show less mass flux dependence. In either case the dependence on mass flux is less than $m^{0.8}$ which has been widely used in correlating α in pure evaporative flow. This suggests that some boiling is present, and is in agreement with the suppression criterion.

Finally, Rig #2 also allows a unique examination of the effect of a step change in heat flux, since preheat and test section heat fluxes were set independently. If the process were completely independent of heat flux, then one would expect the measured heat transfer coefficient in the test section to be greater than that measured in the preheat section, due to a continued increase in vapor quality. If on the other hand, heat flux was dominant, then a large change in heat transfer coefficient should accompany a large step change in heat flux.

One can compare the ratio of measured heat transfer coefficients between the last preheat measuring station and the test section with the ratio of preheat to test section heat fluxes. Figure 4-13a plots such a comparison. Note that as the preheat flux is raised relative to the test section, the heat transfer coefficient ratio increases also, but to a

lesser degree. These comparisons suggest that both mechanisms, boiling and evaporation, are contributing to the heat transfer (at this pressure level), though evaporation is dominant. It thus serves as a further verification of the suppression criterion.

4.8.3 Experimental Results: Mixtures

Four suppression methods were tried for mixtures. The first treats the mixture as an EPF. The next three account for mass transfer resistance in various ways. The 'exact' and SK methods were displayed on Figures 4-4 and 4-5, respectively. The last way is empirical, based on a pool boiling method of Thome. As will be shown in Chapter 7, this method predicts the measured heat transfer coefficient best for a large number of cases.

Figures 4-14 through 4-17 show the effect of heat and mass flux on the heat transfer coefficient at fixed flow rate and initial composition for Rig #1. A strong dependence on heat flux is clearly observed;¹ a weaker dependence on mass flux is also seen. The dependence on pressure appears greater than the dependence on mass flux; this is an indication that boiling is not only present, but dominant.

All criteria predict sufficient heat flux to sustain ebullition. The only exception is Thome's method which predicts suppression at the lower weight compositions of R13B1, and high quality and mass flux. The data

¹The effect of heat flux is slightly exaggerated due to varying pressure from test to test.

indicate the Thome prediction is in error in these cases. However, the error is within the range of uncertainty of the method.

The Rig #1 tests were conducted with various pressure levels. In Rig #2, pressure was maintained generally around 4.75 bar level. The preheat tests were conducted again with heat fluxes varied between 10 and 90 kW/sqm. As before, a dependence on heat flux was observed indicating nucleate boiling to be present (representative Figures 4-9 and 4-10). All suppression criteria predicted sufficient superheat availability. There is only a weak dependence on mass flux.

Some hysteresis tests were also performed with 0.80 wt R13B1. Measurements were taken with preheat fluxes raised (to a maximum of 40kW/sqm) and then lowered. No change in heat transfer coefficient was observed in the preheat section or the test section (at 10kW/sqm). Despite the lack of hysteresis, some effect of preheat flux can be observed.

The preheat results suggest therefore that boiling is not suppressed. For all concentrations, the suppression criteria are verified for the case of nucleate boiling existence.

Representative test section data (low heat flux, high quality) is shown on Figure 4-18. The EPF method predicts $Q_w > Q_{sup}$ (boiling possible) at all compositions and flow rates. The 'exact' method with a Lewis number equal to 5 predicts complete suppression only at the highest mass

flow rates and low compositions of R13B1. The exact method with Lewis equal to 60 and the empirical methods of Stephan and Korner and of Thome predict suppression at all compositions at high flow rates. The measured data show a clear and strong dependence on mass flux. This indicates that convection/evaporation is strong in this region, but does not necessarily imply that boiling is absent.

As was done for pure components, the new approach of the effect of a step change in heat flux was examined. At low heat flux, the data shows a positive dq/dx so that evaporation is much more effective, and could support the notion of complete suppression.

These results show that forced convection/evaporation effects dominate in the test section, but are inconclusive regarding complete suppression of nucleate boiling. If the fact that forced convection/evaporation is dominant is extrapolated to suggest complete suppression, then the EPF methods is incorrect. The exact (Lewis = 60) and the empirical methods would then be validated. Evidence based on heat transfer correlations suggest complete suppression does occur with mixtures at these conditions. This evidence is discussed in Chapters 5 and 7. Measurements at lower heat flux could clearly confirm this conjecture; however the accuracy of such measurements would have been poor.

4.9 Conclusions and Recommendations

1. Conventional suppression theory is supported by experimental tests as well as a critical review of the literature. Contradictory

findings in the literature can in fact be explained by conventional theory. The alternate hypothesis of enhanced nucleate boiling with annular flow boiling is not supported analytically or experimentally.

2. At pressure, flow and heat flux levels of most residential heat pump evaporators, complete suppression of nucleate boiling is not commonly observed with pure refrigerants. However, as pressure is lowered, nucleate boiling may be absent even with low conductive fluids such as refrigerants.
3. The conventional suppression criterion is verified quantitatively for pure refrigerants. For mixed refrigerants the criterion was modified to include mass transfer resistance effects. The result is to lower the heat flux at which complete suppression occurs. Methods were hypothesized from 'exact' and pool boiling theory. These methods were validated in a qualitative sense. It may be possible to have complete suppression for mixtures and not for either pure component.
4. The conclusions of Toral regarding suppression of flowing mixtures may or may not be valid. The problem should be reposed with the correct number of boundary conditions. Analytic development is also needed which accounts for a revised liquid concentration profile in the presence of nucleate boiling. Experimental data

should be taken at sufficiently low pressure that one might expect complete suppression.

5. Incipient and suppressed boiling experiments need to be conducted for mixed fluids in flow boiling. The literature is particularly sparse in this critical area.

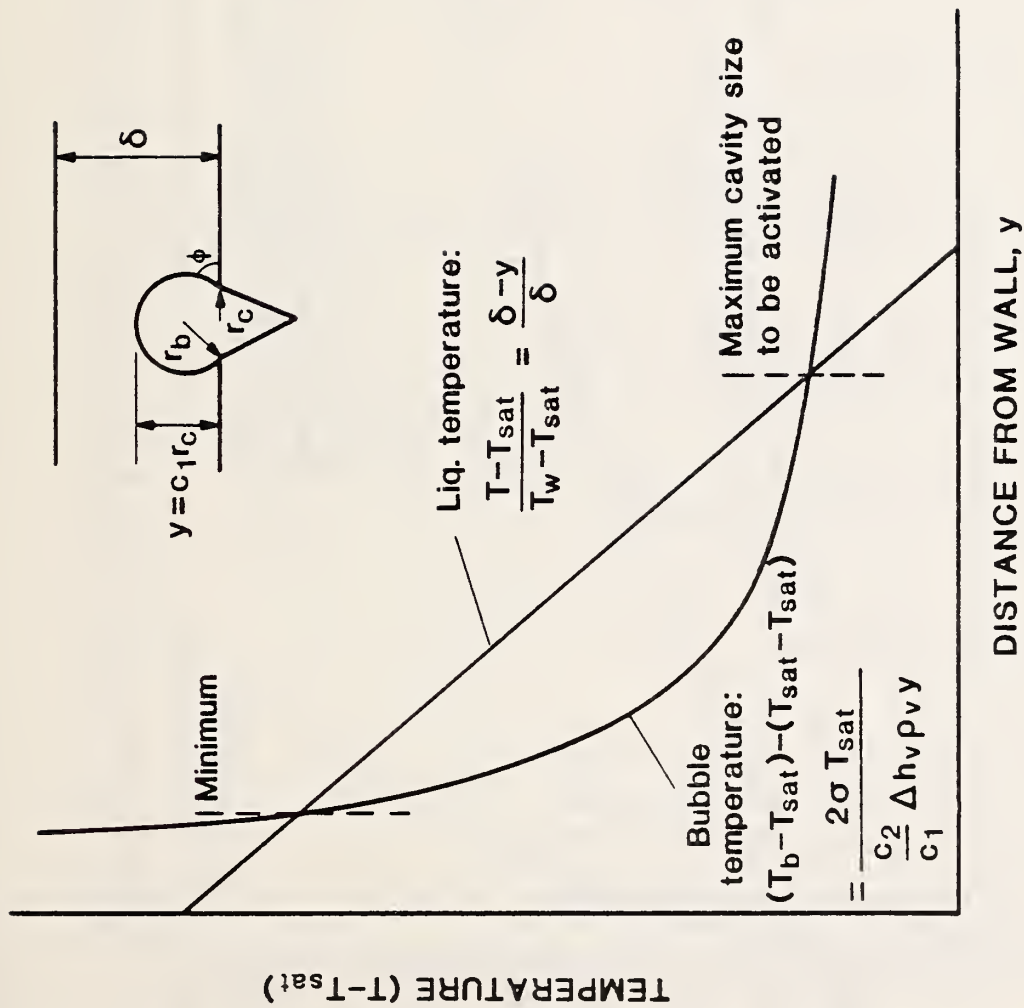


Figure 4-1: Criterion for the Onset of Nucleate Boiling (reprinted from Hs76)

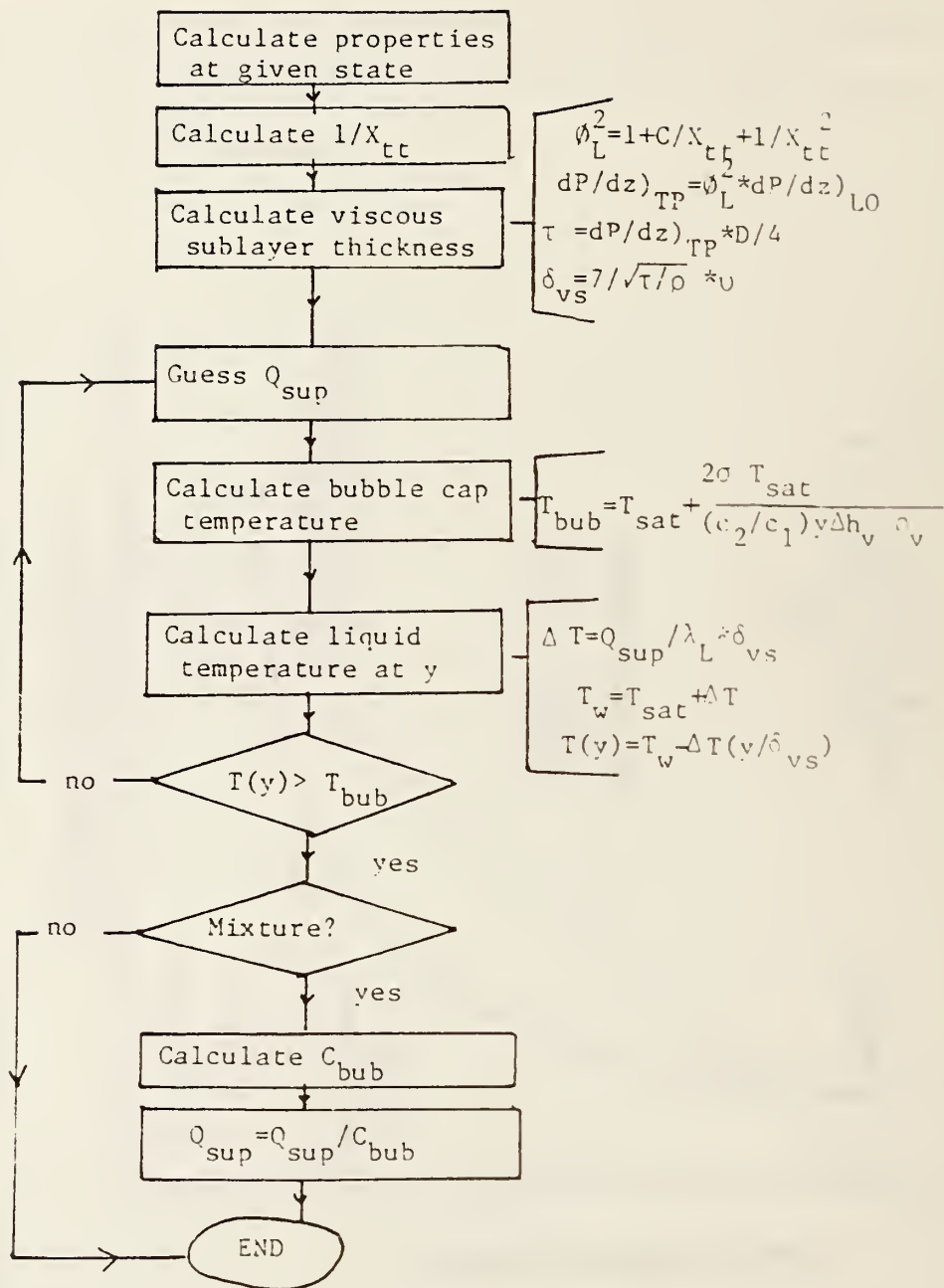


Figure 4-2: Flow Chart for Determining Suppression Heat Flux

CALCULATED SUPPRESSION HEAT FLUX

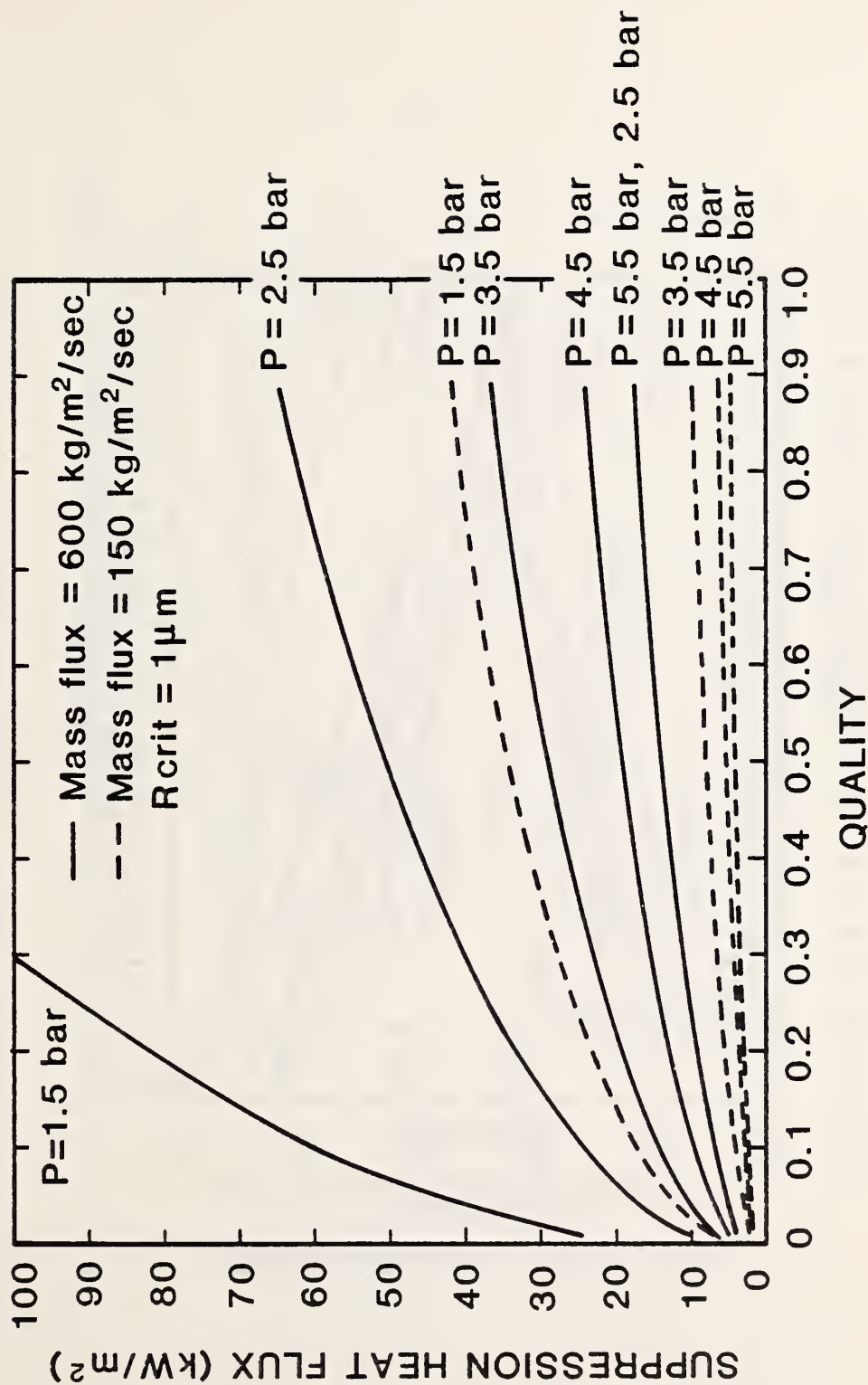


Figure 4-3: Effect of Pressure and Mass Flux on Suppression Heat Flux (R152a)

CALCULATED SUPPRESSION HEAT FLUX

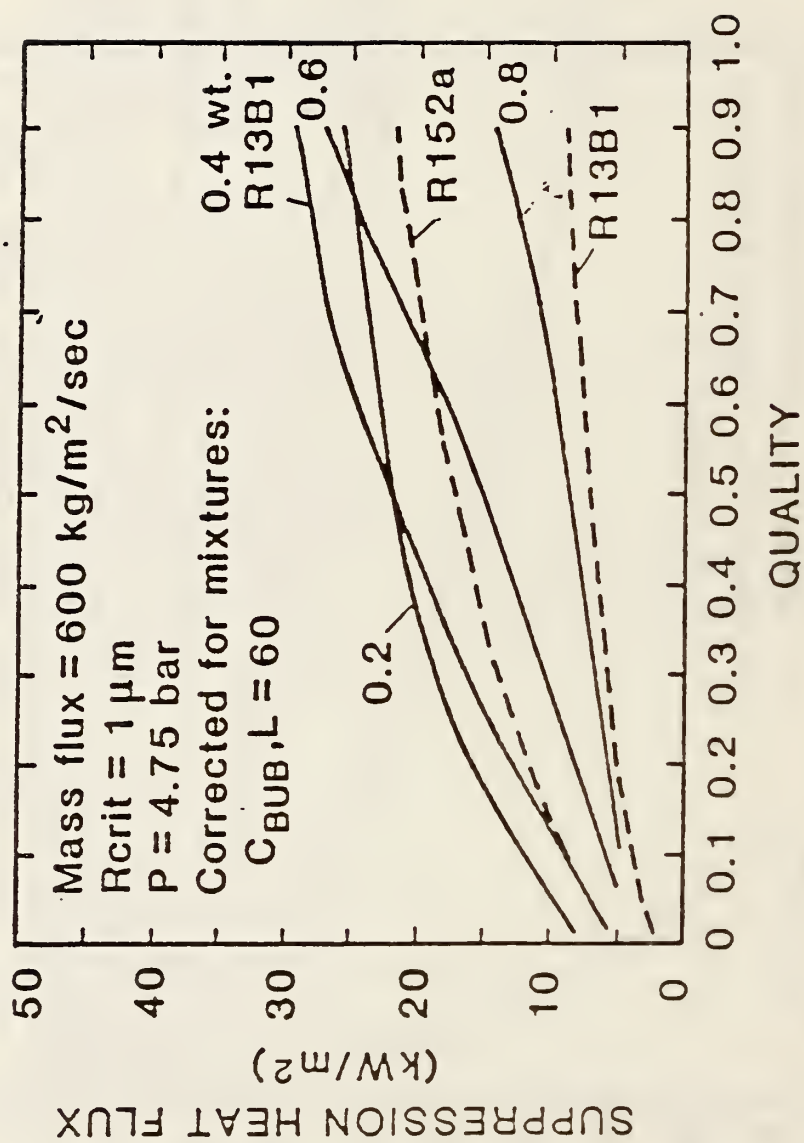


Figure 4-4: Calculated Suppression Heat Flux for Mixtures--Isolated Bubble Theory

CALCULATED SUPPRESSION HEAT FLUX

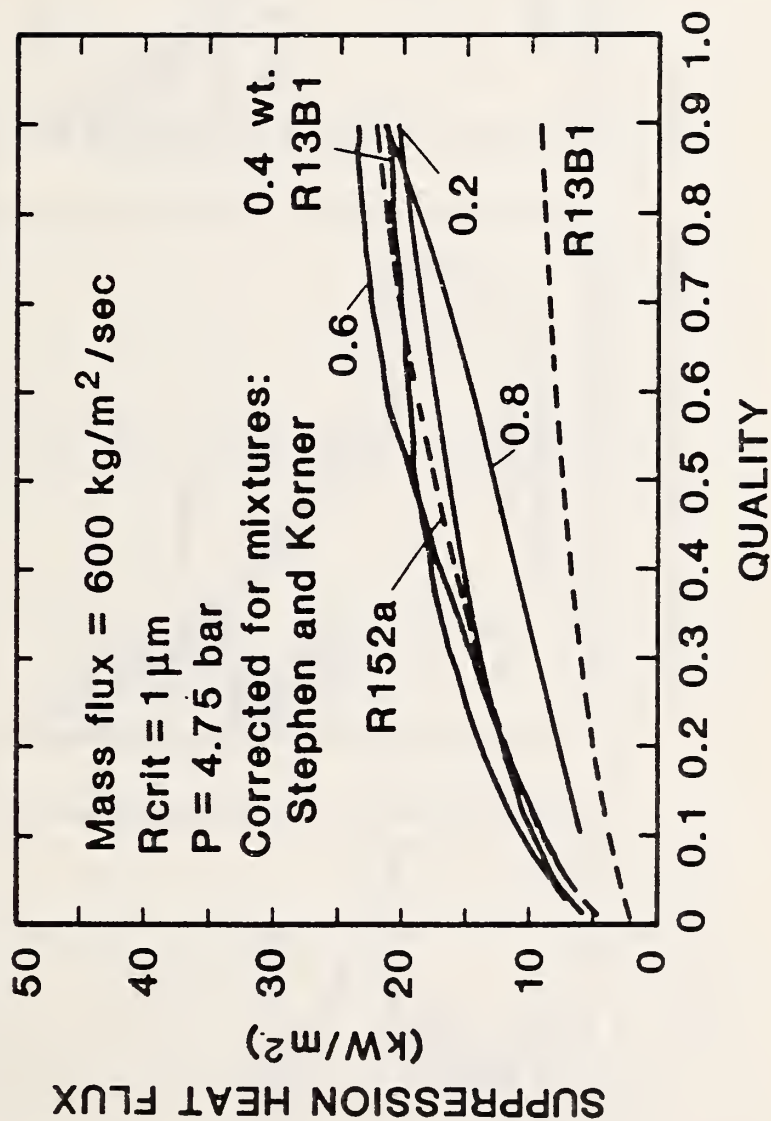


Figure 4-5: Calculated Suppression Heat Flux for Mixtures--Pool Boiling Theory

EFFECT OF HEAT FLUX

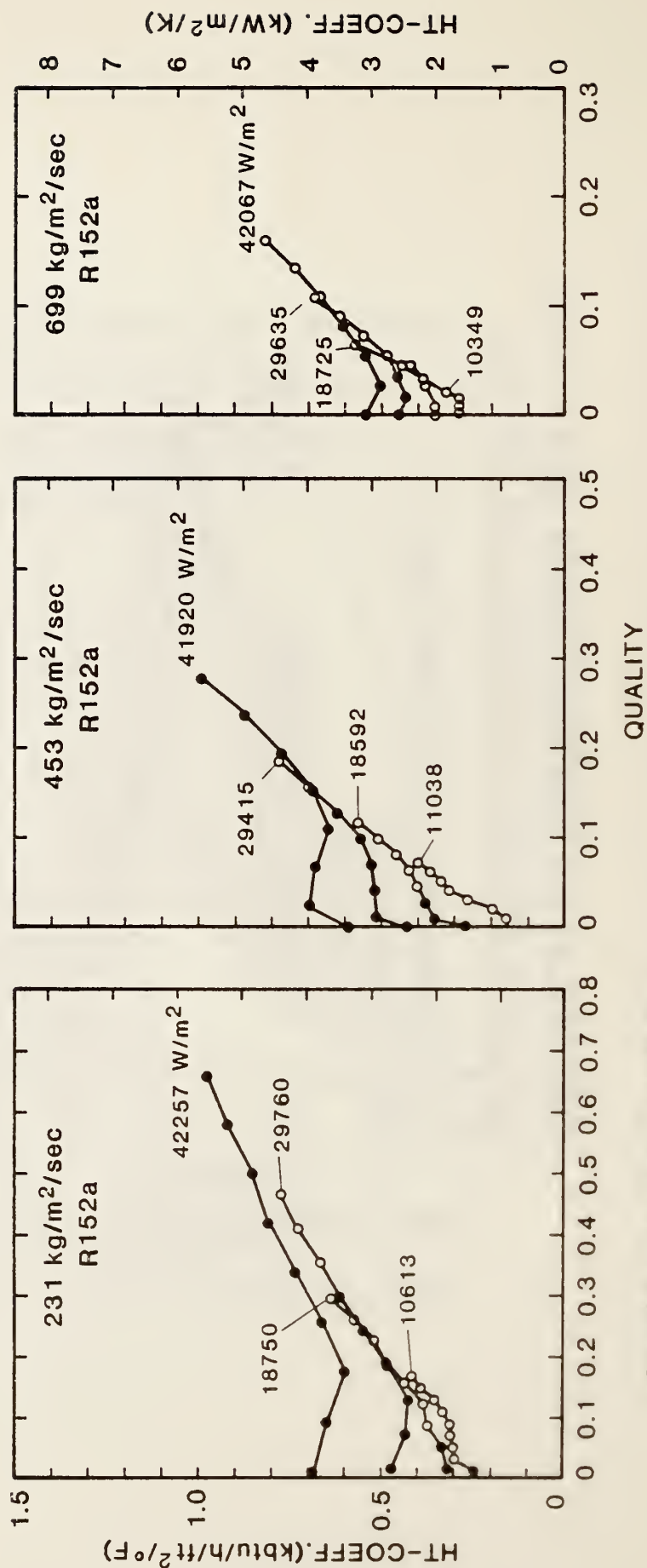


Figure 4-6: Effect of Heat Flux on Pure R152a at Low Pressure

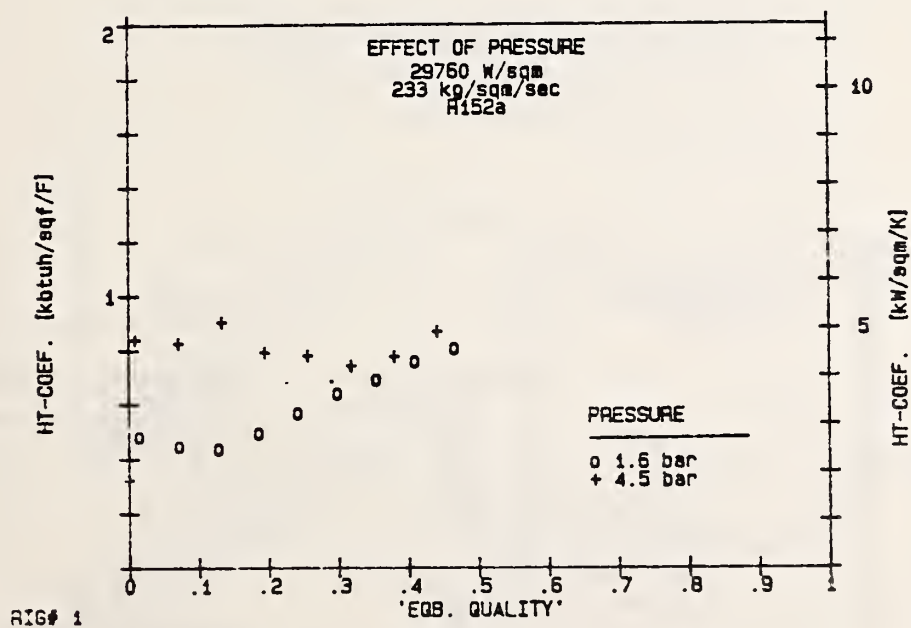
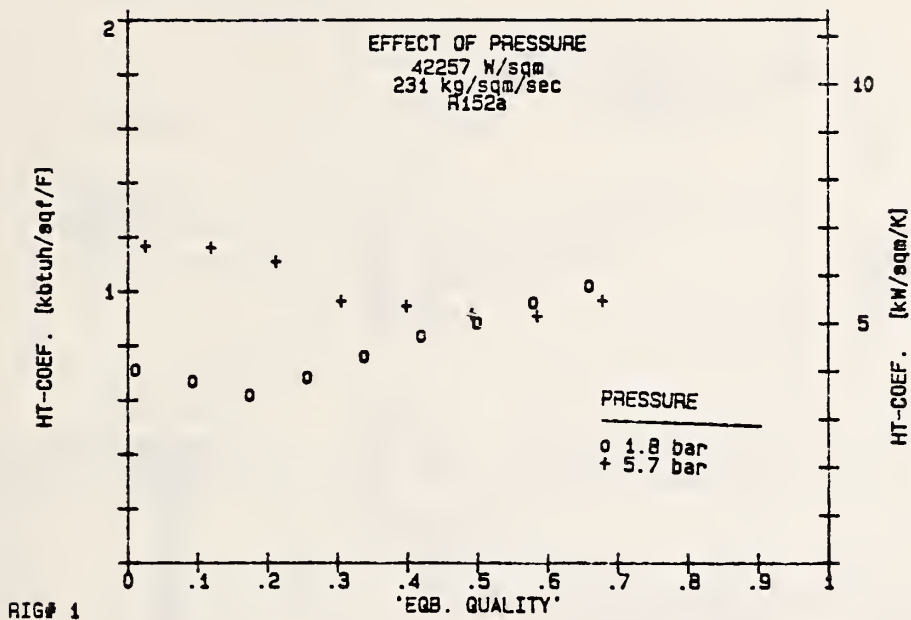
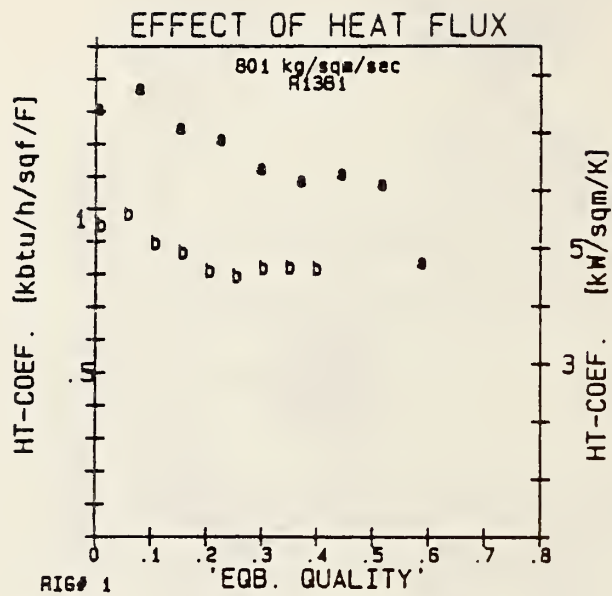


Figure 4-7: Effect of Pressure on Pure R152a. Nucleate boiling dominates at high pressure, even at large quality.



HEAT FLUX

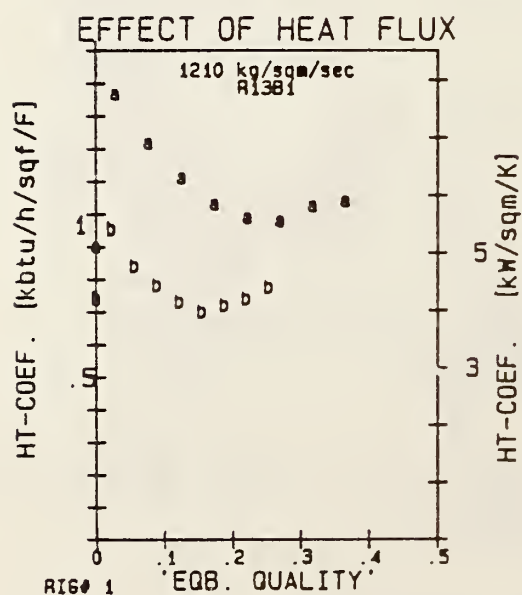
a	42203 W/sqm	(6.4 bar)
	OLD0285	
b	29330 W/sqm	(5.7 bar)
	OLD0286	

SUPPRESSION CRITERION

Vapor Quality	HEAT FLUX (kW/sqm)
---------------	--------------------

.01	2
.05	2.8
.15	3.5
.25	4.2
.35	5.2
.45	5.7
.55	6.1
.65	6.6

Figure 4-8: Effect of Heat Flux on Pure R13B1. Nucleate boiling dominates.



HEAT FLUX

a	42212 W/sqm	(6.4 bar)
	OLD0284	
b	29494 W/sqm	(5.8 bar)
	OLD0283	

SUPPRESSION CRITERION

Vapor Quality	HEAT FLUX (kW/sqm)
---------------	--------------------

.03	2.9
.05	3.0
.10	3.2
.15	3.4
.20	3.6
.25	3.8
.30	4.0
.35	4.2
.40	4.4
.45	4.6
.50	4.8

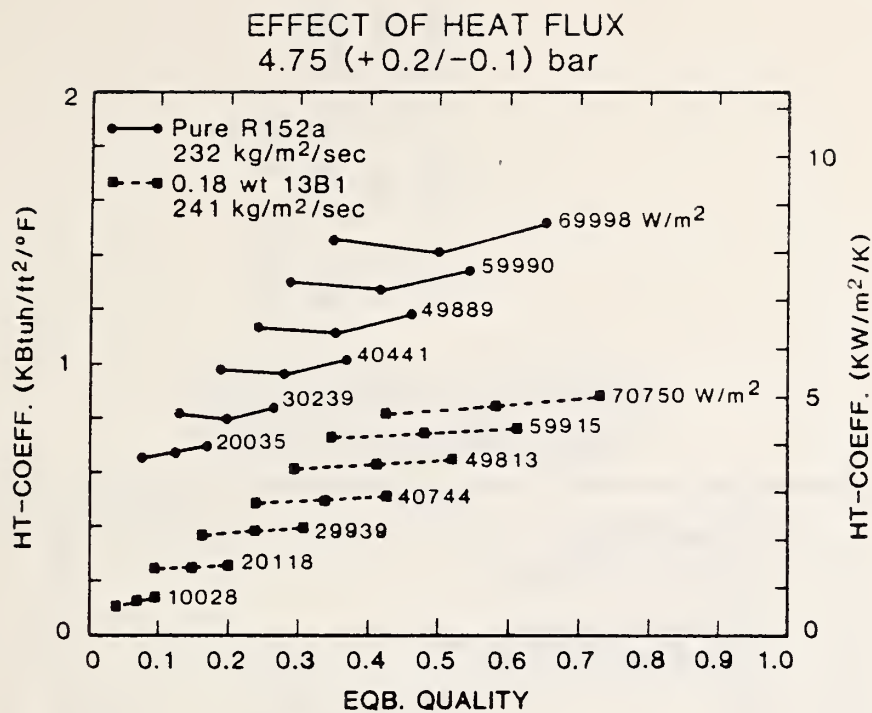
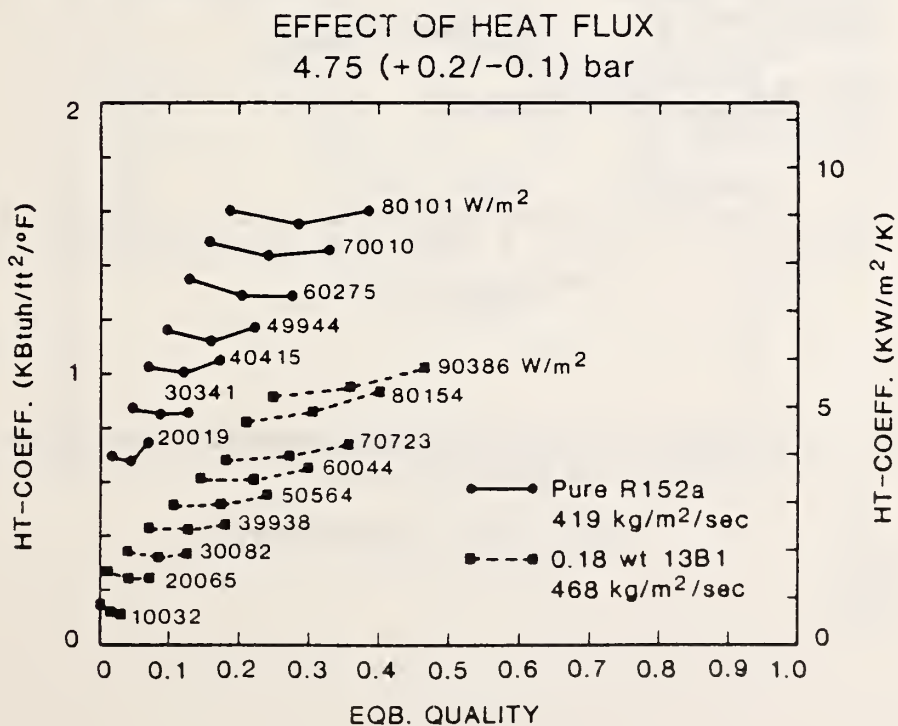


Figure 4-9: Effect of Heat Flux on Pure R152a and P152a/R13B1 Mixture: Preheat Data



EFFECT OF HEAT FLUX 4.75 (+0.2/-0.1) bar

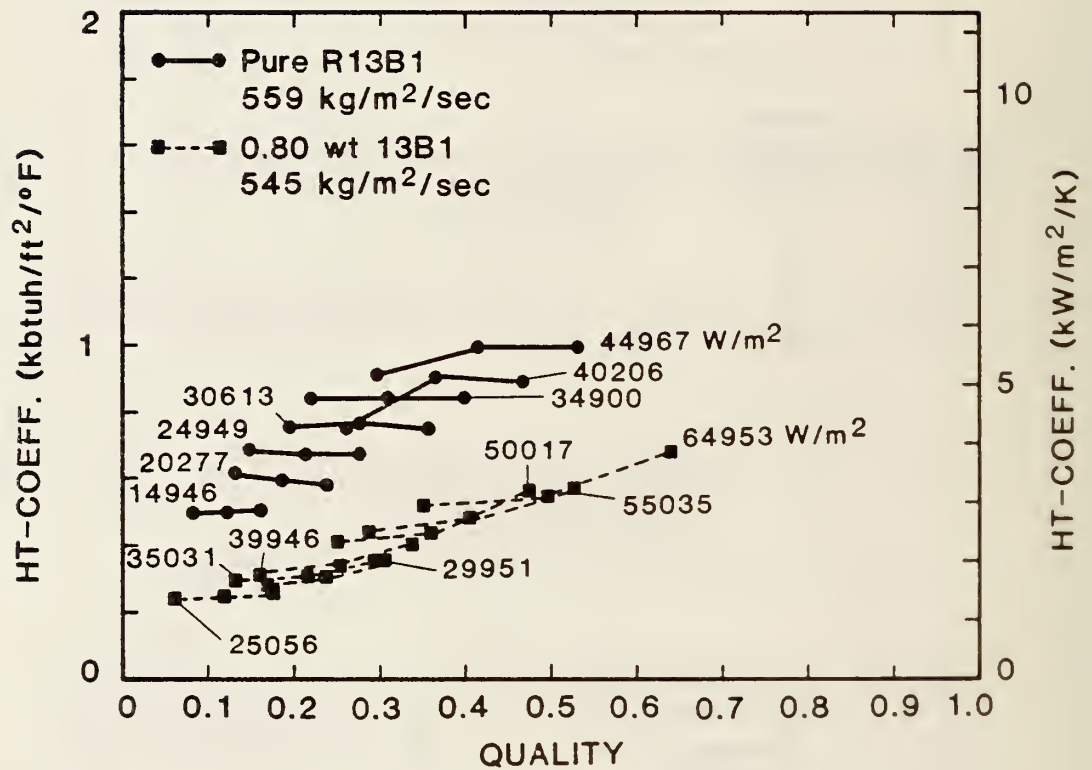


Figure 4-10: Effect of Heat Flux on Pure R13B1 and R152a/R13B1 Mixture: Preheat Data

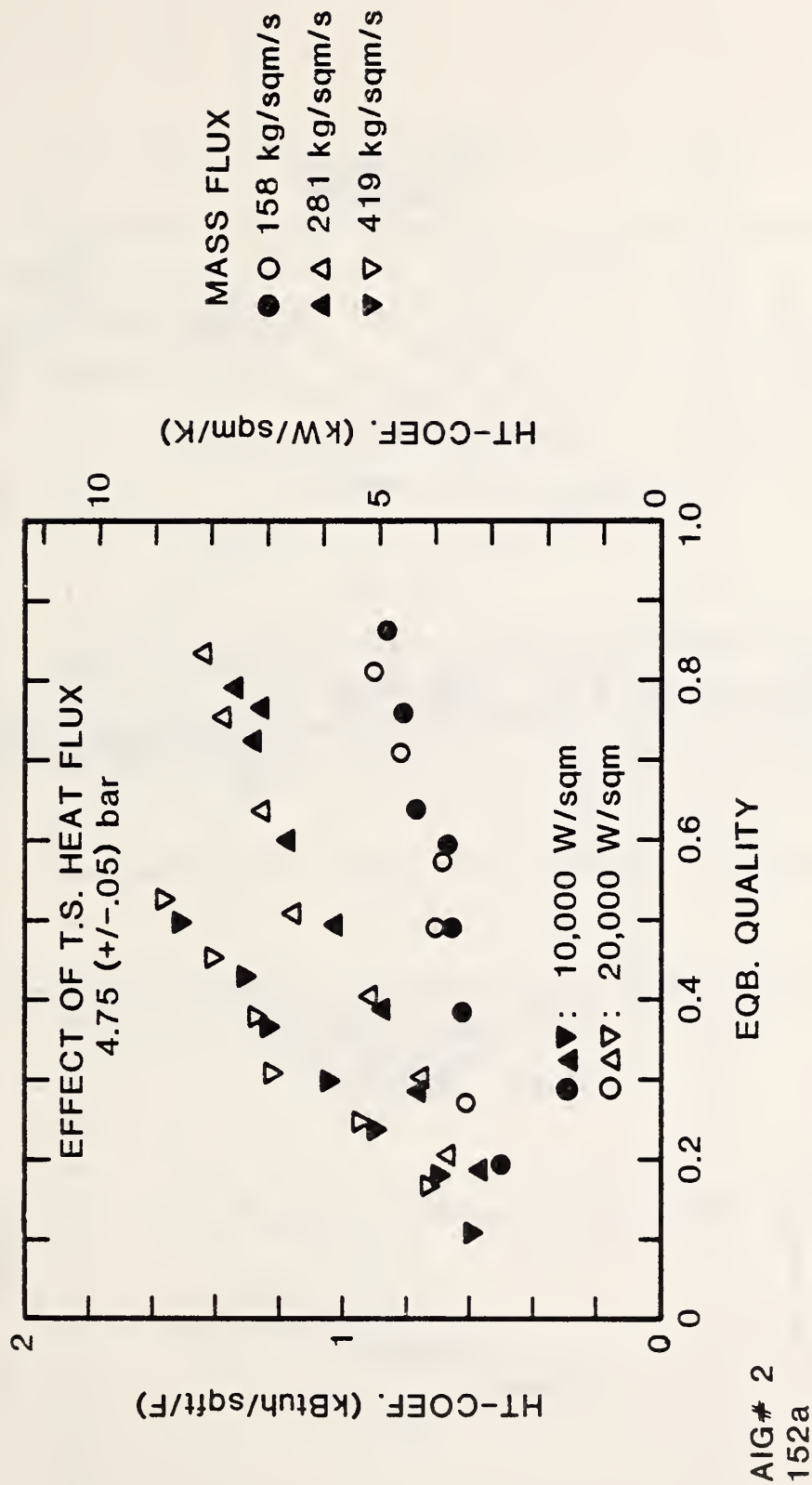


Figure 4-11: Effect of Heat Flux on Pure R152a--Test Section Data

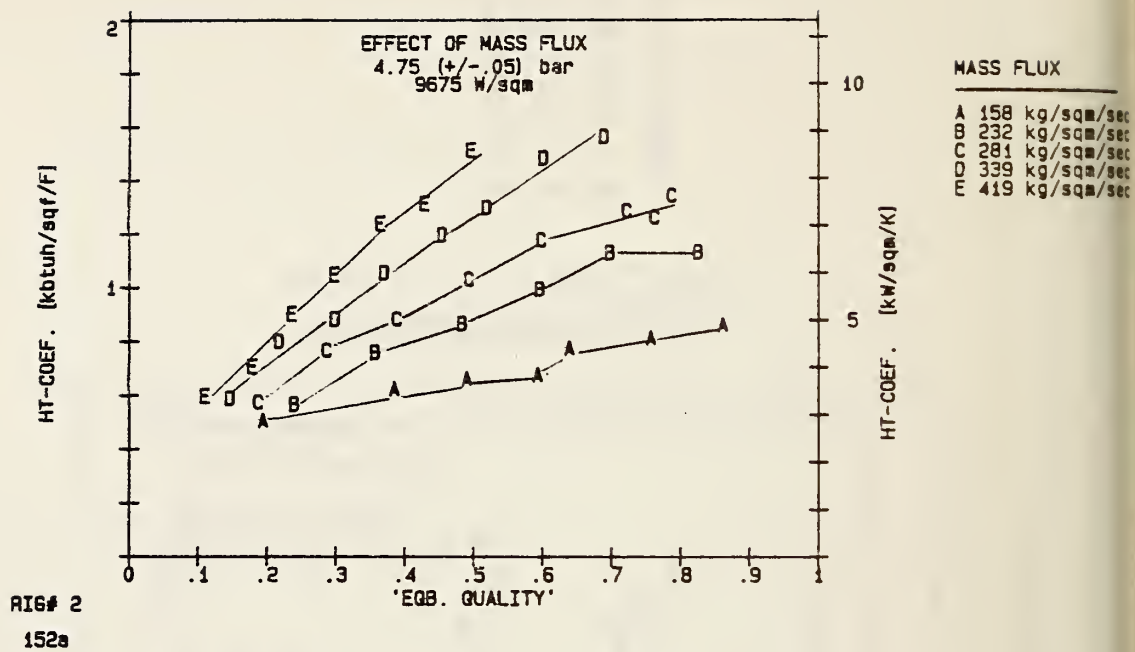
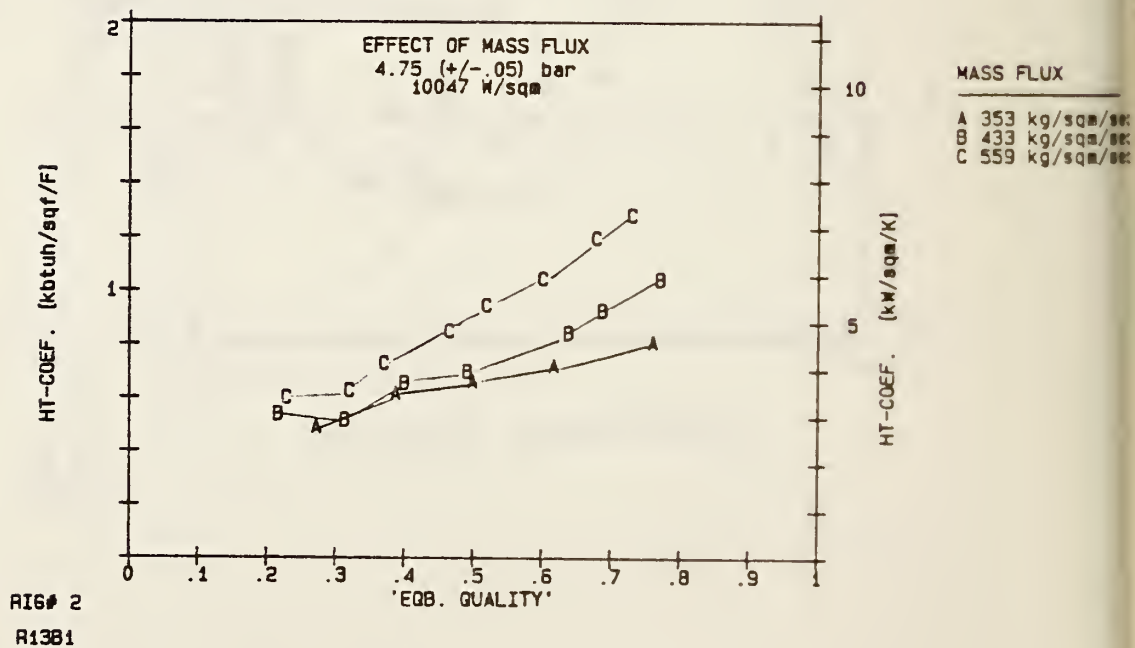


Figure 4-12: Effect of Mass Flux: Test Section Data



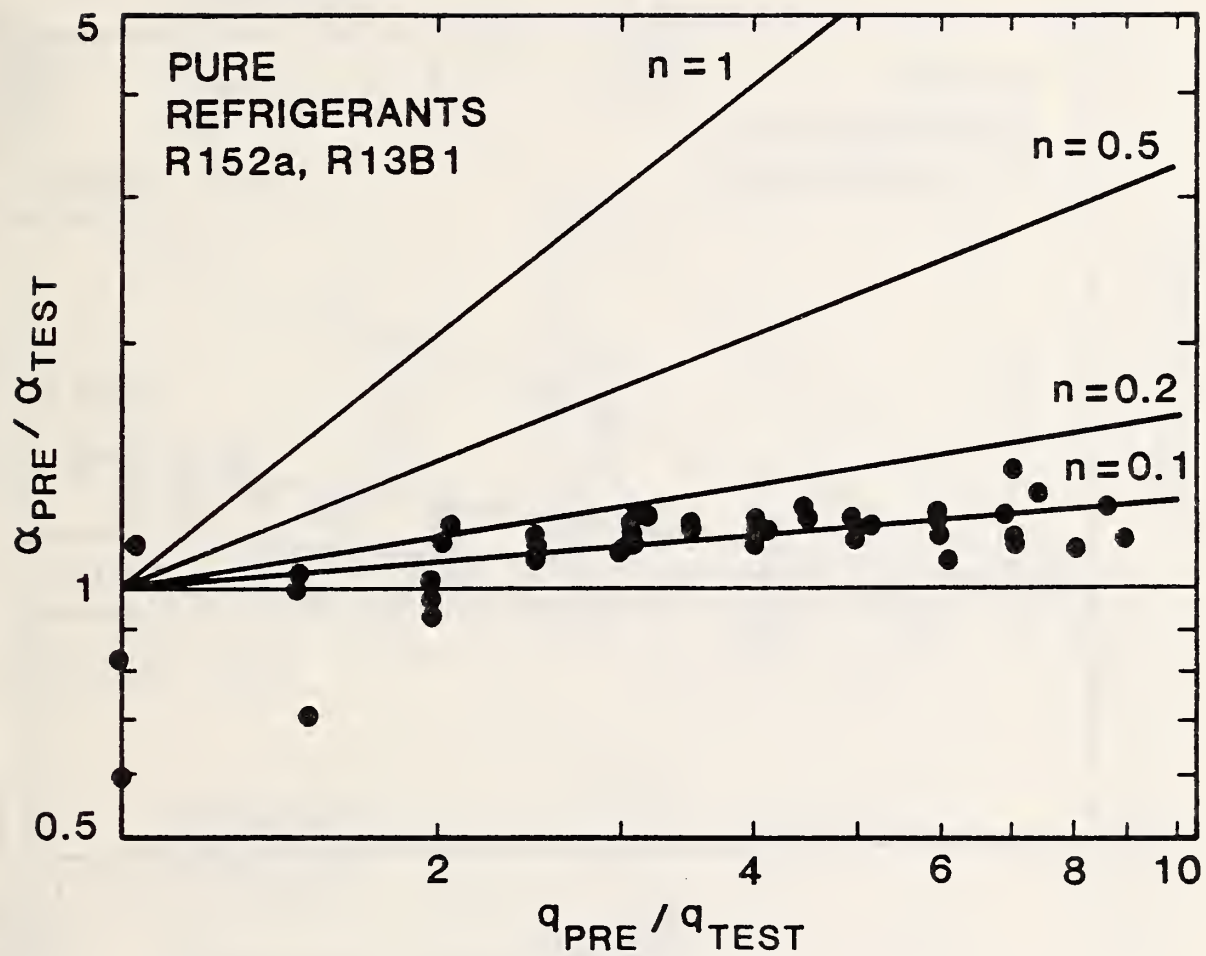


Figure 4-13a: Effect of Step Change in Heat Flux: Pure Refrigerants

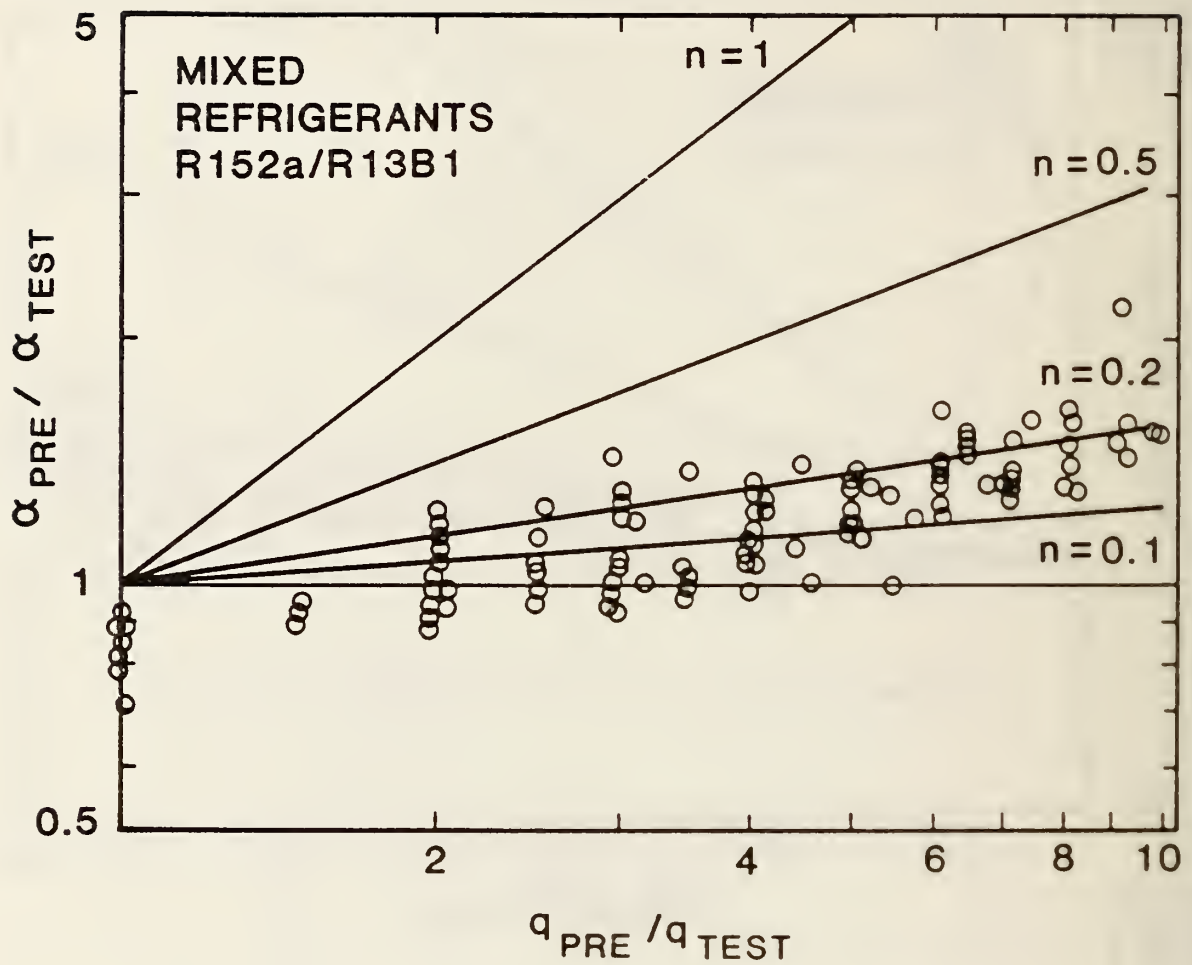


Figure 4-13b: Effect of Step Change in Heat Flux: Mixtures

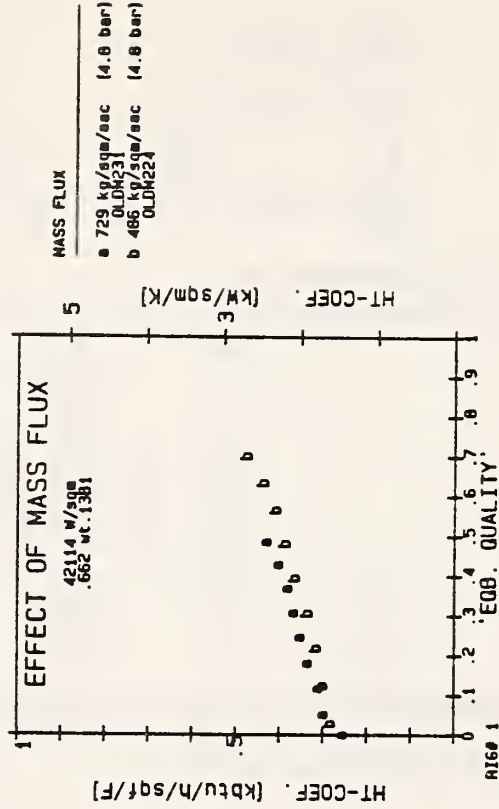
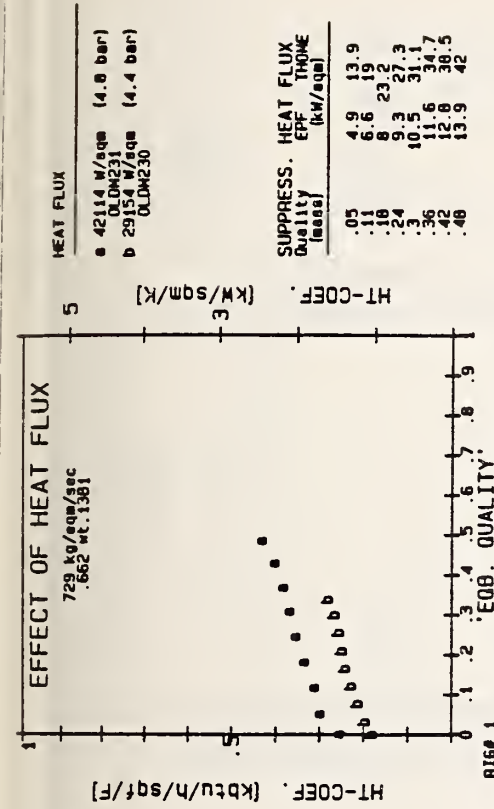
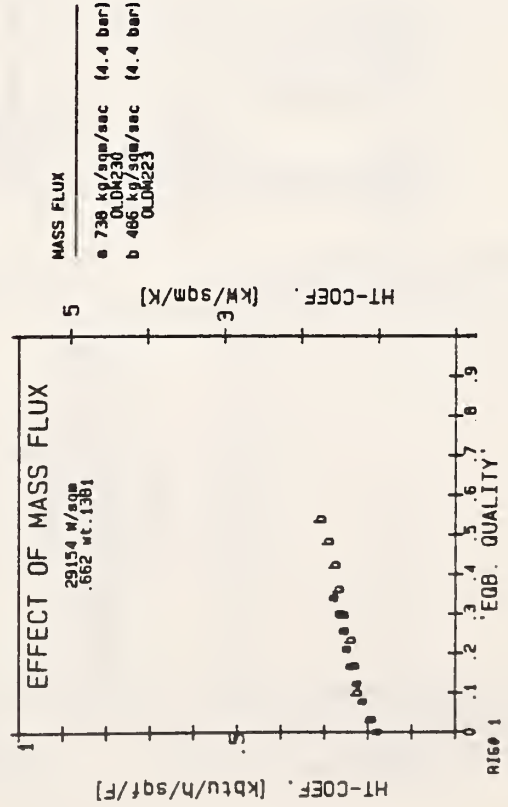
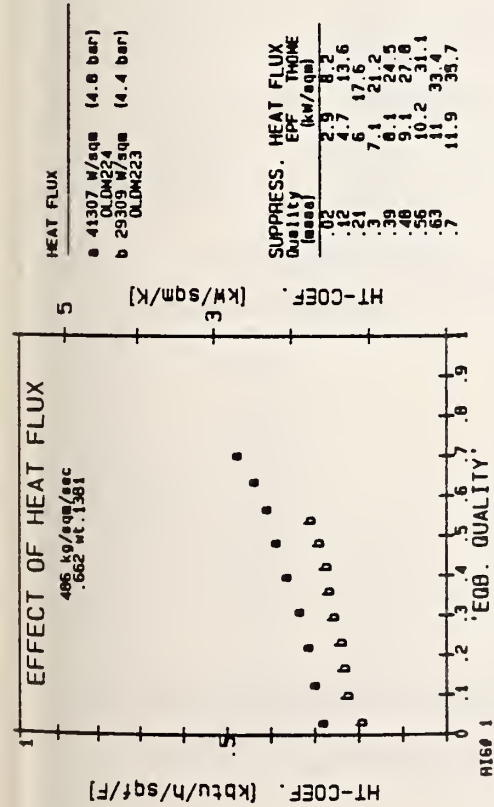


Figure 4-14: Effect of Heat and Mass Flux on 0.662 weight R13B1 mixture. Shown also is the calculated suppression heat flux treating the mixture as an EPF and correcting via Thome's pool boiling method. If q_{act} q_{sup} , then suppression is predicted to not occur.

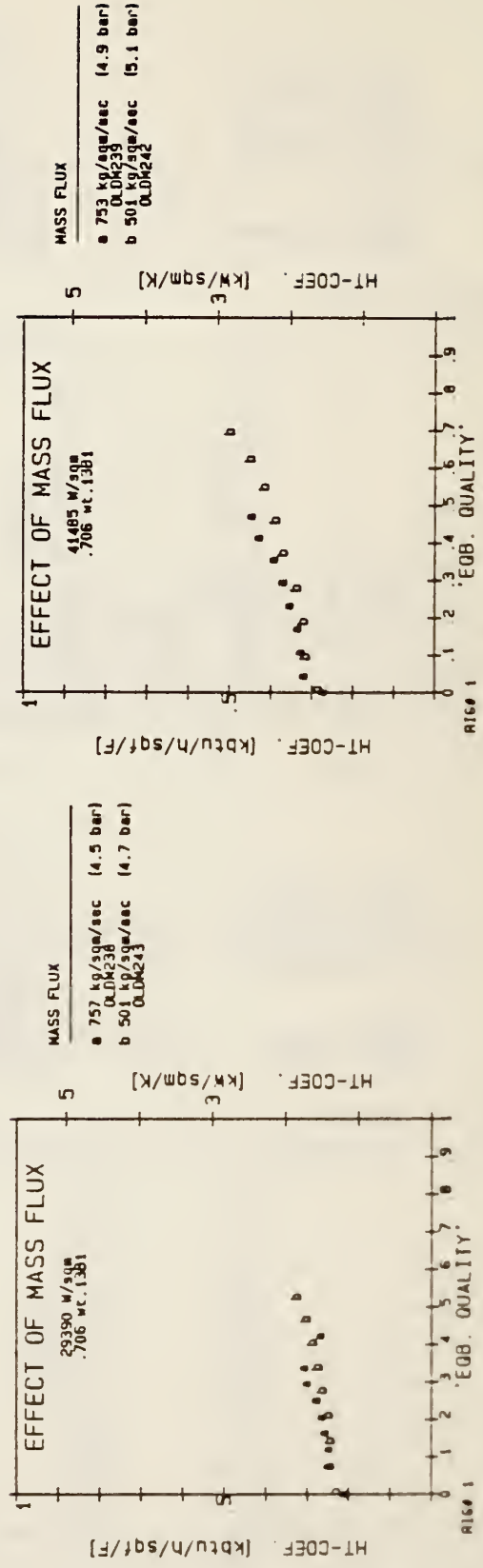
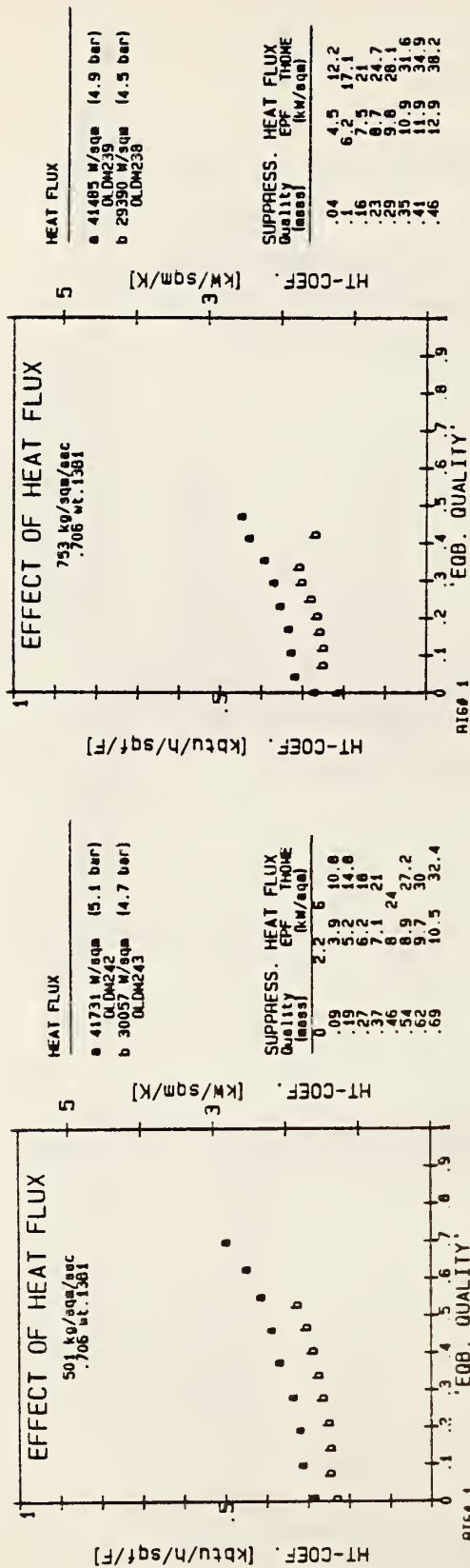


Figure 4-15: Effect of Heat and Mass Flux on 0.706 weight R13B1. Nucleate boiling is not only present, but dominant.

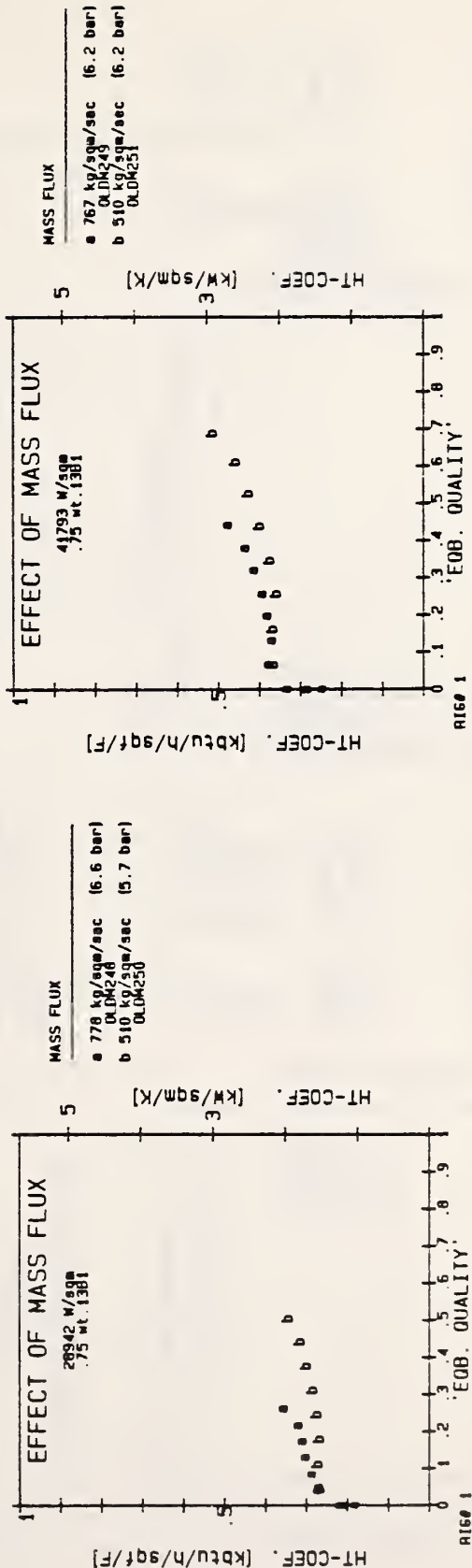
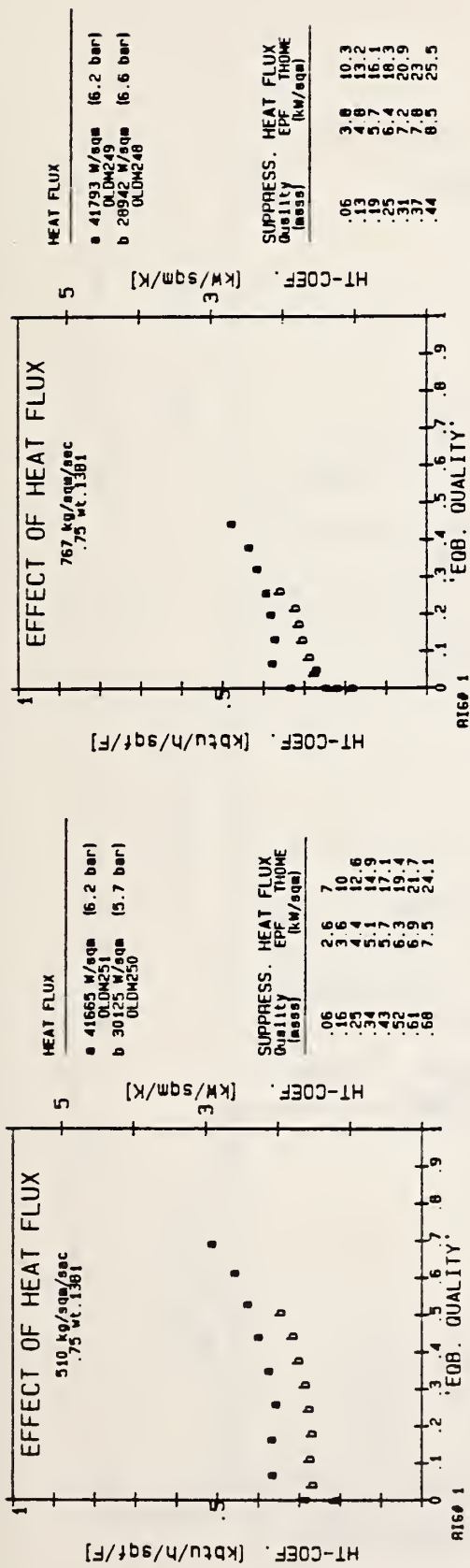


Figure 4-16: Effect of Heat and Mass Flux on 0.75 weight R13B1. Nucleate boiling present, and dominant.

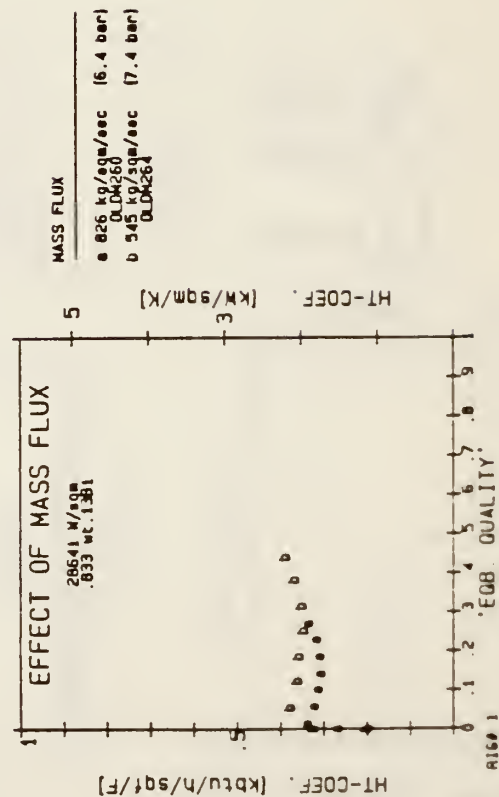
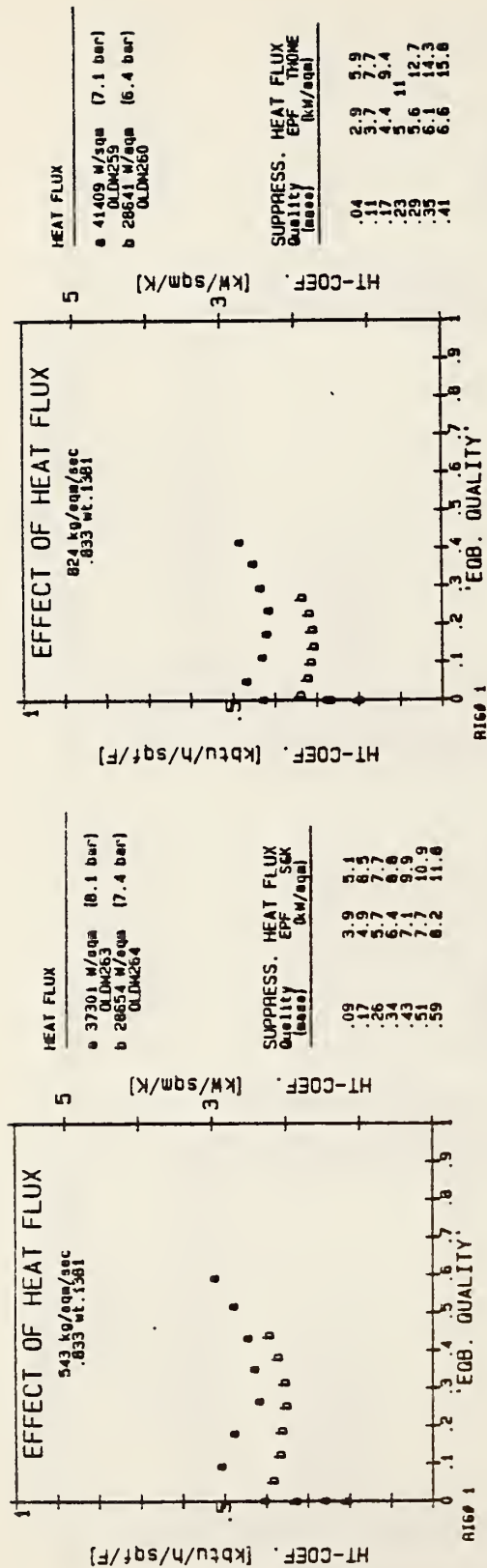


Figure 4-17: Effect of Heat and Mass Flux on 0.833 weight R13B1. Nucleate boiling not only present, but dominant.

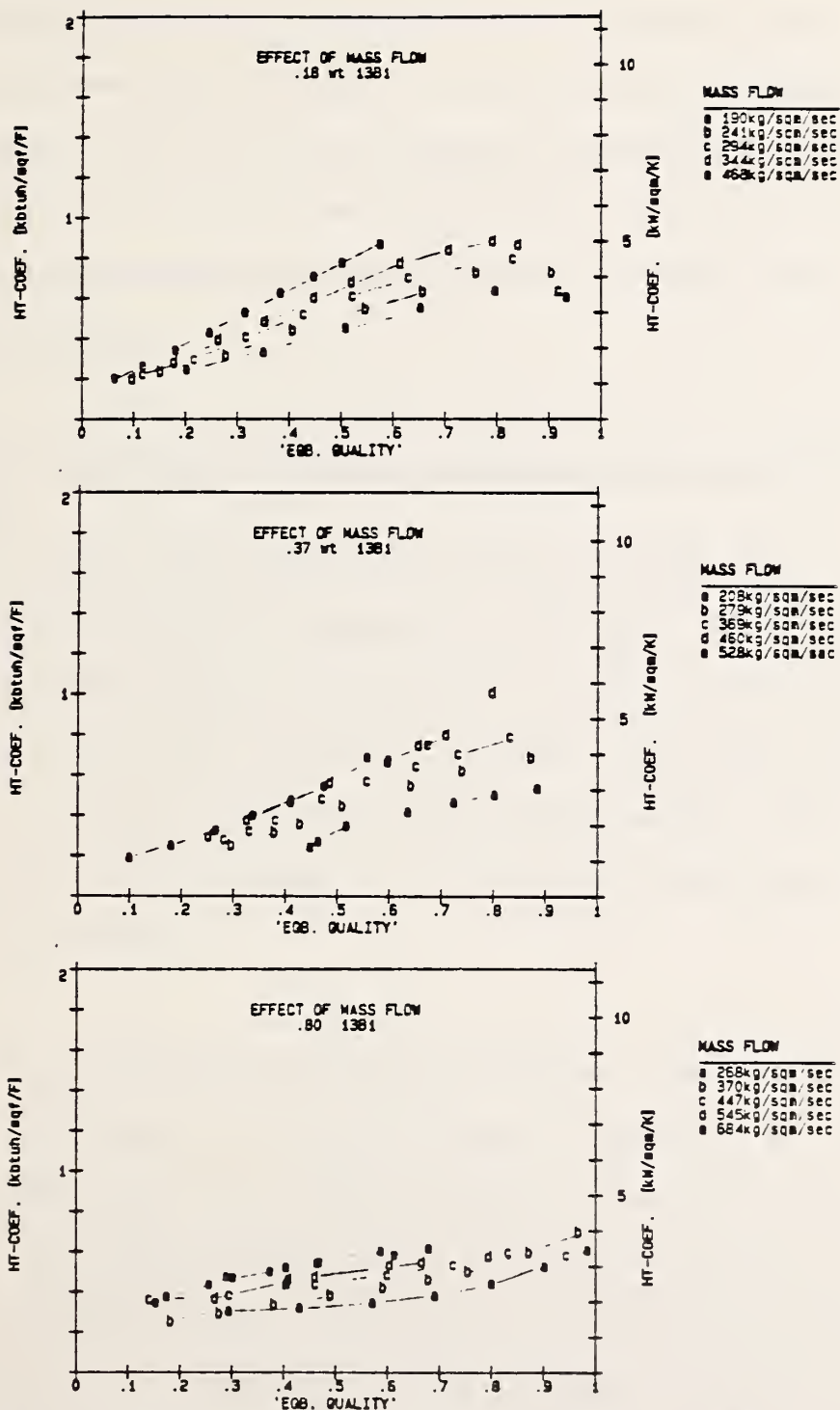


Figure 4-18: Rig#2 Test Section Data. Effect of Mass Flux; Heat Flux= 10 kW/m². Forced Convection/evaporation dominates.

CHAPTER 5: A FURTHER EXAMINATION OF THE DATA

5.1 Introduction

The last chapter revealed some of the features of the experimental data base. They are summarized in Table 5-1. In this chapter, some additional features of the data base are discussed, including new physical phenomena which were observed, and an analytical discussion of the use of equilibrium temperature in the definition of the mixture heat transfer coefficient.

5.2 Circumferential Variation in Heat Transfer in Horizontal Flow Boiling

In horizontal annular flow boiling the liquid film thickness is asymmetric around the inner circumference of the tube. Due to gravity, the film at the tube bottom is thicker than at the tube top. The effect of this thick film for pure fluids is to produce a lower heat transfer coefficient at the tube bottom due to increased resistance. This behavior has been observed widely in the literature [Ch66a,Ra83], and was seen with both rigs.

In the case of horizontal flow boiling of mixtures, a new opposite phenomena was observed, i.e., the heat transfer coefficient at the tube bottom was higher than at the top by an amount far outside experimental uncertainty. The observation was made consistently with both rigs; the rigs utilized different tubes, thermocouples, and test section heaters, and thus should not be a function of these apparatus. The wall temperature measurements determine the circumferential variation and are not dependent on the data analysis technique. The effect was observed with

and without a preheat section, with a variety of heat fluxes, flow rates, and mixture compositions, and over a range of pressures (left uncontrolled in the tests with the first rig).

Figure 5-1 displays a typical data set (Rig #1) for the pure fluids. The heat transfer coefficient at the bottom is seen to be lower than at the tube top, except near $x = 0.8$, where dryout is beginning. In contrast, Figure 5-2 displays similar plots for mixtures. The reversal is noted at qualities greater than 0.2. Identical trends were observed with Rig #2 in both the preheat and the test sections.

One might question why this finding has not been discussed before in the literature. Section 1.7 discusses previous flow boiling of mixture investigations. Three of the previous studies [Sh73, To79, Be80] involved vertical flow with only one thermocouple mounted around the tube circumference. Both the lack of instrumentation and the flow orientation preclude the possibility of observation.

Conjecture can be made regarding the reason for the reversal.

Possibilities include:

- (a) Increased turbulence at bottom of tube
- (b) Nucleate boiling at bottom of tube, and not at the top
- (c) Flow pattern differences between mixtures and pure fluids
- (d) Film boiling at tube top
- (e) Different concentrations at tube bottom and top

The first two reasons may be dismissed in that they should appear for the pure fluids as well. Further, in the case of mixtures, nucleate boiling is more difficult to sustain, so it is unlikely that this is the cause. If any trend should appear in the nucleate boiling dominated region, it is that a greater disparity between top and bottom might occur with mixtures, not a reversal. The third reason may be dismissed in that flow patterns were observed at the outlet. Based on these observations, a greater disparity again might have been expected at a fixed quality. The effect of quality is discussed in the next section.

Film boiling is also a possibility since it will occur first at the tube top. It is not likely since: (a) the wall temperatures were relatively stable; (b) the wall temperatures at the top were not widely different than at the bottom of the tube; (c) the wall temperatures were axially consistent even at low quality. Still, film boiling is a possibility which cannot be entirely dismissed.

The last possibility is believed to be the root cause of the reversal: the higher heat transfer at the tube bottom is due to the relatively greater amount of the more volatile component (R13B1) at the bottom of the tube. The gravity-driven drainage of bulk liquid to the tube bottom provides a larger amount of fluid upon which to draw. Initially vaporization occurs at both tube top and bottom into the annular vapor core. The top portion of the tube, with its thinner film (and initially higher heat transfer rate) vaporizes most of the more volatile component. At some point it becomes starved of this component and the vaporization

rate is diminished. In the bottom portion of the tube, vaporization is initially small then increases relative to the tube top; since it has a greater bulk amount of fluid, it becomes depleted of the more volatile component at a slower rate than the tube top.

There exists then a competition between the depletion of more volatile component and film thickness. If this explanation is correct, one might expect to see in the early portions of the vaporization process α_{top} greater than α_{bot} , as both tube top and bottom have similar compositions. Then as the top becomes depleted of the more volatile component, the two values should merge and then reverse. Figure 5-2 verifies this conjecture.

An attempt was made to correlate the top-to-bottom wall temperature difference with local vapor-liquid composition difference. The latter quantity is correlated with local mass transfer resistance. As seen on Figure 5-3, no clear correlation was seen in the test section data. The relatively small ΔT is due to the low heat flux in this region (constant wall flux and pressure). A similar plot was made with initial composition as the independent variable. Here, there is a general trend that the greater the initial composition of the more volatile R13B1, the greater the observed ΔT . This suggests that the tube bottom has readily available an amount of more volatile component at the higher initial composition, while the top has been depleted.

The finding of the circumferential variation is a further difficulty for those interested in modelling the heat transfer process from first principles. In addition to axial and radial gradients in composition, there appears to exist a circumferential variation in composition. By necessity then, a varying interfacial temperature exists. Furthermore, circumferential diffusion might exist due to the existence of the composition gradient. This latter effect is likely small; if it were large, then the gradient would disappear, as would the reversal in heat transfer coefficient.

5.3 Effect of Equilibrium Quality on Mixture Heat Transfer

When the thermodynamic equilibrium quality, x_{eqb} , is less than zero, some vapor may be present due to subcooled flow boiling. The actual quality then is higher than x_{eqb} when x_{eqb} is small. At values of $x_{eqb} \approx 0.7$, dryout may occur with the remaining liquid entrained in the vapor core. The liquid droplets may persist beyond the point where $x_{eqb} = 1$, due to relatively poor heat transfer through the vapor, so that at large x_{eqb} , $x < x_{eqb}$. At values of x_{eqb} up to 0.2, little vapor was seen for some mixtures at the outlet sight glass. Also dryout was not often measured until x_{eqb} was near or exceeded 1. Inaccuracy of the EOS might explain these observations. Alternatively, the above classic description of quality dependence may need to be altered for mixed fluids. Mixtures have a higher onset of nucleate boiling point than do some fluids. With less subcooled boiling, the actual x may lag x_{eqb} . This effect would explain both the lack of vapor at low x_{eqb} and the lack of dryout at high x_{eqb} . Also the addition of a second less volatile

component may simply delay dryout due to mass transfer resistance (see Appendix 7C). In either case, the quality dependence may be structurally different for mixtures as compared to pure fluids.

In the last chapter the measured heat transfer coefficient of mixtures was proportional to both heat flux and quality. This trend is also opposite that commonly observed for pure fluids. The dependence on heat flux requires the existence of nucleate boiling. In the nucleate boiling regime, a weak inverse proportionality between quality and heat transfer coefficient is usually observed for pure fluids [St82].

The quality dependence da/dx varies with heat flux, composition and quality itself. As seen in Figure 4-20, a larger da/dx is observed at higher heat flux and quality. Again, this is the opposite behavior as that seen with pure fluids.

In this case, the reason might be the use of an equilibrium temperature in the defining relation for the heat transfer coefficient:

$$a = q / (T_w - T_{eqb}) \quad (5-1)$$

If this equation is now partially differentiated by dx to determine the rate of change with quality:

$$\frac{\partial a}{\partial x} = \frac{-q}{(T_w - T_{eqb})^2} \frac{\partial T_w}{\partial x} - \frac{\partial T_{eqb}}{\partial x} \quad (5-2)$$

The experimental values show $\partial\alpha/\partial x > 0$, so

$$\frac{\partial T_{eqb}}{\partial x} > \frac{\partial T_w}{\partial x}$$

The quantity $\partial T_{eqb}/\partial x$ is a function of composition. It is largest when the dew and bubble point temperature difference is largest (at $\Delta X = 1$, $\Delta T_{eqb} = T_{DEW} - T_{BUB}$). Thus, it may be that the apparent dependence on quality is largest in the regions where the dew-bubble temperature difference is largest. In examining the data, a trend of this nature is apparent. The quality dependence then may be an artifact of the defining relation, rather than representative of the heat transfer regime as it is in flow boiling of pure fluids.

5.4 Departure from Nucleate Boiling (DNB) Events

In some of the data taken with Rig #1, DNB events were observed along the tube top. The events occurred generally at large values of heat flux, pressure and concentrations of R13B1. Some of the erratic behavior of R13B1 can be attributed to this occurrence (Figure 5-4). Surprisingly, in the case of mixtures, the bottom and side heat transfer coefficients seem to be little affected by the behavior near the tube top.

Some available data in the literature were examined for the occurrence. The data of [Mi81] for pure R12 and a mixture of R12/R22 shows the same behavior (Figure 5-5). The authors note the 'tube wall temperatures exhibited large fluctuations which indicated the unstable behavior of

boiling . . . the scatter of the tube wall temperature is wider in the case of mixtures than with pure R12.' They did not attribute the scatter to DNB events, and analyzed their data as if it were in an annular flow pattern with conventional nucleate boiling and evaporative heat transfer contributions. Some data of [Ma76] also seems to exhibit scatter at low flow rate and high heat flux, and is suspected of similar events.

For standard heat pump applications with R13B1/R152a and with other refrigerants, there is a possibility that the heat transfer process will be diminished in the first row of coils (where q is largest). In this case, the addition of a less volatile component may actually augment the observed heat transfer. DNB events were never observed with pure R152a, the less volatile component of the tested mixture.

In the following chapters the tests suspected of featuring DNB events are not included in the comparison to the predictive correlations.

5.5 Comparison Between Pure and Mixed Refrigerants

In Chapter 7 the measured heat transfer coefficients for mixtures are compared to predicted values based on treating the mixture as an equivalent pure fluid. In the process of that analysis, a comparison will be made between pure fluids and mixtures when the heat transfer is dominated by nucleate boiling. In that case, the comparison is made at identical pressures and heat fluxes. In the case of flow boiling where flow rate has a sizeable influence on the measured heat transfer coefficient, the comparison is more difficult.

When there is an influence of flow rate, one can compare fluids on any of the following basis:

- (a) same mass flow rate
- (b) same molar flow rate
- (c) same volume flow rate
- (d) same Reynolds/Prandtl number

The mass flow rate comparison is the one with which most engineers are acquainted. On the other hand, chemists and physicists work in molar quantities, and might claim that the weight of a molecule matters less than the number of molecules which flow. The application to a heat pump suggests the same volume flow rate: compressors are effectively constant volume devices. In defense of the last item, single phase scaling laws suggest Re and Pr should be used. These however are derived from the single phase Dittus-Boelter relation; on two phase flow, other parameters affect the results.

Figure 5-6 displays the test section data for both the pure and mixed refrigerants, at identical values of pressure, heat flux and the Martinelli parameter. The measured heat transfer coefficient has been normalized by α_{LO} so that mass flux effects are eliminated from the comparison. The heat transfer coefficient for the mixtures are less than for the pure refrigerants. This finding suggests that there is a distinct mixture effect, possibly due to mass transfer resistance. Shown also on the figure are two correlations to be discussed in Chapters 6 and 7. They are both for pure fluids. The Prandtl number

term is included whenever it is suspected that nucleate boiling has not been suppressed. As can be seen, it appears that nucleate boiling is suppressed for the mixtures, but not for the pure fluids. The presence of nucleate boiling for the pure fluids might also explain their larger heat transfer coefficients. This result is consistent with the suppression criterion prediction of Chapter 4.

5.6 Pressure Drop in Horizontal Flow Boiling of Pure and Mixed Refrigerants

It has been suggested recently that conventional pressure drop prediction methods must be modified to account for mixture effects [Si83a]. Others claim that there is no physical reason for requiring such a change. Arguments might be made for either case. All prediction methods use the quantity x_{eqb} in determining pressure drop. For pure fluids at equilibrium qualities above zero, the vapor quality difference, $x_{act} - x_{eqb}$, is usually small in the annular flow regime. It is well established in nucleate boiling of nonazeotropic mixtures, mass transfer resistance leads to degraded heat transfer. This phenomena could change the vapor generation rate, such that the vapor quality difference, $x_{act} - x_{eqb}$, is dissimilar between pure fluids and mixtures. The dissimilarity could lead to poor prediction using pure fluid methods. On the other hand, it has been established analytically that mass transfer resistance is of minor importance when nucleate boiling has been suppressed and the vapor generation process becomes evaporative only in turbulent annular flow [Sh77].

The Martinelli-Nelson method [Ma48], as modified by Chisholm [Ch67] was selected due to its simple application and success with the pure fluids. The method requires stepwise integration as was described in Chapter 3. For the tests conducted here, the inlet conditions were only slightly subcooled, and single phase pressure drop was neglected. The entire pressure drop was assumed to occur between the calculated position of $x_{eqb} = 0$ and the outlet.

Figure 5-7 displays the comparison between prediction and measurement for the mixtures' data. Agreement is satisfactory, and may be compared to Figure 3-12. No correction for composition is required for this refrigerant.

Rig #1

Table 5-1: Summary of Experimental Data

	Effect of \dot{m}	Effect of \dot{Q}	Effect of x	Dominant Heat Transfer Regime	Final Number of Points
R152a low pressure	strong	negligible at $x > .1$	strong at large x	FC/E	102
high pressure	weak	strong	negative initially	NB	~30
R13B1	weak	strong	negative initially	NB	~40
Mixtures	weak	mildly proportional	mildly proportional	both FC/E and NB	184
Rig #2 Preheat					
R152a	negligible	strong	small	NB	86 [+54 repeats]
R13B1	weak	strong	small	NB	60
mixtures	varied with composition	strong	mildly proportional	both	442
Rig #2 Test Section					
R152a	strong	weak	strong	FC/E	56
R13B1	strong	N/A	strong	FC/E	20
Mixture	strong	N/A	strong	FC/E	141

FC/E: forced convection/evaporation
 NB: nucleate boiling

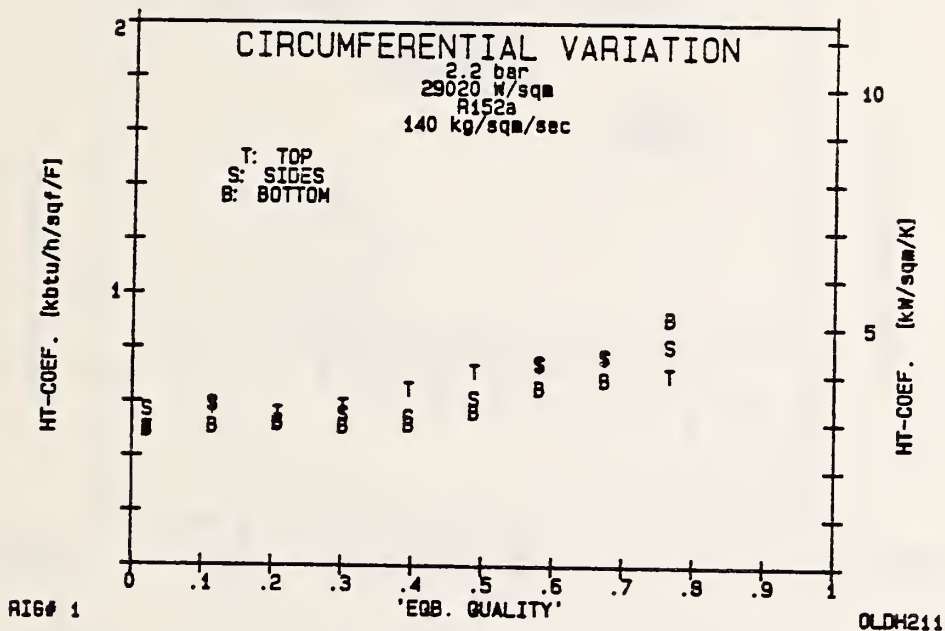
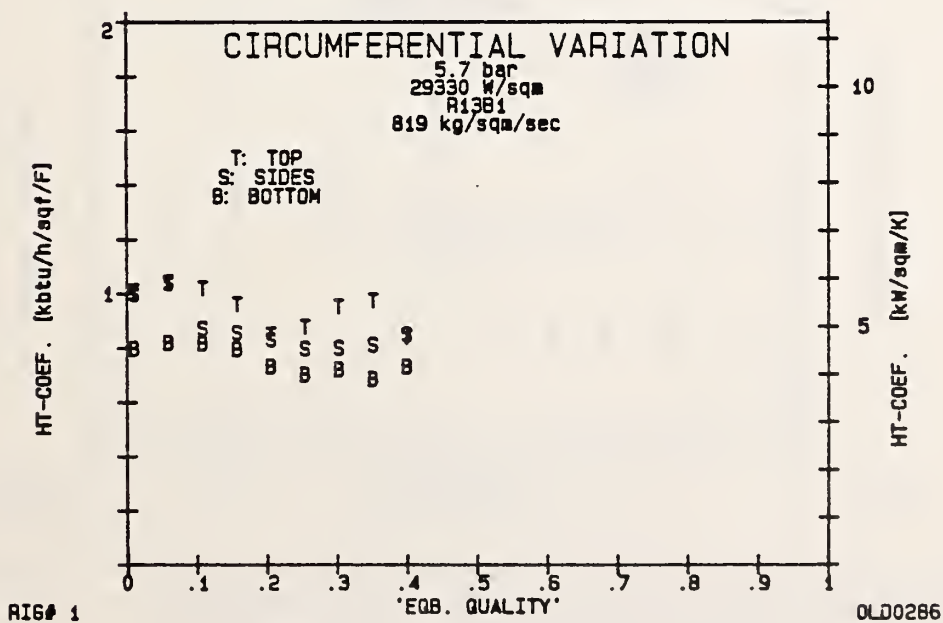


Figure 5-1: Variation in Measured Heat Transfer Coefficient. Heat transfer at tube bottom lower than at top due to thicker film.
 (a) R152a; (b) R13B1



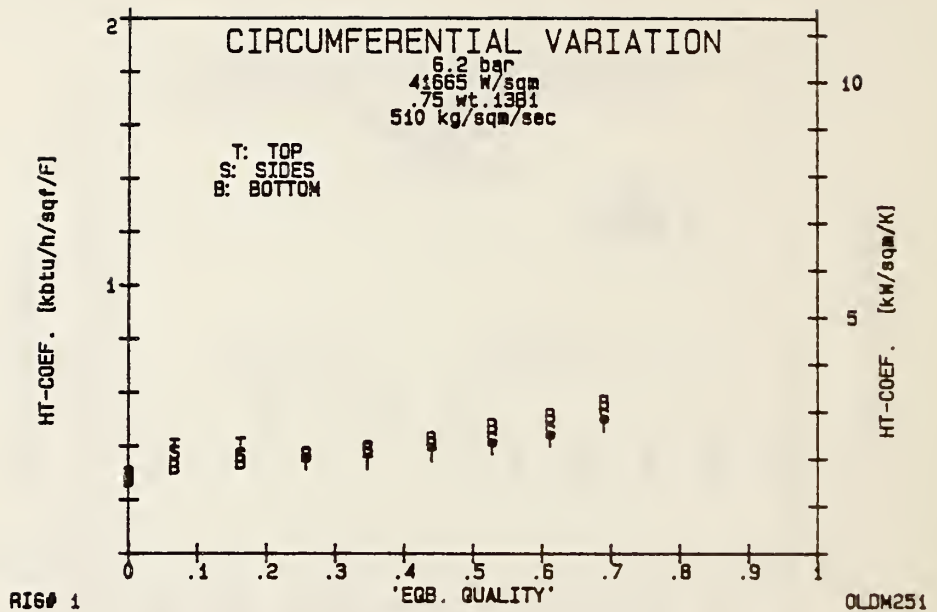
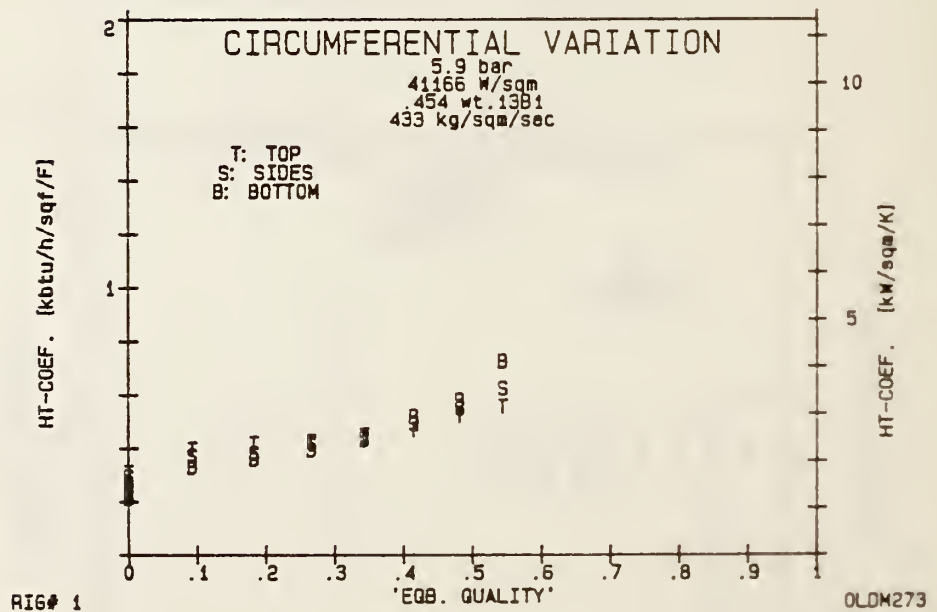


Figure 5-2: Variation in Measured Heat Transfer Coefficient. Heat transfer at tube bottom higher than at top, presumably due to greater availability of more volative component.



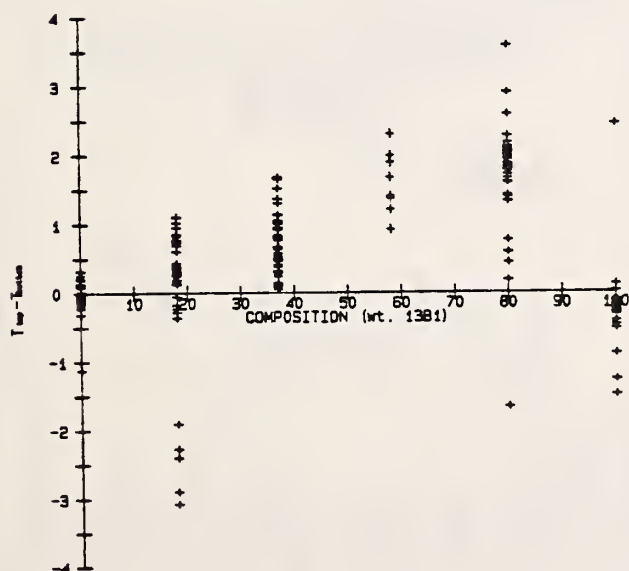
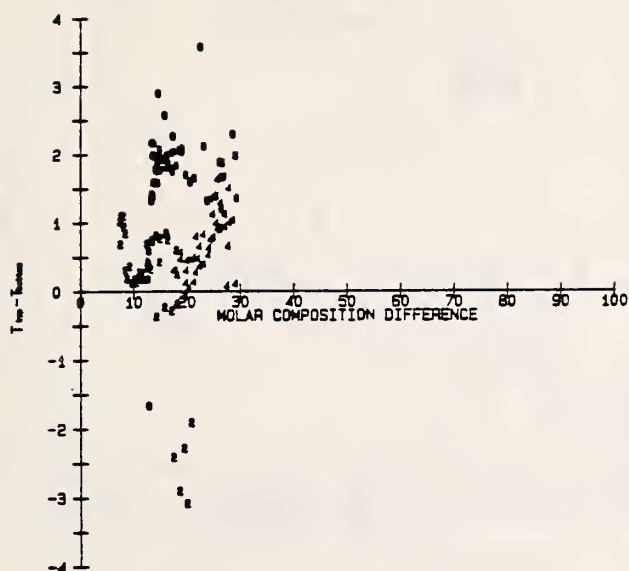


Figure 5-3: Effect of Composition on Top-Bottom Wall Temperature Difference. (a) Effect of Local Molar Composition Difference; (b) Effect of Feed Composition. Outlying Points are due to stratified flow.

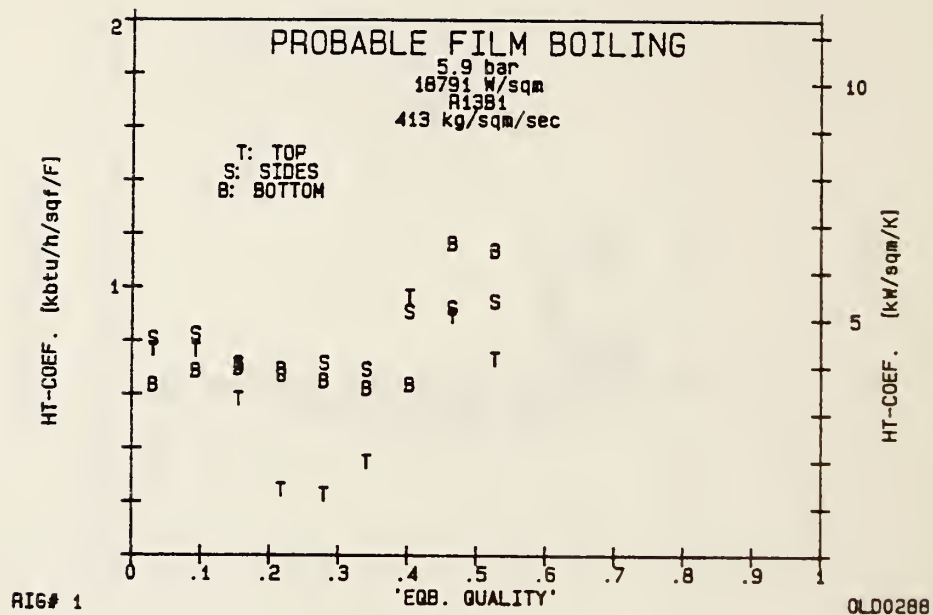
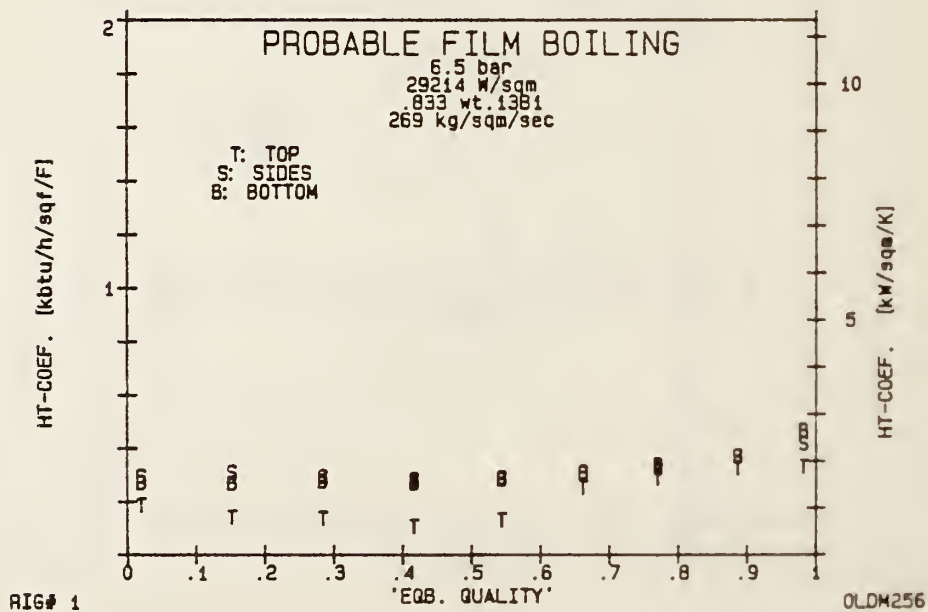
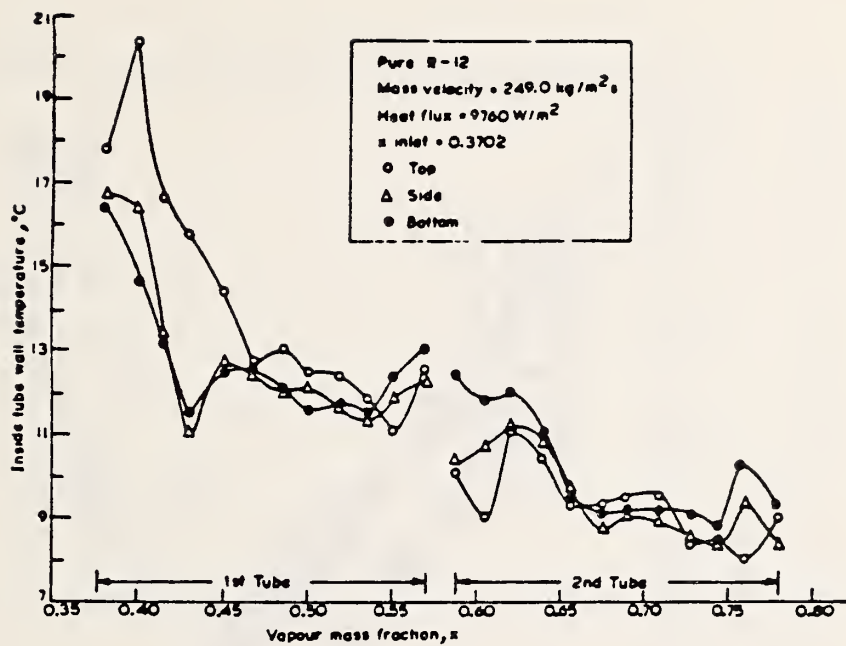
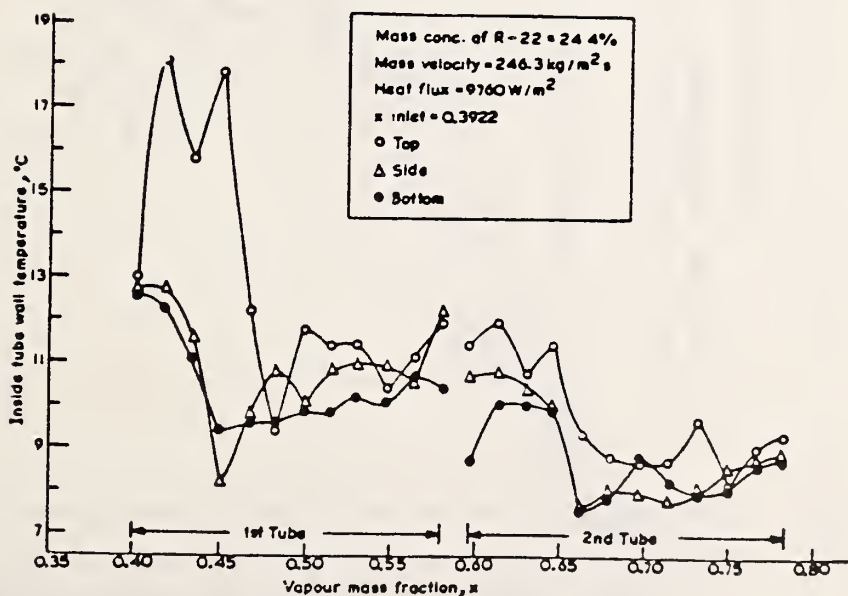


Figure 5-4: Indications of probable film boiling for pure R13B1 and a mixture.





(a) Pure refrigerant 12



(b) Binary mixture

Figure 5-5: Probable Film Boiling in the Data of (Mi81)

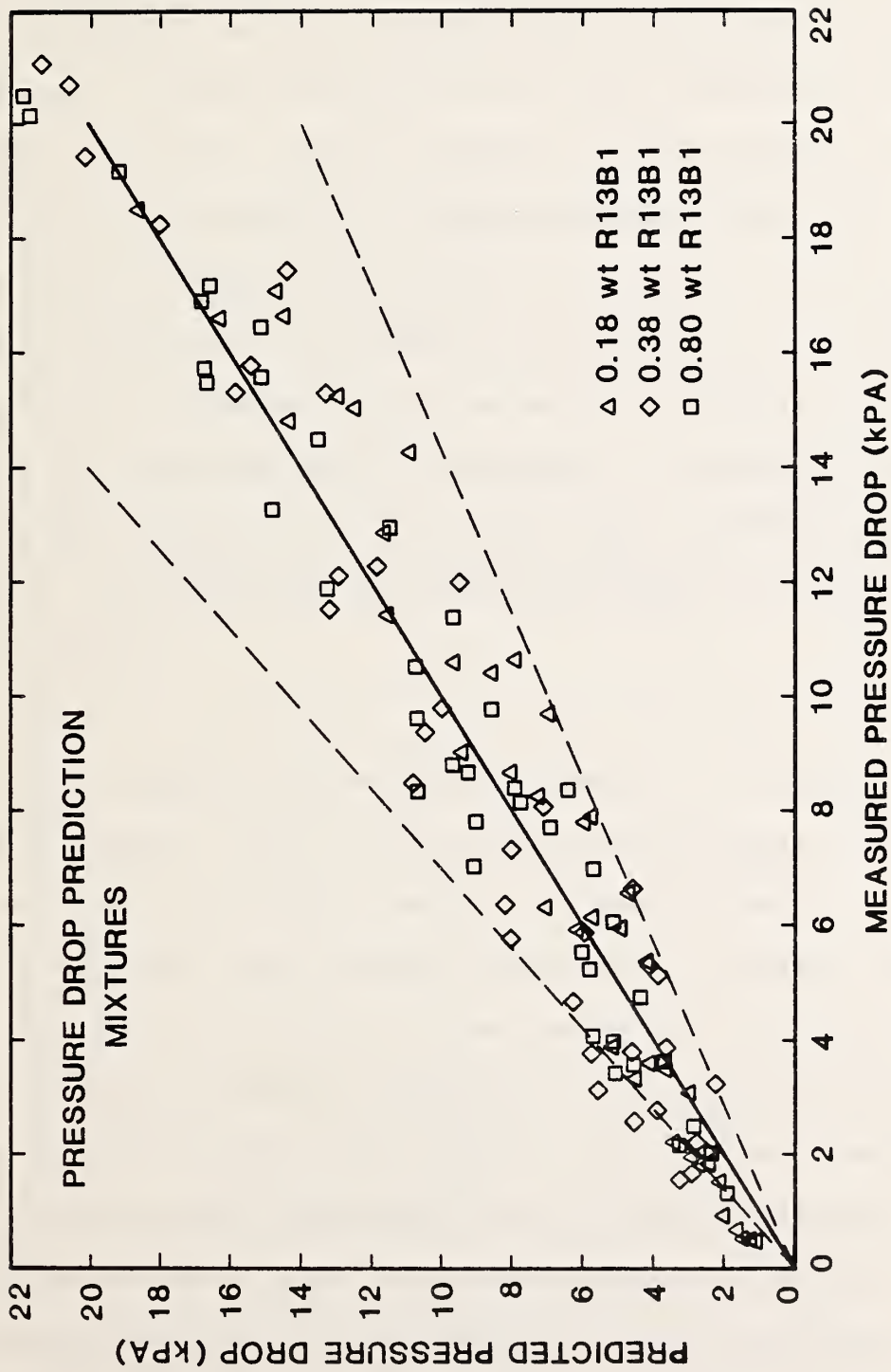


Figure 5-7: Comparison between Predicted and Measured Pressure Drop for Mixtures

CHAPTER 6: PREDICTION OF PURE REFRIGERANT HEAT TRANSFER

6.1 Introduction

In order to understand the effect of mixtures on flow boiling heat transfer, one needs to be able to predict flow boiling behavior with pure components. If such a prediction can be made accurately with a single model/correlation, then the analysis of mixture behavior can begin by treating the mixture as an 'Equivalent Pure Fluids (EPF)', i.e., one which has properties determined by appropriate mixing rules, but which is modelled as if the properties belonged to a pure fluid. If the EPF correlation underpredicts the measured heat transfer for mixtures, then some additional effect attributable to the mixture is augmenting the heat transfer. If, on the other hand, the EPF correlation overpredicts, the mixture has some inhibiting feature, e.g., mass transfer resistance.

The modelling of annular flow boiling heat transfer is not simple. As discussed in Chapter 1, there are many complicating features. Some predictive estimation is needed, however, for design purposes. As such, many correlations have been developed which attempt to consider some of the physical aspects of the flow. In the remainder of this chapter, these correlations are discussed (Section 6.2) and compared with the experimental results of this report (Section 6.3). The best features of various correlations are incorporated into an overall calculation procedure (Section 6.4) which yields excellent agreement with the data. It is then compared favorably with data provided by other researchers. Conclusions and recommendations are described in Section 6.5.

6.2 Correlations for Annular Flow Boiling

In the earlier chapters, the mechanisms of vapor generation in annular flow boiling were seen to be: (a) nucleate boiling at the wall characterized experimentally by a strong dependence of α on heat flux, or (b) evaporation from the vapor-liquid interface characterized by a strong dependence on flow parameters and vapor quality, or (c) a combination of (a) and (b). In the case of refrigerants, both mechanisms commonly contribute, with the more dominant contribution switching from (a) at low quality to (b) at high quality for fixed heat and mass flux.

Correlations have attempted to account for the simultaneous contribution of nucleate boiling and evaporation in an additive sense:

$$\alpha/\alpha_{LO} = A_1 \left(\frac{q}{\dot{m} \Delta h_v} \right)^{C_1} + A_2 (X_{tt})^{C_2}, \text{ with } A_1 = 0 \text{ sometimes} \quad (6-1a)$$

or, a multiplicative sense,

$$\alpha = A_3 \dot{m}^{C_3} q^{C_4} d^{C_5} \quad (6-1b)$$

or, a combination of the two approaches ($S=S(F)$):

$$\alpha = \alpha_{LO}^F + \alpha_{pool}^S \quad (6-1c)$$

Forms (6-1a) and (6-1b) have been used widely in refrigeration industry; form (6-1c) was developed originally by Chen [Ch66] and is commonly

advocated in the nuclear industry. All of the forms have the problem of failing to predict accurately in all circumstances. All forms show distinct contributions of nucleate boiling (seen in the inclusion of q or α_n) and forced convective evaporation (seen in either X_{tt} and/or α_{LO}).

Form (6-1a) has the problem that it particularly has not proven general. In some cases, although a dependence on heat flux could be seen from the data, no improvement was achieved by including it as a correlating parameter, i.e., setting $A_1 = 0$ and defining A_2 and C_2 empirically produced the same or better goodness of fit as including it [Ch79]. This result may merely demonstrate the inadequacy of the correlating parameter or the ability to develop a false correlation. A second difficulty arises in the use of α_{LO} , the single phase heat transfer, as a normalizing parameter. The nucleate boiling contribution is then $\alpha_{LO} A_1 (q / m \Delta h_v)$, which after inserting the usual correlations for α_{LO} , e.g., Dittus-Boelter, indicates nucleate boiling heat transfer to depend on the diameter for no apparent physical reason. Furthermore, the specific fluid-surface combination has been proven important in nucleate boiling heat transfer. The physical influence of the surface is lost in the empirical constants A_1 and C_1 . Still, agreement of form (6-1a) correlations with the data upon which they were developed is ± 25 percent typically. This result is somewhat misleading since: (a) the same correlation applied to a different refrigerant/surface yields poor agreement; (b) the value of X_{tt} , developed to correlate pressure drop with flow parameters, yielded agreement for that purpose of only ± 30 percent; and (3) the Dittus-Boelter equation correlated to measurement

data to ± 13 percent [Sh73]. Despite these problems, the refrigeration industry has typically applied form (6-1) correlations, and several correlations of this type were examined. Table 6-1 lists the form (6-1) correlations.

Form (6-1b) is applicable only to average heat transfer coefficients. Butterworth and Shock [Bu82] have published a summary table of values for C_3 , C_4 , and C_5 which is reproduced here as Table 6-2. The table shows most of the experimental data to be characterized more often by nucleate boiling, i.e., a fairly weak dependence on flow rate (0.1 to 0.25, excepting Danilov) and a dependence on heat flux of exponent 0.5 to 0.7, typical of pool boiling experiments. Form (6-1b) also has the problem of a boiling dependence on tube diameter.

For annular flow, the most widely accepted correlations in the nuclear industry was suggested by Chen [Ch66]. It was developed originally from a large set of data compiled from several authors' experiments; the data are exclusively for vertical flows of water and various organic compounds. The refrigeration industry has rejected its use principally because it has proven inaccurate for refrigerants evaporating in horizontal tubes, and perhaps because of the iterative nature of its solution for the case of constant wall flux. Various researchers in other fields have attempted to improve the methods as will be described.

6.2.1 Miscellaneous Forms

Some other correlations have appeared in the literature and have on occasion predicted refrigerant HTC's with some accuracy. These are the methods recently advanced by Shah [Sh76, Sh82], Dembi et al [De78], and Kandliker [Ka84]. Shah's method was checked with the results shown on Figure 6-1. Due to its suppression criterion which does not include mass flux effects, it selects the wrong heat transfer regime and predicts poorly.

As shown in Appendix 6A, the approach recently has been to compile large sets of data from various experiments and use regression analysis to fit them. Extension of the methods to other data has been disappointing. Furthermore, the regression analysis may lead to correlations which ignore physical features in the data. The approach of this report is to examine the older methods developed from theory and analyze or extend them.

6.2.2 The Original Chen Equation

Rosenhow originally suggested that in the case of flow boiling with nucleation, that the forced convection/evaporative and nucleate boiling contributions might be additive. Following this line, Chen postulated:

$$\alpha = \alpha_e + \alpha_{nbc} \quad (6-2)$$

$$= \alpha_{LOF} + \alpha_n S \quad (6-3)$$

The evaporative portion, α_e , was related in the fashion similar to form (6-1):

$$\alpha_e = \alpha_{LO} F_c(X_{tt}) \quad (6-4)$$

where $F_c(X_{tt})$ is an empirical function of the Martinelli parameter:

$$F_c(X_{tt}) = 2.35 \left(\frac{1}{X_{tt}} + .213 \right)^{.736} \text{ for } \frac{1}{X_{tt}} > 0.1$$

$$\text{ELSE } F_c = 1 \quad (6-5)$$

It accounts for the increase in heat transfer which accompanies an increase in quality when the flow is in a purely evaporative mode. While $F_c(X_{tt})$ was developed empirically, Chen also showed that, through a Reynolds analogy,

$$F_c(\rho_L^2) = \left[\left(\frac{dp}{dz} \right)_{2\phi} / \left(\frac{dp}{dz} \right)_{LO} \right]^{.445} = [\rho_{Ltt}^2]^{.445} \quad (6-5b)$$

so that one finds F related to the pressure drop ratio. This latter ratio is itself correlated by X_{tt} as shown in the Martinelli-Nelson method. The empirical $F_c(X_{tt})$ of equation (6-7a) agrees closely with equation (6-7b) over most of the probable range of X_{tt} values when the original Martinelli-Nelson method is used [Be80].

The nucleate boiling contribution of equation (6-4) was postulated as:

$$a_{nbc} = a_n S_c$$

where a_n is derived from a pool boiling correlation. The suppression factor, S_c , accounts for the general suppression of nucleate boiling as flow rates and/or quality become large. It is derived from the consideration that the temperature field in flow boiling differs from that of pool boiling. The turbulent nature of the liquid film and the excellent heat transfer to the fast moving vapor core tend to reduce the temperature of the liquid near the wall, effectively preventing bubble growth. The suppression factor, S_c , was also determined empirically:

$$S_c = 1 / (1 + 2.53E-6 (Re_{LO} F_c^{1.25})^{1.17}) \quad (6-6a)$$

Chen selected the Forster-Zuber pool boiling relation for a_n :

$$a_n = .00122 \frac{\lambda_L^{.79} C_{pL}^{.45} \rho_L^{.49}}{\sigma^{.5} \mu_L^{.29} \Delta h_v^{.24} \rho_v^{.24}} \Delta T_{sat}^{0.24} \Delta P_{sat}^{0.75} \quad (6-6b)$$

$$= K_1 \Delta T_{sat}^{0.24} \Delta P_{sat}^{0.75} \quad (6-6c)$$

Since, by definition:

$$q_w = (a_e + a_{nbc}) \Delta T_{sat} = a \Delta T_{sat} \quad (6-7a)$$

$$= (a_e + a_n S) \Delta T_{sat} \quad (6-7b)$$

one can substitute (6-6c) into (6-7b) to get:

$$q_w = (\alpha_e + K_1 S \Delta T_{sat}^{0.24} \Delta P_{sat}^{0.75}) \Delta T_{sat} \quad (6-8)$$

The solution of the equation for q_w requires iteratively guessing values of ΔT_{sat} , calculating the nucleate boiling contribution, and either testing that the proper ΔT yields the given heat flux or interpolating graphically toward it [Co80].

6.2.2.1 Closed Form Solution for Chen's Method

Instead of iterating, a simple closed form solution can be found from the following: for small $\Delta T/T$ as is common for evaporating refrigerant applications, Clausius-Clapeyron can be used to eliminate the pressure difference term:

$$\Delta P_{sat}^{0.75} = \Delta T_{sat}^{0.75} \left(\frac{\Delta h_v}{T_{sat} \Delta v_v} \right)^{0.75} \quad (6-9)$$

Now if equation (6-9) is substituted into equation (6-8), then

$$q_w = (\alpha_e + K_2 \Delta T_{sat}^{0.99}) \Delta T_{sat} \quad (6-10)$$

where

$$K_2 = K_1 S \left(\frac{\Delta h_v}{T_{sat} \Delta v_v} \right)^{0.75}, \text{ and } \Delta T = \Delta T_{sat} \text{ for convenience}$$

Approximately $\Delta T^{1.99}$ by ΔT^2 , equation (6-10) becomes a simple quadratic for the unknown ΔT , the solution of which is

$$\Delta T = \frac{-a_e \pm \sqrt{a_e^2 + 4K_2 q_w}}{2K_2} \quad (6-11)$$

Only the positive root is meaningful physically. Substituting this root into (6-7a) gives

$$q_w = [a_e + K_2 \left(\frac{-a_e + \sqrt{a_e^2 + 4K_2 q_w}}{2K_2} \right)] \Delta T = [a_e + a_n] \Delta T \quad (6-12)$$

or, since $q_w = a\Delta T$, the bracketed term is the overall heat transfer coefficient; in simplified form:

$$a = \frac{a_e}{2} + \frac{\sqrt{a_e^2 + 4K_2 q_w}}{2} \quad (6-13)$$

All terms in this equation are known and a can be found directly, eliminating the iterative process. Though the derivation seems obvious, the author has never seen it in print.

6.2.3 Comparing Chen's Correlation to Experimental Data: Literature Review

When compared against the original data bank, Chen's formulation fit the data to an absolute mean deviation of 11 percent. This excellent agreement has been the principal source of the advocacy by the nuclear industry of Chen's method. However, when compared to measured heat transfer coefficients of flow boiling refrigerants, the method tends to underpredict badly in most cases [De78, Ch66a, Pu74], or on occasion

overpredict [e.g., Ch67 data]. Furthermore, the method tends to underpredict the quality dependence. Lastly, though Chen compared his method with five organic fluids, the maximum quality was 0.12. In this range, nucleate boiling dominates. The method then was not really tested in the range of interest to refrigerants. The poor prediction with refrigerants has been attributed by researchers for various reasons:

- (a) the convective contribution is underpredicted due to a negligence of a Prandtl number effect [Be80];
- (b) the nucleate boiling contribution is poorly predicted by the use of the Forster-Zuber correlation. Its contribution is underpredicted [To79] or overpredicted [Ka84] with organic liquids.

The two interpretations may then be directly opposed in trying to understand the physical heat transfer processes.

6.2.4 Modification to Nucleate Boiling Contribution in Chen's Method

Nearly all the terms in Chen's formulation have been suggested for revision. Butterworth and Shock [Bu82] suggested that a different pool boiling relation be used in equation (6-5). They recommended a recent correlation by Stephan and Auracher [St81] which includes the fluid's wetting characteristics and was specialized to various fluid classifications (refrigerants, water, cryogenic fluids, etc.). For the pool boiling of refrigerants, Stephan and Abdelsalam recommended [St80]:

$$\frac{q_{\text{pool}}}{\lambda_L} = 207 \left(\frac{q_d}{\lambda_L L_s} \right)^{.745} \left(\frac{\rho_v}{\rho_L} \right)^{.581} \text{Pr}_L^{.533} \quad (6-14)$$

which Stephan and Auracher modified to include the effect of forced convection:

$$\frac{a_n}{a_{pool}} = 2.9 \left[\frac{\dot{m}D(1-x)}{\mu_L} \right]^{-0.3} \left[\frac{\dot{m}^2(1-x)^2}{\rho_L^2 gD} \right]^{0.2} \quad (6-15)$$

where the bracketed terms are Reynolds and Froude numbers, respectively. The forced convection modification is actually based on Chawla's supposition [Ch67].

Either (6-14) or (6-15) could replace the Forster-Zuber relation in Chen's correlation. Alternately, another nucleate boiling correlation could be used, such as that of Vaihinger [Va79] who correlated recently various pool boiling refrigerant data for a wide range of reduced pressures to within ± 15 percent.

6.2.5 Modification of Forced Convection Contribution

Bennett and Chen recommended recently a modification of the F function for fluids with $Pr_L > 1$ (refrigerants have $2 < Pr_L < 5$) [Be80]. Recalling equation (6-5), they noted the Reynolds analogy used in Chen's original development was valid strictly for $Pr_L = 1$. Bennett and Chen proposed various Prandtl number corrections, the best fitting their data with

$$F_{BC} = \left(\frac{Pr_L + 1}{2} \right)^{0.445} \left(\frac{(dP/dz)_{TPf}}{(dP/dz)_{LO}} \right)^{0.445}$$

$$\approx \text{Pr}_L^{0.296} (\rho_{Ltt}^2)^{.445} \quad (6-16)$$

The frictional pressure drop ratio is to be predicted on a 'best available' basis; commonly this selection is the Martinelli method (and referred by Bennett and Chen as a reasonable approach).

For $\text{Pr}_L > 1$, the recommended modification has the effect of increasing the evaporative and decreasing the nucleate boiling contributions. Development of the Prandtl number correction assumed that ebullition destroys the viscous sublayer. If nucleate boiling is suppressed completely, Bennett and Chen recommend deletion of the Prandtl number correction.

6.2.6 Modification of Suppression Factor

An alternative that has recently been proposed changes the suppression factor. Bennett et al. derived a semi-analytical formulation for S , given as [Be80a]:

$$S_B = \frac{\lambda_L}{a_{LO} Fz} \left(1 - \exp \left(\frac{-a_{LO} Fz}{\lambda_L} \right) \right) \quad (6-18)$$

$$\text{where } z = 0.041 \left(\frac{\sigma}{g(\rho_L - \rho_v)} \right)^{1/2}$$

The only empirical value is 0.041.

6.2.7 Other Modifications to Chen's Method

Polley [Po82] has recently developed a modification to Chen's method with the following characteristics:

- (a) a simpler pool boiling relation
- (b) a criterion to exclude the nucleate boiling contribution if there is insufficient superheat
- (c) a suppression factor based on the magnitude of the pool and evaporative contributions, rather than the flow parameters used in Chen's method

The suppression factor was optimized empirically from a large set of water-steam data. The method produced improved agreement with this data base. His equations are given in Appendix 6B.

6.2.8 Application of Modifications to Chen's Correlation

The previous sections have described several modifications to Chen's original method; prior to this report, none has been applied independently of the data base used by the authors of these modifications. It is interesting to note that virtually every term except the Dittus-Boelter equation used in Chen's original method has been recommended for change.

Considerable care must be taken in testing the changes suggested in the previous sections, as will be shown. Chen's original superposition employed the Forster-Zuber pool boiling relation where $\alpha_{pool} = \alpha_{FZ} = f(\Delta T) = f(T_w - T_{sat})$. This approach is different systematically than $\alpha_{pool} = f(q)$ as suggested by equation (6-14). The pool boiling heat transfer coefficient of Forster and Zuber is:

$$\alpha_{FZ} = C_{FZ} \Delta T^{0.99} \quad (6-19)$$

where $C_{FZ} = C_{FZ}$ (properties), and which may be found by comparison to equation (6-10). By examination of equation (6-10) or (6-11), it can be seen that, for a fixed total heat flux, the calculated ΔT is lowered by the presence of forced convection over that which would occur in pool boiling alone. Consequently, because of the form of equation (6-11), the nucleate boiling contribution is seen to be lower than for the pool boiling beyond that accounted by the suppression factor. Put another way,

$$q_w = q_{fc} + q_{nbc} = \alpha_L F \Delta T + C_{FZ} \Delta T^{1.99} S \quad (6-20)$$

so that $q_{nbc} = q_w$ only in the case of no flow. In contrast, the approach suggested by the use of equation (6-14) implies $q_{nbc} = q_w$. In Polley's development, this problem is resolved due to the reoptimization of the suppression factor.

To use (6-14) in Chen's method, the equation must be reformulated in terms of $\alpha_{SA} = f(\Delta T)$, as follows:

$$\alpha_n = \alpha_{pool} = \alpha_{SA} = C_{SA} q_w^{.745} \quad (6-21)$$

where C_{SA} can be found by comparison to equation (6-14). For pool boiling alone,

$$q_{\text{pool}} = \alpha_{\text{SA}} \Delta T = (C_{\text{SA}} q_{\text{pool}}^{.745}) \Delta T$$

upon eliminating q_{pool}

$$\alpha_{\text{SA}} = C_{\text{SA}}^{3.2916} \Delta T^{2.9216} \quad (6-22)$$

This result can now be substituted into equation (6-3) to get

$$\alpha = \alpha_L F + C_{\text{SA}}^{3.9216} \Delta T^{2.9216} S \quad (6-23)$$

and

$$q = \alpha \Delta T = (\alpha_L F + C_{\text{SA}}^{3.9216} \Delta T^{2.9216} S) \Delta T \quad (6-24)$$

This equation must be solved iteratively for ΔT , and consequently α , in the case of constant wall flux. Thus, the suggested modification of Butterworth and Shock, which might yield more accuracy, pays the cost of increased computational difficulty.

6.3 Experimental Results: Comparison to Measured Data

Recall Table 5-1 for the summary of the data base characteristics.

Table 6-4 displays the many variations of Chen-styled methods which were considered in the analysis.

These characteristics must be considered in the analysis of the predictive ability of correlations.

Table 6-3 displays the results of comparing many of the methods to the experimental results. All methods are compared to the data according to the mean fractional standard deviation:

$$\bar{\sigma} = \frac{\sum_{i=1}^N |(a - a_{\text{meas}})/a_{\text{meas}}|}{N}$$

The best two prediction methods are circled in Table 6-3.

6.3.1 Comparison to Rig #1, R152a Data (Forced Convection/Evaporation Dominant)

All of the form (6-1) equations predict badly. The method of Traviss et al. is derived from condensation research. It underpredicts due most likely to different entrainment rates in evaporation and condensation.

Of the many Chen-styled correlations, the evaporative portion of Chen's original formulation with F_c being empirical and Chen's original formulation with the reformulated Stephan-Abdelsalam method (based on equation (6-24)) predict best. Figure 6-2 displays the variation of a with quality for some of the Chen-styled correlations. Again, the two methods mentioned above predict the slopes very well, though sometimes the magnitude of a is in error. It is interesting to note that Chen's original method overpredicts the measured values. Overprediction with refrigerants has only occurred in one other instance [Ch67].

6.3.2 Comparison of Rig #2 Preheat Data (Nucleate Boiling Dominant)

This data base consisting of about 200 points, includes heat fluxes ranging from 10 to 95 kW/m² and mass fluxes of 100 to 500 kg/sqm/s.

Table 6-3 displays the predictive ability of various correlations against both pure R152a and pure R13B1. None of the form (6-1) correlations do well. Since nucleate boiling is the dominant feature, one might expect pool boiling relations to perform well. The correlation of Stephan and Abdelsalam (equation 6-14) predicts exceptionally well with the data within ± 20 percent and most predictions within 5 to 10 percent. Since equation (6-14) was developed from a large refrigerant data base, the results are pleasingly consistent. Refrigerant R152a was not considered in the authors' equation development, so the experimental data extends the verification of the predictive ability of the method. The effects of mass flux and quality are not accounted by equation (6-14). Equation (6-15) is the attempt made by Stephan and Auracher to account for mass flux and quality. It however overestimates their effect.

After eliminating the film boiling data for R13B1, the remaining data of Rig #1 was seen to be dominated by nucleate boiling. As shown on Table 6-3, the measured values are predicted best by the same pool boiling relations as R152a, adding further verification to the method.

6.3.3 Comparison of Rig #2 Test Section Data (Forced Convection Dominant - Some Nucleate Boiling Contribution Possible)

Again, none of the Form (6-1a) methods predict either the slope da/dx nor the magnitude of α well. The best prediction techniques are those when the Prandtl number correction suggested by Bennett and Chen is combined with the empirical F function:

$$\alpha_e = \alpha_{LO} F_c(X_{tt}) Pr_L^{0.296}$$

and the nucleate boiling contribution is that of Stephan and Abdelsalam (equation 6-24). Figure 6-4 displays the results. There is a larger error, but greater uncertainty with the R13B1 data (section 3.8). If the measured values were based on measured outlet temperature, the R13B1 agreement with the above equation would be superior.

By using equation (6-24) and the Prandtl correction, the nucleate boiling contribution is nearly negligible. Agreement is excellent even when excluding the nucleate boiling contribution (methods (w) and (x) on Table 6-3).

6.4 Discussion of Findings

6.4.1 Nucleate Boiling Dominated Flow Situations

It was found that little or no mass flux correction was needed to fit the data in this situation. Inclusion of the mass flux correction suggested by Chawla and adopted by Stephan and Auercher degraded the predictive ability of the pool boiling correlation of Stephan and Abdelsalam (equation 6-14). In their original paper, Stephan and

Auracher examined eight refrigerant data bases (three with R11, three with R12, one with R22 and one with R114). The R11 data was provided by Chawla, so the forced convection modification, derived from his data, should be expected to fit the data well. Two of the remaining five data bases are not as well predicted.

Further, Vaihinger noted no influence of mass flux in his results, nor has Muller, has Brauer [Va79]. On the other hand, [Ma79] data clearly has a mass flux effect.

The mass flux correction (equation 6-15) has a dependence on tube diameter; though the dependence is weak, there is no physical reason for any functional relation. Also, the heat transfer coefficient is inversely proportional to quality. It agrees with various observations in the literature [Ch67, Ma76, St82] of a heat transfer coefficient reaching a minimum before convective/evaporative processes grow and dominate. Such behavior is also observed with some of the Rig #1 data when it is dominated by nucleate boiling.

Chen-styled correlations explicitly include a forced convection effect, even with small flow rates. The influence of mass flux diminishes as heat flux increases (i.e., as α_{pool} increases). It establishes a proper trend, but never reduces the mass flux effect to zero. It suggests as quality increases, mass flux effects increase in influence, the opposite of Chawla's supposition.

The predictive ability of the complete Chen-styled correlations developed from the literature was not good for this heat transfer regime. The best prediction came with using $\alpha_{\text{pool}} = \alpha_{\text{SA}}(q)$, i.e., using equation (6-14) in conjunction with equation (6-3). As previously discussed, this is an incorrect application of the pool boiling relation in Chen's method. Furthermore, use of the Forster-Zuber pool boiling method instead of the Stephan-Abdelsalam method in Chen's formulation revealed dramatic differences in the predicted α . In their original pool boiling form, the methods are compared in Figure 6-3a. Forster and Zuber underpredicts α at large heat fluxes, e.g., $\alpha_{\text{FZ}} < \alpha_{\text{SA}}$. However when these formulas are used in Chen's method with $\alpha_{\text{pool}} = \alpha_{\text{pool}}(\Delta T)$, their relationship is reversed (Figure 6-3b). The Stephan and Abdelsalam method predicts a larger nucleate boiling contribution. This is due to the methods having a different functional dependence on ΔT .

It is clear that since the original Chen formulation of 1966, progress has been made in predicting pool boiling heat transfer and that the improved capability has as a prerequisite the specification of fluid classifications (and surface characteristics). Given the pool boiling progress, it may be useful to reformulate the suppression factor in Chen's method to improve its overall predictive ability. Any reformulation should allow the forced convection term to diminish in influence to near zero, as shown in the experimental data.

The issue of the influence of mass flux is not settled. It has been observed to be negligible in some cases and apparently not in others.

The predictive ability is not available to determine conditions when a mass flux correction term is needed.

6.4.2 Forced Convection Dominated Flow Situations

None of the form (6-1a) equations fit the data well; this result is not surprising since rarely have they produced satisfactory agreement with data sets other than the ones for which they were originally developed.

The original Chen correlation badly predicted da/dx slopes. This is consistent with many other researchers' findings. The nucleate boiling contribution is overestimated in this flow situation. It is interesting to note that the method overpredicts the Rig #1 data and generally underpredicts the Rig #2 data. Underprediction of refrigerant heat transfer coefficients is more common, although the method has overpredicted in at least one instance [De78].

The use of the analytic form of the F-function (equation (6-5)) degraded the predictive ability. The analytic form $F = F_c(\Delta P)$ has a higher value than the empirical $F = F_c(X_{tt})$ at values of $1/X_{tt} < 2$ corresponding to low quality. It overpredicts in this region. At high quality, the methods nearly agree, and it makes little difference. In general the empirical F was slightly more accurate.

Of the multiple Chen-styled correlations, none fit both the Rig #1 and Rig #2 results. Best agreement with Rig #1 data (R152a only) was achieved including the Stephen-Abdelsalam relation with Chen's original

formulation (equation (6-24)). This approach requires iteration, however, adding to the complexity. Further, it produced poor agreement with both Rig #2 results and importantly the nucleate boiling dominated results previously discussed. In general the agreement with da/dx is good for the Chen predictions without the nucleate boiling contribution.

Best agreement with the Rig #2 data also used the Stephan-Abdelsalam method, but included a Prandtl number correction suggested by Bennett and Chen. The question then naturally arises as to how to predict the need for the Prandtl number correction. An approach is discussed in the next section.

6.4.3 A Complete Correlation

In the previous sections, it was seen that no single correlation fit all the data. However, a particular correlation predicted well in certain situations. In this section, a criterion/procedure will be established which determines when to use a particular correlation.

Following Chawla's suggestion [Ch67], one can determine the heat transfer regime and α by:

$$\alpha = \alpha_{\text{pool}} \quad \text{if } \alpha_{\text{pool}} > \alpha_{\text{FC}}^* \quad (6-25)$$

$$= \alpha_{\text{FC}}^* \quad \text{if } \alpha_{\text{FC}}^* > \alpha_{\text{pool}}$$

The previous sections showed that, at low pressure, when nucleate boiling was completely suppressed, the two best predictive methods were:¹

$$a_{FC}^* = a_{LO}^{F_c}(X_{tt}) + C_{SA}^{3.9216} \Delta T^{2.9216} S \quad [\bar{\sigma} = 0.07] \quad (6-26a)$$

and

$$a_{FC}^* = a_{LO}^{F_c}(X_{tt}) \quad [\bar{\sigma} = .212] \quad (6-26b)$$

At higher pressures, where some nucleate boiling contribution was observed (Chapter 4), the best predictions were with

$$a_{FC}^* = a_{LO}^{F_c}(X_{tt}) Pr_L^{0.296} + C_{SA}^{3.9216} \Delta T^{2.9216} S \quad [\bar{\sigma} = 0.055] \quad (6-27a)$$

and

$$a_{FC}^* = a_{LO}^{F_c}(X_{tt}) Pr_L^{0.296} \quad [\bar{\sigma} = 0.057] \quad (6-27b)$$

The difference between the two methods is the Prandtl correction, which is substantial. To determine when to include the correction, the suppression criterion of Chapter 4 is recommended as the determinant. If the given wall flux is greater than that predicted by the suppression criterion, then equation (6-27a) or (6-27b) should be used. Alternately

¹The pool boiling relation to be used is that of Stephen and Abdelsalam (equation (6-14)).

if the suppression criterion predicts insufficient heat flux, equation (6-26a) or (6-26b) should be used.

Although equation (6-26a) was superior to (6-26b), one might question on theoretical grounds its use. If the data is in fact representative of a completely suppressed nucleate boiling heat transfer regime, then there is no reason to include the nucleate boiling term. In defense of its inclusion, two reasons might be offered:

- (a) The original Chen development/optimization presumed contributions from both regimes, so that F was not optimized for complete suppression.
- (b) The suppression criterion predicts ebullition from large cavities even with very little superheat available. The large cavities may then be 'active' but too few in number to destroy the viscous sublayer (and require the Prandtl number correction). The fact that some cavities are active may justify the inclusion of the nucleate boiling term.

If the nucleate boiling term is included, however, there is an inherent contradiction. With more substantial ebullition (e.g., higher q_w), the Prandtl number correction is invoked, and the evaporative contribution is increased at the expense of the nucleate boiling contribution. Thus while one would expect α_n to be greater at higher q_w ($q_w > q_{sup}$), it may in fact be reduced.

Because of this reason and others to be discussed below, the author prefers the use of equation (6-26b) in the case when $q_w < q_{sup}$. When combined with the criterion of equation (6-25), $\sigma = 0.122$ for Rig #1;

this value is superior to every other method, and yields better agreement than appears in much of the literature for heat transfer correlations.¹

Equation (6-27b) yields nearly as good agreement as (6-27a).

Elimination of the nucleate boiling contribution, though not correct theoretically, offers the practical benefit of a non-iterative solution. The prediction is also more conservative without the nucleate boiling term. The use then of (6-26b) and (6-27b) with the criterion of (6-25) is therefore recommended.

6.4.4 A Comparison with Other Data

As a further test of the approach, spot checks were done against other refrigerant data in the literature.

Heat transfer coefficients for R22 were measured by at least three different authors ($Pr_L \approx 2.5$). Their data is shown on Figure 6-6, with equation (6-27b). The need for the Prandtl correction for the Anderson and Mathur/Chaddock data was supported by an examination of their raw data. The Anderson data is predicted very well; it is known that it excludes dryout data. The Mathur/Chaddock data is predicted very well in the low and middle quality range. At high quality, the approach slightly overpredicts: however this data is for dryout conditions. At low quality, the data exhibits considerable scatter. The scatter is due to the effect of heat flux, neglected by [Ch79]. The use of equation

¹Figure 6-5 shows the results of using the criteria.

(6-25) would have improved agreement in this region; however property values were not available to perform the calculation.

Chaddock and Noerager measured R12 ($Pr = 3.1$) and fit the average α to $\pm 15\%$ with

$$\alpha = \alpha_{LO}(3/X_{tt}) \quad 0.2 < X_{tt} < 0.5$$

Again, their data showed a fairly strong heat flux dependence, so equation (6-27b) is appropriate. Agreement is fair: -30% for $X_{tt} = 0.2$ and -2% at $X_{tt} = 0.5$. The underestimates may be due to the effect of heat flux.

Recall that only one data set from the literature [Ch67] was badly overpredicted by the Chen correlation. However, the data of Chawla exhibited no heat flux dependence. In this case, equation (6-26b) is the correct one for use, and reduces the prediction by more than 50%. This will place the prediction in the appropriate range.

6.5 Closing Remarks: Conclusions and Recommendations

A large data base was developed which included data from all possible heat transfer regimes. A comparison was made between published correlations and the data base. All form (6-1) correlations, widely used in the refrigeration industry, predicted poorly. The result is not surprising as they have tended in the past to suffer from a lack of generality. The new Shah correlation also predicted badly.

In the nucleate boiling dominated regime, a recent pool boiling correlation (equation (6-14)) predicted exceptionally well. A correction for forced convection was unnecessary and its inclusion degraded the agreement. Therefore, a criterion is needed for predicting the onset and amount of a mass flux influence. The Chen correlation implicitly includes one which is not correct. Forced convection should be allowed to have little or no influence in certain cases.

The forced convection dominated regime was predicted best by Chen's original method modified to include equation (6-14) for the Rig #1 data. A Prandtl number correction was needed to achieve good agreement with the Rig #2 data. The discrepancy between the results is believed due to sustained ebullition. A criterion was developed to determine when to apply the Prandtl number correction.

The complete Chen styled correlation is the most widely used method outside the refrigerant industry for predicting heat transfer coefficients. The literature has shown it to predict poorly for organic fluids with blame placed and corrections suggested on various terms of the original correlation. None of these corrections however had been checked prior to this report. All changes suggested in the literature were tested, alone and in combination. Certain forms of the correlation predicted well. A procedure was developed to determine when to apply the various forms. It was shown that the superposition principle could be abandoned in favor of a single dominant mode (either nucleate boiling or evaporation). In this respect, it draws upon the success of Shah,

Chawla, and portions of Polley. It also eliminates the need for iteration. It includes the recent suggestion by Bennett and Chen for a Prandtl number correction.

If one chose to retain the complete Chen styled correlation, virtually every term in the original formulation (equation (6-3)) could be changed to improve agreement. As such each term will be discussed separately.

To date no one has suggested revising the q_L term in equation (6-3). Yet, the Dittus-Boelter relation is accurate to ± 13 percent, so that agreement between two-phase (evaporative only) data and prediction may be limited to this range of uncertainty. More accurate single-phase relations are available, e.g., Petukhov's method [Pe70] which is believed to be accurate to ± 5 to 6 percent. This could be used without adding much complexity since it is non-iterative.

In this chapter, a closed form solution was derived for Chen's original method. Thus, iterative solutions, as suggested in recent texts, may be discarded for conditions away from the critical point. The original method employed the Forster-Zuber pool boiling correlation. However, substantial progress has been made in pool boiling since the Forster-Zuber development. It has been found that the best correlations for pool boiling are fluid-specific, i.e., classes of fluid such as refrigerants require their own empirical correlations. The pool boiling predictive ability of Forster and Zuber's relation is poor when applied to refrigerants.

The use of an analytic F-function, such as that found through Reynolds analogy, suffers from the practical lack of predicting closely the pressure drop. Available pressure drop correlations such as Martinelli-Nelson predict refrigerants to at best $\pm 20\%$. This uncertainty combined with the uncertainty of predicting single-phase heat transfer coefficients yields an overall uncertainty of at least ± 25 percent in predicting α in the simplest case of evaporation without nucleate boiling. The use of the empirical F-function in Chen's original supposition produced better agreement with the measured data. Future work might concentrate on improving pressure drop correlations, perhaps treating separately the cases of nucleate boiling and evaporation.

The semi-analytical S-function developed by Bennett et al., aggravated the overprediction of the nucleate boiling contribution. This represented the first test of their approach. Since F and S were developed empirically, and since it has been shown that pool boiling predictions are specialized to classes of fluids, a reoptimization of the F and S functions for refrigerants is recommended with:

- a) α_{LO} derived from Petukhov
- b) $\alpha_n = \alpha_{pool}$ from Stephan and Abdelsalam, kept in its original form to escape the need for iteration
- c) a criterion included to eliminate forced convection effects ($F=0$) in some cases
- d) a criterion included to eliminate nucleate boiling effects ($S=0$) in some cases, and
- e) a large data base of similarly determined experimental data (i.e., all with subcooled inlet, or all with two-phase inlet) over a wide pressure and heat flux range.

Finally the experimental data existent in the literature should be more closely analyzed and stratified by experimental technique. If this is done, improved predictive ability will likely be achieved. The author also hopes that the complete correlation outlined in Section 6.4.3 will be tested further.

Table 6-1: Some Simple Correlations for Flow Boiling of Pure Refrigerants

Form 6-1a: $A_1(Bo)^{C_1} + A_2(1/X_{tt})^{C_2} = \alpha/\alpha_{LO}$

A_1	C_1	A_2	C_2	Authors
--	--	3	1	Chaddock and Noeranger [Ch66]
6700	1	23.45	0.66	Collier and Pulling [Co64]
--	--	3.5	0.5	Dengler and Addoms [De56]
(English Units)		$0.64q^{.11}$	0.74	Bennett et al [Be63]

Miscellaneous References and Relevant Refrigerants

o Lavin and Young [La67]	R12
o Shah [Sh76, Sh82]	many
o Dembi et al [De78]	many
o Kandlikar [Ka84]	many
o Chaddock and Mathur [Ch79, Ma79]	R22
o Stephan and Auracher [St81]	many
o Chawla [Ch67]	R11
o Bendel and Schlander [Ba74]	R12
o Rhee and Young [Rh72]	R12, R22
o Pierre [Pi56]	R12
o Singal et al [Si83]	R13

Table 6-2: Simple Correlations for Average Heat Transfer of Flow Boiling Refrigerants

$$\alpha \sim m^{\cdot C_3} q^{\cdot C_4} d^{\cdot C_5}$$

Authors	C ₃	C ₄	C ₅	Refrigerants
<hr/>	<hr/>	<hr/>	<hr/>	<hr/>
Danilova [Da69]	0.5	0.5	-1	R11
Aljarrah and Duminil [Al77]	0.25	0.55	-.2	R12, R22, R502, R13 B1
Riedle and Purciple [Pu72]	0	0.7	-.6	R11, R12, R113
Slipevic [Sl70]				
high m	1.4	0	-.54	many
low m	0.1	0.7	-.54	many
Bogdanov	0.2	0.6	-.6	R11, R12, R22, R113

[reprinted from [Bu82]]

METHOD Form 6-1a	EVAP. PORTION	NUC. PORTION	152a	13B1	Preheat		Test Section	
					152a	13B1	152a	13B1
(A) Chaddock/Noerager	See Table 6-1	--	0.404	0.347	0.37	0.224	0.371	0.308
(B) Collier and Pulling	See Table 6-1	See Table 6-1	0.212	0.181	0.276	0.16	0.365	0.352
(C) Danglar and Addome	See Table 6-1	See Table 6-1	0.358	0.281	0.355	0.193	0.165	0.139
(D) Bennett et al	See Table 6-1	See Table 6-1	0.366	0.61	0.696	0.638	0.591	0.611
(E) Travlee et al	--	--	0.29	0.405				
Form 6-1b								
(F) Levin and Young			0.199	0.195	0.411	0.246	0.234	0.191
Pool Boiling Methods								
(G) Stephan and Abdelaleem	--	$a_{SA}(q)$	0.282	0.167	0.055	0.142		
(H) Forster and Zuber	--	$a_{FZ}(q)$	0.142	0.189	0.14	0.162		
Form 6-1c								
(I) Chen Original	$F_c(X_{tt})$	a_{FZ}	0.276	0.197	0.124	0.163	0.143	0.143
(J) Bennett and Chen Original	$F_c(\theta_L) \cdot Pr_L^{0.296}$	a_{FZ}	0.779	0.153	0.112	0.151		
(K) Bennett and Chen $Pr_L^{0.296}$	$F_c(X_{tt}) \cdot Pr_L^{0.296}$	a_{FZ}					0.092	0.102
(M) Chen Original	$F_c(\theta_L)$	a_{FZ}	0.419	0.191				
(N) Chen and Stephen (Q)	$F_c(X_{tt})$	$a_{SA}(q)$	0.249	0.125	0.078	0.133		
(O) Chen and Stephen (AT)	$F_c(X_{tt})$	$a_{SA}(\Delta T)$	0.07	0.305				
(P) Bennett and Stephen (Q)	$F_c(\theta_L) Pr_L^{0.296}$	$a_{SA}(q)$	0.839	0.137	0.107	0.144		
(Q) Bennett and Stephen (AT)	$F_c(\theta_L) Pr_L^{0.296}$	$a_{SA}(\Delta T)$	0.615	0.213				
(R) Bennett and Chawla (Q)	$F_c(\theta_L) Pr_L^{0.296}$	$a_{SA}(q)$	1.1	0.169	0.407	0.269		
(S) Chen and Stephen (AT, Pr_L) ³	$F_c(X_{tt}) Pr_L^{0.296}$	$a_{SA}(\Delta T)$					0.055	0.155
(U) Chen (X_{tt}) and Bennett S	$F_c(X_{tt}) Pr_L^{0.4}$	$a_{FZ} \cdot S_B$					0.101	0.099
(V) Chen Orig.-Evap. Only	$F(X_{tt})$	--	0.212	0.547	0.643	0.546		
(W) Chen $Pr_L^{0.296}$ - Evap. Only	$F(X_{tt}) \cdot Pr_L^{0.296}$	--			0.363	0.21	0.057	0.164
Complete Correlation								
(Y) Higher of (I) or (O)			0.068	0.167			0.055	
(Z) Higher of (I) or (V)			0.122	0.167				

Table 6-4: Summary of Chen-Styled Methods

$$\alpha = \alpha_{LO} F + \alpha_n S$$

$$\alpha_{LO} = 0.023(\lambda_L/D)(G(1-x)/\mu_L)^{0.8} Pr_L^{0.4}$$

METHOD	F	α_n	S	As Shown on Table 6-3
Chen Original	$F_c(X_{tt})$ (6-5a)	$\alpha_{FZ}(\Delta T)$ (6-6a)	$S_c(F)$ (6-5c)	I
Bennett and Chen Original	$F_c(\rho_L^2) Pr_L^{0.296}$ (6-15)	$\alpha_{FZ}(\Delta T)$ (6-6a)	$S_c(F)$ (6-5c)	J
Bennett and Chen Empirical F	$F_c(X_{tt}) Pr_L^{0.296}$ (6-26b)	$\alpha_{FZ}(\Delta T)$ (6-6a)	$S_c(F)$ (6-5c)	K
Chen, Analytic F	$F_c(\rho_L^2)$ (6-5a)	$\alpha_{FZ}(\Delta T)$ (6-6a)	$S_c(F)$ (6-5c)	M
Chen with Stephan's Pool Boiling Method	$F_c(X_{tt})$ (6-5a)	$\alpha_{sa}(q)$ (6-13)	$S_c(F)$ (6-5c)	N
Chen with Reformulated Stephan Method	$F_c(X_{tt})$ (6-5a)	$\alpha_{sa}(\Delta T)$ (6-21)	$S_c(F)$ (6-5c)	O
Bennett/Chen with Stephan's Method	$F_c(\rho_L^2)^{0.296}$ (6-15)	$\alpha_{sa}(q)$ (6-13)	$S_c(F)$ (6-5c)	P
Bennett/Chen with Reformulated Stephan	$F_c(\rho_L^2)^{0.296}$ (6-15)	$\alpha_{sa}(\Delta T)$ (6-21)	$S_c(F)$ (6-5c)	Q
Bennett/Chen with Stephan/Chawla	$F_c(\rho_L^2)^{0.296}$ (6-15)	$\alpha_{sa}(Q) \cdot C_{Ch}$ (6-13)	$S_c(F)$ (6-5c)	R
Same as Q, but with Empirical F	$F_c(X_{tt}) Pr_L^{0.296}$ (6-21b)	$\alpha_{sa}(\Delta T)$ (6-21)	$S_c(F)$ (6-5c)	S
Same as S, but with $Pr_L^{0.4}$	$F_c(X_{tt}) Pr_L^{0.2956}$	$\alpha_{sa}(\Delta T)$ (6-21)	$S_c(F)$ (6-5c)	T
Same as K, but with Analytic S	$F_c(X_{tt}) Pr_L^{0.296}$ (6-21b)	$\alpha_{FZ}(\Delta T)$ (6-6a)	S_B (6-16)	U
Chen Original (Evaporative Contribution Only)	$F_c(X_{tt})$ (6-5a)	—	—	V
Bennett and Chen (Evaporative Only)	$F_c(X_{tt}) Pr_L^{0.296}$ (6-26b)	—	—	W

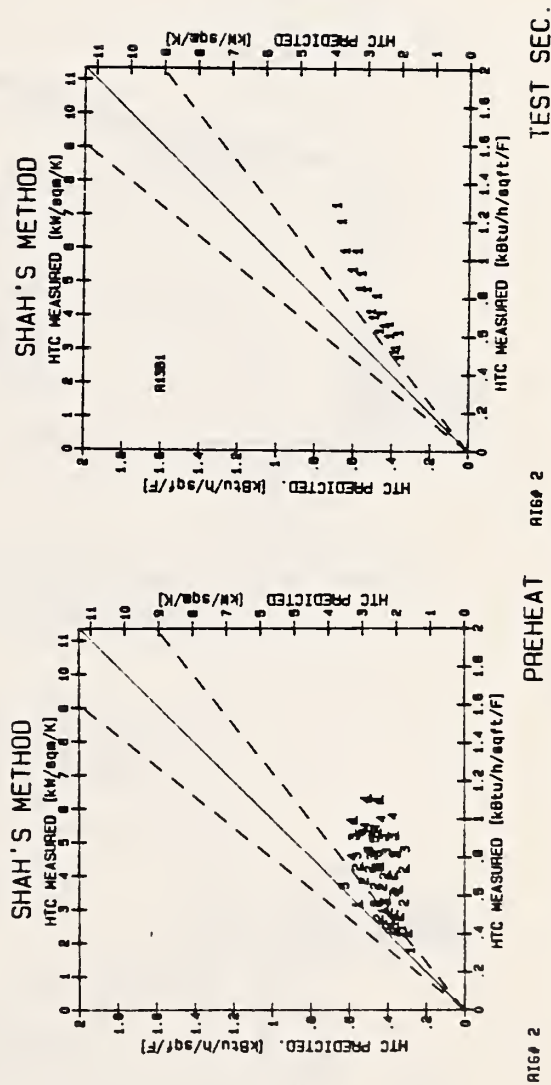
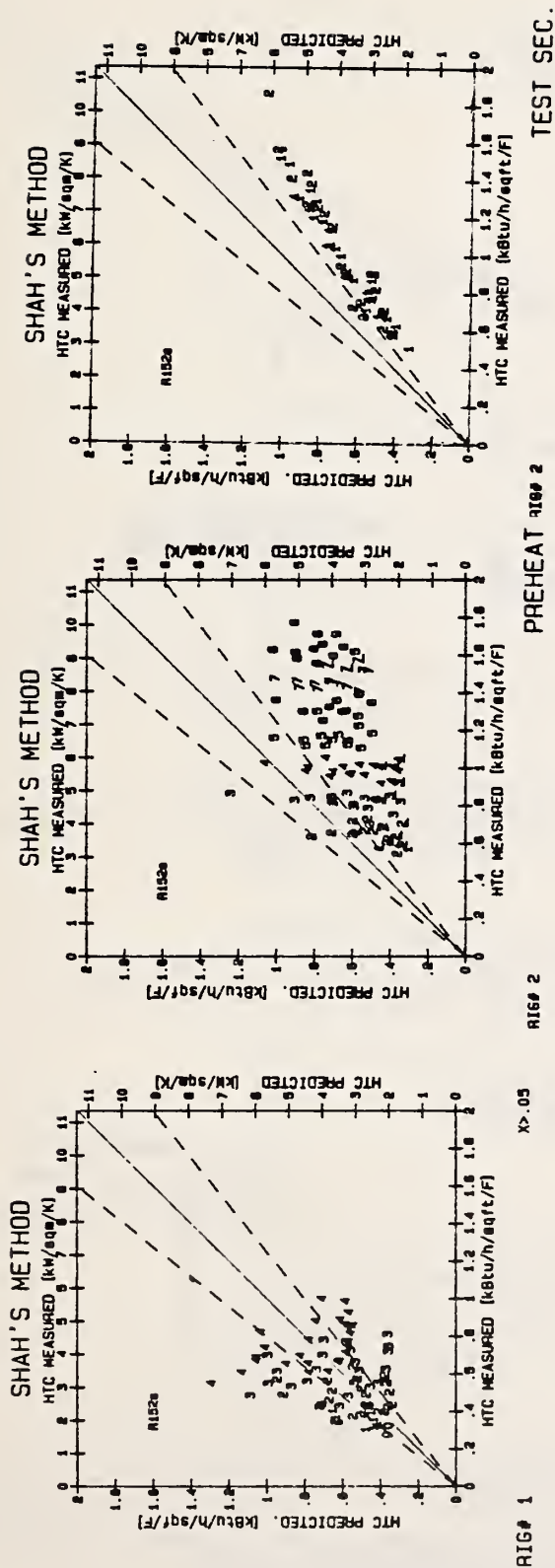


Figure 6-1: Comparison of Shah's Method to Experimental Data. Error bars are for $\pm 20\%$.² The numbers 1 through 9 indicate heat flux levels ($1: 10000 \text{ W}/\text{m}^2$, $2: 90000 \text{ W}/\text{m}^2$). The underscoring numbers are for half step increments ($1: 15000 \text{ W}/\text{m}^2$).

F FUNCTION: EMPIRICAL AND ANALYTICAL

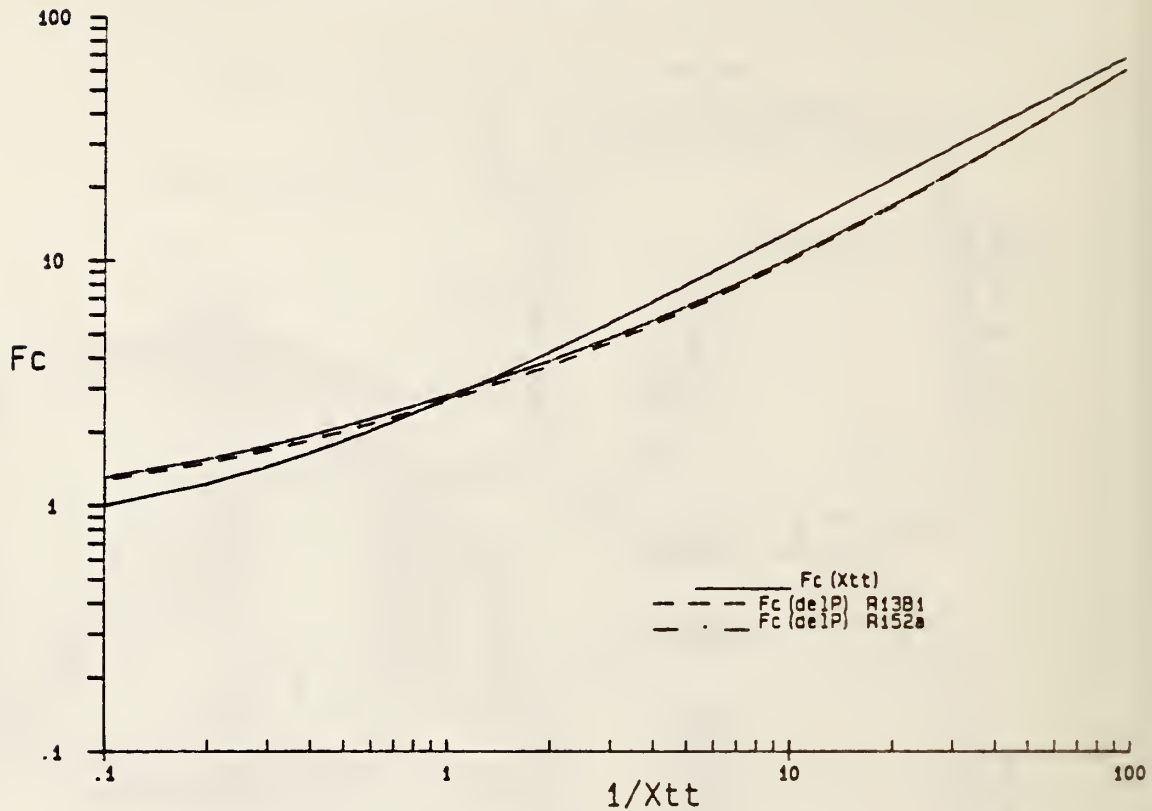
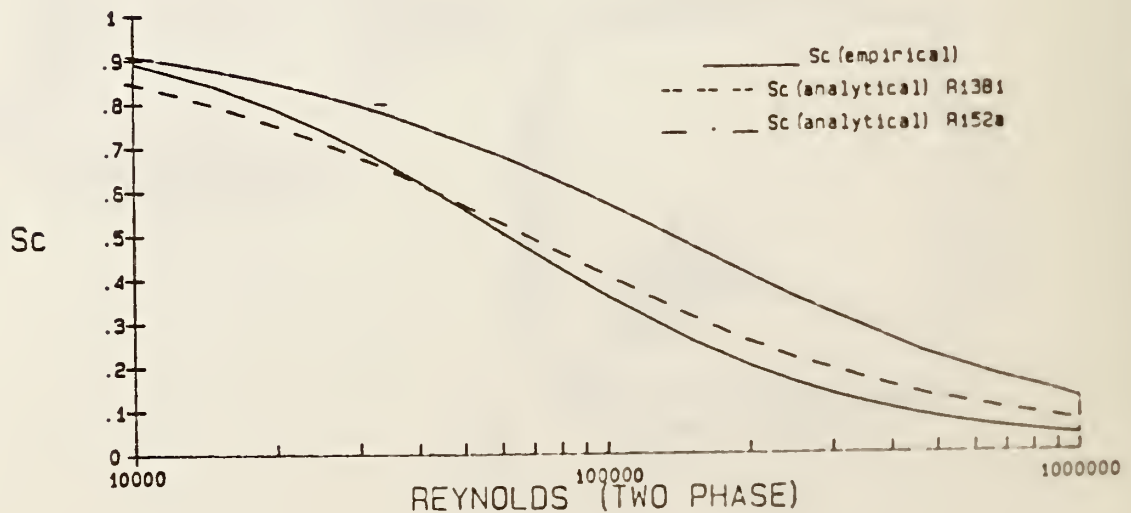


Figure 6-2: Comparison of Empirical and Analytical Functions in Chen's Method. Pressure= 4.75 bar.

S FUNCTION: EMPIRICAL AND ANALYTICAL



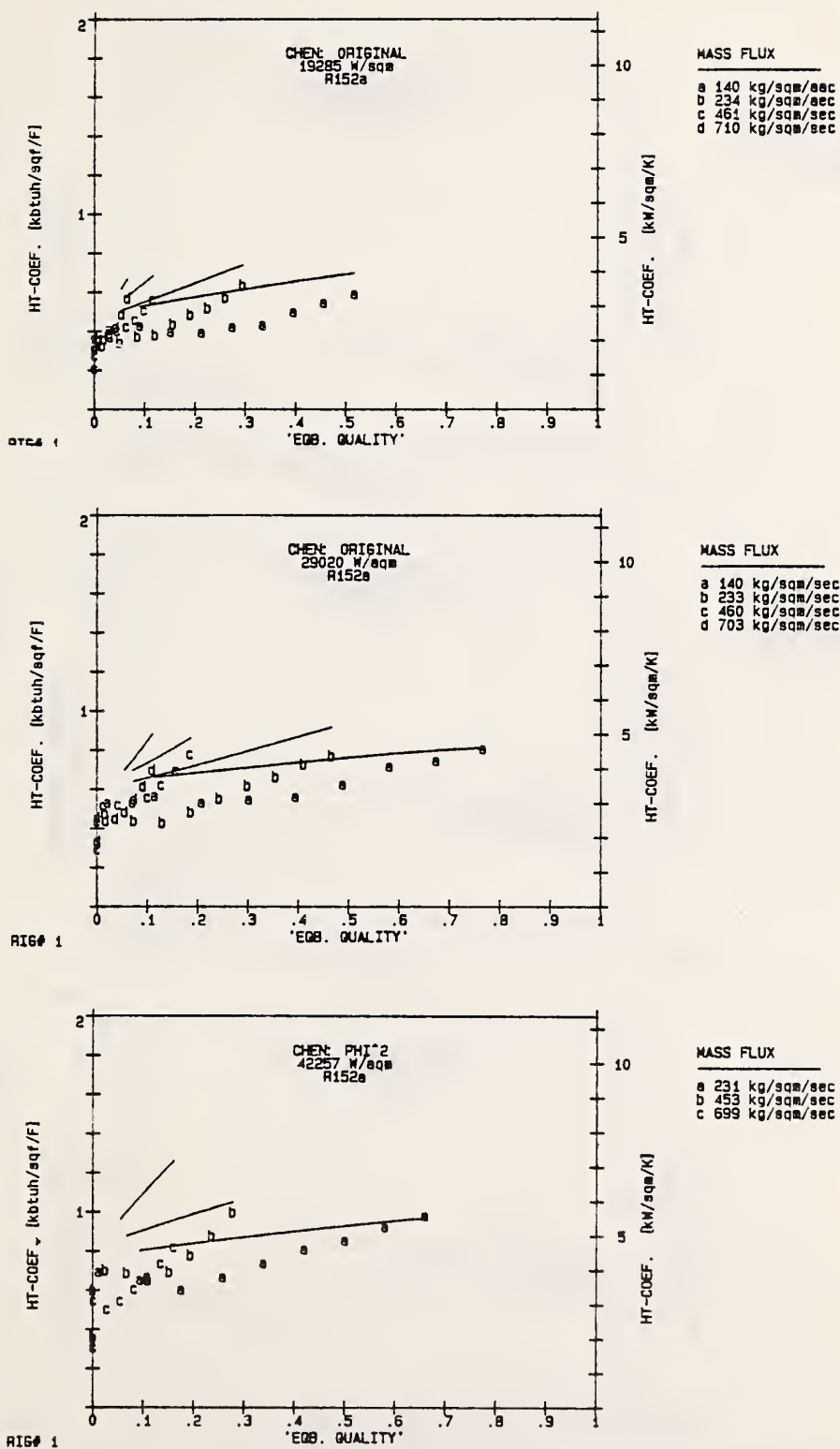


Figure 6-3: Comparison of Chen-Styled Methods to Experiments. Over-prediction is due to nucleate boiling contribution. Use of analytic F-function aggravates overprediction at low x.

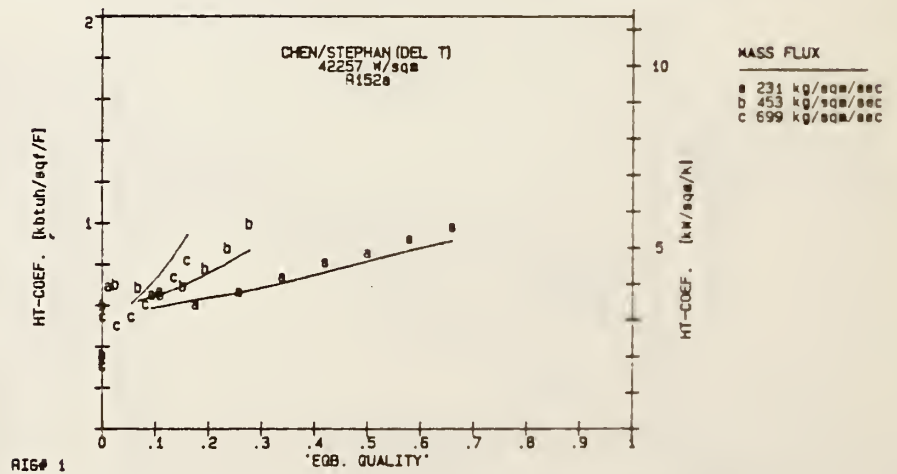
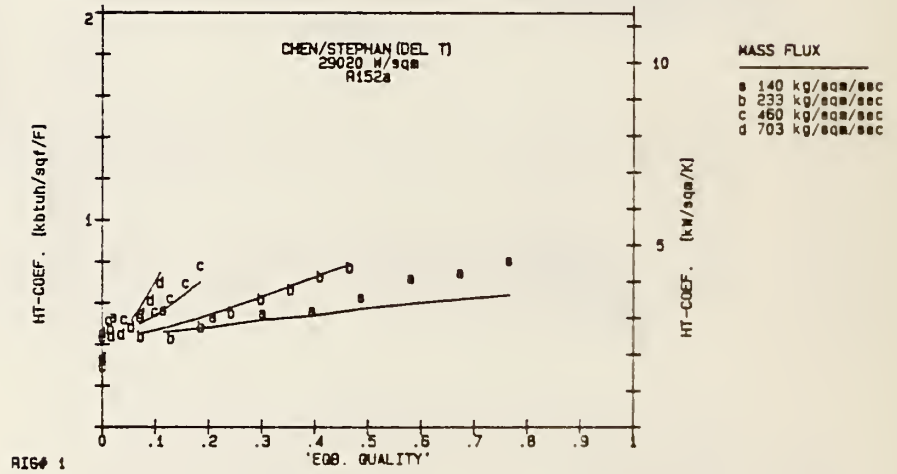
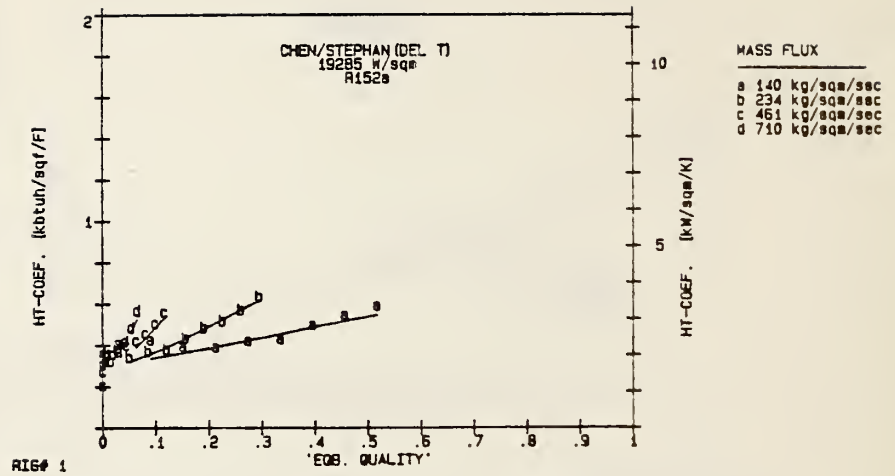


Figure 6-3: Comparison of Chen-Styled Methods to Experiments.

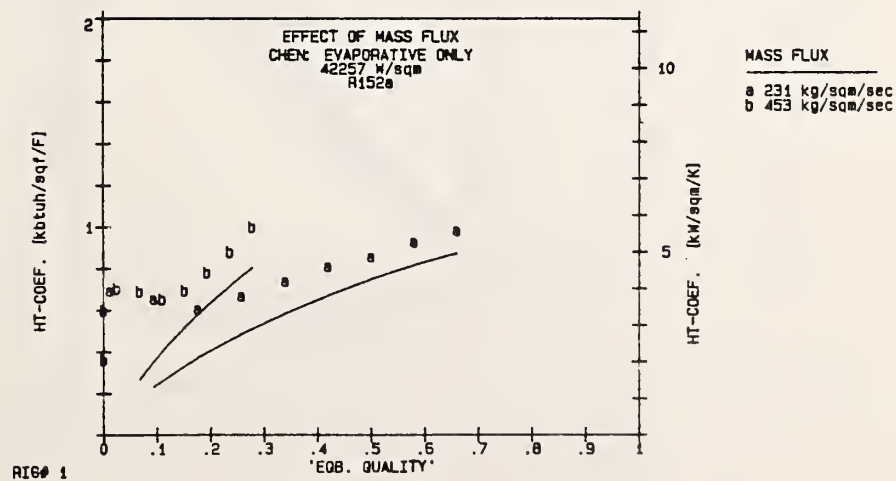
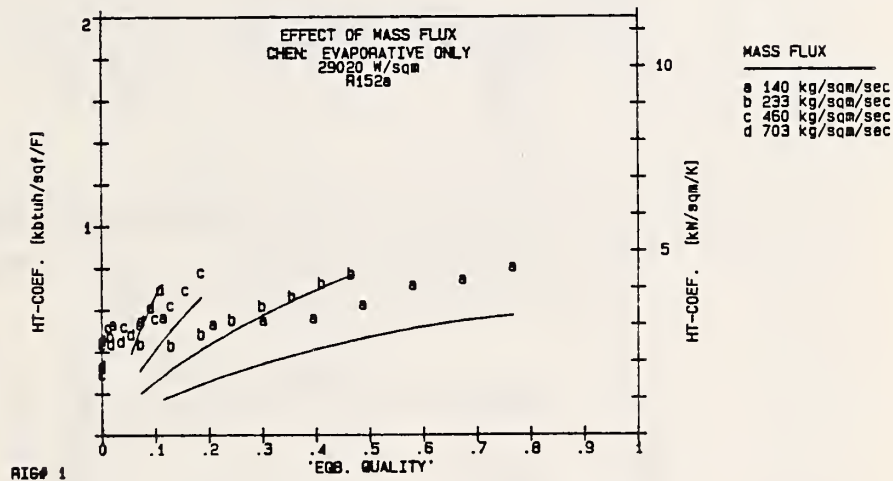
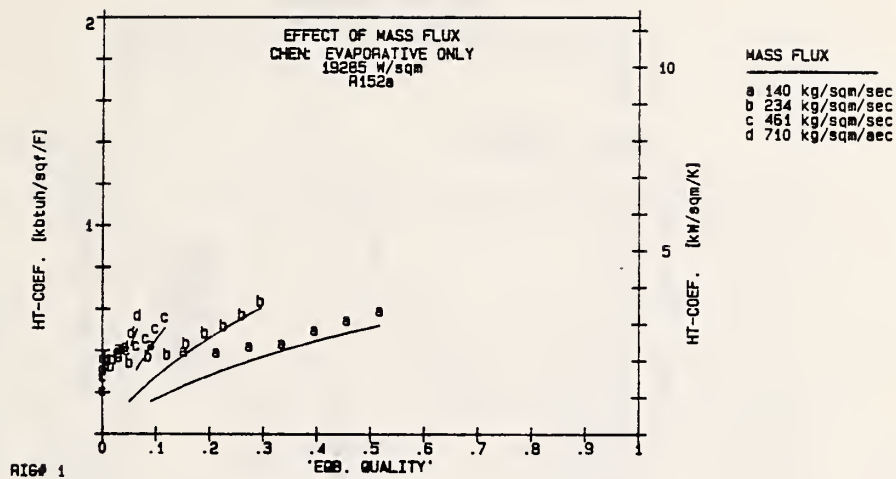
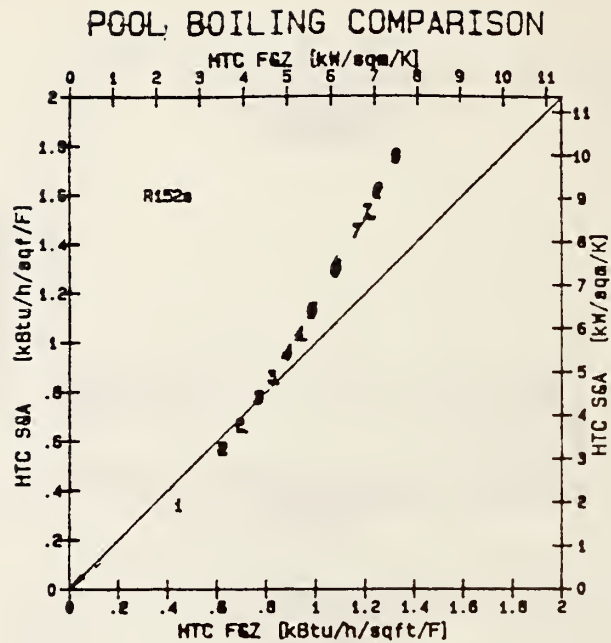


Figure 6-3 (cont): Comparison of Chen-Styled Methods to Experiments.



NUC. BOIL. CONTRIBUTION COMPARISON: CHEN

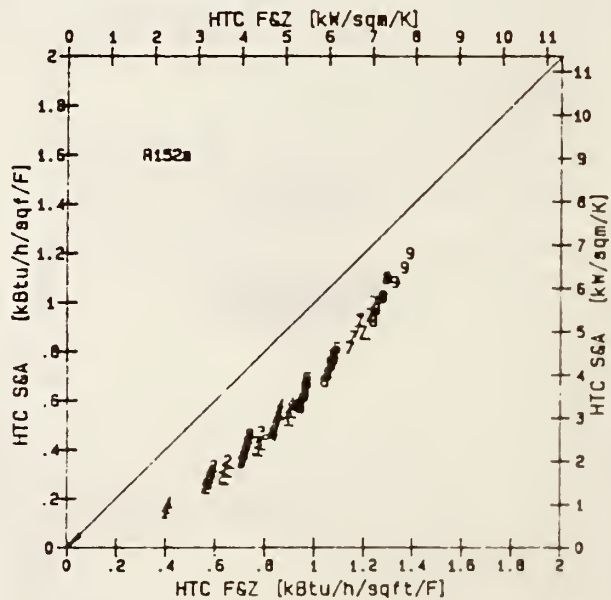


Figure 6-4: Comparison of SA and FZ Methods. When put in their original pool boiling form, SA method predicts greater than FZ. When used in Chen's correlation, the opposite trend occurs.

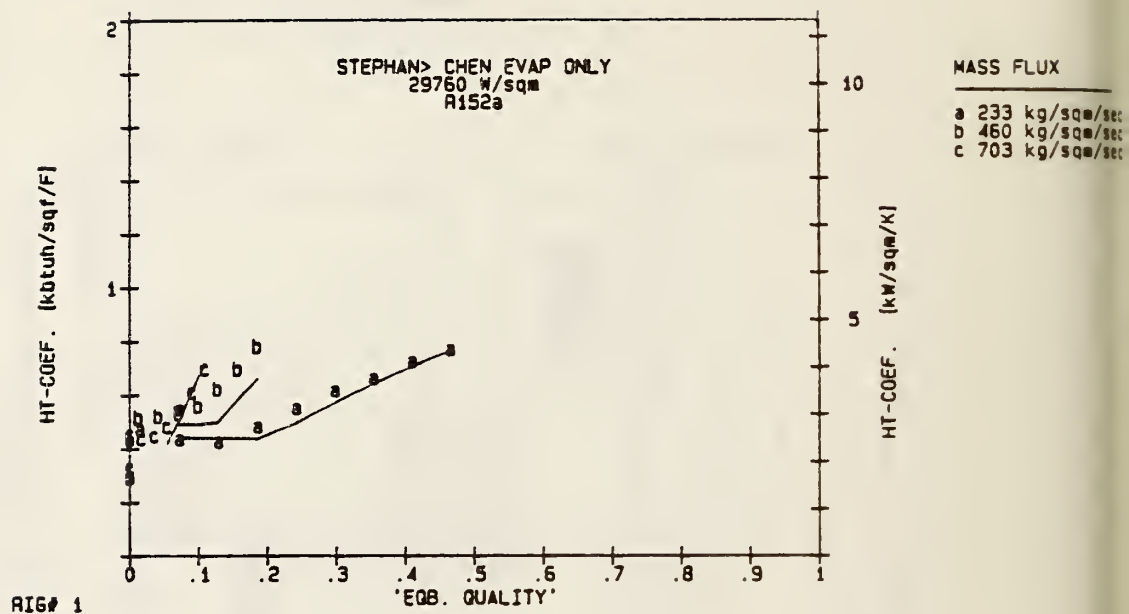
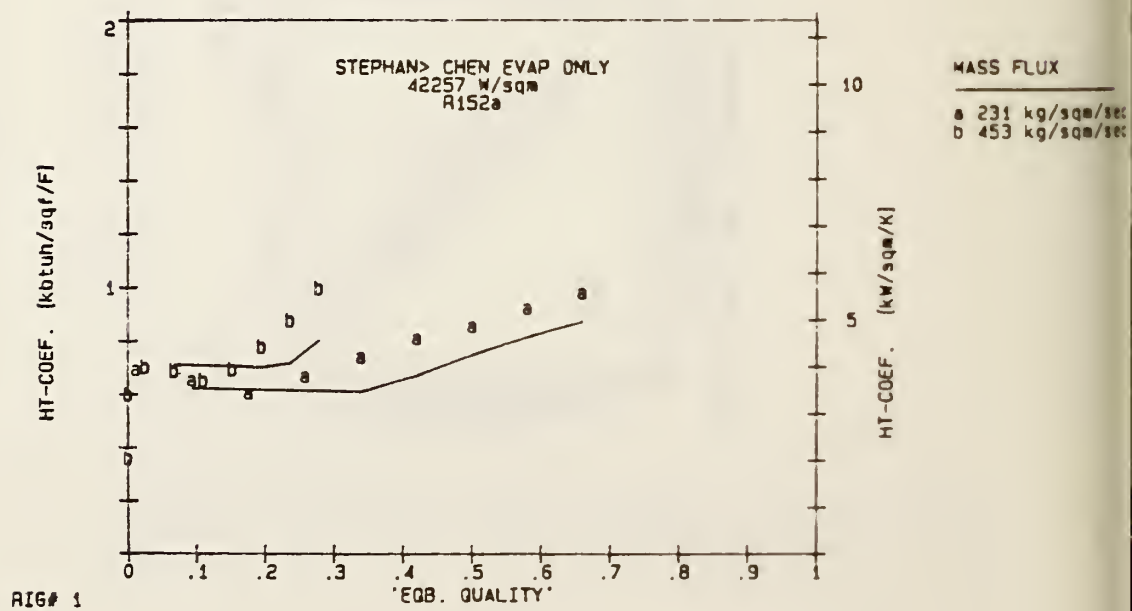


Figure 6-6: Comparison of Complete Correlation with selected Rig#1 data. Chawla's criterion improves agreement.



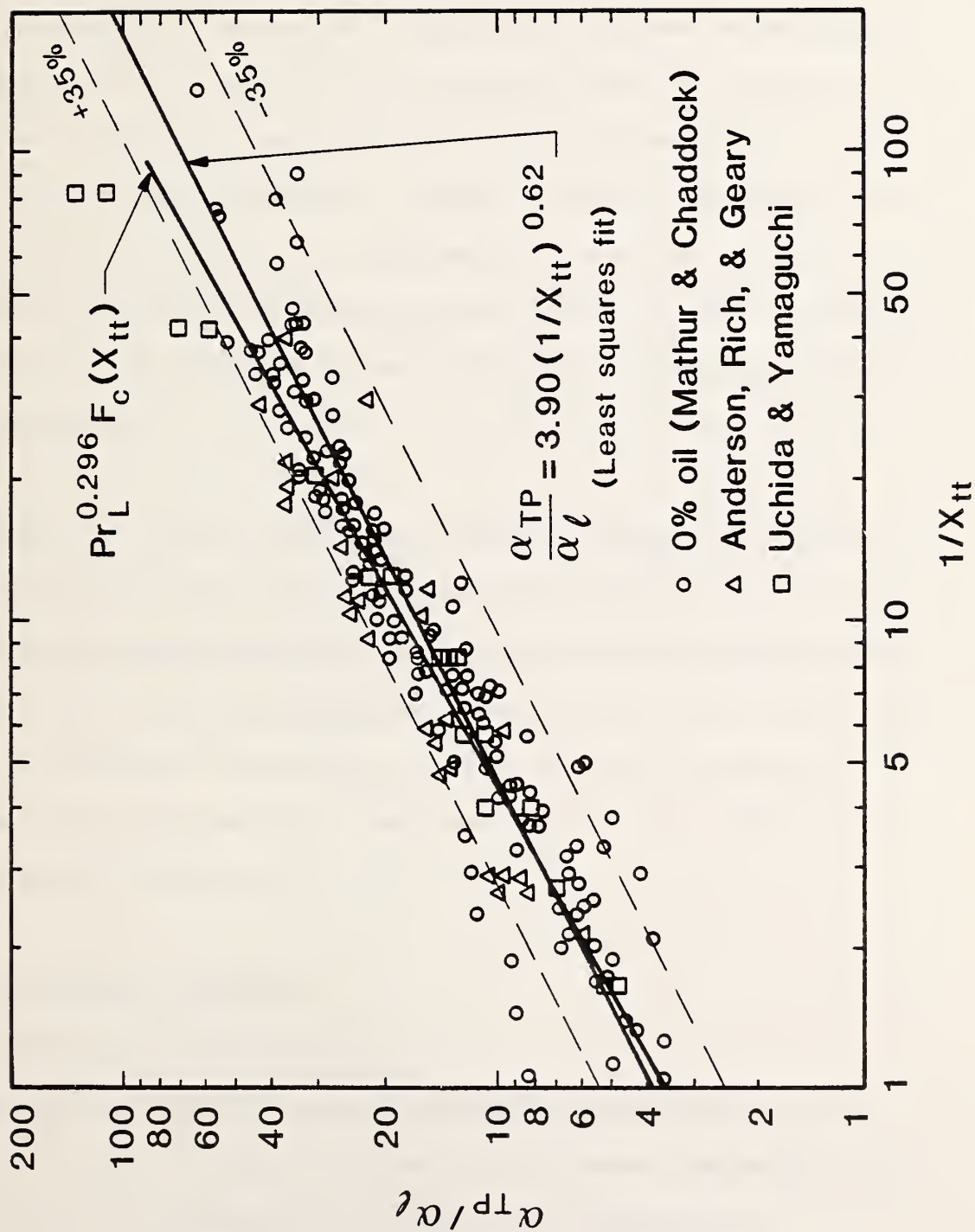


Figure 6-7: Comparison of correlation with others' data

CHAPTER 7: PREDICTION OF HEAT TRANSFER WITH MIXED REFRIGERANTS

7.1 Introduction

As has been seen in the previous chapters, heat transfer may be dominated by evaporation from the vapor-liquid interface or by nuclear boiling at the wall surface. Thus, an understanding of each process, and how it is changed by the addition of a second component, is necessary. To date, relatively little work has been done in flow boiling of mixtures. In contrast, a large experimental base exists for pool boiling of mixtures. As with pure fluids no analytic model is available for predicting heat transfer in pool boiling, and correlations have been developed instead.

This chapter will review briefly the analytic modelling of individual bubbles, discussing their implications on the real situation (section 7.2.1), pool boiling correlations for mixtures (7.2.2), analytic modelling of forced convection/evaporation mixtures and relation correlations (7.3). Then complete correlations for flow boiling of mixtures are described (7.4) and compared to experimental data (7.5). The findings are discussed in section 7.6.

7.2 Pool Boiling of Mixture

7.2.1 Modelling of Single Bubbles

As discussed in Chapter 1, mixtures differ from pure fluids in two fundamental ways: (1) vapor is formed of a different composition than liquid, and (2) the saturation or bubble point temperature is

non-isothermal, being a function of local composition. The consequence of these differences can be illustrated qualitatively:

Consider a liquid mixture of overall composition of X_e which is superheated to temperature T_e , i.e., the amount of superheat is $T_e - T_{\text{bub}}(X_e)$, as shown in Figure 7-1. As a spherical vapor bubble forms and grows¹, it is formed preferentially of the more volatile component. Due to mass continuity, the liquid in the region near the bubble has a lower composition than the bulk liquid. The liquid and vapor compositions at the bubble interface are considered to be in equilibrium. As such the interfacial bubble point temperature is not $T_{\text{bub}}(X_e)$ but $T_{\text{bub}}(X_i)$, and the appropriate driving force [the amount of superheat] is not $T_e - T_{\text{bub}}(X_e)$, but $T_e - T_{\text{bub}}(X_i)$, the latter being the smaller quantity. This loss of available superheat is commonly accepted as the principal reason for reduced bubble growth rates, and lower nucleate boiling heat transfer coefficients observed with mixtures as compared to an equivalent pure fluid.

Several authors have analyzed the growth rate reduction [Sc59, Va67, Sh83]. The results of their analysis, all of which start with simple heat and balances, is:

¹ Its initial growth rate is controlled by inertial forces, i.e., its ability to push outwards the surrounding liquid fluid, the process is simply that of an expanding sphere and governed by Rayleigh's equation. Following the initial growth period, the growth of the bubble is controlled by the rate at which heat can diffuse to the bubble interface. In the case of mixtures, the growth rate is also influenced by the rate at which the more volatile component can diffuse to the interface.

$$\dot{R} = \frac{\dot{R}_{EPF}}{1 - \frac{C_{PL}}{\Delta h_v} \frac{a_T}{a_D} (Y^* - X_e) \frac{dT_{bub}}{dX_e}} = C_{BUB} \dot{R}_{EPF}$$

where R_{EPF} is the growth rate of a bubble of an equivalent pure fluid superheated by $T_e - T_{bub}(X_e)$. The terms of this equation can be examined: as might be expected by the previous discussion, the liquid-vapor composition difference $(Y-X)$ and the ratio of thermal and mass diffusivities $\partial T / \partial D$ appear. The term dT_{BUB} / dX_e is the slope of the bubble point line. It should be noted that this term and $(Y-X)$ always have opposite sign, so that the denominator is always greater than 1, and a reduced growth rate is predicted. This relation has been verified experimentally [Fl 74]. However, the above equation is valid only for the unrealistic situation of an isolated spherical bubble in a uniformly superheated liquid. Several efforts have been made to analyze microlayer evaporation under a binary bubble near a heated wall surface as described in Appendix 7C.

7.2.2 Boiling of Mixtures versus Pure Fluid

All of the models described in Appendix 7C point to the vapor-liquid composition difference as a principal factor in the degradation of heat transfer observed in mixtures. This quantity is therefore a likely candidate to be used as a correlating parameter. Before discussing correlations however, a few other differences between mixtures and pure fluids should be noted. As shown in section 4.4, a larger superheat with a mixture is required to sustain bubble growth from a cavity of

fixed radius. In a similar fashion, for a fixed superheat, only larger cavities will be activated for mixtures as compared to pure fluids.

Since the population of cavity sizes is

$$n \sim \frac{1}{r}$$

there will be fewer sites which will be active at a given superheat. This finding suggests again a degradation in heat transfer occurs, due to the reduced number of activated sites with mixtures.

When a site has been activated, observations have shown that the bubble departure size and frequency is less for mixtures than for pure fluids. This leads to less coalescence with neighboring bubbles. The implication of the reduced frequency is again degraded heat transfer.

7.2.3 Mixture Correlations for Pool Boiling

None of these detailed points are considered in mixture correlations. Virtually all correlations consist of correction factors to a pool boiling heat transfer coefficient which would be predicted if the fluid were considered to be pure or ideal. Table 7-1 lists the correction factors. Note the parameter $|Y-X|$ appears repeatedly. Experiments by Happel and Stephan have shown that the maximum reduction in heat transfer as compared to that predicted by ideal molar mixing occurs when $|Y-X|$ is maximum. They also found no degradation when the mixture is at its azeotropic composition, as shown in Figure 7-2. These authors noted

a pressure dependence on the degradation, as in earlier experiments by Stephan which led to equation (7-24). Shock recently reviewed some of these correlations, and prioritized their application as:

- (1) Use a correlation if it was developed from actual experimental data for the fluid pair of interest.
- (2) If one new experimental data point is available, use equation (7-14) with the constant A_0 determined from the experimental value.
- (3) Use equation (7-13)
- (4) Use equation (7-14) with $A_0 = 1.53$

Section 6.3.2 showed that the pure refrigerant data was predicted to $\pm 15\%$ by the correlation of Stephan and Abdelsalam (equation 6-14). Thus this equation might be used as the basis for analyzing the mixtures' methods shown in Table 7-1. The pure refrigerant data was calculated at the given system pressure and heat flux. An ideal heat transfer coefficient, α_{id} , was then calculated using mole fraction weighting of the pure refrigerant α 's. This α_{id} was then corrected for mixture effects by the use of equations 7-13, 7-14, and 7-15. The general curve shapes of these equations is shown on Figure 7-3. Note that the methods produce a maximum degradation in heat transfer at roughly the same molar composition. However the size of the maximum degradation differs considerably between methods. Also the general shape of the method of Thome predicts a larger degradation over a wider composition range.

A heat transfer coefficient based on treating the mixture as an equivalent pure fluid was calculated with equation 6-14. Note that α_{EPF} is greater than α_{id} . This result is in contrast to that for the evaporative situation as described in Section 2.4. An analysis, similar to that done in Section 2.4, was conducted with equation 6-14, with the result:

$$\frac{\alpha_m}{\alpha_{id}} \approx \frac{\rho_{vm}}{\rho_{vid}}^{.581} \frac{\rho_{Lid}}{\rho_{Lm}}^{.454} \frac{\mu_{Lm}}{\mu_{Lid}}^{.533} \frac{C_{PLm}}{C_{PLid}}^{.533} \frac{\lambda_{Lid}}{\lambda_{Lm}}^{.278}$$

The last three dimensionless groups have values greater than one. The density ratios have values of about 0.9 or greater, and their opposing effect is thus small. In this case, then, if it were not for other mixture effects, an increased pool boiling coefficient (over an ideal fluid) would be observed.

7.3 Forced Convection/Evaporation of Mixtures

7.3.1 Analytic Modelling

Shock has examined in detail an ethanol water mixture in turbulent flow, evaporating due to constant wall heat flux [Sh76]. This analysis neglects entrainment phenomena and the presence of waves. Additional assumptions included: a) negligible sensible heating of liquid; b) equilibrium at the vapor-liquid interface; c) negligible axial density and velocity gradients; d) constant shear. The liquid flow velocity profile was approximated via mixing length theory, using eddy diffusivities due to Deissler (near the wall) and Von Karman. He then assumed the eddy diffusivity for mass to have the same value, i.e.

$$\varepsilon_D \approx \varepsilon_M$$

Vapor side heat and mass transfer diffusivities were estimated via the Chilton-Colburn analogy, which relates these coefficients to the friction factor (calculated via Blasius equation):

$$j_H = j_D = f/2$$

He then solved the basic continuity and energy equations to determine the interfacial temperature and composition in a stepwise fashion along the length of the tube. He examined changes in the magnitude of the resistances, the heat flux, and the pressure gradient to determine their relative importance. As a base case he assumed no mass transfer resistance, and equilibrium flash vaporization, i.e. $\bar{X}_{BULK} = \bar{X}_1$, $\bar{Y}_{BULK} = \bar{Y}^*(X_B)$.

He found:

- (a) mass transfer resistance (MTR) on the liquid side has a negligible effect on the interfacial temperature and composition.
- (b) MTR on the vapor side controls what effects do appear;
- (c) however, the MTR effect is negligible, i.e. assuming equilibrium vaporization leads to little error in estimating the temperature drop through the film.
- (d) the error introduced by (c) is lessened with reduced heat flux
- (e) the inclusion or exclusion of pressure gradient has no effect on the above conclusions, and
- (f) very little sensible heating of vapor occurs over the range of tested variables ($T_G \approx T_i$).

The effect of finding (c) is that the mixture can be treated as an EPF if the process is strictly evaporative. Any deviation in the heat transfer coefficient from an ideal mole fraction weighting would be caused by non-ideal property behavior, not mass transfer effects. This finding then is in sharp contrast to the conclusion of the preceeding section on pool boiling of mixtures. This is also in mild contrast to condensation of vapors with noncondensable gases (NG); NG cause severe degradation in condensing coefficient with stagnant vapor. A 20% - 30% degradation can also be found when the vapor stream is in laminar flow. There is unfortunately no literature on turbulent in-tube condensation of vapor with NG.¹ Recently Stoecker [St85] noted a condensing coefficient for an R-12/R-114 mixture which was lower than either pure refrigerant. He attributed without analysis the degradation to slip, and not mass transfer resistance.² Appendix 7D has additional comments on Shock's analysis.

7.3.2 Predictive Modelling for Forced Convective/Evaporation of Mixture (Bell and Ghaly Model)

Given the findings of the previous section, it is not surprising that Shock has recommended the use of a simplified equilibrium model [Sa82,Sh83]: the Bell and Ghaly method [Be72]. It was developed originally for film condensation of a superheated vapor. It can however be rederived for forced convection/evaporation, as is done in Appendix 7E.

¹Webb [We82] examined turbulent flow over a tube and found in condensation of water vapor with 2% air (by volume) a 20% reduction in condensing coefficient.

²It may be due to non-ideal property behavior, but this possibility was not analyzed.

A summary of the assumptions in the method is:

- (1) No sensible heating of the liquid.
- (2) Over a small axial distance, the change in bulk vapor temperature is equal to the change in equilibrium temperature.
- (3) Mass transfer resistance is neglected. To balance the error of this assumption, single phase heat transfer coefficients are employed rather than the (higher) two phase values.

The effective heat transfer coefficient is then given by:

$$\frac{1}{a_{\text{eff}}} = \frac{1}{a_{\text{LO}}} + \frac{x C_{\text{PG}} dT_{\text{eqb}}/dh}{a_{\text{G}}} \quad (7-1)$$

Assumption (3) was later revised so that two phase heat transfer coefficients are now recommended. For evaporation, the sensible heating of vapor is small, so that the above equation reduces roughly to

$$\frac{1}{a_{\text{eff}}} \approx \frac{1}{a_{\text{LO}}|_{\text{TP}}} = \frac{1}{a_{\text{Lo}}(\rho_{\text{Ltt}}^2)^{.445}} \quad (7-2)$$

The term is identical to Chen's evaporative term for pure component evaporation. Thus, with little sensible heating of the vapor stream the Bell and Ghaly model is actually a pure fluid liquid film correction.

7.4 Complete Mixtures' Correlations

The previous sections have described each heat transfer regime, and methods to calculate α for mixtures. This section describes methods of calculation when both evaporation and nucleate boiling are present.

7.4.1 Modification to Bell and Ghaly to include Nucleate Boiling

Sardesai, Shock, and Butterworth suggested recently a modification to the Bell and Ghaly method to include nucleate boiling [Sa82]. In this case, equation (7E-1) of Appendix E becomes:

$$q_{TOT} = a_{LO}(T_W - T_i) + a_n(T_W - T_{bub}(\bar{X})) \quad (7-3)$$

where a_n is found from the methods described in section 7.2.3. The problem then is to estimate $T_{bub}(X)$. If one sets $T_{bub}(X) = T_i$, then, equation (7-1) becomes

$$a_{eff} = \frac{1}{\frac{1}{a_{LO} + a_n} + \frac{q_G/q_{TOT}}{a_G}} \quad (7-3)$$

If instead $T_{bub}(X) = T_G$, then equation (7-1) becomes

$$a_{eff} = \frac{1 + a_n/a_{LO}}{\frac{1}{a_{LO}} + \frac{q_G/q_{TOT}}{a_G}} \quad (7-4)$$

The authors however do not suggest when to include the nucleate boiling contribution, or if a suppression factor should be included. If in fact one is included then equation (7-3) becomes very similar to Chen's method described in the last chapter.

7.4.2 Modification to Bennett and Chen's Method to include Mixture Effects

Bennett and Chen developed an extension of their method to include mixture effects [Be80]. Their approach is dissimilar in its assumptions to those advanced in all the previous sections. Specifically, sensible heating of the vapor is neglected, but sensible heating of the liquid is accounted. Additionally mass transfer resistance in the liquid (and not in the vapor) is assumed and accounted semi-empirically. Lastly, a much different approach is taken to account for reduced nucleate boiling heat transfer.

In the case of mixtures, the nucleate boiling contribution is considered reduced by the same factor as described in section 7.2.1 for single bubbles (equation 7-0)

$$C_{BUB} = \frac{1}{1 - \frac{C_{PL}}{\Delta h_v} \frac{a_T}{a_D} (Y^* - X_e) \frac{dT_{BUB}}{dX_e}} \quad (7-5)$$

so that the nucleate boiling part of equation (6-3) becomes

$$a_n = a_{pool} C_{BUB} S \quad (7-6)$$

The forced convection term is also modified to account for mass transfer resistance in the liquid film. It is hypothesized that, due to this resistance, the real interfacial temperature is higher than calculated

from equilibrium. In this manner, the driving potential, $T_W - T_i$ is less for mixtures than for an equivalent pure fluid. Thus, for a pure fluid,

$$\dot{q}_L = a_{LO} (T_W - T_{eqb})$$

and for a binary mixture,

$$\dot{q}_{BL} = a_{LO} (T_W - T_i)$$

$$= a_{LO} \frac{(T_W - T_i)}{(T_W - T_{eqb})} (T_W - T_{eqb})$$

$$= a_{LO} C_{Con} (T_W - T_{eqb}) \quad (7-7)$$

The problem remains to eliminate the unknown interfacial temperature.

Appendix 7A shows how this elimination was achieved through the introduction of a mass transfer coefficient:

$$C_{con} = 1 + \frac{q \, y^* \frac{dT_{BUB}}{dX_e}}{\rho_L \beta_L \Delta h_v (T_W - T_{eqb})} \quad (7-8)$$

where β_L = mass transfer coefficient

The mass transfer coefficient was assumed to behave as

$$\beta_L = B \frac{a_D}{D} \text{Re}_L^{0.8} \text{Sc}^{0.4}$$

where B was determined empirically to be 0.023. The authors note the coincidental agreement with the Dittus - Boelter constant. The authors next account for sensible heating of the liquid phase. A derivation of this accounting is given in Appendix 7B; the equations (7-5) and (7-8) should be replaced by an effective heat of vaporization:

$$\Delta h_{\text{veff}} = \Delta h_v - C_{pL}(Y^* - X_e) \frac{dT_{\text{BUB}}}{dX_e} \quad (7-9)$$

and $B = 0.015$ gives better agreement with their data when Δh_{veff} is used. The author noted little change in agreement resulted with the inclusion or exclusion of equation (7-9).

7.4.3 Other Modifications to Chen's Method to include Mixture Effects

Collier and Shock [Co80, Sh73] have suggested modifying the nucleate boiling contribution when mixtures are used. They suggest treating the components as separate resistances in series, and including a correction factor for mixtures:

$$\frac{1}{\alpha_{\text{pool}} S} = \frac{\bar{X}_A}{\alpha_{\text{pool}_A} S} + \frac{1 - \bar{X}_A}{\alpha_{\text{pool}_B} S} \frac{1}{C} \quad (7-10)$$

where C is found from Table 7-1. Tacitly they assume that sensible heating of liquid and vapor are negligible. Consistent with Shock's earlier findings, they assume the turbulent evaporation process to be unaffected by mixtures so α_{L0} , F, and S are unaffected.

7.4.4 Other Correlations for Flow Boiling of Mixtures

Varma et al. [Va79] studied a binary mixture of R12/R22, as discussed in Chapter 1. They correlated their data to $\pm 30\%$ for low mass fractions of R22 and $\pm 15\%$ for higher mass fractions, using the following form:

$$\frac{\alpha}{\alpha_{LO}} = 8.275 \frac{1}{X_{tt}}^{.253} \frac{\dot{q}}{\dot{m}\Delta h_v}^{.12} (1 - |\bar{Y}_e^* - \bar{X}|)^{-.9} \quad (7-11)$$

By its nature, the correlation does not consider the physical processes involved in the flow boiling of mixtures. It is interesting to examine the only term which is explicit to mixtures:

$$(1 - |\bar{Y}^* - \bar{X}_e|)^{-.9} \quad (7-12)$$

This term is always greater than unity, suggesting the use of a mixture augments the heat transfer process over an EPF. Their experimental data did show a higher heat transfer coefficient for the mixture than for pure R12. No tests were done with pure R22. As previously noted, the mixture degrades the heat transfer in nucleate boiling dominated situations. In forced convection dominated situations, the term $(1/X_{tt})$ generally appears to the exponent $2/3$ to $3/4$. Their correlation suggests neither regime. The agreement between (7-11) and the data is therefore not expected to be general. It however should not be dismissed, since the heat and mass flux range they tested is quite similar to that used in the test section of rig #2.

In the only other known study, Singal et al. measured R13/R12 mixtures [Si83]. Their results produced erratic behavior with quality and composition; there was a clear dependence on mass and heat flux. Average heat transfer coefficient was compared with the Pierre correlation for average heat transfer coefficient and agreement was poor (wide scatter, both positive and negative).

7.4.5 Summary of Mixtures' Models

At this point, the literature may be summarized along the following lines:

- (1) Experiments with pool boiling of mixtures have shown severe degradation in heat transfer coefficient when compared to ideal or equivalent pure fluid values. The degradation has been accounted by various correction factors. Since pool boiling methods have been extrapolated successfully in the prediction of flow boiling of pure fluids, the same extrapolation has been hypothesized as valid for mixtures.
- (2) Shock's analytic treatment suggests that mass transfer resistance (MTR) and sensible heating are negligible in turbulent flow evaporation. His conclusions are generally supported by condensation research. He concludes that non-mixture methods are adequate for predicting the heat transfer. If MTR is included, Shock suggests the dominant MTR is on the vapor side. In sharp contrast, Bennett and Chen have advanced a true mixtures' model which includes both MTR and sensible heat only on the liquid side; they correlated a large data set with their model.
- (3) Other authors in the literature have either attempted to use non-mixture relations in the presence of nucleate boiling, or have produced curvefits which are structurally flawed in their interpretation of the physical phenomena.

Table 7-2 lists the complete mixture methods and their related assumptions.

7.5 Comparison to Measured Data

Table 7-3 displays 46 variations of the models described in the previous sections. Because the mass diffusion coefficient is unknown, parametric runs were made, assuming a range of Lewis numbers. The best methods are discussed in the following sections.

7.5.1 Comparison to Preheat Data of Rig #2

While the mixtures data of this section shows effects of mass flux and quality, it is primarily affected by heat flux, suggesting that it might be best represented by a pool boiling correlation corrected for mixture effects, as discussed in Section 7.2.3.

Figure 7-4 displays some of the measured data superposed on the predicted coefficients. In all cases, a severe degradation in heat transfer is observed (about 40-50% as compared to α_{id} , and 70% compared to α_{EPF}). Hidden in these figures are the effects of mass flux and quality. Also there is an uncertainty in the actual local liquid composition, given that a mass transfer resistance and a non-equilibrium condition are part of the physical process. These complications can be mitigated by examining only that experimental data closest to equilibrium, i.e. the first thermocouple group in the preheat section. At this group, the vapor quality is lowest, so that the liquid composition will be close to the known subcooled inlet composition. At this point also, the evaporative mode should contribute only weakly, so that mass flux and vapor quality levels should not be significant. Figure 7-5 displays this data, along with the predictive methods. In this

figure, unlike the previous set, the Stephan and Korner method is evaluated using $A_0 = 2.64$; this value was selected to predict exactly one of the experimental data points. The vertical scatter is due to the neglect of the mass flux effect. This approach was discussed in Section 7.2, and was in fact successful in evaluating Toral's subcooled flow boiling data [To79].

Table 7-3 shows that the best correlations of the data are a pure evaporative, non-mixture model ($\alpha = \alpha_{LOFC}(X_{tt})$) and two pool boiling relations. The agreement between the evaporative model and the data may be coincidental; the data itself does not exhibit the strong mass flux dependence predicted by the model. Instead it exhibits a strong heat flux dependence ignored by the evaporative model. Of the pool boiling relations, the method of Thome and the specialized Stephan and Korner methods predict the measured data fairly well. Thome's method is both more conservative and more accurate in the mixture concentrations at which heat pumps are recommended for operation. It predicts the observed level of degradation at points away from the maximum degradation better than Stephan and Korner.

7.5.2 Comparison to Rig #1 Data

This data set consists of 184 points with equilibrium qualities between .05 and 0.90. The data includes a wide range in molar composition (though not weight composition as shown in Table 3-1). A variety of pressures were used so that a comparison between runs is difficult;

however the pressure variation provides an additional parameter upon which to check the ability of the correlations.

The data shows a proportional dependence on heat flux, quality and weakly mass flux. This suggests that nucleate boiling is principally contributing to the vapor generation process; in this manner it is like the previous data set.

All of the pure fluid correlations overpredict the measured values by an amount exceeding their overprediction of the pure fluids. This is a first indication of a degraded heat transfer with mixtures.

Of all the correlations, a few stand out for their predictive ability. Since α is a strong function of heat flux, the pool boiling methods were again examined. Here Thome's method is superior to Stephan and Korner because much of the data has a greater molar composition of R13B1 than was the case in Section 7.5.2. The Stephan and Korner method is only superior at small molar compositions of R13B1. While Thome's method yielded the lowest mean deviation, it did not represent well the data trends. By its nature, Thome's method produces an inverse relationship between vapor quality and heat transfer coefficient, opposite of the measured observation. It tends to overpredict the measurements at low quality and underpredict at high quality (Figure 7-6). Because of this feature, it predicts the average heat transfer coefficient very well. The two other methods which predict the data with any accuracy are evaporative only, non-mixture modeling: Chen's original method

without Prandtl correction, and Bell and Ghaly's method. They are actually very similar, as is discussed shortly.

7.5.3 Comparison to Rig #2: Test Section Data

This data base consists of 141 points with equilibrium qualities between 0.05 and 0.90, and shows significant mass flux effects. It therefore is likely dominated by forced convection/evaporation. The poor predictive ability of the pool boiling methods offers further verification of this conclusion.

Several methods shown on Table 7-3 [(B), (J), (CC), (FF), (HH) (II)] yielded mean deviations less than 0.20. The "evaporative only", nonmixture correlation of (B) which is simply equation (6-26b):

$$\alpha = \alpha_{LO} F_c(\bar{X}_{tt})$$

yielded one of the best agreements. This same equation predicted well for the pure R152A data when nucleate boiling was completely suppressed. However, unlike its underpredictive tendency with the pure fluids it overpredicts the mixtures' data (Figure 7-7). Slightly better prediction is achieved with methods (BB) and (FF) which do include a mass transfer resistance effect. However the predictive ability of (BB) and (FF) is artificial. First the terms Pr_L , Δh_{eff} and $\Delta T/\Delta T_e$ tend to compensate each other and produce a value near 1. The Lewis number of 1 is unrealistic in any case. Finally the term $\Delta T/\Delta T_e$ was calculated based on some nucleate boiling contribution, i.e. the complete Bennett and

Chen correlation was employed, and the nucleate boiling contribution subtracted out. This is physically unrealistic. For these reasons, methods (BB) and (FF) are not recommended.

Method (HH) is a Bell and Ghaly styled method, which reduces effectively to the same method as (B) since the liquid film dominates. It therefore is not really a new approach. It has all the same features as (B) described above. The use of $F_c(\rho_{Ltt}^2)$ made little difference, since the methods produced similar values in this pressure and quality range.

Method (J) yields the best agreement of the complete Bennett/Chen-styled correlations. It however tends to underpredict the dependence on vapor quality and overpredict the nucleate boiling contribution. Agreement at this stage of analysis can only be considered coincidental. The method badly predicted the experimental data in the heat transfer regime dominated by nucleate boiling.

7.6 Discussion of Findings

The complete Chen-styled correlations predicted poorly. In general they tended to overpredict the magnitude of α , and underpredict the dependence on quality, $d\alpha/dx$. The overprediction is a principal result of the treatment of the fluid as an equivalent pure fluid with the Forster and Zuber correlation (i.e. calculating with EPF properties). This results in a large nucleate boiling contribution, as was shown in Figure 7-3. Secondly, the term C_{BUB} reduces the nucleate boiling contribution to a lesser extent than the methods in Table 7-1.

Furthermore a structural problem was revealed in the mass transfer resistance inclusion in the evaporative term (equation 7-7). At Lewis numbers of five or greater, as might be common for most organic fluids, the term

$$C_{BUB} = \Delta T / \Delta T_e = \text{equation (7-5)}$$

could become negative at reasonable values of ΔT_e (close to measured values). A negative value of $\Delta T / \Delta T_e$ has no physical meaning. As such it was set to zero in these cases. This caused the method to reduce to a pure nucleate boiling method, equal to $\alpha_{EPF} C_{BUB} S$. Since the α_{EPF} is too large, the method tends to overpredict.

Many perturbations of the Chen-styled correlation were tried, including a few new approaches:

- a) Collier and Shock's nucleate boiling contribution was changed so that α_A and α_B was determined via equation (6-17) corrected via Thome's method:

$$\alpha_n S = \left| \frac{\bar{X}_A}{\alpha_n S} + \frac{(1 - \bar{X}_A)}{\alpha_B S} \right|^{-1} C_{TH}^{-1}$$

- b) Bennett and Chen's method without the Prandtl correction; this was tried since pure R152a measured values were predicted well without the correction (section 6.4).

These modifications yielded improvements over the original approaches, but did not give satisfactory agreement.

In the nucleate boiling regime, pool boiling methods corrected for mixture effects were seen to be the most accurate. They failed however to predict the observed quality dependence. Thome's method is very simple to apply and is the most accurate and conservative, and is thus recommended.

In the forced convection/evaporative regime, a non-mixture method which assumes nucleate boiling suppression predicted the data best. This result is consistent with recent turbulent flow evaporation theory. The best predictor for this data was also the best predictor for the completely suppressed pure refrigerant data, lending further credibility to Chen's evaporative correlation. Unlike pure fluids through it tended to overpredict the mass flux effect. It is tempting to attribute the overprediction to MTR, though no definitive statement can be made. MTR may however account in a subtle way for the fact that the measured mixtures data, α/α_{LO} , was less than the pure fluid values at the same pressure, heat flux and Martinelli parameter. This was shown on Figure 5-6.

It is known that MTR reduces bubble growth rates and decreases the heat flux where complete suppression is predicted. The reduced α for mixtures may be the result then of nucleate boiling having been suppressed for the mixtures but not for the pure fluids. With ebullition, the viscous sublayer may be destroyed, thus increasing both the evaporative and the nucleate boiling contributions. Such a theory would explain the measured reduction and be consistent with turbulent flow evaporation theory and the correlation results.

Table 7-1: Pool Boiling Correction Factors for Binary Mixtures

<u>Authors</u>	<u>α</u>	<u>C</u>	<u>Equation</u>
Palen and Small [Pa64]	$\alpha = \alpha_{id} C_{PS}$	$\exp(-0.27(T_{dew} - T_{bub})), T[^\circ K]$	(7-13)
Stephan and Korner [St69]	$\alpha = q_w / \Delta T_{id} / C_{Sk}$	$A_o(.88 + .12P) Y^* - X_o + 1$	(7-14)
	$\Delta T_{id} = \bar{X}_A \frac{q_w}{\alpha_A} + \bar{X}_B \frac{q_w}{\alpha_B}$		
Thome [Th78]	$\alpha = \alpha_{id} C_{TH}$	$\Delta T_{id} / (\Delta T_{id} + T_{dew} - T_{bub})$	(7-15)
Calus and Rice [Ca72]	$\alpha = \alpha_{EPR} C_{CR}$	$1 / [1 + (\frac{a_T}{a_D}) Y^* - X_o]^{0.7}$	not examined
Afgan [Af68]	$\alpha = \alpha C_f$	$1 - C_7 Y^* - X_o $	not examined

Table 7-2: Summary of Assumptions in Mixtures' Models

Method	Mixture effect on α_e	Mixture effect on α_n	Sensible Heating of Liquid	Sensitive Heating of Vapor	Suppression Factor
Bell and Ghaly	no	N/A	no	yes	none
Sardesai, Shock and Butterworth (ie. Bell + nucleate boiling)	no	pool boiling methods	no	yes	none
Collier/Shock	no	pool boiling methods	no	no	S_c
Bennett and Chen	yes semi-empirical	isolated bubble growth theory	yes	no	S_c
Varma et al.	empirical		no	no	none

Table 7-3: Comparison of Mixed Refrigerant Correlations and Experimental Data

Method	Evaporative Portion	Nucleate Portion	$\sigma = \frac{1}{N} \sum_{i=1}^N \left \frac{\alpha - \alpha_{\text{meas}}}{\alpha_{\text{meas}}} \right $	Comments	
Chen-Styled Correlations					
(A) Chen Original	$F_o(X_{tt})$				
(B) Evap Only					
(C) Original	$F_o(X_{tt}, Pr_L)$				
(D) Evap Only					
Bennett and Chen					
(E) Original L=1	$F_o(\delta_L^2) Pr_L, \Delta T / \Delta T_o$	$\alpha_{FZ} C_{BUB}$	0.967		$\alpha_o = 0$ Frequently
(F) L=5			0.603		
(G) L=10			0.426		
(H) L=30			0.321		
(I) Original L=1	$F_o(X_{tt}, Pr_L, \Delta T / \Delta T_o)$	$\alpha_{FZ} C_{BUB}$	1.085	0.727	0.453
(J) L=5			0.671		0.182
(K) L=10			0.304		
(L) $\Delta H_v(\text{eff})$ L=1	$F_o(X_{tt}, Pr_L, \Delta h_{v, \text{eff}}, \Delta T / \Delta T_o)$	$\alpha_{FZ} C_{BUB}$	0.907	0.554	0.292
(M) L=5			0.452		0.198
(N) L=10			0.304		
(O) No Pr_L L=1	$F_o(X_{tt}, \Delta T / \Delta T_o)$	$\alpha_{FZ} C_{BUB}$	0.624	0.345	0.220
(P) L=5					0.203
(Q) L=1	$F_o(X_{tt}, \Delta h_{v, \text{eff}}, \Delta T / \Delta T_o)$		0.756		$\alpha_o = 0$ usually
(R) L=5			0.603		
(S) L=30			0.318		

Table 7-3 (Continued)

Method	Evaporative Portion	Nucleate Portion	Mean Deviation		
			Rig #1 Preheat	Rig #2 Test	
			1st	Group	All
<u>Collier/Shock</u>					
(T) Original	$F_o(X_{tt})$	$a_{KZ}(Q), C_{SK}$	1.027		
(U)	$F_o(X_{tt})$	$a_{SA}(\Delta T), C_{TH}$	0.582	0.692	0.501
(V)	$F_o(X_{tt}, Pr_L)$	$a_{SA}(\Delta T), C_{TH}$	1.032	1.032	0.793
<u>Evap Only</u>					
(W) Ben/Chen Original	L-1 $F_o(\phi_L^2) Pr_L \Delta T / \Delta T_o$	Calculated, but not included	0.387		0.303
(X)	L-5		0.426		
(Y)	L-30		1		
(Z) $F(X_{tt})$	L-1 $F_o(X_{tt}, Pr_L, \Delta T / \Delta T_o)$		0.499	0.402	0.395
(AA) Original	L-5		0.368		0.192
(BB) No Pr_L correction	L-1 $F_o(X_{tt}, DT / DT_o)$		0.404		0.163
(CC)	L-5		0.504		0.441
(DD)	L-10		0.743		
(EE)	L-30		1		
(FF) Δh_v effective	L-1 $F_o(X_{tt}, Pr_L, \Delta T / \Delta T_o, \Delta h_{v,eff})$		0.387	0.402	0.395
<u>Boill/Ghaly</u>					
(HH)		$F_o(X_{tt})$	0.337		0.188
(II)		$F_o(\phi_L^2)$	0.26		0.185
(JJ)		$F_o(X_{tt}, Pr_L)$	0.645	0.345	0.259
					0.616

Table 7-3 (Continued)

Method	Evaporative Portion	Nucleate Portion	Mean Deviation		
			Rig #1 Preheat lat Group	Rig #2 Test	All
(KK)	$F_o(\delta_L^2)$	$\alpha_{FL}(Q), C_{SC}^{SC}Chen$	0.754		0.247
(LL)	$F_o(X_{tt})$	$\alpha_{TH}^{SC}Chen$	0.705		
(MM)	$F_o(X_{tt}, Pr_L)$	$\alpha_{SA}(\Delta T), C_{TH}$	1.032	0.651	0.793
<u>Yarman, et al</u>					
(NN)	$F(X_{tt}, B_o, \bar{Y}-\bar{X})$		1.251		0.598
<u>Non Mixture Correlations</u>					
(OO) Chaddock and Noeranger	$f(X_{tt})$	-	1.237		
(PP) Dengler and Addams	$f(X_{tt})$		1.183		1.119
(QQ) Collier and Pulling	$f(X_{tt})$	$f(B_o)$	1.311		
<u>Pool Boiling Correlations</u>					
(RR) Thome	-	$(Q/\Delta T_{id})C_{TH}$	0.161	0.305	0.257
(SS) Stephan and Korner	-	$(Q/\Delta T_{id})/C_{SK}$	0.802	0.225	0.225
(TT) Palen and Small	-	$\alpha_{id}C_{PS}$	1.061		.443

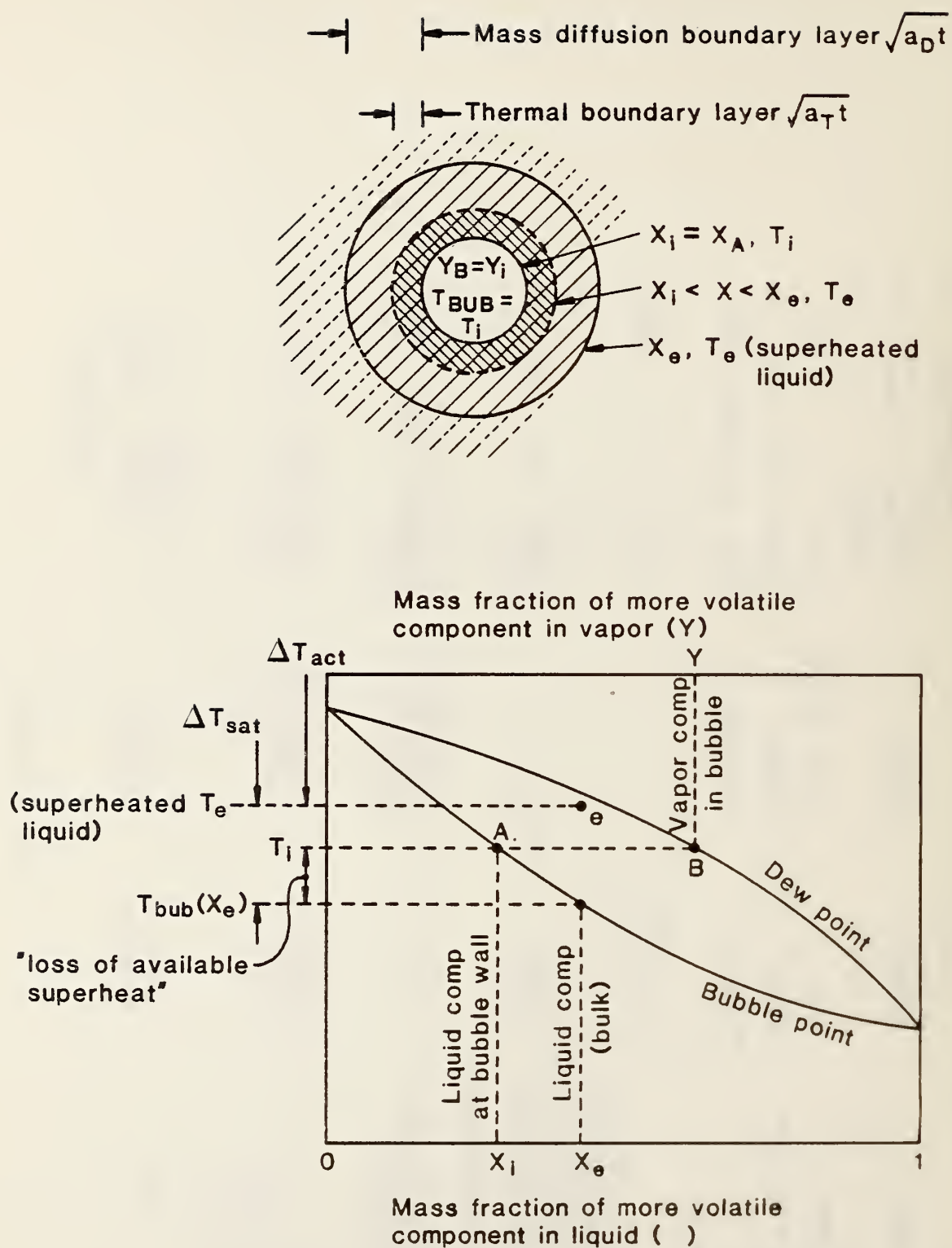


Figure 7-1: Isolated Bubble Growing in a Superheated Binary Liquid.

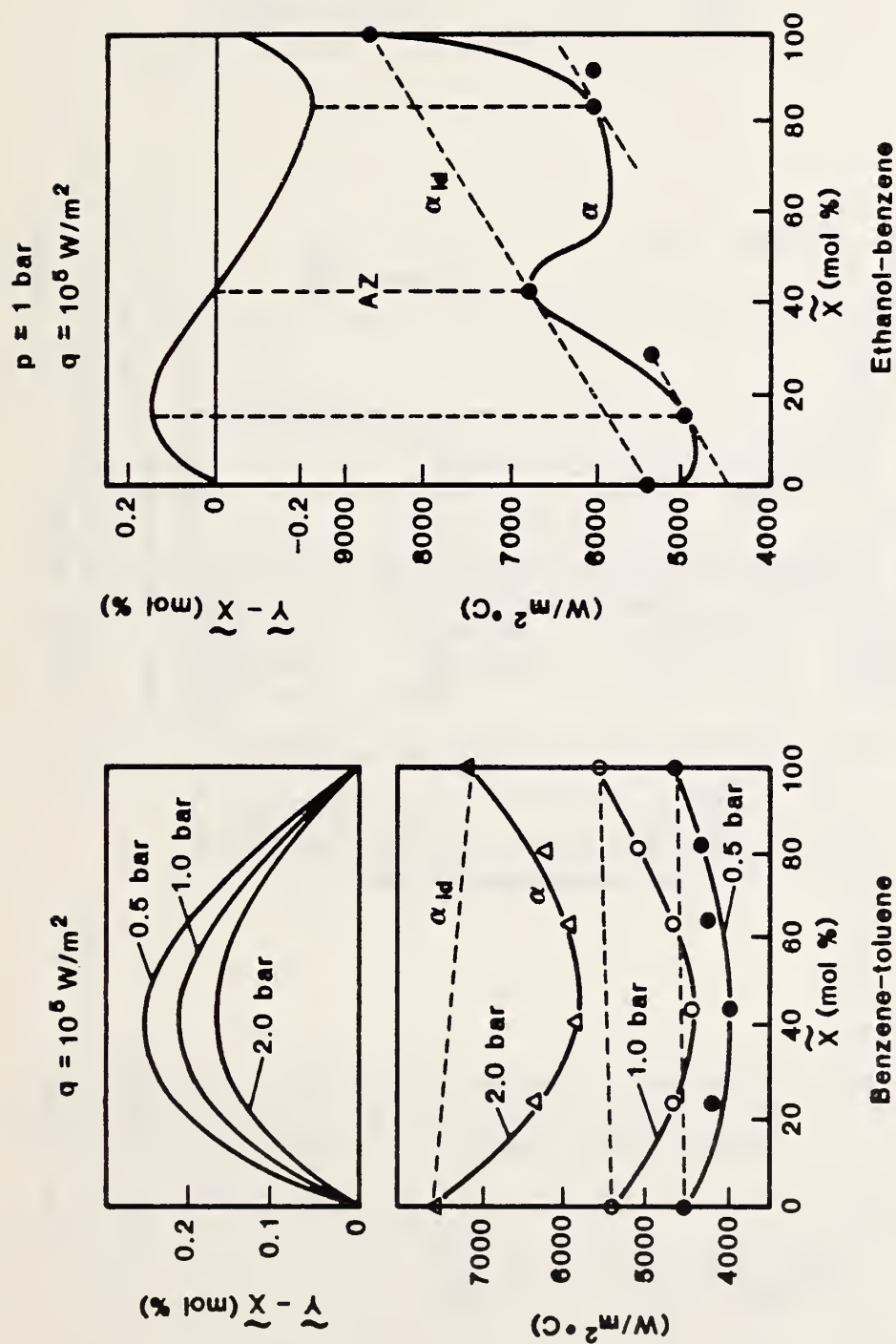


Figure 7-2: Pool Boiling Experiments of Happel and Stephan with binary mixtures.
Reduction in heat transfer coefficient correlated with vapor-liquid composition difference.

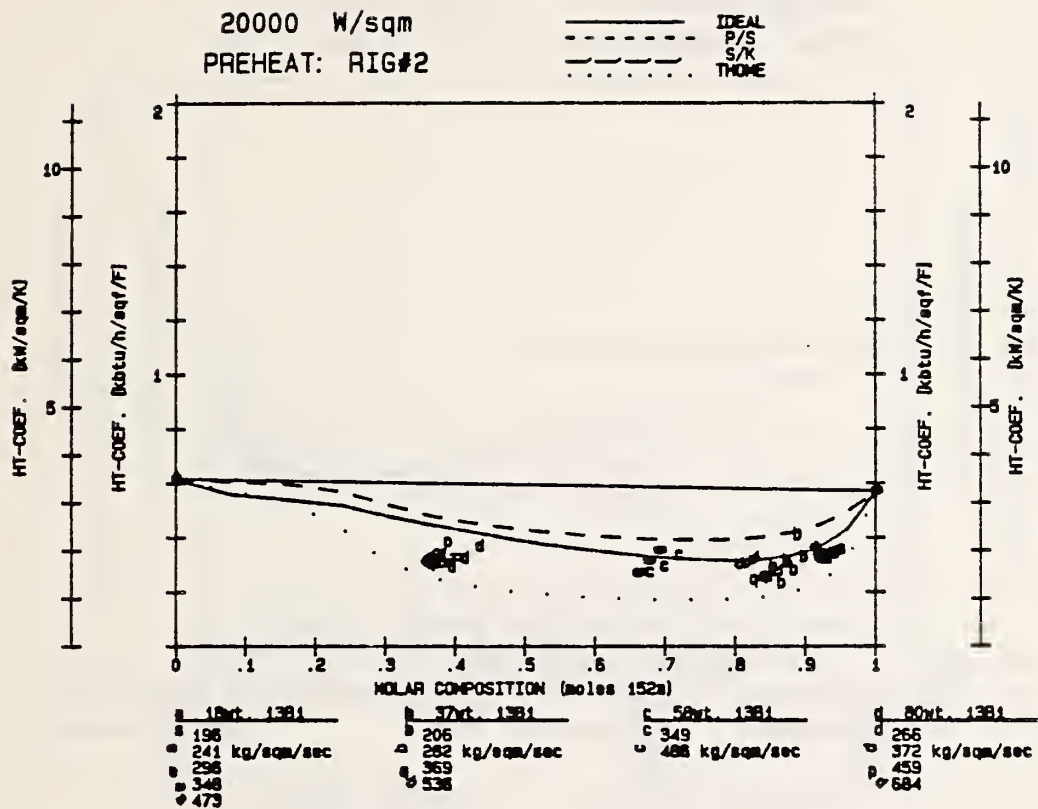
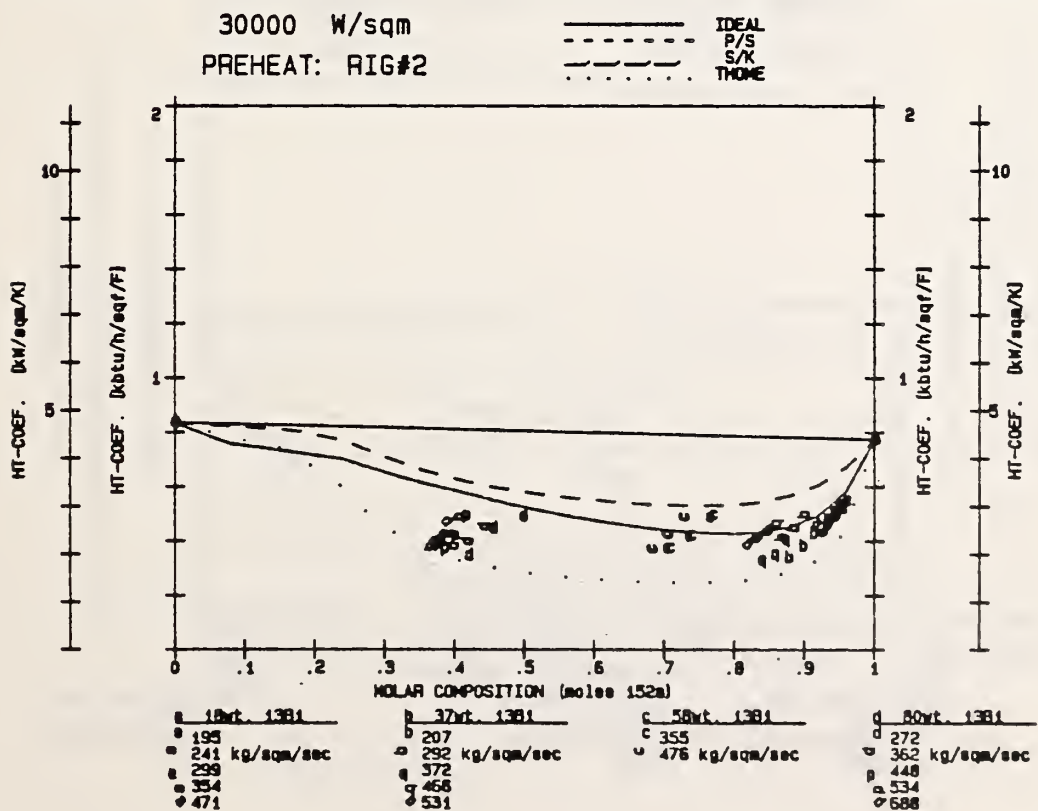


Figure 7-4: Comparison of Preheat Data to Pool Boiling Models



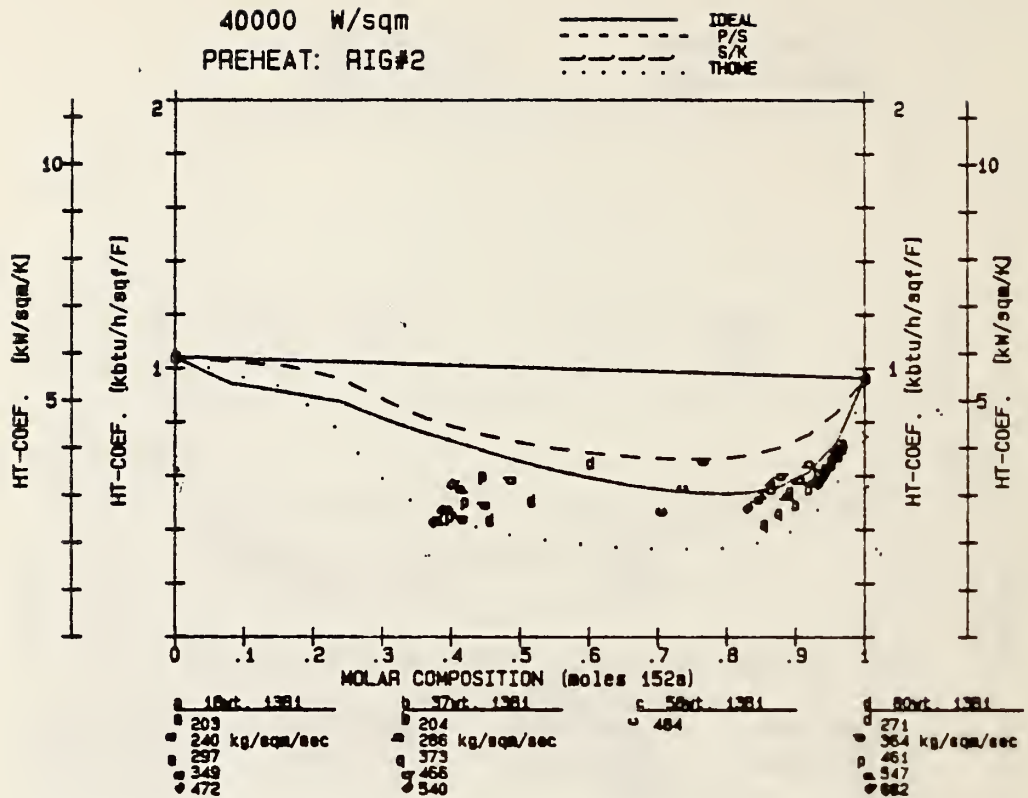
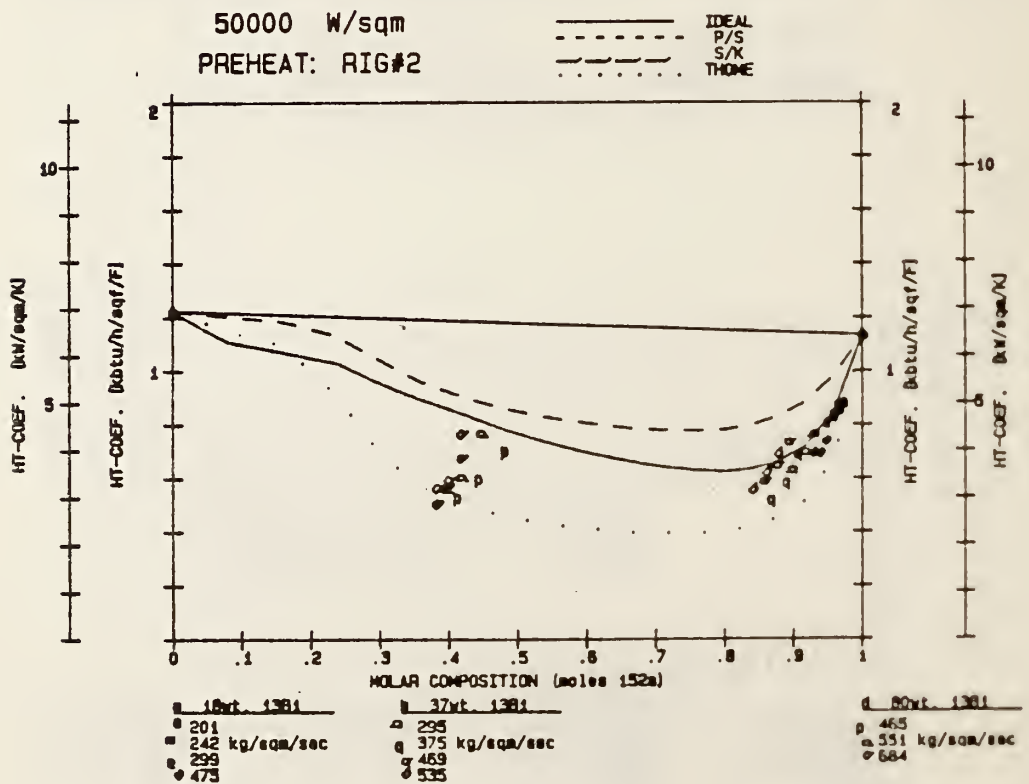


Figure 7-4 (cont): Comparison of Preheat Data to Models



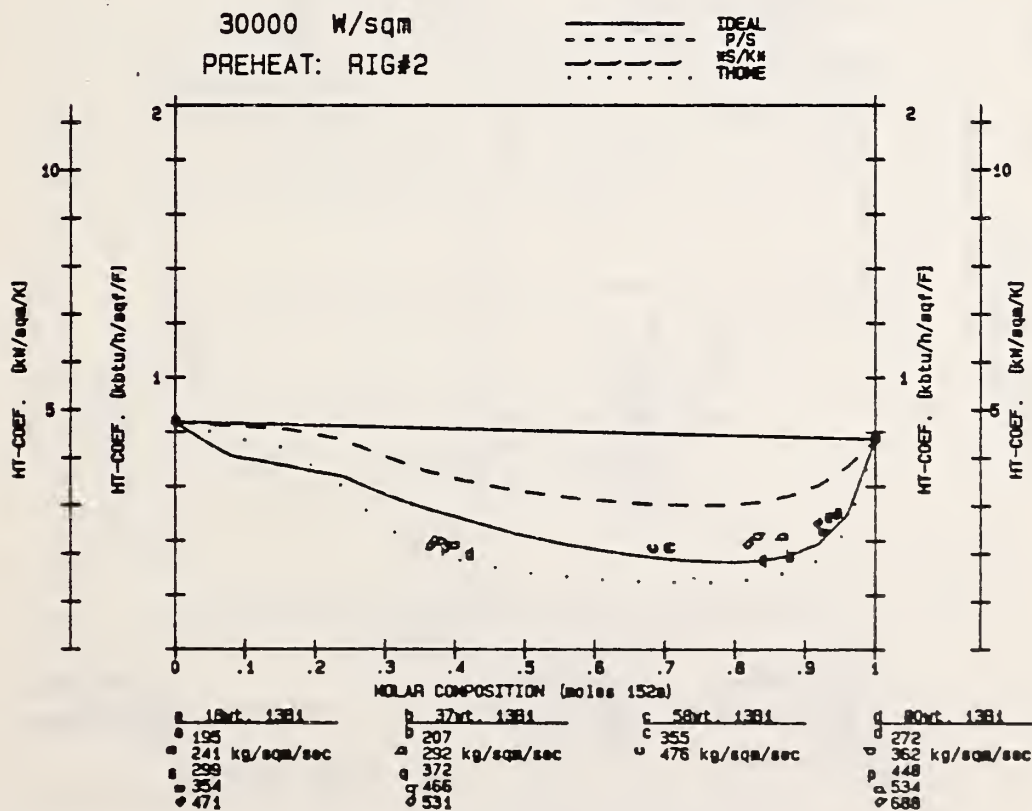
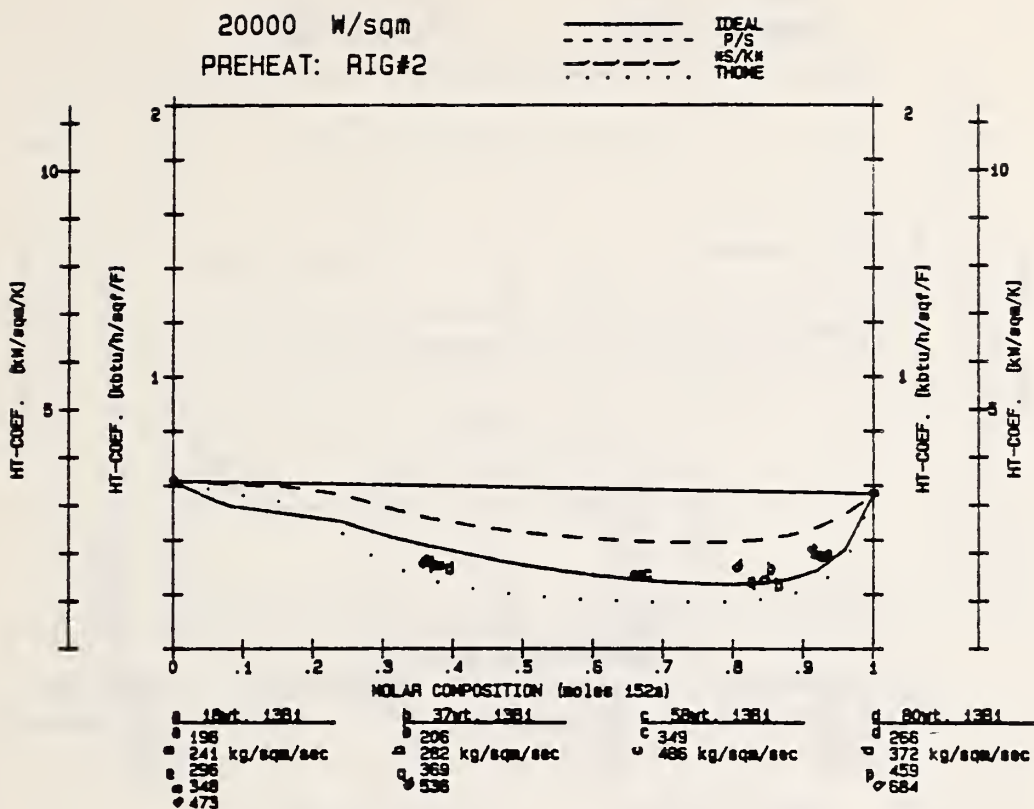


Figure 7-5: Comparison of 1st Station Preheat Data to Pool Boiling Models

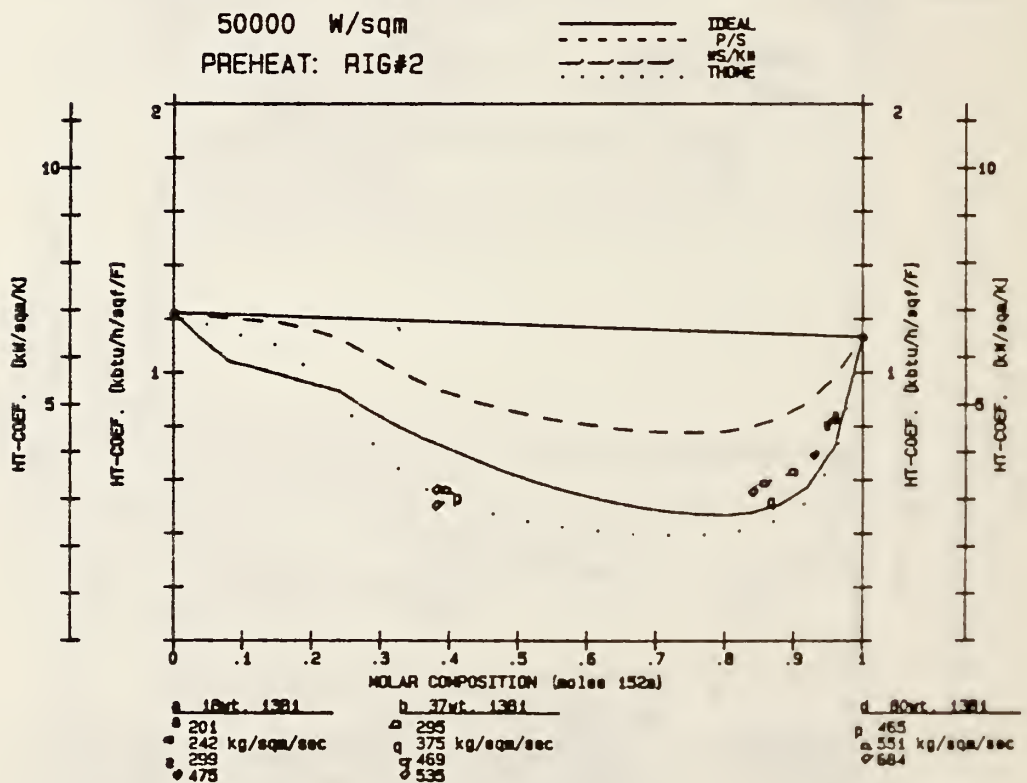
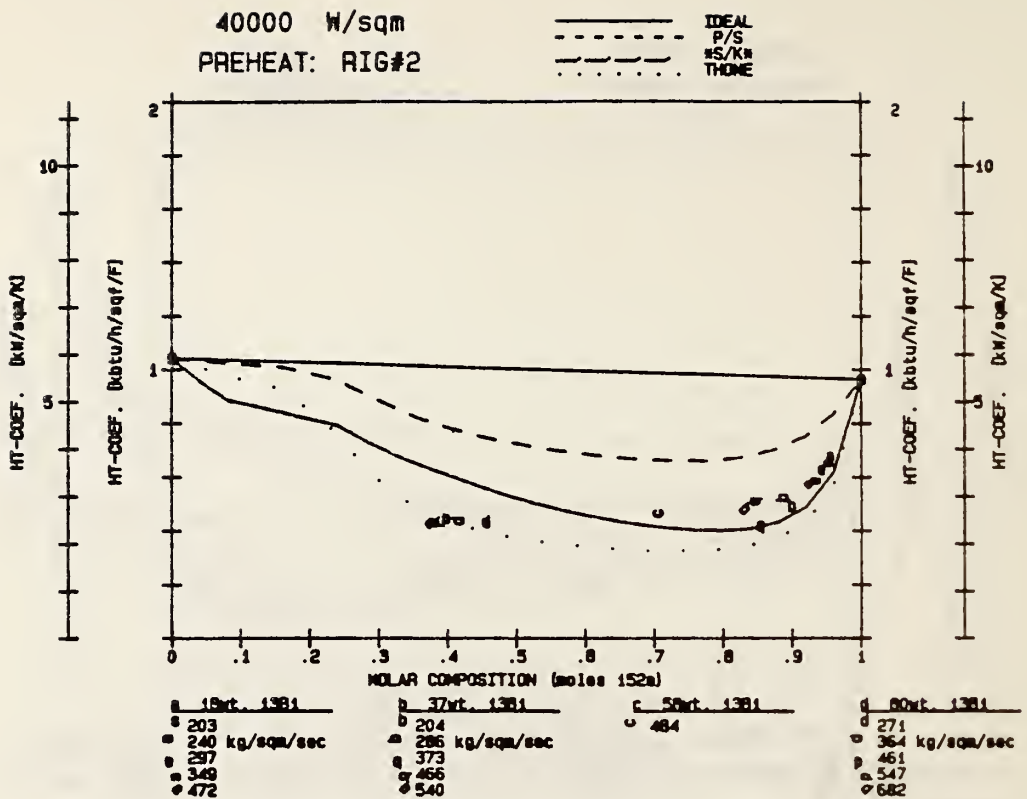


Figure 7-5 (cont): Comparison of 1st Station Preheat Data to Pool Boiling Models

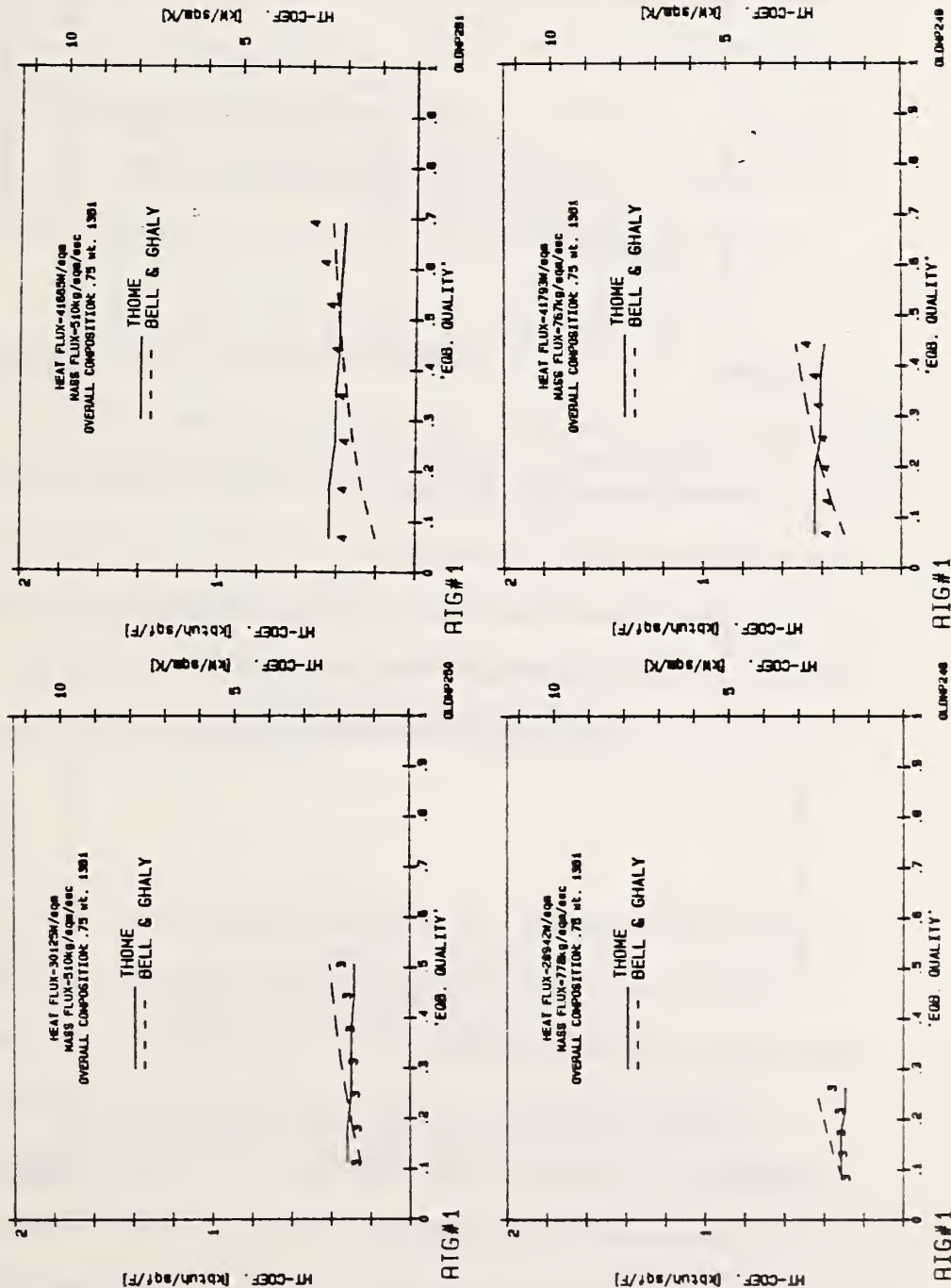


Figure 7-6: Comparison of Rig#1 Data to Thome's and Bell and Ghaly's Methods. Bell and Ghaly model produces same results as Chen's evaporative only method.

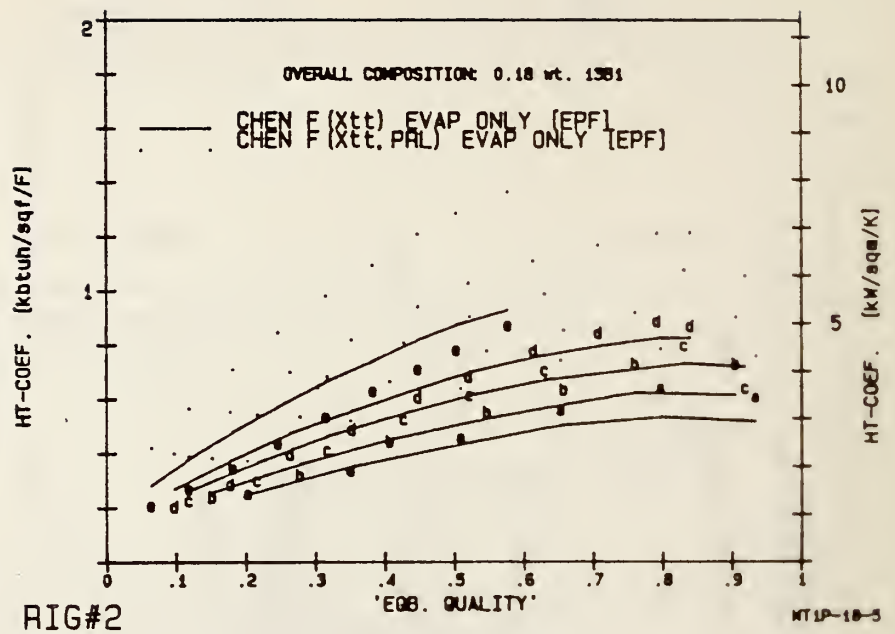
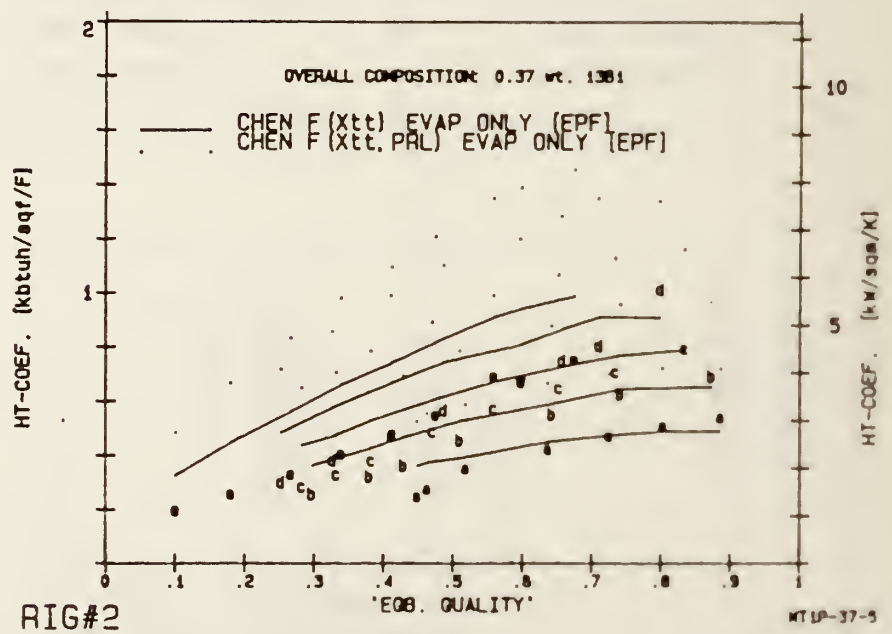


Figure 7-7: Comparison of Measured Test Section Data to Evaporative Only Methods



CHAPTER 8: CONCLUSIONS AND RECOMMENDATIONS FOR FURTHER RESEARCH

8.1 Summary of Findings and Contributions

The research described in this report involved determining experimental heat transfer coefficients, (HTC) examining the phenomena involved in the physical process, and analyzing the predictive ability of available models and correlations. This work was done for both pure and mixed refrigerants. Over 1,000 data points were collected, covering a wide range of pressure, composition, quality, and heat and mass flux.

Several data collection and reduction factors were shown to influence the experimental heat transfer coefficients. The use of pressure taps and instream thermocouples may affect the wall temperature measurements (Chapter 3). The use of a preheater introduces concerns about entrainment and liquid film superheat, though the effect was seen to be minimal. The use of equilibrium temperature in the definition of the HTC may itself cause a quality dependence to appear in the results (Chapter 5).

It is very important to be able to predict the dominant heat transfer regime and the point of complete suppression of nucleate boiling (Chapters 4 and 6). A controversy in the current literature regarding suppression of nucleate boiling was resolved by critical analysis in favor of traditional theory. It was seen that with pure refrigerants complete suppression occurs only at lower pressures than would occur in residential heat pump applications. A suppression criterion was applied to pure refrigerants at a selected cavity size, and shown to predict

quantitatively the quality at which suppression occurs for a given pressure, heat and mass flux. The method was extended to mixed refrigerants via several hypotheses, and illuminated questions about predicting suppression with mixtures. The method predicted that ebullition might be easier to achieve with mixtures than for pure R152a unless mass transfer resistance was included. In contrast, inclusion of a mass transfer resistance term suggests that suppression would be easier to achieve. Various methods were suggested, and partially verified, for including a mixture effect in the suppression criterion.

Many pure fluid correlations were examined critically (27 in total). Older correlations proved to be inaccurate with data bases other than the ones with which they were originally developed. The new method by Shah was shown to be inaccurate due to its treatment of the suppression point. The complete Chen correlation and its many variations were tested. The complete correlation predicts badly, generally overestimating the nucleate boiling contribution. The use of the semi-analytic suppression factor which has been suggested recently aggravated the overprediction. In the nucleate boiling regime, the new method of Stephan and Abdel salam [St82] was validated. The inclusion of this method [St82] into Chen's correlation required special reformulation, and the method then predicted particularly well in the forced convection dominated region. A Prandtl number correction suggested by Bennett and Chen [Be80] was used in a new procedure to predict HTC's for pure refrigerants. The new procedure incorporates a pool boiling method [St82], the evaporative portion of the [Be80] method and uses the

suppression criterion verified in Chapter 4. For these reasons it is better grounded in theory than recent regression-based correlations. It predicted the measured behavior better than calculations which have appeared in the literature, and can be used in a non-iterative manner with little loss in accuracy. The method was also checked against other independent data bases, and predicted the values well.

Sudden departure from nucleate boiling (DNB) events were observed in some of the pure fluid and mixtures' measurements. In examining other data sets of refrigerants, similar events could be seen, though they remained unattributed as such by their original authors. These events may be the cause of some of the data scatter found in the literature; the data in the literature should be critically reviewed for these events. The occurrence of DNB events suggest reduced heat transfer in the first row of coils in heat pump evaporators; methods could be developed to prevent their occurrence (e.g., addition of a second component and/or modified).

In the case of mixtures, previously unrecognized physical phenomena were noted: the circumferential variation in HTC may be opposite for mixtures than observed for pure fluids. This observation suggests the existence of a circumferential gradient in concentration and interfacial temperature (Chapter 5). Modelling then of mixture heat transfer is further complicated in that gradients exist in axial, radial and circumferential directions. In the flow boiling of mixtures when the onset of nucleate boiling is more difficult to predict and when mass transfer

resistance occurs, the actual quality may lag the 'equilibrium' quality in a different way than for pure fluids. This problem poses another difficulty for the correlations/models suggested to date.

For mixtures it was shown that the measured HTC would be different from ideal, even in the absence of mass transfer resistance, due to non-ideal property behavior. In the nucleate boiling dominated regime, α_{EPF} is greater than α_{id} (Chapter 7). In contrast, in the forced convection/evaporation, regime, α_{EPF} is less than α_{id} (Chapter 2). The measured values in each regime showed a degradation in heat transfer over that predicted by equivalent pure fluid correlations, presumably due to mass transfer resistance (Chapter 7). The degradation compared to either pure fluid was seen to be sometimes very severe (greater than 50%). In the nucleate boiling mode, this is due to mass transfer resistance restricting bubble growth. In the forced convection/evaporation mode, it may be due to mass transfer resistance suppressing the nucleate boiling for the mixture, but not for the pure components.

A total of 46 methods were examined for predicting heat transfer with flow boiling of mixtures (Chapter 7). Many methods were simple variations of the few existing techniques or were designed originally for pure fluids. Of the actual mixtures' models/correlations, some were found to be flawed on physical grounds. The regression-based correlation of Varma et al suggests that heat transfer is enhanced by the use of refrigerant mixtures over equivalent fluids; this has not been observed to date. The method of Bennett and Chen is also problematic at

large Lewis numbers. Its correction term for mass transfer resistance in evaporative flow becomes negative (not physically possible) in this range. It should be excluded from further use.

None of the mixtures' calculation methods achieved closure with measured values to the same degree as was achieved with pure fluids. Closure, however, was typical of that reported in the literature for mixtures. In the nucleate boiling dominated regime, the method of Thome, suggested for pool boiling of mixtures, achieved the best agreement with the measured heat transfer coefficient. It however predicted the opposite quality dependence than was observed in the data. It was able to predict the average heat transfer coefficient in this regime very well, and is thus recommended. In the forced convection evaporative regime, none of the methods predicted particularly well. The best fit to the data was achieved by the evaporative portion of Chen's original equation. This method then neglects any mixture effect, i.e., MTR, and suggests the absence of nucleate boiling. It does however tend to overpredict, particularly at high mass flow rates. This tendency is opposite that observed for pure fluids. Unlike the case of pure refrigerants, no general complete correlation could be developed for mixtures. Chawla's original supposition, which worked very well for pure fluids, sometimes selected the less accurate predictive method. However, failing an alternative, it is still recommended for use. This result, while disappointing, illustrates the difficulty with the prediction of mixture behavior. It also suggests the wide need for more experiments in the area.

8.2 Further Research Needs

Several new efforts could be supported which would add to the understanding of flow boiling of mixtures. First the experimental rig could be redesigned in order to increase the speed with which data could be collected. An example of such a rig is shown in Figure 8-1. The rig, modular in orientation, could have removable tubes for special studies (e.g., enhanced surfaces, artificial nucleation sites, effect of pressure and temperature taps). It also could include one tube which is designed for constant temperature operation and flow visualization. Valving could be used to allow flow through the tubes in any order. Thermocouples could be placed to determine the onset of nucleate boiling point, film boiling occurrences, and instream temperatures (microthermocouples could be tried). U-tubes with different radii of curvature could be installed between passes to allow studies of the effect of evaporator bends.

On a more fundamental basis, the principal efforts for pure fluids could be to understand and predict: (a) entrainment and deposition rates, and (b) pressure drop. Data on the former is particularly scarce. For the latter, pressure drop should be measured in an experiment with simple evaporation (complete suppression) and again in an experiment with nucleate boiling dominant. This might provide information to develop a more accurate pressure drop correlation. An improved ΔP correlation would assist both the heat transfer and suppression predictions.

For mixtures, there is a fundamental need to know concentration on both a bulk stream and local gradient basis. Because virtually no measurements have been taken to date, even intrusive measurements would help. To this end, isokinetic sampling probes or hot wire techniques could be used in principle. In the immediate future, measurements of other mixtures should be done. If possible, an ideal mixture should be used. The measurement program should vary parametrically, pressure, concentration, mass and heat flux, and cover the full quality range. The pressure levels should cover a range which suggests complete suppression. This would provide information about possible mass transfer resistance and non-equilibrium in the pure evaporative mode.

The issue of onset and suppression of nucleate boiling for mixtures needs to be resolved. The literature offers few papers on experimentally determined ONB values and boiling site densities for mixtures. The new experimental rig could be designed to include boiling from artificial nucleation sites in a glass section (visualization studies would then be possible). If in this section, constant temperature, rather than constant heat flux, could be maintained, then excellent resolution of the ONB point should be possible. Hysteresis studies would also be assisted in the use of such a section.

In all cases, any future studies occur in parallel with measurements of transport properties of the mixed fluids. Precise knowledge of these properties would allow the separate determination of the contribution of mass transfer resistance to each heat transfer regime.

Even without further measurements, the existing data base and correlations can be examined further. There are near endless combination of portions of existing correlations which could be tested against the data. Data in the literature should be examined critically for experimental technique and data interpretation. In particular, inlet conditions (subcooled liquid versus two phase) may have an effect on results. DNB events for mixed refrigerants also needs to be studied further. Some of the scatter in the predictive ability in correlations may in fact be due to poor experimental technique or interpretation rather than a problem with the correlations.

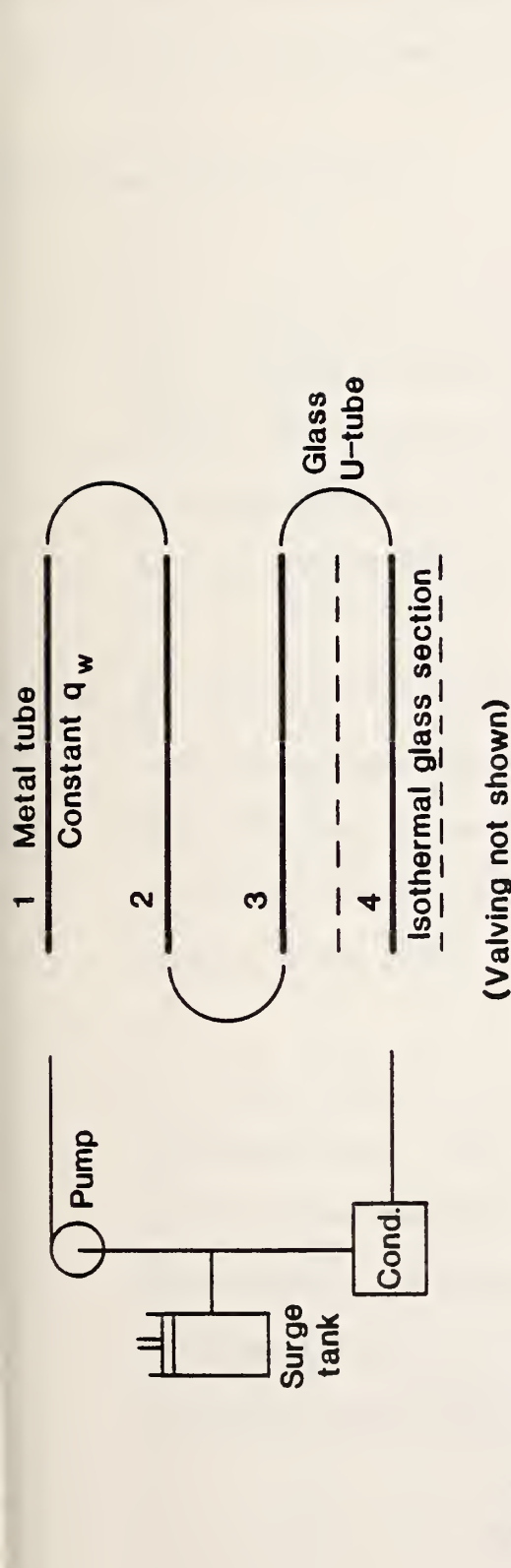


Figure 8-1: Proposed New Test Rig.

APPENDIX 3A: EXPERIMENTAL DATA SUMMARY

The following lists the data collected for this report. It is arranged so that other researchers may use it most easily.

These items should be noted:

- (a) The tests where film boiling occurred at the tube top are: 225, 236, 237, 252, 253, 256, 265, 274, 275. Though the average heat transfer coefficient is only partially affected, this data should not be used for comparison to annular flow boiling correlations.
- (b) The heat transfer coefficients, HTC, for values of $x = 0.00$ may be incorrect. The actual thermodynamic quality was less than 0.00, however in many cases, HTC was mistakenly calculated with the $T_f = T_{sat}$, instead of $T_f = T_{sc}$. These values should not be used.
- (c) 'Feed Comp' refers to the measured composition at the subcooled inlet. 'Mass Quality' refers to the calculated quality based on weight, not moles. 'Liquid Comp' and 'Vapor Comp' refer to calculated compositions at the local pressure, enthalpy and given feed composition. 'T_{eqb}' refers to the calculated fluid temperature assuming equilibrium conditions.

TEST SECTION DATA: R16#1 R152a

ROW	MASS FLUX kg/sq.m/s	HEAT FLUX W/sq.m	QUALITY	HTC W/sq.m/K	Test degK
194	699	42068	0.00	1750	257.5
	699	42068	0.00	1782	262.7
	699	42068	.00	3117	264.5
	699	42068	.03	2870	264.0
	699	42068	.05	3120	263.4
	699	42068	.08	3459	262.8
	699	42068	.11	3613	262.0
	699	42068	.13	4197	261.2
	699	42068	.16	4670	260.4
195	703	29636	0.00	1861	256.6
	703	29636	0.00	1892	260.3
	703	29636	0.00	2588	261.1
	703	29636	.02	2501	260.6
	703	29636	.04	2553	260.1
	703	29636	.05	2753	259.6
	703	29636	.07	3119	259.0
	703	29636	.09	3463	258.3
	703	29636	.11	3969	257.6
196	711	18725	0.00	1759	254.0
	711	18725	0.00	1776	256.3
	711	18725	0.00	2068	257.5
	711	18725	.01	2009	257.2
	711	18725	.02	2049	256.9
	711	18725	.03	2112	256.5
	711	18725	.04	2389	256.1
	711	18725	.05	2765	255.6
	711	18725	.06	3237	255.2
197	713	10350	0.00	1763	252.7
	713	10350	0.00	1760	254.0
	713	10350	0.00	1761	254.8
	713	10350	.00	1645	254.5
	713	10350	.01	1640	254.3
	713	10350	.02	1631	254.0
	713	10350	.02	1833	253.7
	713	10350	.03	2121	253.4
	713	10350	.03	2603	253.0
198	465	11038	0.00	1158	257.4
	465	11038	0.00	1109	258.8
	465	11038	.01	915	259.7
	465	11038	.02	1126	258.6
	465	11038	.03	1507	258.5
	465	11038	.04	1796	258.4
	465	11038	.05	1929	258.2
	465	11038	.06	2083	258.1
	465	11038	.07	2279	257.9

TEST SECTION DATA: R16#1 R152a

RUN	MASS FLUX kg/sq m/s	HEAT FLUX W/sq m	QUALITY	HTC W/sq m/K	Tsat degK
199	462	18592	0.00	1192	256.1
	462	18592	0.00	1571	261.6
	462	18592	.01	2044	262.1
	462	18592	.03	2197	261.9
	462	18592	.04	2291	261.8
	462	18592	.06	2417	261.6
	462	18592	.08	2616	261.4
	462	18592	.10	2868	261.1
	462	18592	.12	3195	260.9
200	460	29415	0.00	1668	260.2
	460	29415	0.00	2470	265.6
	460	29415	.01	2935	267.3
	460	29415	.04	2965	267.1
	460	29415	.07	3027	266.6
	460	29415	.10	3164	266.6
	460	29415	.13	3546	266.3
	460	29415	.16	3962	266.0
	460	29415	.18	4455	265.6
201	453	41920	0.00	2043	262.5
	453	41920	0.00	3402	270.3
	453	41920	.02	3993	272.1
	453	41920	.07	3914	271.9
	453	41920	.11	3706	271.7
	453	41920	.15	3949	271.5
	453	41920	.19	4432	271.2
	453	41920	.24	4997	270.9
	453	41920	.28	5675	270.6
202	235	18750	.02	1649	258.7
	235	18750	.05	1955	258.5
	235	18750	.09	2120	258.4
	235	18750	.12	2166	258.2
	235	18750	.16	2476	258.0
	235	18750	.19	2763	257.7
	235	18750	.23	2950	257.4
	235	18750	.26	3253	257.1
	235	18750	.29	3617	256.9
203	237	10614	.01	1413	257.3
	237	10614	.03	1698	257.3
	237	10614	.05	1708	257.2
	237	10614	.07	1762	257.2
	237	10614	.09	1768	257.1
	237	10614	.11	1872	257.1
	237	10614	.13	2007	257.0
	237	10614	.15	2215	257.0
	237	10614	.17	2361	256.9
204	229	4671	0.00	982	253.5

TEST SECTION DATA: R16#1 R152a

RUN	MASS FLUX kg/sq m/s	HEAT FLUX W/sq m	QUALITY	HTC W/sq m/K	Test degK
205	229	4671	.00	1267	259.0
	229	4671	.01	1527	258.9
	229	4671	.02	1556	258.6
	229	4671	.03	1764	258.7
	229	4671	.04	1928	258.6
	229	4671	.05	1937	258.5
	229	4671	.06	1839	258.4
	229	4671	.07	1572	258.3
	233	29761	.02	2657	261.7
	233	29761	.07	2491	261.5
	233	29761	.13	2439	261.2
	233	29761	.19	2750	261.0
	233	29761	.24	3142	260.8
	233	29761	.30	3514	260.5
	233	29761	.35	3776	260.1
	233	29761	.41	4133	259.7
206	233	29761	.47	4336	259.3
	232	42257	.01	3947	265.4
	232	42257	.09	3722	265.1
	232	42257	.18	3453	264.8
	232	42257	.26	3306	264.5
	232	42257	.34	4215	264.2
	232	42257	.42	4622	263.7
	232	42257	.50	4875	263.2
	232	42257	.58	5267	262.6
	232	42257	.66	5592	262.0
210	140	19285	.03	2340	262.8
	140	19285	.09	2438	262.7
	140	19285	.15	2234	262.6
	140	19285	.21	2238	262.5
	140	19285	.27	2415	262.4
	140	19285	.33	2471	262.3
	140	19285	.40	2852	262.1
	140	19285	.46	3124	261.9
	140	19285	.52	3382	261.8
	141	29021	.02	3025	268.5
211	141	29021	.11	3223	268.4
	141	29021	.21	3027	268.3
	141	29021	.30	3135	268.1
	141	29021	.39	3204	268.0
	141	29021	.47	3566	267.8
	141	29021	.58	4095	267.6
	141	29021	.67	4248	267.4
	141	29021	.77	4591	267.2
212	236	41722	.02	3483	263.9
	236	41722	.10	3449	263.6

TEST SECTION DATA: R1501 R152a

RUN	MASS FLUX kg/sq m/s	HEAT FLUX W/sq m	QUALITY	HTC W/sq m/K	Tsat deg F
	236	41722	.18	3482	263.3
	236	41722	.25	3764	263.0
	236	41722	.33	4045	262.7
	236	41722	.41	4391	262.1
	236	41722	.49	4732	261.5
	236	41722	.57	4914	261.0
	236	41722	.64	5057	260.4
214	216	27681	0.00	1793	280.6
	216	27681	.01	4525	289.5
	216	27681	.07	4459	289.5
	216	27681	.13	4849	289.4
	216	27681	.19	4278	289.4
	216	27681	.26	4210	289.3
	216	27681	.32	4022	289.2
	216	27681	.38	4194	289.2
	216	27681	.44	4675	289.1
215	427	27814	0.00	1601	290.7
	427	27814	0.00	2313	285.9
	427	27814	0.00	4129	291.2
	427	27814	.03	5259	292.3
	427	27814	.06	4712	292.3
	427	27814	.09	4537	292.2
	427	27814	.12	4211	292.1
	427	27814	.15	4234	292.1
	427	27814	.18	4747	292.0
216	415	39971	0.00	2007	285.0
	415	39971	0.00	3192	292.6
	415	39971	.01	7367	299.4
	415	39971	.03	7103	299.4
	415	39971	.10	6511	299.3
	415	39971	.15	5997	299.3
	415	39971	.20	5441	299.2
	415	39971	.25	5283	299.1
	415	39971	.29	5746	299.0
218	646	28191	0.00	1893	285.3
	646	28191	0.00	1940	288.8
	646	28191	0.00	1989	292.3
	646	28191	0.00	3342	295.7
	646	28191	.01	4049	297.2
	646	28191	.03	4277	297.2
	646	28191	.06	4372	297.1
	646	28191	.08	4199	297.0
	646	28191	.10	4014	296.9
219	645	40589	0.00	1862	283.4
	645	40589	0.00	2524	288.4
	645	40589	0.00	3751	293.4

TEST SECTION DATA: RIG#1 R152a

RUN	MASS FLUX kg/sqa/s	HEAT FLUX W/sqa	QUALITY	HTC W/sqa/K	Tsat degK
645	40589	.06	5636	297.6	
645	40589	.04	5619	297.5	
645	40589	.07	5407	297.4	
645	40589	.10	5370	297.4	
645	40589	.13	5122	297.3	
645	40589	.16	5137	297.2	

TEST SECTION DATA: R1681 R1381

RUN	MASS FLUX kg, sqm/s	HEAT FLUX W/sqm	QUALITY	HTC W/sqm/K	Test degK
282	764	10649	0.00	1497	259.5
	764	10649	.00	2601	261.8
	764	10649	.02	2662	261.8
	764	10649	.04	2900	261.8
	764	10649	.06	3125	261.8
	764	10649	.08	3401	261.7
	764	10649	.10	3619	261.7
	764	10649	.12	3489	261.6
	764	10649	.13	3205	261.6
283	1219	29494	0.00	4216	261.4
	1219	29494	.02	5428	262.4
	1219	29494	.06	4788	262.2
	1219	29494	.09	4451	262.0
	1219	29494	.12	4162	261.9
	1219	29494	.15	3990	261.7
	1219	29494	.19	4103	261.4
	1219	29494	.22	4213	261.2
	1219	29494	.25	4416	261.0
284	1210	42212	0.00	5127	263.7
	1210	42212	.03	7780	265.9
	1210	42212	.08	6925	265.7
	1210	42212	.13	6319	265.5
	1210	42212	.17	5859	265.3
	1210	42212	.22	5623	265.0
	1210	42212	.27	5567	264.7
	1210	42212	.32	5920	264.5
	1210	42212	.37	5915	264.2
285	802	42204	.01	7436	265.3
	802	42204	.08	7789	265.2
	802	42204	.15	7093	265.1
	802	42204	.23	6900	264.9
	802	42204	.30	6383	264.8
	802	42204	.37	6172	264.6
	802	42204	.44	6300	264.4
	802	42204	.52	6111	264.1
	802	42204	.59	4752	263.9
286	820	29330	.01	5097	261.6
	820	29330	.06	5590	261.5
	820	29330	.11	5083	261.4
	820	29330	.16	4925	261.3
	820	29330	.21	4603	261.2
	820	29330	.25	4511	261.0
	820	29330	.30	4655	260.8
	820	29330	.35	4664	260.6
	820	29330	.40	4644	260.4

TEST SECTION DATA: RIG#1 R13B1

RUN	MASS FLUX kg/sqm/s	HEAT FLUX W/sqm	QUALITY	HTC W/sqm/K	Tsat degK
287	413	29188	.05	5611	262.5
	413	29188	.15	5433	262.4
	413	29188	.25	5331	262.4
	413	29188	.34	5271	262.3
	413	29188	.44	5392	262.3
	413	29188	.54	4896	262.2
	413	29188	.63	5211	262.1
	413	29188	.73	5917	262.0
	413	29188	.83	6534	261.9
	413	29188	.93	6534	261.9
288	414	18792	.03	4279	261.8
	414	18792	.09	4396	261.7
	414	18792	.15	3645	261.7
	414	18792	.22	3237	261.7
	414	18792	.29	3279	261.6
	414	18792	.34	3348	261.5
	414	18792	.40	4854	261.4
	414	18792	.46	5539	261.3
	414	18792	.53	5744	261.2
	414	18792	.53	5744	261.2
289	403	10522	0.00	1775	262.9
	403	10522	.02	3769	265.8
	403	10522	.05	3823	265.7
	403	10522	.09	4321	265.7
	403	10522	.12	4169	265.6
	403	10522	.16	5646	265.6
	403	10522	.20	3492	265.5
	403	10522	.23	4170	265.4
	403	10522	.27	4100	265.3
	403	10522	.27	4100	265.3
290	803	18758	0.00	1709	260.4
	803	18758	0.00	2798	264.5
	803	18758	.01	4787	267.4
	803	18758	.04	5279	267.4
	803	18758	.08	5239	267.3
	803	18758	.11	5249	267.3
	803	18758	.14	5520	267.2
	803	18758	.17	6065	267.1
	803	18758	.21	5909	267.1
	803	18758	.21	5909	267.1
291	1220	18814	0.00	1896	259.5
	1220	18814	0.00	2517	261.2
	1220	18814	0.00	3810	264.0
	1220	18814	.01	5313	265.0
	1220	18814	.04	5325	264.9
	1220	18814	.06	5268	264.6
	1220	18814	.08	5545	264.7
	1220	18814	.10	6125	264.6
	1220	18814	.12	5682	264.5
	1220	18814	.12	5682	264.5

TEST SECTION DATA: RIG#1

RUN	MASS FLUX kg/sqcm	HEAT FLUX W/sqcm	MASS QUALITY	HTC W/sqcm/K	Teqb degK	LIQUID COMP.	VAPOR COMP.	FEED COMP.	PRESSURE bars
223	486	29309	.03	1168	260.2	.66	.86	.662	4.62
	486	29309	.10	1288	260.4	.64	.86		4.67
	486	29309	.17	1331	260.7	.62	.85		4.65
	486	29309	.23	1374	261.0	.61	.85		4.63
	486	29309	.30	1467	261.3	.59	.84		4.62
	486	29309	.36	1529	261.7	.56	.84		4.59
	486	29309	.42	1577	262.1	.54	.83		4.56
	486	29309	.48	1661	262.5	.51	.83		4.53
	486	29309	.54	1769	263.1	.48	.82		4.50
224	487	41308	.03	1617	262.8	.66	.85	.662	5.08
	487	41308	.12	1724	263.1	.64	.85		5.06
	487	41308	.22	1809	263.6	.61	.84		5.04
	487	41308	.31	1920	264.0	.58	.84		5.02
	487	41308	.40	2083	264.7	.55	.83		4.99
	487	41308	.48	2216	265.4	.51	.82		4.96
	487	41308	.57	2336	266.3	.47	.81		4.92
	487	41308	.63	2502	267.1	.43	.79		4.88
	487	41308	.70	2711	268.1	.40	.78		4.83
225	252	28671	.08	1126	260.1	.65	.86	.662	4.64
	252	28671	.20	1045	260.7	.61	.85		4.63
	252	28671	.32	1122	261.5	.58	.84		4.62
	252	28671	.44	1337	262.5	.53	.83		4.61
	252	28671	.54	1494	263.9	.48	.81		4.60
	252	28671	.64	1640	265.3	.43	.79		4.55
	252	28671	.73	1766	266.8	.37	.77		4.57
	252	28671	.80	1929	268.2	.33	.74		4.55
	252	28671	.97	2068	269.5	.30	.72		4.53
226	259	41190	.09	1570	262.7	.64	.85	.662	5.02
	259	41190	.27	1434	263.7	.60	.84		5.01
	259	41190	.43	1731	265.0	.54	.83		5.00
	259	41190	.58	2084	266.9	.47	.80		4.99
	259	41190	.70	2395	268.9	.40	.77		4.97
	259	41190	.81	2651	271.0	.34	.74		4.96
	259	41190	.91	2848	272.8	.29	.70		4.94
	259	41190	1.00	3137	274.4	.25	.66		4.92
	259	41190	1.00	1353	275.9	.22	.62		4.90
230	739	29154	0.00	1037	253.0	.66	1.00	.662	4.60
	739	29154	.03	1129	259.5	.66	.86		4.59
	739	29154	.08	1227	259.6	.65	.86		4.57
	739	29154	.12	1301	259.7	.64	.86		4.55
	739	29154	.17	1386	259.8	.62	.85		4.52
	739	29154	.21	1431	259.9	.61	.85		4.50
	739	29154	.26	1474	260.0	.60	.85		4.47
	739	29154	.30	1528	260.1	.58	.85		4.44
	739	29154	.34	1602	260.2	.57	.84		4.41

TEST SECTION DATA: RIG#1

RUN	MASS FLUX kg/sqm/s	HEAT FLUX W/sqm	MASS QUALITY	HTC W/sqm/K	Temp degK	LIQUID COMP.	VAPOR COMP.	FEED COMP.	PRESSURE bars
231	729	42115	0.00	1461	261.0	.66	1.00	.662	5.06
	729	42115	.05	1710	262.6	.65	.85		5.06
	729	42115	.12	1780	263.0	.64	.85		5.04
	729	42115	.18	1920	263.2	.62	.85		5.02
	729	42115	.25	2023	263.4	.60	.84		4.99
	729	42115	.31	2109	263.7	.58	.84		4.96
	729	42115	.37	2191	263.9	.56	.83		4.92
	729	42115	.43	2305	264.2	.54	.83		4.87
	729	42115	.49	2463	264.6	.51	.82		4.83
234	497	29340	.01	1110	258.9	.70	.87	.706	4.65
	497	29340	.08	1366	259.1	.69	.87		4.63
	497	29340	.15	1326	259.3	.68	.86		4.62
	497	29340	.22	1387	259.5	.66	.86		4.61
	497	29340	.28	1474	259.7	.65	.86		4.59
	497	29340	.34	1533	260.0	.63	.85		4.57
	497	29340	.41	1599	260.3	.61	.85		4.54
	497	29340	.47	1685	260.6	.59	.84		4.52
	497	29340	.53	1824	261.1	.56	.84		4.49
235	507	41411	.01	1620	262.1	.70	.87	.706	5.14
	507	41411	.10	1761	262.4	.69	.86		5.12
	507	41411	.20	1910	262.6	.67	.86		5.10
	507	41411	.29	1920	263.0	.65	.85		5.08
	507	41411	.38	2074	263.4	.62	.85		5.06
	507	41411	.46	2199	263.9	.59	.84		5.02
	507	41411	.54	2320	264.5	.56	.83		4.98
	507	41411	.62	2493	265.2	.52	.82		4.94
	507	41411	.69	2742	266.1	.47	.81		4.90
236	247	29231	.09	1155	258.5	.69	.87	.706	4.55
	247	29231	.22	1039	259.1	.66	.86		4.54
	247	29231	.35	1159	259.8	.63	.85		4.53
	247	29231	.47	1328	260.7	.59	.84		4.50
	247	29231	.58	1530	261.9	.53	.83		4.52
	247	29231	.69	1669	263.4	.47	.81		4.50
	247	29231	.78	1821	265.1	.41	.79		4.48
	247	29231	.86	1982	266.6	.36	.76		4.47
	247	29231	.94	2190	268.2	.31	.73		4.45
237	247	36019	.10	1393	259.6	.69	.86	.706	4.55
	247	36019	.26	1228	260.5	.65	.86		4.72
	247	36019	.41	1393	261.5	.61	.85		4.71
	247	36019	.56	1733	262.9	.54	.83		4.70
	247	36019	.69	1961	264.7	.47	.81		4.69
	247	36019	.80	2179	266.7	.40	.78		4.67
	247	36019	.90	2417	268.7	.34	.75		4.65
	247	36019	1.00	2722	270.7	.29	.71		4.63
	247	36019	1.00	2232	272.6	.24	.66		4.61
238	758	29391	0.00	1216	257.5	.71	1.00	.706	4.72

TEST SECTION DATA: R16#1

RUN	MASS FLUX kg/sec/m ²	HEAT FLUX W/sqcm	MASS QUALITY	HTC W/sqcm/K	Temp degK	LIQUID COMP.	VAPOR COMP.	FEED COMP.	PRESSURE bars
	758	29391	.42	1541	261.5	.60	.85		4.71
	758	29391	.07	1423	259.4	.69	.87		4.68
	758	29391	.12	1426	259.4	.68	.86		4.68
	758	29391	.16	1479	259.5	.68	.86		4.64
	758	29391	.21	1520	259.5	.67	.86		4.62
	758	29391	.25	1601	259.5	.65	.86		4.59
	758	29391	.30	1728	259.6	.64	.86		4.56
	758	29391	.34	1762	259.7	.63	.85		4.53
239	754	41485	0.00	1561	259.9	.71	1.00	.706	5.19
	754	41485	.04	1630	262.4	.70	.86		5.17
	754	41485	.11	1876	262.5	.69	.86		5.15
	754	41485	.17	1916	262.7	.67	.86		5.12
	754	41485	.23	2029	262.8	.66	.86		5.10
	754	41485	.29	2120	262.9	.65	.85		5.06
	754	41485	.35	2245	263.1	.63	.85		5.02
	754	41485	.41	2455	263.2	.61	.85		4.98
	754	41485	.47	2556	263.4	.59	.84		4.95
242	502	41732	.01	1630	263.4	.70	.86	.706	5.34
	502	41732	.10	1797	263.6	.69	.86		5.33
	502	41732	.19	1829	263.9	.67	.86		5.31
	502	41732	.28	1927	264.3	.65	.85		5.29
	502	41732	.37	2108	264.8	.62	.85		5.27
	502	41732	.46	2219	265.3	.59	.84		5.25
	502	41732	.55	2365	266.0	.56	.83		5.22
	502	41732	.62	2563	266.8	.52	.82		5.18
	502	41732	.70	2844	267.7	.48	.81		5.15
243	501	30058	.01	1319	260.5	.70	.87	.706	4.89
	501	30058	.08	1406	260.7	.69	.86		4.87
	501	30058	.14	1400	260.9	.68	.86		4.86
	501	30058	.21	1427	261.1	.66	.86		4.85
	501	30058	.28	1512	261.4	.65	.86		4.84
	501	30058	.34	1569	261.6	.63	.85		4.82
	501	30058	.41	1643	262.0	.61	.85		4.79
	501	30058	.47	1731	262.4	.59	.84		4.77
	501	30058	.53	1861	262.8	.56	.84		4.75
244	247	28776	.07	1182	259.6	.69	.87	.706	4.72
	247	28776	.20	1206	260.1	.67	.86		4.71
	247	28776	.33	1198	260.6	.63	.85		4.70
	247	28776	.45	1395	261.7	.59	.84		4.69
	247	28776	.57	1541	262.9	.54	.83		4.69
	247	28776	.67	1679	264.2	.48	.82		4.67
	247	28776	.77	1864	265.9	.42	.79		4.65
	247	28776	.84	2068	267.4	.37	.77		4.64
	247	28776	.92	2347	269.0	.33	.74		4.63
246	779	29943	0.00	1049	259.8	.75	1.00	.750	6.75
	779	29943	0.00	1259	264.6	.75	1.00		6.75

TEST SECTION DATA: RIG#1

RUN	MASS FLUX kg/sq.m/s	HEAT FLUX W/sq.m	MASS QUALITY	HTC W/sq.m/K	Teqb degK	LIQUID COMP.	VAPOR COMP.	FEED COMP.	PRESSURE bars
	779	28943	.05	1553	270.4	.74	.87		6.75
	779	28943	.04	1570	270.3	.75	.87		6.74
	779	28943	.08	1648	270.4	.74	.87		6.72
	779	28943	.13	1735	270.4	.73	.86		6.71
	779	28943	.17	1784	270.5	.73	.86		6.69
	779	28943	.22	1835	270.6	.72	.85		6.68
	779	28943	.26	2044	270.6	.71	.85		6.66
249	767	41793	0.00	1425	261.0	.75	1.00	.750	6.46
	767	41793	0.00	1909	266.8	.85	.91		6.45
	767	41793	.07	2161	266.8	.74	.87		6.44
	767	41793	.13	2123	266.9	.73	.87		6.42
	767	41793	.20	2183	269.1	.72	.86		6.40
	767	41793	.26	2248	269.2	.71	.86		6.38
	767	41793	.32	2372	269.3	.70	.86		6.33
	767	41793	.38	2485	269.4	.69	.85		6.32
	767	41793	.44	2729	269.6	.67	.85		6.29
250	511	30125	0.00	1206	261.9	.75	1.00	.750	5.81
	511	30125	.04	1529	265.3	.74	.87		5.81
	511	30125	.11	1561	265.5	.73	.87		5.80
	511	30125	.18	1536	265.6	.72	.87		5.79
	511	30125	.25	1578	265.6	.71	.86		5.78
	511	30125	.31	1634	266.0	.70	.86		5.77
	511	30125	.38	1721	266.2	.69	.85		5.75
	511	30125	.44	1898	266.5	.67	.85		5.73
	511	30125	.51	1972	266.8	.65	.85		5.71
251	510	41666	0.00	1630	265.0	.75	1.00	.750	6.40
	510	41666	.07	2094	266.6	.74	.87		6.39
	510	41666	.16	2097	266.3	.73	.86		6.38
	510	41666	.26	2046	269.1	.71	.86		6.36
	510	41666	.35	2142	269.4	.69	.86		6.35
	510	41666	.44	2281	269.8	.67	.85		6.33
	510	41666	.53	2436	270.3	.65	.84		6.30
	510	41666	.61	2614	270.9	.62	.84		6.28
	510	41666	.69	2935	271.6	.58	.83		6.25
252	251	29222	.05	1269	264.6	.74	.87	.750	5.68
	251	29222	.18	1160	265.0	.72	.87		5.67
	251	29222	.31	1226	265.5	.70	.86		5.67
	251	29222	.44	1303	266.1	.67	.85		5.66
	251	29222	.57	1521	267.0	.65	.84		5.65
	251	29222	.68	1675	268.1	.63	.83		5.64
	251	29222	.78	1824	269.5	.62	.81		5.63
	251	29222	.87	2082	271.2	.60	.79		5.62
	251	29222	.95	2373	272.9	.60	.77		5.61
253	254	34447	.05	1463	266.2	.74	.87	.750	5.96
	254	34447	.21	1354	266.6	.72	.86		5.95
	254	34447	.36	1384	267.3	.69	.86		5.95

TEST SECTION DATA: R1681

RUN	MASS FLUX kg/sqm/s	HEAT FLUX W/sqm	MASS QUALITY	HTC W/sqm.K	Temp degK	LIQUID COMP.	VAPOR COMP.	FEED COMP.	PRESSURE bars
	254	34447	.51	1552	268.1	.85	.85		5.94
	254	34447	.64	1265	269.3	.60	.83		5.93
	254	34447	.77	2109	270.9	.53	.82		5.92
	254	34447	.87	2518	272.8	.47	.79		5.91
	254	34447	.97	2958	274.8	.40	.76		5.90
	254	34447	1.00	2416	276.8	.34	.73		5.89
256	269	29215	.02	1489	267.7	.83	.90	.833	6.57
	269	29215	.15	1462	267.9	.82	.90		6.55
	269	29215	.28	1424	268.1	.81	.89		6.57
	269	29215	.42	1339	268.3	.80	.89		6.56
	269	29215	.54	1415	268.7	.78	.88		6.56
	269	29215	.66	1682	269.1	.76	.87		6.55
	269	29215	.77	1811	269.6	.73	.86		6.53
	269	29215	.89	2039	270.5	.69	.85		6.52
	269	29215	.98	2319	271.8	.63	.84		6.51
259	825	41410	0.00	1593	261.3	.83	1.00	.833	7.26
	825	41410	0.00	2447	269.7	.83	1.00		7.26
	825	41410	.05	2675	271.0	.83	.90		7.25
	825	41410	.11	2458	271.1	.83	.90		7.23
	825	41410	.17	2400	271.1	.82	.89		7.22
	825	41410	.24	2370	271.1	.82	.89		7.20
	825	41410	.29	2484	271.1	.81	.89		7.17
	825	41410	.36	2573	271.1	.80	.89		7.14
	825	41410	.42	2762	271.0	.80	.88		7.11
260	826	28642	0.00	1147	259.2	.83	1.00	.833	6.61
	826	28642	0.00	1540	264.4	.83	1.00		6.61
	826	28642	.01	1939	267.8	.83	.90		6.60
	826	28642	.06	1847	267.8	.83	.90		6.59
	826	28642	.10	1796	267.8	.83	.90		6.57
	826	28642	.14	1759	267.8	.82	.90		6.56
	826	28642	.19	1777	267.7	.82	.89		6.54
	826	28642	.23	1816	267.7	.82	.89		6.52
	826	28642	.27	1921	267.7	.81	.89		6.50
262	528	22463	0.00	1094	260.7	.83	1.00	.833	7.29
	528	22463	0.00	1644	267.9	.83	1.00		7.29
	528	22463	.02	2241	271.1	.83	.90		7.28
	528	22463	.08	2081	271.2	.82	.90		7.28
	528	22463	.13	2037	271.2	.82	.89		7.25
	528	22463	.18	1951	271.2	.82	.89		7.24
	528	22463	.24	1912	271.2	.82	.89		7.22
	528	22463	.29	2002	271.2	.81	.89		7.20
	528	22463	.34	2096	271.2	.81	.89		7.18
263	543	37301	0.00	1469	265.2	.83	1.00	.633	8.25
	543	37301	0.00	2287	273.1	.97	.98		8.24
	543	37301	.09	2673	275.6	.83	.89		8.23
	543	37301	.18	2700	275.7	.82	.89		8.22

TEST SECTION DATA: R15#1

RUN	MASS FLUX kg/sqcm/s	HEAT FLUX W/sqcm	MASS QUALITY	HTC W/sqcm/K	T _{eq} degK	LIQUID COMP.	VAPOR COMP.	FEED COMP.	PRESSURE bars
	543	37301	.26	2356	275.8	.81	.89		8.21
	543	37301	.35	2424	275.9	.81	.88		8.20
	543	37301	.43	2516	276.0	.80	.88		8.19
	543	37301	.52	2710	276.1	.79	.88		8.15
	543	37301	.59	2746	276.3	.78	.87		8.13
264	546	28655	0.00	1162	263.2	.83	1.00	.633	7.59
	546	28655	0.00	1853	272.0	.83	1.00		7.57
	546	28655	.06	2162	272.6	.83	.90		7.53
	546	28655	.12	2664	272.6	.82	.89		7.57
	546	28655	.19	2045	272.7	.82	.89		7.56
	546	28655	.25	1984	272.8	.81	.89		7.54
	546	28655	.31	2005	272.8	.81	.89		7.53
	546	28655	.38	2098	272.8	.80	.88		7.51
	546	28655	.44	2222	272.9	.79	.88		7.49
265	266	18598	.01	1110	265.7	.83	.90	.633	6.20
	266	18598	.09	1246	265.8	.83	.90		6.20
	266	18598	.18	1243	265.9	.82	.90		6.19
	266	18598	.26	1125	266.1	.81	.89		6.19
	266	18598	.34	1067	266.2	.80	.89		6.19
	266	18598	.42	1066	266.4	.79	.89		6.18
	266	18598	.51	1136	266.6	.78	.88		6.18
	266	18598	.58	1235	266.8	.77	.88		6.17
	266	18598	.66	1350	267.1	.75	.87		6.16
266	525	41457	0.00	1995	266.8	.83	1.00	.633	7.57
	525	41457	.05	2974	272.6	.83	.90		7.59
	525	41457	.15	3123	272.7	.82	.89		7.57
	525	41457	.25	2582	272.8	.81	.89		7.55
	525	41457	.35	2671	272.9	.80	.89		7.54
	525	41457	.44	2650	273.1	.79	.88		7.52
	525	41457	.53	2754	273.2	.78	.88		7.50
	525	41457	.62	3014	273.4	.77	.87		7.48
	525	41457	.71	3431	273.7	.75	.87		7.45
270	423	18539	0.00	745	259.4	.45	1.00	.454	5.37
	423	18539	0.00	939	264.8	.45	1.00		5.37
	423	18539	.03	1039	270.2	.44	.79		5.37
	423	18539	.04	1022	270.2	.44	.79		5.35
	423	18539	.09	1085	270.6	.42	.78		5.34
	423	18539	.13	1131	271.0	.41	.77		5.33
	423	18539	.17	1144	271.5	.39	.76		5.31
	423	18539	.21	1217	271.9	.37	.76		5.29
	423	18539	.25	1329	272.4	.36	.75		5.27
272	428	28781	0.00	929	263.6	.45	1.00	.454	6.14
	428	28781	0.00	1264	271.7	.45	1.00		6.14
	428	28781	.04	1467	274.9	.44	.78		6.13
	428	28781	.11	1543	275.7	.42	.77		6.13
	428	28781	.17	1619	276.5	.39	.75		6.12

TEST SECTION DATA: R19#1

RUN	MASS FLUX kg/sq-m/s	HEAT FLUX W/sq-m	MASS QUALITY	HTC W/sq-m/K	Teqb degK	LIQUID COMP.	VAPOR COMP.	FEED COMP.	PRESSURE bars
273	428	28781	.23	1749	277.3	.37	.74		6.12
	428	28781	.25	1849	278.1	.35	.72		6.12
	428	28781	.34	2009	279.0	.32	.71		6.11
	428	28781	.39	2295	279.9	.30	.69		6.10
	433	41167	0.00	1256	262.7	.45	1.00	.454	6.01
	433	41167	0.00	1662	270.7	.55	.82		6.01
	433	41167	.09	2087	274.7	.42	.77		6.00
	433	41167	.18	2128	275.8	.39	.75		5.99
	433	41167	.27	2345	277.0	.35	.73		5.98
	433	41167	.34	2500	278.2	.32	.71		5.97
	433	41167	.41	2795	279.4	.29	.68		5.95
	433	41167	.48	3124	280.4	.27	.66		5.94
	433	41167	.54	3589	281.4	.24	.63		5.92
274	213	40459	0.00	1671	277.2	.45	1.00	.454	6.29
	213	40459	.17	1945	280.7	.40	.74		6.28
	213	40459	.33	2142	283.0	.33	.70		6.26
	213	40459	.47	2579	285.4	.28	.65		6.26
	213	40459	.59	3219	287.4	.24	.60		6.27
	213	40459	.70	3737	289.0	.21	.55		6.26
	213	40459	.82	4288	290.4	.18	.52		6.25
	213	40459	.92	5622	291.6	.16	.46		6.25
	213	40459	1.00	6654	292.7	.14	.44		6.24
	215	28745	0.00	1018	269.1	.45	1.00	.454	5.75
275	215	28745	.11	1215	271.2	.41	.78		5.73
	215	28745	.24	1353	272.9	.36	.75		5.73
	215	28745	.34	1471	274.6	.32	.71		5.77
	215	28745	.44	1751	276.4	.28	.68		5.77
	215	28745	.53	2048	278.0	.24	.64		5.77
	215	28745	.61	2286	279.3	.22	.61		5.77
	215	28745	.69	2497	280.6	.19	.57		5.76
	215	28745	.76	2707	281.6	.17	.54		5.76

PREHEAT SECTION DATA: R1642 R152a

RUN	MASS FLUX kg/sq-m/s	HEAT FLUX W/sq-m	QUALITY	HTC W/sq-m/K	Tsat degK
229	155	10026	.06	3254	290.5
	155	10026	.09	3317	290.6
	155	10026	.12	3211	290.6
268	157	20002	.14	3561	290.4
	157	20002	.21	3087	290.4
	157	20002	.28	3391	290.4
287	154	25024	.19	3436	290.0
	154	25024	.28	3619	290.0
	154	25024	.36	3997	290.0
293	157	30697	.24	3949	290.4
	157	30697	.35	4273	290.3
	157	30697	.45	4664	290.3
296	164	35079	.26	4675	290.4
	164	35079	.38	4838	290.3
	164	35079	.49	5219	290.3
284	159	39996	.32	5209	290.2
	159	39996	.45	5279	290.1
	159	39996	.59	5584	290.1
285	159	45020	.37	5709	290.3
	158	45020	.52	5707	290.3
	158	45020	.67	5921	290.2
320	232	20036	.08	3676	290.6
	232	20036	.12	3764	290.6
	232	20036	.17	3921	290.5
295	238	30240	.13	4593	290.6
	238	30240	.20	4465	290.5
	238	30240	.26	4734	290.5
298	238	40442	.19	5319	290.4
	238	40442	.29	5456	290.3
	238	40442	.37	5751	290.2
302	240	49890	.24	6391	290.3
	240	49890	.35	6291	290.2
	240	49890	.46	6723	290.1
304	246	59991	.29	7396	290.9
	246	59991	.42	7249	290.9
	246	59991	.54	7676	290.8
310	246	69998	.35	8215	290.8
	246	69998	.50	8011	290.7
	246	69998	.65	8632	290.6
322	282	20008	.05	3607	290.2
	282	20008	.09	3745	290.2
	282	20008	.13	3980	290.1
294	285	30250	.10	4615	290.6
	285	30250	.15	4511	290.5
	285	30250	.21	4766	290.5

PREHEAT SECTION DATA: R16#2 R152a

RUN	MASS FLUX kg/sq@/s	HEAT FLUX W/sqm	QUALITY	HTC W/sqm/K	Tsat degK
289	289	40694	.14	5578	290.6
	289	40694	.22	5470	290.5
	289	40694	.29	5771	290.4
290	283	49986	.19	6534	291.0
	283	49986	.28	6512	290.9
	283	49986	.38	6954	290.3
291	283	59992	.24	7535	290.7
	283	59992	.35	7418	290.5
	283	59992	.46	7904	290.3
292	277	70003	.30	8310	290.7
	277	70003	.43	8143	290.6
	277	70003	.57	8646	290.4
293	281	74967	.32	8782	290.9
	281	74967	.46	8658	290.8
	281	74967	.60	8932	290.5
324	287	80118	.33	9421	291.1
	287	80118	.47	9337	290.9
	287	80118	.62	9193	290.7
321	340	20038	.04	3667	290.6
	340	20038	.07	3725	290.5
	340	20038	.10	4074	290.5
296	354	30225	.06	4711	290.6
	354	30225	.11	4665	290.6
	354	30225	.15	4922	290.5
297	356	40447	.10	5585	290.5
	356	40447	.16	5419	290.4
	356	40447	.22	5715	290.4
301	359	49930	.13	6539	290.9
	359	49930	.21	6363	290.3
	359	49930	.28	6697	290.8
303	356	59981	.17	7388	290.5
	356	59981	.26	7120	290.4
	356	59981	.35	7722	290.2
309	367	69993	.20	8324	290.7
	367	69993	.30	8068	290.5
	367	69993	.40	8301	290.4
311	366	80036	.24	9173	290.9
	366	80036	.35	8838	290.7
	366	80036	.47	9070	290.5
316	363	89907	.28	10068	290.9
	363	89907	.41	9718	290.7
	363	89907	.54	9712	290.4
323	419	20020	.02	3867	290.8
	419	20020	.04	3781	290.7
	419	20020	.07	4143	290.7

PREHEAT SECTION DATA: R16#2 R152a

RUN	MASS FLUX kg/sqm/s	HEAT FLUX W/sqm	QUALITY	HTC W/sqm/K	Tsat degK
328	418	30342	.05	4913	290.7
	418	30342	.09	4795	290.6
	418	30342	.13	4817	290.5
299	425	40416	.07	5621	290.9
	425	40416	.12	5702	290.8
	425	40416	.17	5968	290.7
300	427	49945	.10	6594	290.9
	427	49945	.16	6349	290.8
	427	49945	.22	6658	290.7
305	430	60275	.15	7746	291.3
	430	60275	.20	7392	291.1
	430	60275	.29	7403	290.9
308	430	70011	.16	8369	290.8
	430	70011	.24	8127	290.7
	430	70011	.33	8242	290.5
312	429	80101	.19	9254	290.9
	429	80101	.29	8995	290.8
	429	80101	.36	9275	290.6
351	148	10086	.09	3339	290.3
	148	10086	.12	3306	290.3
	148	10086	.16	3307	290.3
340	153	20421	.20	3341	290.4
	153	20421	.27	3431	290.4
	153	20421	.34	3659	290.4
350	149	25846	.22	3497	290.2
	149	25846	.31	3639	290.1
	149	25846	.40	4080	290.1
338	150	30731	.30	4390	290.4
	150	30731	.41	4611	290.4
	150	30731	.52	4832	290.3
349	150	35105	.36	4982	290.2
	150	35105	.49	5028	290.1
	150	35105	.61	5224	290.1
332	156	39937	.32	5293	290.3
	156	39937	.46	5397	290.3
	156	39937	.59	5355	290.2
339	286	20404	.05	3694	290.4
	286	20404	.09	3712	290.4
	286	20404	.12	3783	290.3
337	288	30700	.09	4867	290.8
	288	30700	.15	4939	290.8
	288	30700	.20	5157	290.7
331	286	39891	.14	5697	290.2
	286	39891	.21	5569	290.1
	286	39891	.29	5672	290.0

PREHEAT SECTION DATA: RIG#2 R152a

RUN	MASS FLUX kg/sqm/s	HEAT FLUX W/sqm	QUALITY	HTC W/sqm/K	Tsat degK
334	285	50004	.19	6717	290.7
	285	50004	.23	6646	290.6
	285	50004	.37	6716	290.5
342	287	60008	.26	7766	290.9
	287	60008	.37	7736	290.8
	287	60008	.48	7927	290.7
344	285	70761	.32	8473	291.0
	285	70761	.45	8512	290.9
	285	70761	.58	8812	290.7
346	293	80452	.36	9737	290.9
	293	80452	.50	9773	290.7
	293	80452	.65	10139	290.4
336	423	30684	.02	5092	290.8
	423	30684	.06	5050	290.8
	423	30684	.10	5243	290.7
330	428	39887	.07	5873	290.3
	428	39887	.12	5669	290.2
	428	39887	.17	5737	290.1
333	429	50004	.09	6935	291.1
	429	50004	.16	6751	291.0
	429	50004	.22	6628	290.9
341	426	59966	.13	7819	290.9
	426	59966	.20	7746	290.8
	426	59966	.27	7933	290.7
343	426	70761	.16	8799	291.4
	426	70761	.25	8604	291.3
	426	70761	.34	8745	291.0
345	424	79772	.20	9506	291.1
	424	79772	.30	9219	290.9
	424	79772	.40	9122	290.6
347	424	89915	.23	10315	291.4
	424	89915	.35	10034	291.2
	424	89915	.46	9984	290.9

PREHEAT SECTION DATA: RIG#2 R13B1

RUN	MASS FLUX kg/sq m/s	HEAT FLUX W/sq m	QUALITY	HTC W/sq m/K	Tsat degK
506	353	10029	.10	2276	254.4
	353	10029	.14	2246	254.4
	353	10029	.18	1755	254.4
502	360	15178	.16	2293	254.4
	360	15178	.22	2225	254.3
	360	15178	.28	2231	254.3
503	359	19955	.21	2353	254.3
	359	19955	.29	2743	254.3
	359	19955	.37	3189	254.2
504	359	25015	.27	2505	255.0
	359	25015	.37	3551	255.0
	359	25015	.47	4174	254.9
505	356	30766	.34	3201	254.7
	356	30766	.46	4619	254.6
	356	30766	.59	4730	254.5
491	433	10006	.08	2601	254.3
	433	10006	.11	2541	254.3
	433	10006	.14	2413	254.2
499	434	15026	.12	2952	254.2
	434	15026	.17	2796	254.2
	434	15026	.22	2720	254.1
490	441	19973	.17	2750	254.5
	441	19973	.23	2952	254.5
	441	19973	.30	3477	254.4
487	451	25216	.21	3166	254.8
	451	25216	.29	3991	254.8
	451	25216	.37	3969	254.7
483	432	30786	.29	4273	255.1
	432	30786	.39	4713	255.0
	432	30786	.50	4615	254.9
488	445	35215	.31	4563	255.0
	445	35215	.42	5123	254.9
	445	35215	.54	5149	254.8
473	451	41013	.34	4705	254.9
	451	41013	.47	5673	254.8
	451	41013	.60	5751	254.7
492	559	14947	.08	3122	254.6
	559	14947	.12	3136	254.5
	559	14947	.16	3197	254.5
486	556	20278	.13	3634	254.5
	556	20278	.18	3680	254.5
	556	20278	.24	3653	254.4
493	564	24949	.15	4243	254.8
	564	24949	.21	4160	254.8
	564	24949	.28	4223	254.7

PREHEAT SECTION DATA: R1642 R1721

RUN	MASS FLUX kg/sq.m	HEAT FLUX W/sqm	QUALITY	HTC W/sqm/K	Test degK
462	554	30613	.19	4596	255.0
	554	30613	.27	4766	254.9
	554	30613	.35	4646	254.8
494	562	34900	.22	5153	255.0
	562	34900	.31	5253	254.9
	562	34900	.40	5232	254.8
472	560	40206	.26	4544	254.9
	560	40206	.36	5467	254.3
	560	40206	.47	5405	254.6
495	555	44968	.30	5609	255.4
	555	44968	.41	6256	255.2
	555	44968	.53	6211	255.0
477	566	51293	.31	3691	255.3
	566	51293	.44	5301	255.1
	566	51293	.57	5081	254.9

PREHEAT SECTION DATA: R18B2

.90 wt R18B1

RUN	MASS FLUX kg/sq.m/s	HEAT FLUX W/sq.m	MASS QUALITY	HTC W/sq.m/K	T _{eqb} degK	LIQUID COMP.	VAPOR COMP.
533	268	10009	.10	1138	259.0	.79	.89
	268	10009	.15	1154	259.1	.79	.89
	268	10009	.19	1442	259.2	.78	.89
535	268	15020	.17	1429	259.3	.79	.89
	268	15020	.24	1526	259.4	.78	.89
	268	15020	.31	1796	259.6	.77	.89
534	266	20041	.24	1679	259.3	.79	.89
	266	20041	.34	1961	259.6	.78	.88
	266	20041	.43	2111	259.8	.75	.88
533	268	25008	.31	1822	259.8	.77	.86
	268	25008	.42	2152	259.2	.75	.86
	268	25008	.50	2449	259.6	.72	.87
532	272	30059	.37	1997	259.9	.76	.88
	272	30059	.50	2556	259.4	.70	.87
	272	30059	.63	2815	260.0	.69	.87
531	272	35062	.44	2245	259.1	.74	.86
	272	35062	.59	2940	259.8	.71	.87
	272	35062	.73	3215	260.9	.65	.86
530	271	40041	.50	2467	259.5	.70	.87
	271	40041	.67	2975	260.4	.66	.86
	271	40041	.80	3674	262.1	.60	.84
528	370	10021	.04	1127	257.6	.80	.89
	370	10021	.07	1216	257.6	.79	.89
	370	10021	.11	1246	257.7	.79	.89
525	373	15027	.09	1482	259.1	.79	.89
	373	15027	.14	1479	259.2	.79	.89
	373	15027	.19	1561	259.3	.78	.89
524	373	20028	.14	1705	259.0	.79	.89
	373	20028	.21	1759	259.1	.78	.89
	373	20028	.27	1871	259.2	.77	.89
523	366	25057	.20	1971	259.1	.78	.89
	366	25057	.29	2006	259.3	.77	.86
	366	25057	.36	2208	259.5	.76	.88
522	362	30044	.25	2170	259.5	.77	.89
	362	30044	.33	2264	259.7	.76	.88
	362	30044	.43	2577	259.9	.74	.88
521	366	34959	.30	2349	259.3	.77	.88
	366	34959	.42	2535	259.1	.75	.88
	366	34959	.53	2945	259.5	.72	.87
527	364	39750	.34	2481	259.0	.76	.88
	364	39750	.47	2772	259.4	.74	.88
	364	39750	.59	3307	259.9	.71	.87
529	362	45890	.41	2707	259.5	.75	.88
	362	45890	.57	3194	260.0	.71	.87
	362	45890	.71	3680	260.9	.66	.86
547	372	55110	.48	3289	259.6	.70	.87

PREHEAT SECTION DATA: R16B2

.80 wt R13B1

RUN	MASS FLUX kg/sq.m	HEAT FLUX W/sq.m	MASS QUALITY	HTC W/sq.m/K	T _{avg} degK	LIQUID COMP.	VAPOR COMP.
	372	55110	.65	3694	260.4	.69	.86
	372	55110	.81	4504	261.9	.61	.85
537	447	9984	.02	1143	257.6	.80	.89
	447	9984	.05	1374	257.6	.80	.89
	447	9984	.08	1611	257.6	.79	.89
538	459	19946	.10	1712	257.9	.79	.89
	459	19946	.15	1865	258.0	.79	.89
	459	19946	.21	2152	258.1	.78	.89
539	449	29950	.18	2086	258.6	.78	.89
	449	29950	.27	2357	258.7	.77	.89
	449	29950	.35	2777	258.9	.76	.88
543	461	40909	.25	2489	258.9	.77	.89
	461	40909	.36	2801	259.1	.76	.88
	461	40909	.46	3348	259.4	.74	.88
544	465	49831	.32	2964	259.0	.76	.88
	465	49831	.45	3355	259.3	.74	.88
	465	49831	.58	3948	259.7	.71	.87
545	467	57963	.38	3380	259.5	.75	.88
	467	57963	.53	3796	260.0	.72	.87
	467	57963	.67	4409	260.6	.68	.86
550	460	67675	.46	3992	259.6	.74	.88
	460	67675	.63	4408	260.3	.69	.87
	460	67675	.79	5102	261.6	.62	.85
556	546	25056	.06	1913	258.0	.80	.89
	546	25056	.12	1979	258.1	.79	.89
	546	25056	.18	2072	258.1	.78	.89
519	535	35031	.13	2259	258.4	.79	.89
	535	35031	.22	2412	258.5	.78	.89
	535	35031	.30	2758	258.7	.77	.88
540	534	29951	.17	2233	258.5	.78	.89
	534	29951	.24	2399	258.5	.78	.89
	534	29951	.31	2771	258.6	.77	.88
518	547	39946	.16	2435	258.8	.79	.89
	547	39946	.26	2661	258.9	.77	.89
	547	39946	.34	3107	259.0	.76	.88
548	551	50017	.23	3167	258.9	.77	.89
	551	50017	.36	3411	259.1	.76	.88
	551	50017	.48	4342	259.3	.73	.88
546	550	55035	.29	3320	259.0	.77	.88
	550	55035	.41	3646	259.2	.75	.88
	550	55035	.53	4307	259.5	.72	.87
551	540	64953	.35	3969	259.4	.76	.88
	540	64953	.50	4208	259.8	.73	.87
	540	64953	.64	5223	260.4	.69	.86
511	625	20055	.02	1802	257.6	.80	.89
	665	20055	.06	1747	257.6	.80	.89

PREHEAT SECTION DATA: RIG#2

.80 wt R13B1

RUN	MASS FLUX kg/sqm/s	HEAT FLUX W/sqm	MASS QUALITY	HTC W/sqm/K	Teqb degK	LIGUID COMP.	VAPOR COMP.
	685	20055	.10	1841	257.7	.79	.89
542	684	20134	.04	1861	258.1	.80	.89
	684	20184	.06	1830	258.1	.79	.89
	684	20184	.12	1966	258.2	.79	.89
510	688	30180	.07	2164	258.1	.90	.89
	688	30180	.13	2191	258.1	.79	.89
	688	30180	.18	2428	258.1	.78	.89
541	679	29911	.10	2265	258.1	.79	.89
	679	29911	.16	2333	258.1	.79	.89
	679	29911	.21	2692	258.2	.76	.89
513	691	35085	.09	2390	258.5	.79	.89
	691	35085	.15	2377	258.5	.79	.89
	691	35085	.22	2738	258.6	.78	.89
508	682	40729	.13	2445	258.3	.79	.89
	682	40729	.20	2691	258.4	.76	.89
	682	40729	.28	3240	258.4	.77	.89
512	693	44758	.14	2727	258.4	.79	.89
	693	44758	.23	2939	258.4	.78	.89
	693	44758	.31	3525	258.5	.77	.88
509	684	49814	.17	2879	258.8	.78	.89
	684	49814	.27	3243	258.9	.77	.88
	684	49814	.36	3845	259.0	.76	.88
549	683	49973	.18	3210	258.9	.78	.89
	683	49973	.27	3580	259.0	.77	.88
	683	49973	.36	4354	259.1	.76	.89
553	693	64826	.22	4021	259.0	.78	.89
	693	64826	.34	4112	259.1	.76	.88
	693	64826	.46	5339	259.3	.74	.88
552	681	64923	.25	4035	259.7	.77	.89
	681	64923	.36	4140	259.9	.76	.88
	681	64923	.49	5376	260.0	.73	.87
554	700	74948	.27	4375	259.3	.77	.88
	700	74948	.41	4719	259.5	.75	.88
	700	74948	.54	5940	259.7	.72	.87

RUN	MASS FLUX kg/sq2/s	HEAT FLUX W/sq2	MASS QUALITY	HTC W/sq2/K	Temp degK	LIQUID COMP.	VAPOR COMP.
407	202	25102	.15	1416	270.6	.32	.73
	205	25102	.23	1553	272.4	.27	.69
	206	25102	.32	1750	274.1	.24	.65
410	206	20081	.22	1674	272.1	.28	.69
	206	20081	.30	1805	273.6	.25	.66
	206	20081	.37	2342	274.9	.22	.60
445	200	20392	.27	1343	273.1	.26	.67
	200	20392	.34	1610	274.5	.23	.64
	200	20392	.42	1885	275.9	.20	.60
411	202	29584	.32	1957	274.0	.24	.65
	202	29584	.42	2192	275.8	.20	.60
	203	29584	.51	2459	277.4	.17	.56
415	205	35122	.38	2791	275.3	.22	.62
	205	35122	.49	3127	277.3	.18	.57
	205	35122	.59	3812	278.9	.16	.52
412	205	39638	.42	2803	276.0	.20	.60
	205	39638	.54	3129	278.0	.17	.54
	205	39638	.66	3471	279.6	.14	.49
416	204	44884	.47	3402	277.1	.19	.58
	204	44884	.60	3751	279.1	.15	.51
	204	44884	.73	4439	280.6	.13	.46
445	230	15015	.13	1220	270.2	.32	.73
	230	15015	.17	1233	271.0	.30	.71
	230	15015	.22	1356	271.9	.28	.69
442	283	20496	.18	1446	271.5	.30	.71
	283	20496	.24	1558	272.5	.27	.69
	283	20496	.29	1732	273.6	.25	.66
438	289	24887	.21	1917	272.0	.28	.70
	289	24887	.28	1987	273.3	.26	.67
	289	24887	.34	2126	274.5	.23	.64
453	292	30041	.27	2367	273.1	.26	.67
	292	30041	.34	2585	274.5	.23	.64
	292	30041	.42	2842	275.8	.20	.60
452	297	40262	.35	2978	274.9	.23	.64
	297	40262	.45	3313	276.6	.19	.59
	297	40262	.53	3657	277.9	.17	.55
448	295	50285	.41	3581	276.1	.21	.61
	295	50285	.52	3962	277.9	.17	.55
	295	50285	.62	4341	279.3	.15	.51
447	289	60589	.48	4156	277.3	.18	.57
	289	60589	.61	4540	279.1	.15	.51
	289	60589	.73	4902	280.5	.13	.46
441	369	20375	.11	1356	269.9	.32	.73
	369	20375	.16	1429	270.3	.30	.72
	369	20375	.21	1600	271.6	.28	.70
439	363	24638	.14	1855	270.2	.31	.73

PREHEAT SECTION DATA: R1842

.33 wt R10B1

RUN	MASS FLOW kg/sec/m ²	HEAT FLUX W/secm	MASS QUALITY	HTC W/secm ² /K	Temp degK	LIQUID CONF.	VAPOR CONF.
	363	24838	.20	1952	271.3	.29	.70
	363	24838	.25	2027	272.3	.26	.68
395	373	30944	.16	1841	271.0	.30	.72
	373	30944	.23	1966	272.3	.27	.69
	373	30944	.30	2245	273.4	.25	.66
397	374	39839	.21	2336	272.0	.28	.70
	374	39839	.30	2575	273.5	.23	.66
	374	39839	.37	3039	274.9	.22	.62
398	376	49660	.27	2897	273.4	.26	.67
	376	49660	.37	3263	275.1	.22	.63
	376	49660	.46	3861	276.7	.19	.58
399	372	59445	.33	3560	274.7	.24	.65
	372	59445	.44	4007	276.6	.20	.59
	372	59445	.54	4609	278.1	.17	.54
400	374	69055	.38	4159	275.8	.22	.62
	374	69055	.50	4738	277.8	.18	.56
	374	69055	.61	5276	279.3	.15	.51
401	372	79804	.43	4853	277.0	.20	.59
	372	79804	.57	5471	279.1	.16	.53
	372	79804	.69	5940	280.5	.14	.47
440	460	24818	.09	1905	269.7	.34	.74
	460	24818	.14	1937	270.5	.31	.73
	460	24818	.18	1990	271.3	.29	.71
454	467	29981	.15	2350	270.8	.31	.72
	467	29981	.20	2455	271.2	.29	.70
	467	29981	.25	2631	272.7	.26	.68
451	467	40110	.20	2274	272.2	.29	.70
	467	40110	.27	3060	273.4	.26	.67
	467	40110	.33	3365	274.5	.24	.65
455	469	49796	.24	3318	273.2	.27	.68
	469	49796	.32	3648	274.5	.24	.65
	469	49796	.40	4142	275.9	.21	.61
445	447	60525	.32	3548	274.3	.24	.65
	447	60525	.41	4111	276.0	.21	.61
	447	60525	.50	4645	277.3	.18	.56
456	458	69850	.35	4106	275.2	.23	.63
	458	69850	.46	4752	277.0	.19	.59
	458	69850	.55	5448	278.3	.17	.54
459	467	79856	.38	4633	275.9	.22	.62
	467	79856	.50	5342	277.6	.19	.56
	467	79856	.60	6003	278.9	.15	.51
460	446	90060	.42	5264	277.0	.20	.60
	446	90060	.55	6083	278.9	.17	.54
	446	90060	.67	6735	280.2	.14	.48
468	528	10052	.02	1123	268.7	.36	.76
	528	10052	.04	1144	269.0	.35	.75

PREHEAT SECTION DATA: R1682

.38 wt R13B1

RUN	MASS FLUX kg/sq-m/s	HEAT FLUX W/sq-m	MASS QUALITY	HTC W/sq-m/K	Temp deg-c	LIQUID COMP.	VAPOR COMP.
	528	10052	.09	1150	269.3	.35	.75
467	537	20028	.06	1720	269.2	.35	.75
	537	20038	.09	1746	269.9	.33	.74
	537	20038	.13	1837	270.3	.32	.73
466	532	30070	.10	2512	270.0	.33	.74
	532	30070	.15	2746	270.8	.31	.72
	532	30070	.20	2916	271.6	.29	.70
465	541	40281	.14	2726	270.7	.31	.72
	541	40281	.20	2943	271.6	.29	.70
	541	40281	.26	3235	272.9	.26	.68
464	535	49957	.18	3171	271.9	.30	.71
	535	49957	.26	3550	273.1	.28	.68
	535	49957	.33	3726	274.3	.25	.65
463	543	60165	.22	3692	272.7	.28	.69
	543	60165	.30	4111	274.3	.24	.66
	543	60165	.38	4591	275.6	.22	.62
457	542	69767	.29	4016	274.0	.28	.68
	542	69767	.38	4581	275.3	.22	.62
	542	69767	.46	5299	276.9	.19	.59
462	546	80304	.30	4524	274.6	.25	.66
	546	80304	.40	5203	276.3	.21	.61
	546	80304	.50	5744	277.8	.18	.58
461	552	89942	.34	4675	275.3	.23	.64
	552	89942	.44	5755	277.1	.19	.59
	552	89942	.56	6374	278.4	.16	.53

PREHEAT SECTION DATA: F1282

.12 wt R1081

ROW	MASS FLUX kg/sqm ²	HEAT FLUX W/sqm ²	WEE QUALITY	HTC W/sqm ² K	T _{avg} degK	LIQUID COMP.	VAPOR COMP.
544	190	9993	.06	922	278.4	.15	.52
	190	9993	.10	1074	279.1	.14	.50
	190	9993	.13	1207	279.9	.13	.47
575	196	20140	.13	1956	279.9	.13	.47
	196	20140	.20	2024	281.1	.12	.43
	196	20140	.26	2055	282.0	.10	.39
579	196	29981	.22	2221	282.0	.11	.42
	196	29981	.30	2985	283.2	.09	.37
	196	29981	.39	3153	284.1	.08	.33
584	202	40729	.29	3855	282.6	.10	.38
	202	40729	.41	3940	283.6	.08	.32
	202	40729	.51	4089	284.7	.07	.28
585	202	49992	.37	4779	284.0	.09	.34
	202	49992	.50	4686	285.2	.07	.29
	202	49992	.64	5006	286.0	.06	.25
590	205	60132	.44	5643	284.3	.08	.31
	205	60132	.60	5705	285.3	.06	.26
	205	60132	.75	6093	286.0	.05	.22
598	242	10028	.04	854	279.4	.16	.53
	242	10028	.07	1022	279.1	.15	.51
	242	10028	.09	1115	279.7	.15	.50
577	241	20118	.09	1890	279.9	.15	.50
	241	20118	.15	1913	280.0	.13	.46
	241	20118	.20	2004	280.9	.12	.43
580	241	29939	.16	2909	280.7	.13	.45
	241	29939	.24	2951	282.0	.11	.41
	241	29939	.31	3087	282.9	.09	.37
583	240	40744	.24	3696	282.2	.11	.41
	240	40744	.34	3772	283.5	.09	.35
	240	40744	.42	3938	284.3	.08	.31
586	242	49813	.29	4660	282.7	.10	.37
	242	49813	.41	4809	284.0	.08	.32
	242	49813	.52	4955	284.3	.07	.28
589	249	59915	.35	5464	283.7	.09	.35
	249	59915	.48	5604	284.9	.07	.29
	249	59915	.61	5730	285.7	.06	.25
592	246	70750	.42	6276	284.5	.06	.32
	246	70750	.58	6394	285.6	.06	.26
	246	70750	.73	6833	286.3	.05	.23
597	295	10003	.02	886	278.0	.17	.55
	295	10003	.05	1055	278.5	.16	.53
	295	10003	.07	1133	279.0	.15	.51
576	296	20109	.06	1905	278.9	.16	.52
	296	20109	.11	1796	279.9	.14	.49
	296	20109	.15	1929	280.7	.13	.46
581	300	29960	.11	2727	279.9	.14	.48

PREHEAT SECTION DATA: R1342

.18 wt R13B1

RUN	MASS FLUX kg/sq2/s	HEAT FLUX W/sqm	MASS QUALITY	HTC W/sqm/K	Tavg degK	LIQUID COMP.	VAPOR COMP.
	300	29960	.17	2975	281.0	.12	.44
	300	29960	.24	2986	282.0	.11	.41
582	298	39911	.17	3517	280.9	.12	.45
	298	39911	.25	3694	282.1	.10	.40
	299	39911	.33	3920	283.1	.09	.36
587	299	49785	.22	4517	291.9	.11	.41
	299	49785	.32	4703	283.2	.09	.36
	299	49785	.41	4899	284.0	.08	.32
588	298	59873	.26	5263	282.9	.10	.38
	298	59873	.39	5499	284.2	.08	.33
	298	59873	.50	5708	285.0	.07	.29
593	300	79923	.38	6758	284.2	.08	.33
	300	79923	.53	6984	285.4	.07	.23
	300	79923	.66	7984	286.1	.05	.24
594	305	89872	.43	7549	284.6	.06	.31
	305	89872	.59	7740	285.6	.06	.26
	305	89872	.75	8597	286.2	.05	.22
596	345	10069	.01	853	277.8	.17	.55
	345	10069	.03	706	278.2	.17	.54
	345	10069	.06	766	278.7	.16	.52
595	349	20095	.04	1955	278.3	.16	.53
	349	20095	.08	1796	279.2	.15	.51
	349	20095	.12	1876	280.0	.14	.48
596	354	30743	.08	2450	279.3	.15	.51
	354	30743	.14	2711	280.4	.13	.47
	354	30743	.19	2755	281.4	.12	.43
599	350	39885	.13	3313	280.0	.13	.47
	350	39885	.20	3484	291.2	.12	.43
	350	39885	.27	3578	282.2	.10	.39
560	351	51196	.19	4266	281.5	.12	.44
	351	51196	.27	4459	282.6	.10	.39
	351	51196	.35	4630	283.7	.09	.35
562	354	59907	.22	4968	282.5	.11	.41
	354	59907	.32	5160	283.7	.09	.36
	354	59907	.41	5364	284.6	.08	.32
563	351	69847	.27	5717	282.9	.10	.39
	351	69847	.38	5864	284.2	.08	.33
	351	69847	.49	6136	285.0	.07	.29
564	348	79720	.32	6464	283.6	.09	.36
	348	79720	.45	6587	284.8	.07	.31
	348	79720	.57	6914	285.5	.06	.26
565	351	90237	.36	7196	284.4	.09	.34
	351	90237	.51	7308	285.5	.07	.28
	351	90237	.65	7699	286.2	.06	.24
566	349	95147	.39	7545	284.6	.08	.33
	349	95147	.54	7648	285.7	.07	.27

PREHEAT SECTION DATA: R1332

.18 wt R1331

RUN	MASS FLUX kg/sqm/s	HEAT FLUX W/sqm	MASS QUALITY	HTC W/sqm/K	Temp degK	LIQUID COMP.	VAPOR COMP.
	349	95147	.69	8207	286.3	.05	.23
595	468	10032	.00	1206	277.4	.18	.56
	468	10032	.02	982	277.7	.17	.55
	468	10032	.03	941	279.1	.17	.54
574	473	20065	.01	2101	277.5	.17	.55
	473	20065	.04	1874	278.2	.16	.53
	473	20065	.07	1876	278.8	.15	.51
572	472	30082	.04	2666	279.1	.16	.54
	472	30082	.08	2484	279.0	.15	.50
	472	30082	.13	2518	279.9	.14	.48
572	473	39938	.07	3223	279.2	.15	.51
	473	39938	.13	3237	280.3	.14	.47
	473	39938	.18	3382	281.2	.12	.44
571	475	50064	.10	3958	279.9	.14	.49
	475	50064	.17	3950	281.0	.12	.44
	475	50064	.24	4199	282.0	.11	.40
570	473	60044	.14	4660	281.0	.12	.46
	473	60044	.22	4610	282.2	.11	.41
	473	60044	.30	4955	283.2	.10	.37
569	479	70723	.18	5274	281.6	.12	.44
	479	70723	.27	5322	282.9	.10	.39
	479	70723	.36	5655	283.7	.09	.34
568	460	80154	.21	6253	282.2	.11	.42
	480	80154	.31	6545	283.4	.09	.37
	480	80154	.40	7132	284.2	.08	.32
567	473	90386	.25	6940	282.9	.11	.40
	473	90386	.36	7209	284.2	.09	.34
	473	90386	.46	7830	284.9	.07	.30

PREHEAT SECTION DATA: RIS#2

.58 wt R1391

RUN	MASS FLUX kg/sqa/s	HEAT FLUX W/sqa	MASS QUALITY	HTC W/sqa/K	T _{eb} degK	LIQUID COMP.	VAPOR COMP.
640	350	20042	.20	1574	264.7	.52	.82
	350	20042	.25	1702	265.3	.49	.82
	350	20042	.33	1933	265.9	.47	.81
637	355	30305	.28	2147	265.7	.49	.81
	355	30305	.37	2393	266.7	.45	.80
	355	30305	.45	2799	267.8	.41	.79
639	351	20048	.20	1578	264.7	.52	.82
	351	20048	.27	1697	265.3	.49	.82
	351	20048	.33	1924	265.9	.47	.81
636	349	30311	.30	2158	265.8	.48	.81
	349	30311	.39	2428	266.8	.44	.80
	349	30311	.47	2856	268.0	.40	.78
635	475	10002	.01	987	262.5	.58	.84
	475	10002	0.00	904	261.3	.62	.85
	475	10002	0.00	862	260.2	.67	.86
630	486	20404	.14	1532	263.6	.54	.83
	486	20404	.18	1801	263.9	.52	.83
	486	20404	.23	2012	264.3	.51	.82
634	481	10006	.07	1040	263.0	.56	.84
	481	10006	.09	1077	263.1	.55	.83
	481	10006	.12	1174	263.3	.54	.83
631	476	20406	.15	1564	263.7	.53	.83
	476	20406	.20	1811	264.1	.52	.82
	476	20406	.25	2029	264.5	.50	.82
628	476	30046	.21	2104	264.7	.51	.82
	476	30046	.28	2407	265.3	.49	.81
	476	30046	.34	2779	266.0	.46	.80
625	484	40429	.27	2640	265.3	.49	.81
	484	40429	.36	3131	266.2	.45	.80
	484	40429	.44	3709	267.2	.41	.79
632	479	20407	.14	1561	263.7	.54	.83
	479	20407	.19	1788	264.1	.52	.82
	479	20407	.24	2008	264.5	.50	.82
629	479	30046	.21	2134	264.3	.51	.82
	479	30046	.27	2429	265.0	.49	.82
	479	30046	.34	2793	265.7	.46	.81
624	479	40436	.28	2650	265.3	.49	.81
	479	40436	.36	3145	266.2	.45	.80
	479	40436	.45	3720	267.3	.41	.79
616	476	19998	.12	1774	275.3	.55	.81
	476	19998	.17	1779	275.6	.53	.81
	476	19998	.22	1844	276.1	.52	.80
611	478	30104	.19	2121	276.1	.52	.80
	478	30104	.26	2186	276.7	.50	.79
	478	30104	.33	2406	277.4	.48	.78
617	478	70452	.43	3598	278.9	.44	.77

RUN	MASS FLUX kg/sqm/s	HEAT FLUX W/sqm	MASS QUALITY	HTC W/sqm/K	Teqb degK	LIQUID COMP.	VAPOR COMP.
	478	70452	.57	4157	280.8	.38	.73
	478	70452	.68	4694	282.7	.33	.70
615	475	20011	.12	1776	275.3	.55	.81
	475	20011	.16	1768	275.7	.53	.81
	475	20011	.21	1832	276.1	.52	.80
612	475	30138	.19	2148	276.1	.53	.80
	475	30138	.26	2204	276.9	.50	.79
	475	30138	.33	2436	277.5	.48	.78
609	476	40672	.27	2400	277.0	.50	.79
	476	40672	.35	2619	277.9	.47	.78
	476	40672	.44	3002	279.0	.43	.76
618	482	70459	.42	3714	279.2	.44	.77
	482	70459	.55	4245	281.1	.38	.73
	482	70458	.67	4805	283.0	.33	.70
614	479	20037	.11	1776	275.5	.55	.81
	479	20037	.16	1754	275.8	.53	.81
	479	20037	.21	1823	276.3	.52	.80
613	474	30136	.19	2150	276.1	.53	.80
	474	30136	.26	2217	276.9	.50	.79
	474	30136	.32	2452	277.5	.48	.78
608	471	40714	.27	2267	277.1	.50	.79
	471	40714	.36	2534	278.1	.46	.78
	471	40714	.45	2898	279.2	.43	.76
620	517	49540	.30	3193	267.4	.48	.81
	517	49540	.40	3590	268.5	.44	.79
	517	49540	.49	4129	269.8	.39	.77
621	475	49502	.33	3237	266.3	.46	.81
	475	49502	.43	3694	267.5	.42	.79
	475	49502	.53	4299	268.9	.37	.76
607	482	60042	.36	3476	278.2	.46	.78
	482	60042	.48	3945	279.7	.41	.75
	482	60042	.59	4663	281.4	.36	.72
619	477	70430	.42	3323	278.8	.44	.77
	477	70430	.56	4346	280.7	.38	.74
	477	70430	.67	4942	282.6	.33	.70

TEST SECTION DATA: RIG#2 R152a

RUN	MASS FLUX kg/sqm/s	HEAT FLUX W/sqm	QUALITY	HTC W/sqm/K	Test degK
329	158	9675	.19	2878	290.6
288	157	10103	.39	3544	290.3
287	154	10095	.49	3760	289.9
283	157	9954	.59	3839	290.2
286	164	10076	.54	4400	290.2
284	159	10011	.76	4616	290.0
285	158	10031	.86	4903	290.1
320	232	9759	.24	3217	290.5
295	238	10125	.36	4310	290.4
292	238	10121	.48	4919	290.1
302	240	10116	.60	5650	289.9
304	246	10102	.70	6420	290.5
310	246	9976	.83	6433	290.3
322	282	9675	.19	3259	290.1
294	285	10203	.29	4365	290.4
289	289	10158	.39	5022	290.3
290	293	10163	.49	5859	290.6
291	293	10159	.60	6686	290.0
292	277	10199	.72	7302	290.1
293	281	10125	.76	7165	290.2
324	287	9315	.79	7625	290.3
321	340	9730	.15	3333	290.4
296	354	10132	.22	4545	290.4
297	356	10121	.30	5017	290.2
301	359	10101	.37	5999	290.5
303	356	10098	.45	6302	290.0
309	367	10017	.52	7374	290.0
311	366	9975	.60	8418	290.1
316	363	10074	.69	8975	289.9
323	419	9698	.11	3389	290.6
328	418	9569	.18	4010	290.4
299	425	10104	.24	5123	290.5
300	427	10098	.30	5955	290.5
305	430	9954	.36	7035	290.6
308	430	9983	.43	7459	290.0
312	429	9978	.50	8590	290.1
351	148	19067	.27	3458	290.2
340	153	20214	.49	4019	290.3
350	149	19660	.57	3909	290.0
338	150	20248	.71	4640	290.2
349	150	19438	.81	5105	290.0
332	156	20037	.81	5120	290.1
339	286	20221	.20	3821	290.2
337	288	20202	.30	4277	290.6
331	286	20057	.40	5191	289.9
334	295	20083	.51	6560	290.3

TEST SECTION DATA: R16#2 R152a

RUN	MASS FLUX kg/sq m/s	HEAT FLUX W/sq m	QUALITY	HTC W/sq m/K	Tsat degk
342	287	19563	.53	7109	290.4
344	285	18930	.75	7832	290.4
346	293	19191	.83	9159	290.0
336	423	20183	.17	4104	290.6
330	428	19999	.25	5350	289.9
333	429	20042	.31	6927	290.6
341	426	19597	.38	7204	290.4
343	426	18605	.45	7586	290.6
345	424	19143	.52	8857	290.1
347	424	19358	.60	10560	290.5

TEST SECTION DATA: R16#2 R13B1

RUN	MASS FLUX kg/sq m/s	HEAT FLUX W/sq m	QUALITY	HTC(P) W/sq m/K	HTC(T) W/sq m/K	Tsat(P) degk
506	353	10048	.27	2785	2525	254.3
502	360	10048	.39	3598	3097	254.2
503	359	10053	.50	3758	3275	254.1
504	359	10042	.62	4093	3497	254.6
505	356	10057	.76	4598	3789	254.3
491	433	10115	.22	3059	2758	254.2
489	434	10107	.31	2931	2633	254.0
490	441	10113	.40	3719	3227	254.3
487	451	10104	.49	3955	3370	254.5
483	432	10005	.64	4785	3888	254.7
468	445	10107	.69	5262	4113	254.6
473	451	9988	.77	5923	4632	254.4
492	559	10117	.23	3410	3005	254.4
486	558	9992	.32	3557	3094	254.2
493	564	10107	.37	4136	3436	254.5
482	554	9987	.46	4819	3909	254.5
494	562	10105	.52	5368	4192	254.5
472	560	10081	.60	5934	4632	254.3
495	555	10100	.68	6798	4745	254.7
477	566	9983	.73	7263	5134	254.5

TEST SECTION DATA: R1642

.58 wt R13B1

RUN	MASS FLUX kg/sqm/s	HEAT FLUX W/sqm	MASS QUALITY	HTC W/sqm/K	Teqb degK	LIQUID CONF.	VAPOR CONF.
350	19873	.45	2434	267.5	.41	.78	
355	20258	.59	3285	269.9	.34	.74	
351	30274	.48	2807	267.9	.40	.78	
349	30260	.62	3721	270.5	.32	.73	
475	9998	.17	1376	263.6	.53	.83	
486	10067	.30	1810	265.0	.48	.81	
481	20019	.20	1793	263.9	.52	.82	
476	20019	.34	2479	265.5	.46	.81	
476	20013	.45	3133	267.5	.41	.78	
484	20013	.56	3980	269.0	.35	.75	
479	30217	.36	2843	265.8	.45	.80	
479	30911	.47	3604	267.5	.40	.78	
479	30609	.59	4509	269.5	.34	.75	
476	9997	.29	1949	276.7	.49	.79	
478	10000	.42	2297	278.5	.44	.77	
478	10034	.80	3290	284.6	.28	.65	
475	20015	.31	2329	277.0	.46	.79	
475	20040	.44	2977	278.9	.43	.76	
476	20048	.56	3234	280.8	.38	.73	
482	19937	.81	4644	285.2	.28	.65	
479	30109	.33	2587	277.5	.48	.78	
474	30008	.46	3338	279.2	.42	.76	
471	29969	.59	3421	281.3	.36	.72	
517	30821	.63	5091	271.9	.33	.73	
475	30856	.67	5246	271.2	.30	.71	
482	30924	.75	6194	283.8	.30	.67	
477	30276	.83	5196	285.1	.27	.64	

TEST SECTION DATA: R16#2

.18 wt R13B1

RUN	MASS FLUX kg/sqm/s	HEAT FLUX W/sqm	MASS QUALITY	HTC W/sqm/K	Temp degK	LIQUID COMP.	VAPOR COMP.
190	9971	.20	1438	291.1	.11	.43	
196	9972	.35	1923	293.2	.09	.35	
196	9961	.51	2500	285.1	.07	.28	
203	9891	.65	3185	285.4	.06	.24	
202	9885	.80	3646	285.5	.05	.21	
205	9910	.93	3464	295.5	.04	.19	
242	9972	.15	1359	280.8	.13	.46	
241	9983	.28	1810	292.1	.10	.38	
241	9974	.41	2517	283.9	.08	.32	
240	9852	.55	3123	285.1	.05	.27	
242	9892	.66	3610	285.5	.06	.24	
249	9891	.76	4142	285.2	.05	.22	
246	9916	.90	4147	286.7	.04	.19	
255	9979	.12	1298	290.0	.14	.48	
296	9885	.22	1705	281.8	.11	.42	
300	9981	.32	2341	283.0	.09	.36	
298	9972	.43	2986	284.0	.08	.31	
299	9900	.52	3491	284.8	.07	.28	
298	9897	.63	4011	285.6	.06	.25	
300	9923	.83	4535	285.4	.05	.20	
305	9910	.92	3641	286.5	.04	.19	
345	9962	.10	1155	279.6	.14	.47	
349	9986	.19	1628	281.0	.12	.44	
354	9887	.26	2250	282.4	.10	.39	
350	9889	.35	2770	283.1	.09	.35	
351	9855	.45	3440	284.5	.07	.31	
354	9845	.52	3876	285.2	.07	.28	
351	9849	.61	4415	285.5	.06	.25	
348	9841	.71	4794	285.9	.05	.23	
351	9834	.79	5032	286.5	.05	.21	
349	9835	.84	4925	286.6	.05	.20	
468	9973	.06	1184	278.8	.15	.52	
473	9995	.12	1530	279.7	.14	.48	
472	9995	.18	1969	280.8	.12	.44	
473	9977	.25	2478	282.1	.11	.40	
475	9962	.31	3043	282.8	.09	.36	
473	9957	.38	3583	283.9	.08	.33	
479	9944	.45	4046	284.3	.07	.31	
480	9863	.50	4439	284.7	.07	.29	
473	9844	.58	4959	285.3	.06	.26	

TEST SECTION DATA: RIG42

.80 wt R13B1

RUN	MASS FLUX kg/sq.m/s	HEAT FLUX W/sq.m	MASS QUALITY	HTC W/sq.m.K	T _{avg} degF	LIQUID COMP.	VAPOR COMP.
269	10073	.29		1757	258.4	.77	.88
268	10074	.43		1848	258.9	.74	.88
266	10073	.57		2006	259.4	.71	.87
269	10065	.69		2202	260.6	.67	.86
272	10045	.90		2530	261.6	.61	.85
272	10060	.96		3022	263.4	.54	.83
271	10054	.98		3467	265.4	.46	.81
370	10210	.18		1464	257.6	.78	.89
373	10201	.28		1695	259.4	.77	.88
373	10211	.38		1930	259.5	.75	.88
366	10159	.49		2195	259.9	.73	.88
362	10160	.59		2422	259.5	.71	.87
366	10174	.68		2639	260.3	.68	.86
364	10170	.75		2870	261.1	.64	.85
362	10062	.87		3407	262.9	.57	.84
372	10094	.97		3984	264.9	.46	.81
447	10102	.14		2086	257.7	.79	.89
459	10086	.29		2200	258.2	.77	.88
449	10082	.46		2505	259.1	.74	.88
461	10127	.60		2775	259.9	.70	.87
465	10134	.73		3061	260.6	.65	.86
467	10123	.83		3414	262.2	.59	.84
460	10050	.94		3334	264.3	.50	.82
546	9991	.27		2099	258.2	.77	.88
535	10018	.40		2533	259.8	.75	.88
534	10244	.41		2651	259.8	.75	.88
547	10029	.46		2719	259.3	.74	.88
551	10143	.60		3052	259.7	.70	.87
550	10140	.67		3127	260.0	.68	.86
540	10075	.79		3295	261.5	.62	.85
685	10145	.15		1997	257.7	.79	.89
684	10265	.18		2165	258.2	.78	.89
688	10129	.26		2504	258.2	.77	.89
679	10291	.29		2728	259.2	.77	.89
691	10136	.30		2694	259.6	.77	.88
682	10097	.37		2868	258.4	.75	.88
693	10146	.40		2988	259.5	.75	.88
694	10114	.46		3102	259.0	.74	.88
693	10154	.47		3152	259.1	.74	.88
693	10118	.59		3451	259.5	.71	.87
681	10096	.61		3342	260.3	.70	.87
700	10089	.68		3526	260.2	.68	.86

TEST SECTION DATA: RIG#2

.38 wt R13B1

RUN	MASS FLUX kg/sq.m/s	HEAT FLUX W/sq.m	MASS QUALITY	HTC W/sq.m/K	Temp degK	LIQUID COMP.	VAPOR COMP.
208		9922	.45	1447	276.4	.19	.59
208		6821	.46	1572	276.6	.19	.58
200		9934	.52	2008	277.6	.17	.55
208		10115	.64	2404	279.1	.15	.50
205		10105	.72	2682	290.5	.13	.46
205		10106	.80	2856	291.1	.12	.43
204		10091	.88	3072	282.0	.11	.40
280		10192	.30	1450	273.3	.25	.66
283		10032	.38	1812	275.2	.22	.62
289		9935	.43	2051	276.1	.20	.60
292		10036	.51	2573	277.3	.18	.56
287		10015	.64	3131	279.4	.14	.50
295		10013	.74	3557	280.5	.13	.46
289		9995	.87	3924	291.7	.11	.41
369		9988	.28	1616	272.9	.25	.67
363		9969	.33	1861	273.7	.23	.65
373		9801	.38	2159	275.0	.22	.62
374		9800	.47	2770	276.5	.19	.58
376		9771	.56	3259	278.1	.16	.53
372		9758	.65	3686	279.5	.14	.49
374		9746	.73	4021	280.5	.13	.46
372		9731	.83	4503	281.6	.11	.42
460		9967	.25	1696	272.4	.27	.68
467		10064	.33	2165	273.9	.24	.65
467		10045	.41	2673	275.8	.21	.61
469		10043	.49	3213	277.2	.18	.57
447		10039	.60	3604	278.5	.15	.52
459		10001	.66	4261	279.4	.14	.49
467		10025	.71	4557	280.0	.13	.47
446		9986	.80	5747	291.3	.12	.43
528		10027	.10	1118	269.8	.33	.74
537		10041	.12	1464	271.2	.30	.71
532		10034	.27	1878	272.7	.26	.68
541		10031	.34	2307	274.1	.23	.64
535		10029	.41	2728	275.6	.20	.61
543		10010	.47	3118	276.9	.19	.57
545		10039	.56	3932	278.0	.16	.53
546		9990	.60	3856	278.9	.15	.51
536		10012	.67	4286	279.6	.14	.48

APPENDIX 4A: ALTERNATE SUPPRESSION CRITERION

Three alternate suppression criterion were found in the literature. All are based somewhat on Chawla's original suggestion: to decide on the paper heat transfer regime one should calculate the heat transfer coefficient based on an accurate pool boiling relation, and again on an accurate forced convection/evaporative relation (e.g., one based solely on m or X_{tt} , but not heat flux). The larger α determines the correct heat transfer regime.

Collier has used Dengler and Addoms relation:

$$\alpha/\alpha_{LO} = A(1/X_{tt})^B = q/\Delta T \qquad A = 3.5, B = 0.5$$

and combined it with an 'onset of nucleate boiling' criterion of Davis and Anderson similar to that derived by Hsu:

$$\Delta T = \frac{8\sigma q T_{sat}}{\Delta h_v \lambda_L \rho_v}^{0.5} \qquad (4A-1)$$

to yield

$$q = \frac{49\alpha_{LO}^2}{\lambda_L X_{tt}} \frac{2\sigma T_{sat} \alpha_{LO}}{\Delta h_v} \qquad (4A-2)$$

Polley employed a similar approach; however, he used Chen's equation combined with (4A-1) to yield:

$$\Delta T_i = \frac{2\sigma T_{sat}}{\Delta h_v} (V_v - V_L) \frac{1}{r_c (1 - \frac{Fa}{\lambda_L} r_c)}$$

If the given $\Delta T < \Delta T_i$, the flow is considered to be absent of nucleate boiling.

Shah has recently correlated a large amount of refrigerant data with a new correlation described in Chapter 6. He utilizes Chawla's suggestion exactly and employs the dimensionless number

$$Co = \frac{1-x}{x}^{0.8} \frac{\rho_v}{\rho_L}^{0.5} \quad (4A-4)$$

and relates Co to an evaporative heat transfer coefficient. By a separate relation, he calculates a nucleate boiling α . The larger of the two determines the flow regime. His method therefore equates dominant evaporative heat transfer regime with the complete suppression regime. This may not be true. As shown in Chapter 6, the criterion frequently selected the wrong flow regime and badly predicted the experimental data.

APPENDIX 4B: REVIEW OF CORRELATIONS α/α_L WITH X_{tt}

A common form of a correlation of the heat transfer coefficient with fluid flow parameters is

$$\frac{\alpha}{\alpha_L} \text{ vs } f\left(\frac{1}{X_{tt}}\right) \quad (4B-1)$$

Mesler (9) has examined such a form noting:

$$\alpha_L = 0.023 \frac{\lambda_L}{D} \left(\frac{4G}{\pi D \mu_L}\right)^{0.8} \left(\frac{\rho_L}{\lambda_L}\right)^{0.4} \quad (4B-2)$$

$$\left(\frac{1}{X_{tt}}\right) = \left(\frac{x}{1-x}\right)^{0.9} \left(\frac{v_v}{v_L}\right)^{0.5} \left(\frac{\mu_v}{\mu_L}\right)^{0.1} \quad (4B-3)$$

$$\alpha = \frac{q/A_c}{\Delta T} \quad (4B-4)$$

He then approximates:

$$\left(\frac{x}{1-x}\right)^{0.9} \cong x \quad (4B-5)$$

and

$$xG\Delta h_v = \int_0^z \frac{q}{A} \pi D dz$$

or

$$x = \frac{\int_0^z (q/A) \pi D \, dz}{G \Delta h_v} \quad (4B-6)$$

where z is the distance from the point of interest and the saturated BPL.

Equation 4B-6 assumes saturation conditions at $z = 0$. Substituting equations 4B-2 and 4B-4 into the left side of 4B-1, and 4B-6 into 4B-5 and 4B-5 into 4B-3, one gets:

$$\frac{\frac{q/A}{\Delta T}}{0.023 \frac{\lambda_L}{D} \frac{4G}{\pi D \mu_L}^{0.8} \frac{C_p \mu_L}{\lambda_L}^{0.4}} \text{ vs. } \frac{\int_0^z (q/A) \pi D \, dz}{G \Delta h_v} \frac{v_v^{0.5}}{v_L} \frac{\mu_v^{0.1}}{\mu_L} \quad (4B-7)$$

If one now assumes slowly varying properties, the equation reduces to:

$$\frac{\frac{q/A}{\Delta T}}{G^{0.8}} \cong \frac{\int_0^z (q/A) \, dz}{G} C_1 \quad (4B-8)$$

where $C_1 \cong$ a constant made up of fluid properties. Mesler then approximates $G^{0.8}$ as G to get

$$\frac{1}{G} \frac{q/A}{\Delta T} \cong C_1 \frac{1}{G} \int_0^z \frac{q}{A} \, dz \quad (4B-9)$$

The right side must remain in integral form since in the Dengler and Addoms experiment with which Mesler is concerned, there was an axial

variation of heat flux.¹ If the integral does not vary sharply in the axial direction, one should get a strong correlation between the two sides of equation 4B-9.

This is as far as Mesler took the derivation. If one has a constant axial heat flux, then the last equation reduces to:

$$\Delta T \approx ct = C_2 \quad (4B-10)$$

where the constant includes the presupposed slowly varying fluid properties. Yet, temperature differences do not remain constant in evaporating flows. This derivation leads then to an apparent contradiction: on the one hand, $\alpha/\alpha_L = f(1/X_{tt})$ yields good agreement since many of the same parameters appear on both sides of the equation. On the other hand, when the derivation is extended to constant heat flux, resulting in equation 4B-10, disagreement appears between experimental data and the form of the equation.

The contradiction in fact results, not from the extension to constant heat flux, but from the overabundance of rounding and approximation. The assumption put forth in equation 4B-5 is valid only at relatively low qualities. At a quality of .5, the error in the assumption is 100%, at large qualities the error is even greater. Thus, the $(x/(1-x))^{0.9}$ parameter should not be approximated as stated in (4B-5) except at qualities less than 0.2. This accounts for the variation one sees in

¹In protesting Mesler's analysis, Standiford points out that (q/A) varied axially, and that Mesler did not consider this fact. Actually, Mesler is very careful in this regard, as seen above.

heat transfer coefficient in evaporating flow, and helps explain the legitimacy of using $(1/X_{tt})$ as a correlating parameter.

APPENDIX 4C: VISUAL EVIDENCE: REVIEW OF LITERATURE

Hewitt et al [He63] built an experimental rig designed specifically to observe nucleation on a steam core-water film vertical flow, as shown in Figure 4C-1. A double annulus was formed with an inner metal rod and two glass tubes. Water could be introduced as a film attached around the rod and steam introduced in parallel with the water in the remainder of the inner annulus. The glass tube wall was kept clear and free of condensation by forcing hot air through the outer annulus. Both steam and water were introduced near saturation conditions, and heat applied directly through the inner metal rod. The experimental arrangement allowed film thickness, flow rate and heat flux to be varied. High speed films were used to observe rapid processes. The authors observed qualitatively that bubble nucleation depended on the flow rates involved. At high steam velocity, as occur in flow boiling processes, no bubbles were seen; this study therefore supports the notion of a complete suppression of nucleate boiling. The authors also noted that, for lower steam velocities, when nucleate boiling was observed, that the heat flux determined the number of sites and activity level of nucleation. The high speed film was shown recently [He84] and one could observe nucleation at a particular site whenever a liquid wave passed over it. When the wave passed and the film thickness receded, the nucleation disappeared.

Tippets [Ti62] attempted to observe flow patterns of vertical upward flow of high pressure boiling water at various heat fluxes. A rectangular channel was built with heater strips on two sides. High speed

films (4300 frames/sec) were taken through the unheated sides (Figure 4C-1b). In the annular flow regime and qualities of 45-60% (i.e., very thin films), the author noted less but clear agitation of the liquid film on the unheated surfaces as compared to the heated surfaces. He considered this agitation the result of bubble growth within the liquid film; calculations revealed there to be sufficient wall superheat for bubble formation.

Hosler [Ho63] noted that the Tippetts study suffered from a lack of depth perception. He constructed a horizontal rectangular channel with the bottom surface being electrically heated. The two sides were made of quartz prisms, allowing the sides as well as the top to be viewed simultaneously (see Figure 4C-1c). He filmed medium pressure boiling water at 4000 frames/sec as well as took still photographs of 0.5 μ -sec exposure duration. His still photographs were much clearer than those of Tippetts. An annular flow pattern was observed at a 10% calculated quality. Very few bubbles were observed, and he concludes, 'when the vapor column nearly fills the channel, the mechanism of heat transfer apparently changes from bubble generation to surface evaporation.'

There may, however, be a bias in Hosler's study: he mentions, in passing, that the heater strip was 'machined' to ensure uniform heat generation. The machining process may have eliminated many nucleation sites, restricting potential bubble growth.

The study of Berensen and Stone [Be63] differs from those previously mentioned in several interesting ways. They observed the vaporization

of R113 in a horizontal tube using constant temperature air as the heat source. It therefore differs from the studies in terms of fluid type, flow orientation, and boundary condition (constant temperature, rather than constant heat flux). The refrigerant flowed inside a pyrex tube which was surrounded by a rectangular quartz duct (Figure 4C-1d). Inside the annulus, 800°F air passed in counterflow to the refrigerant. Subcooled refrigerant entered the heated chamber and exited at moderate to high quality, depending on the amount of subcooling. Initially high speed films (7000 frames/sec) had poor resolution between the liquid and vapor; the authors then added a refrigerant-coloring agent (used in leak detection) in a concentration of about 1% wt. They considered resolution to be excellent. Berenson and Stone observed a few bubbles in the film but considered the effect on the rate of vapor generation to be negligible. The authors conclude:

'[Although] nucleation of bubbles on the wall was observed whenever the wall was wet, in all flow regimes, (. . .) the dominant heat transfer mechanism in annular flow is conduction and convection through the liquid film on the wall. The vapor formation process occurs primarily at the interface between the liquid annulus and the vapor core, and not by the formation of bubbles within the liquid annulus.'

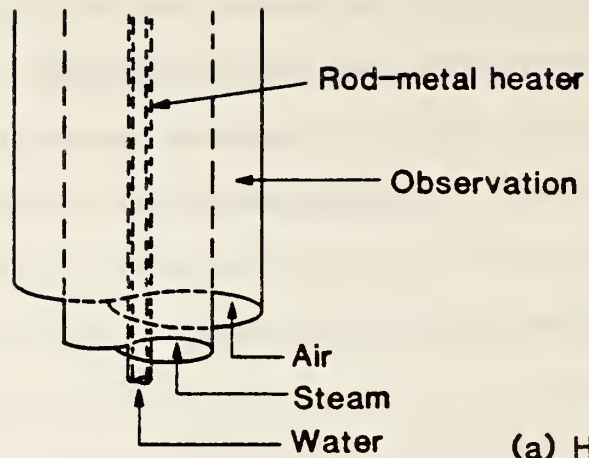
Unfortunately this study, like that of Hosler, suffers from the potential lack of nucleation sites in that a pyrex tube was used. Also R113 has a very small contact angle (4°) [Be84], so that very few cavities were unwetted in all likelihood.

Staub and Zuber [St66] also observed flow patterns with R22 flowing vertically in a glass tube (quality range 0.14 to 0.22). An electrically conducting transparent coating was bonded to the inside of the tube. Observations and photographs were made with the conclusion about the annular flow regime: 'this well-defined mechanism consists of a vapor core with or without entrained droplets and a liquid annulus on the wall that is often quite thick and wavy and sometimes still contains very small vapor bubbles.'

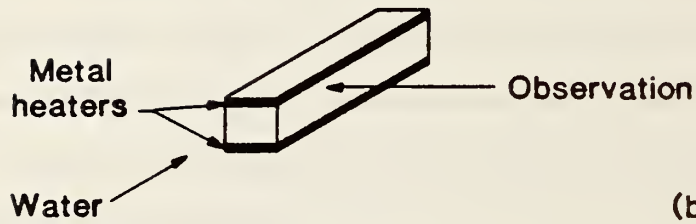
Gouse and Common [Go65] used a similar arrangement as [St66] with R113 except that the coating was placed on the outside of the tube. They observed suppression of nucleation whenever an annular flow was observed. Again, their glass tubes did not contain the full range of activation sites, and R113 has a very small contact angle.

Mesler [Me77] reviews several studies of nucleate boiling in stationary and moving thin liquid films. In his own study, high speed movies were taken of boiling of stationary water on a metal surface. An artificial nucleation site was created in the surface; very near the site, a rapid response small thermocouple was installed and polished flush with the surface. Films were taken which photographed simultaneously the bubbles

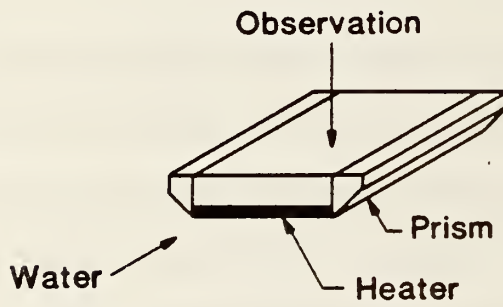
growing and departing the surface and the thermocouple reading on an oscilloscope face. With this arrangement he was able to monitor local cooling (i.e., heat transfer) rates and bubble position. He observed high heat transfer rates in the small area under the bubble for short periods. It is the high heat transfer rate which led him to consider boiling as the principal mechanism with all thin films.



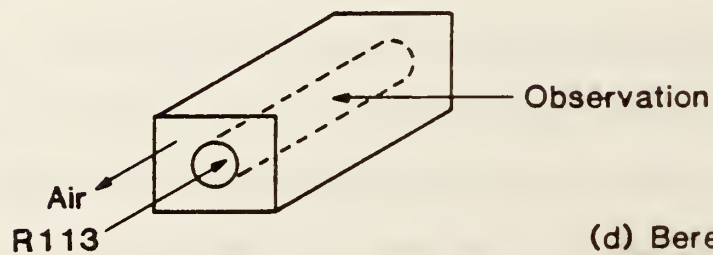
(a) Hewitt et al



(b) Tippetts



(c) Hosler



(d) Berenson and Stone)

Figure 4C-1: Visualization Methods

APPENDIX 4D: DEPENDENCE ON HEAT AND MASS FLUX

Nucleate boiling suppression was first proposed by Dengler and Addoms [De56] based on an experiment with vaporizing water which flowed inside 1 in. OD copper tubes. Steam was used as a heat source in five separate sections of a 20 foot copper tube. Wall thermocouples were embedded in the tube wall, and pressure taps were installed at the entrance and exit of each section. Of note, the void fraction was measured to within 10% using a radioactive tracer. The idea of suppression was advanced on the following experimental and theoretical observations:

- (1) Heat flux increased sharply along the tube; the quality increased as well but the wall-steam temperature difference remained constant, i.e., heat transfer coefficient increased sharply with quality.
- (2) Both liquid and vapor velocities could be obtained from the measured void fraction and mass flow rates. An average velocity of the two phase mixture was calculated and used in a single phase convection heat transfer correlation to predict the heat transfer rate. Good agreement was achieved over much of the tube, excepting the low quality portion.
- (3) The use of a flow parameter, $1/X_{tt}$, correlated the data fairly well, except at low quality.
- (4) Previous studies showed that forced convection raised the value of the wall superheat necessary to initiate nucleate boiling. Thus, if one raised the velocity sufficiently, nucleation should cease.

At low quality, Dengler and Addoms considered both convection and nucleate boiling to be important, and their effects to be superposed. This conclusion is derived from the underprediction of heat transfer at low quality by the correlation techniques described in observations (2) and (3) above.

Mesler [Me77] examined in detail the data of Dengler and Addams. Dengler and Addoms claimed no correlation between measured heat flux and wall superheat (observation (1) above). Mesler reviewed the raw data from Dengler's report, and rejects for various reasons (dryout, highly fluctuating wall temperatures, erratic thermocouples) over 100 of Dengler's original 185 data points. The original Dengler and Addoms plot of α/α_L versus $1/X_{tt}$ showed a few points at low quality to have relatively high values of α/α_L , and the authors attributed these points to have been caused by the presence/addition of nucleate boiling. Mesler replots their data with only his 'acceptable' points, and shows that nucleate boiling, if it is the proper explanation, contributes at all qualities. Using only the acceptable data, Mesler also plots heat flux versus $\Delta T_{\text{superheat}}$, the slope of which represents the heat transfer coefficient. He then plots in the same fashion the data of five pool boiling experiments and shows them to have a similar, general shape as the flow boiling data of Dengler and Addams. He thus establishes a general relation between heat flux and wall superheat and draws from the data precisely opposite conclusions of the physical process than the authors who first collected and explained the data. In a brief letter of response, Standiford (15) points out an error in one of the five pool

boiling experiments, which Mesler accepts but points to the remaining experiments.

Mesler also considers observation (3) of Dengler and Addoms, the correlation of α/α_L with $(1/X_{tt})$ on a log-log basis. He argues about two potential pitfalls of such an approach. First the use of log-log plots tends to reduce the appearance of variation. Secondly, he points out that there are several common variables in α/α_L and X_{tt} , and that with slowly varying fluid properties, one should automatically expect a strong correlation, as Dengler and Addams achieved. His analysis is reviewed in more detail in Appendix 4B.

Mesler goes on to note that as convection of the vapor increases, $(1/X_{tt})$ must increase. At the same time, with stronger convection one would expect a smaller ΔT . Mesler then states 'This, in turn, predicts that when α/α_L , which tends to increase with $1/X_{tt}$, is multiplied by ΔT , which tends to decrease with $1/X_{tt}$, the quantity obtained should vary less with $1/X_{tt}$ than did α/α_L . The actual data . . . contradict this prediction.' Since convection does not explain the data trends sufficiently, Mesler argues that nucleate boiling may be the phenomena, and compares the Dengler and Addams data to pool boiling data as previously discussed.

In further arguing for nucleate boiling as the dominant mechanism for all flow boiling situations, Mesler cites several studies of boiling with thin moving films.

Beattie and Lawther have presented briefly evidence to support the notion of bubble existence in thin turbulent flowing films [Be79]. They maintain that attached bubbles exist and serve to enhance surface roughness. The bubble contribution to surface roughness is dependent on surface tension and shear forces. They then find agreement between a flow model which includes these forces (rather than say, a model including Reynolds Number) to experimental data of velocity profile and friction factor in annular flows with thin films. This agreement, they conclude is 'consistent with the existence of attached wall bubbles in the film . . . [and] that the nucleate boiling mechanism can contribute to heat transfer in thin film annular flows.' The notion of attached bubbles is not new: Lacey et al discuss the possibility, suggesting that bubbles might remain fixed within the viscous sublayer [La62].

Turning to refrigerants, Chawla [Ch67] noted that vaporization data taken with many flowing refrigerants indicated two separate regimes for heat transfer. The first regime showed near independence of the heat transfer coefficient from mass flow rate but a strong dependence on heat flux. This regime in behaving similarly to pool boiling experiments was considered to be dominated by nucleation. A second regime showed complete independence from heat flux but a strong dependence on mass flow. This second regime was characterized as being convection-dominated. A small region between these two general regimes is considered to be of transitive nature, with nucleation and evaporative mechanisms suppressed. Chawla's correlation of his data actually suggests a suppression criterion (see Appendix 4A). Additionally, an independence of

the heat transfer coefficient from heat flux has been observed with benzene, toluene and in at least one case R12 [Da65,St65]. These studies suggest then an absence of nucleate boiling phenomena. Others have previously observed similar behavior with vertical flow of water; several studies are cited in Lacey, Hewitt, and Collier [La62].

In the most definitive study to date, Aounallah et al [Ao82] have recently built an apparatus to determine if two phase heat transfer coefficients can be indeed completely independent of heat flux for a given flow rate, film thickness and quality. The comparison is potentially difficult since the amount of droplet entrainment is a weak function of heat flux; entrainment affects the thickness of the liquid film. All previous experiments cited above used a uniform heat flux. For a given inlet condition and mass flow rate, the point at which a certain quality is reached is related directly to this heat flux (as shown in Chapter 3); with a larger heat flux, the same vapor quality will be achieved at a different location in the flow. A comparison of the effect of heat flux would require then a comparison of heat transfer coefficients at different positions along the tube and is complicated by the fact that boiling is a function of local surface conditions. To avoid this problem, Aounallah et al built an apparatus similar in many ways to the second test rig used in this report. They used a vertical tube comprised of three sections: a preheat section, a 'calming' adiabatic section, and a test section. The preheat section was used to bring the flow to the desired quality. The calming section was included to bring the flow to estimated 'hydrodynamic equilibrium' at the inlet

of the test section. Hydrodynamic equilibrium is achieved when the rate of entrainment exactly equals the rate of droplet deposition under adiabatic conditions. In this manner, not only the quality but the film thickness could be controlled at the test section inlet. The test section was outfitted with several closely spaced wall thermocouple stations; at each station, four thermocouples were mounted circumferentially. Fluid temperature was assumed as saturated and calculated from pressure measurements along the test section.

The authors then determined heat transfer coefficients for water at a fixed flow rate and quality for five heat flux values. The heat transfer coefficients were found to be constant, i.e., independent of heat flux. These results were reported for four different qualities (.05 to .42), showing that as quality increased, so did the heat transfer. Their results therefore support the notion of the complete suppression of nucleate boiling. It should be noted that their measured values were not predicted well by a detailed film flow model but were predicted to about $\pm 20\%$ by the forced convective portion of the Chen correlation [Ch66].

Beattie and Green [Be84] responded to the publication of Aounallah et al by examining in detail an old experiment by Bertolletti et al whose experimental apparatus closely resembled that of Aounallah. The Bertolletti data is at much higher pressure, flow rates, and heat fluxes though also with flowing water. The data of Bertolletti did not show a constant heat transfer coefficient, but instead one which 'varied

significantly with heat flux, having negligible dependent on mass flux, quality, tube diameter, and distance from the inlet of the heated section'. Beattie and Green also compared the Bertoletti data to the pool boiling correlation of Aladiev et al. Agreement, as shown on a log-log plot is excellent.

APPENDIX 4E: MIXTURES - LITERATURE REVIEW

Little work has been done specifically addressing suppression or incipience of nucleate boiling of mixtures. However, the general study of nucleate boiling of nonazeotropic mixtures is itself a large and growing field major portions of tests have been devoted to this subject. As such a comprehensive review of all features of nucleate boiling of mixtures is beyond the scope of this report. In this appendix certain critical features of bubble growth as applied to the suppression question are introduced.

Equation (4-1) for the superheat requirement for a vapor nucleus of radius r_c to exist in pure fluids is also applicable for mixtures. However there are important differences in the values of the terms of equation (4-1). First the term dP_{sat}/dT for a mixture differs from that of a pure fluid or an ideal mixture as given by Collier:

$$\frac{dP_{sat}}{dT} = \left(\frac{\partial P}{\partial T} \right)_{\bar{X}} + \left(\frac{P}{RT} \frac{\partial \bar{X}}{\partial T} \right)_P + (K - 1) \bar{Y} \left(\frac{\partial^2 g}{\partial \bar{X}^2} \right)_{P, T}$$

where K is the equilibrium constant (\bar{Y}/\bar{X}) and g is the Gibbs free energy. The term $\partial P/\partial T)_{\bar{X}}$ is identical to what would appear for a pure fluid. The second term on the right side is always negative so that dP_{sat}/dT for a mixture is always less than that for an ideal mixed fluid. On applying this finding to equation (4-1), the incipient superheat requirements for mixtures is increased over that of an ideal mixed fluid.

This change, however, has been shown by Shock (Sh77) to be less important than the behavior of the mixture's surface tension. Small additions of a second component may have drastic consequences on surface tension, such that the superheat requirement may decrease substantially over that of one of the pure fluids or that presupposed of an ideal mixture.

Three studies of the onset of nucleate boiling (onb) with binary mixtures were found in the literature. Thome, Shakir, and Mercier [Th82] performed a careful study of the activation of a single first boiling site on a polished heated surface with mixtures of liquid nitrogen-argon and ethanol-water. The composition of the cryogenic mixture had no effect on the activation of the single site. However, composition yielded a strong effect on their results with ethanol water. The results in both cases are due to the wetting characteristics of the mixtures. The cryogenic mixture components have similar contact angles, whereas the addition of slight amounts of ethanol to water has a drastic effect on surface tension and therefore the contact angle. The authors did not consider the effect of mass transfer resistance (mtr) in their results. In fact, the cryogenic mixture results suggest no effect of mtr. However, the onb point for ethanol water is underpredicted by treating the analysis as an equivalent pure fluid.

Shock evaluated binary mixtures of ethanol-water and ethanol-benzene, with similar conclusions regarding the influence of wetting characteristics [Sh77]. The onb point was found by wall temperature

measurement in his flow boiling experiments. He suggests that suppression of boiling of mixtures might not be strictly treated as the same as the onb problem, due to the possible existence of local concentration gradients around established nuclei. He leaves open the possibility of mtr effects.

Toral studied ethanol-cyclohexane, which behaves in a more ideal fashion than the previous ethanol mixtures, in a flow boiling apparatus similar to Shock's [To79]. He differentiates between activation of an isolated cavity and the sudden transition to multiple cavity activation. The latter mechanism, more relevant to the work of this report, is called the onb by Toral. He concludes that composition has a considerable influence on multiple cavity activation, 'indicating the presence of mtr effect and suggesting that onb is governed by bubble growth dynamics . . . ' If Toral's conclusions are correct, then mtr should be considered in subsequent prediction methods for mixtures.

Toral [To79] also attempted a basic theoretical study of the potential for nucleate boiling in thin film flow of two non-azeotropic mixtures: an aqueous solution of methanol and one of ethanol-cyclohexane. He posed the following problem:

'A thin liquid film flows in upward direction on a flat plate of infinite depth by the action of shear stress imposed upon it by vapor flowing concurrently. Thermodynamic equilibrium is assumed between liquid and vapor phases with uniform temperature

distribution due to the adiabatic condition at the boundary with the flat plate. At time $t = 0$ heat flux q_w is applied at this boundary over the axial length $x = 0$ to $x = L$. The temperature profile begins to develop. A net rate of evaporation begins when the heat flux reaches the interface. It is assumed that for $t > 0$ heat flux at the wall remains constant at q_w .

As time goes on, the thickness of the layer decreases due to evaporation, the film thickness also decreases with downstream distance.

The basic equations governing the problem are:

Momentum

$$\rho e_m \frac{\partial^2 u}{\partial y^2} = -\rho g + \frac{dp}{dx} = ct$$

Energy or Mass Transfer

$$\frac{\partial \theta}{\partial t} + u \frac{\partial \theta}{\partial x} = \epsilon \theta \frac{\partial^2 \theta}{\partial y^2}$$

$\theta = T$ in energy equation

$\theta = C$ in mass equation

The boundary conditions he used are discussed later.

Toral investigates the effect of assuming various thermal and mass diffusivities ($\epsilon \theta$) in the above expression. Most researchers have assumed a single phase eddy diffusivity throughout the layer, i.e., a

growing turbulence as one proceeds toward the interface. Some research has shown that the turbulence may be damped in the vicinity of the interface, providing an increase of thermal and mass transfer resistance.¹ The damped and undamped diffusivity models produced widely different results. Using an undamped profile, a small wall superheat developed for the non-azeotropic mixture, one which would be insufficient for nucleation. Using a damped profile, the calculated wall superheat increased by a factor of 6, to the point that nucleation was likely. For the aqueous mixture, wall superheat was too low to initiate bubble growth in either case. He concludes that only with high conductivity fluids, such as with aqueous mixtures, can one anticipate the suppression of nucleate boiling, if in fact turbulence damping occurs at the interface. It is important to note that the conductivity of water or aqueous mixtures is roughly 100 times that of many other fluids, including most common refrigerants.

Toral's work is most relevant to this report since it is concerned with non-azeotropic mixtures. A detailed review of his posed problem reveals some potential difficulties with his analysis.

The parabolic form of the energy and mass transfer equations requires the use of only one boundary condition on x . Toral however uses:

¹In the vicinity of the interface, the eddy diffusivity in the energy equation reduced to the thermal diffusivity, $\lambda/\rho C_p$.

$$T(0, y, t) = T_{\text{bub}}(C_{\text{bulk}})$$

$$c(0, y, t) = C_{\text{bulk}}$$

$$dT(L, y, t)/dx = 0$$

$$dc(L, y, t)/dx = 0$$

The use of two x boundary conditions converts the solution technique from a 'forward marching' one to a closed form type. The effect of specifying the downstream condition propagates upstream in the solution technique. Toral even notes $\partial T/\partial x = 0$ shortly after the inlet. Thus, the use of two boundary conditions is mathematically incorrect.

The physical meaning of $\partial T/\partial x = 0$ can be interpreted simply with the use of a control volume heat is transferred into the control volume by diffusion away from the wall and by convection. It is transferred out by convection and by diffusion toward the interface. The difference must be the amount of heat stored. If $\partial T/\partial x = 0$, there is no sensible heating of the liquid, and net flow of heat must either be to storage or toward the interface. A similar explanation is valid for the mass transfer equation.

The mathematical error might not have serious consequences, a marching type solution could produce the same result, since the specification of 'no sensible heating' may or may not be valid. Many condensation researchers consider the term to be small, and that, at steady-state, all wall heat flux is transferred to the interface (e.g., [Co37]). Bennett and Chen in their flow boiling study of an ethylene-glycol/water mixture considered sensible heating of the liquid layer, and achieved only a slightly improved agreement with data [Be80]. On the other hand,

Toral called the stored heat 'sensible heat', and noted it represented 40-50% of the total heat flux in the damped cases.

Despite its potential difficulties, Toral's posed problem is of substantial interest. An alternate means of solution would be to assume steady-state and approximate an initial film thickness $\delta(x = 0) = \delta_0$, and march downstream until the film is depleted. In the case of refrigeration cycles, the initial condition in the x-direction can be simply equilibrium vapor and liquid compositions, since a two phase mixture in fact enters an evaporator from an isenthalpic expansion device. At the entering vapor quality of about 20% the phases separate into an annular flow pattern very near the evaporator inlet. At each Δx step, the film thickness must be calculated from energy and species balances. Such a solution requires as input the same y-boundary conditions and x initial condition as Toral assumes.



APPENDIX 6A: MISCELLANEOUS HEAT TRANSFER FORMS

The graphical method of Shah, like Chen's method, attempts to predict α in either heat transfer regime. Mass flux and quality effects are considered in the nucleate boiling regime through the single phase heat transfer coefficient where

$$\alpha = \alpha_{nbc} = \alpha_{LO}(f(Bo)) \tag{6A-1}$$

Like form 6-1a equations, the nucleate boiling has a dependence on tube diameter (explicit in α_{LO}). The forced convection dominated regime, called by Shah the 'fully suppressed nucleate boiling regime,' yields

$$\alpha = \alpha_{FC} = \alpha_{LO}f(Co) \tag{6A-2}$$

where

$$Co = \left(\frac{1-x}{x}\right)^{0.8} \left(\frac{\rho_v}{\rho_L}\right)^{0.5} \tag{6A-3}$$

and Co is called the convection number. Co is similar to X_{tt} without the dimensionless viscosity term.

The correlation was compared to 810 data points from R11, R12, and R22 experiments with a mean fractional deviation of 23% and a tendency to underpredict [De78]. Shah recently computerized the method [Sh82], and the algorithm was compared to the experimental data of this report. In general, the method predicted poorly (figure 6-1). The suppression

criterion was incorrect, so that the algorithm selected a heat transfer coefficient calculated from equation (6-2b) instead of the more appropriate equation (6-2a). All of the Rig #2 data tended to be underpredicted, less severely for the forced convection regime. The Rig #1 data was also poorly predicted (figure 6-1), though the mean deviation is reduced.

After analyzing Shah's correlation and others; Dembi et al. introduced a new correlation for the forced convective/evaporative regime of the form [De78]:

$$\alpha = 0.115 \frac{\lambda_L}{D} (x^4(1 - x^2))^{0.11} \left(\frac{G^2 \Delta h_v}{g \rho_L \sigma} \right)^{0.44} (Pr_L)^{0.7} \quad (6A-4)$$

It correlated the same 810 point data base to a mean deviation of 0.15. However, the coefficients were determined by regression analysis of the data base, so good agreement might be expected. It is interesting to note that heat flux does not appear in the equation though a weak dependence on heat flux was observed in the experimental data. No attempt was made to apply this correlation. It is also interesting to note that the Prandtl number dependence is to the 0.7 power, similar to Bennett and Chen's correlation.

Most recently, Kandlikar [Ka84] has developed, via regression analysis, a correlation which yields good agreement with a large body of experimental data on refrigerants, water, and organic fluids in both

horizontal and vertical orientations. The method involves the classic superposition of convective/evaporation and nucleate boiling. It contains seven empirically determined constants, one of which is dependent on fluid type (and therefore fitted to the individual experiment with that fluid). Test with R152a and R13B1 are not included in this data base, and therefore the correlation could not be checked.

APPENDIX 6B: POLLEY'S METHOD

Polley has recently modified Chen's method and suggested a different pool boiling relation due to Cooper [Po82]:

$$a_n = a_{pool} = C_1 \left(\frac{P}{P_c} \right)^{.126} \left(1 - \frac{T}{T_c} \right)^{-.70} q^{.69} \quad (6B-1)$$

where C_1 varying between 3 and 4.1 for refrigerants, and other values for different fluids. Also, he modified the suppression factor:

$$S = 1.0 \text{ if } \frac{a_e}{a_{pool}} < 0.15 \quad (6B-2)$$

$$= -.5271 \ln \left(\frac{a_e}{a_{pool}} \right) \text{ if } 0.15 < \frac{a_e}{a_{pool}} < 1.0 \quad (6B-3)$$

$$= 0 \text{ if } \frac{a_e}{a_{pool}} > 1.0 \quad (6B-3)$$

The justification for the changes were given as:

- (a) The pool boiling relation is simpler to apply, as it requires fewer properties;
- (b) The suppression factor is based on heat transfer contributions directly; and most importantly,
- (c) The revised form fit a very large data bank of steam-water data to a higher degree of accuracy than Chen's equation.

Polley included an additional criterion to determine if a nucleate boiling contribution should be included. He suggested that the Davis and Anderson incipient superheat, ΔT_i , be calculated (see Appendix 4A). If the given ΔT is less than that calculated, then no nucleate boiling should be included. It is, however, not clear how to apply it in the case of constant wall flux where ΔT is not known a priori.

APPENDIX 7: DEVELOPMENT OF COON (MASS TRANSFER EFFECT ON LIQUID SIDE) IN BENNETT AND CHEN'S METHOD

Bennett and Chen postulated mass transfer does not affect α , but does effect the driving force.

For a pure fluid

$$q_{\text{evap}} = \alpha_{\text{LO}}(T_{\text{W}} - T_{\text{eqb}}) \quad T_{\text{eqb}} = \text{equilibrium temp, for pure fluid } T_{\text{eqb}} = T_{\text{sat}}$$

For a binary

$$q_{\text{BIN}} = \alpha_{\text{LO}}(T_{\text{W}} - T_{\text{i}}) \quad T_{\text{i}} = \text{interfacial temp.}$$

$$= \alpha_{\text{LO}} \frac{T_{\text{W}} - T_{\text{i}}}{T_{\text{W}} - T_{\text{eqb}}} (T_{\text{W}} - T_{\text{eqb}})$$

$$= \alpha_{\text{LO}} C_{\text{COON}} (T_{\text{W}} - T_{\text{eqb}}) \quad (7A-1)$$

Since T_{i} is unknown, Bennett derived a way of eliminating it from (7A-1), as follows (steps not shown in Bennett's report):

Define a mass transfer coefficient, β_{L} :

$$\dot{m}_{\text{mv}} = \rho_{\text{L}} \beta_{\text{L}} (X_{\text{eqb}} - X_{\text{i}}) \quad (7A-2)$$

mv = more volatile

Now, assume all heat input results in evaporation

$$\dot{q}_{\text{evap}} = m \Delta h_v = \frac{\dot{m}_{mv}}{Y} \Delta h_v \quad (7A-3)$$

and assume $Y = Y^*$, i.e., $Y^* = Y^*(X_{\text{eqb}})$, not Y_i (this is not strictly correct) and since

$$\frac{T_W - T_i}{T_W - T_{\text{eqb}}} = \frac{T_W - T_{\text{bub}}(X_i)}{T_W - T_{\text{bub}}(X_{\text{eqb}})} \quad (7A-4)$$

equations (7A-2), (7A-3) and (7A-4) can be combined to give C_{OON} as follows:

From (7A-2) and (7A-3),

$$X_{\text{eqb}} - X_i = \frac{\dot{m}_{mv}}{\rho_L \beta_L} = \frac{\dot{q} Y^*}{\Delta h_v \beta_L} \quad (7A-5)$$

Also

$$X_{\text{eqb}} - X_i = \frac{dX_{\text{eqb}}}{dT_{\text{bub}}} (T_B - T_i) \quad (7A-6)$$

combining (7A-5) and (7A-6)

$$\frac{dX}{dT_{\text{bub}}} (T_{\text{eqb}} - T_i) = \frac{\dot{q} Y^*}{\Delta h_v \rho_L \beta_L}$$

or

$$T_{eqb} - T_i = \frac{\dot{q}Y^* \frac{dT_{bub}}{dX}}{\rho_L \beta_L \Delta h_v}$$

Add and subtract T_W , and multiply by -1

$$(T_W - T_{eqb}) - (T_W - T_i) = \frac{-qY^* dT_{bub}/dX_{eqb}}{\rho_L \beta_L \Delta h_v}$$

Divide by $(T_W - T_{eqb})$

$$1 - \frac{T_W - T_i}{T_W - T_{eqb}} = \frac{-qY^* dT_{bub}/dX}{\rho_L \beta_L \Delta h_v (T_W - T_{eqb})}$$

or

$$\frac{T_W - T_i}{T_W - T_{eqb}} = 1 + \frac{qY^* dT_{bub}/dX_{eqb}}{\rho_L \beta_L \Delta h_v (T_W - T_{eqb})}$$

Note that (+) sign. In Bennett and Chen's paper they have a (-) sign.

The difference is due to definition. In the development here, X is defined in terms of the more volatile component. Bennett and Chen used X as the less volatile component. If defined in that manner, a (-) is correct.

APPENDIX 7B: BENNETT AND CHEN'S INCLUSION OF SENSIBLE HEATING OF LIQUID

$$\dot{Q} = \dot{Q}_{\text{evap}} + \dot{Q}_{\text{sens}_L} + \dot{Q}_{\text{sens}_v}$$

$$\dot{Q}_{\text{evap}} = \dot{m} \Delta h_v \quad (7B-1a)$$

$$\dot{Q}_{\text{sens}_L} = \frac{1}{\pi D} \dot{M}_L C_{PL} \frac{dT_{\text{bub}}}{dz} \quad (7B-1b)$$

so

$$\dot{Q} = \dot{m} \Delta h_v + \frac{1}{\pi D} \dot{M}_L C_{PL} \frac{dT_{\text{bub}}}{dz} \quad (7B-1c)$$

Mass balances give

$$\text{total mass:} \quad -d(\dot{M}_L) = \dot{m} \pi D \, dz \quad (7B-2)$$

$$\text{component mass:} \quad -d(\dot{M} X_L) = \dot{m} Y^* \pi D \, dz$$

$$-X_B d\dot{M}_L - \dot{M}_L X_B = \dot{m} Y^* \pi D \, dz \quad (7B-3)$$

Rearranging (7B-3)

$$\frac{dX_B}{dz} = \frac{-\dot{m} Y^* D}{\dot{M}_L} \frac{X_B}{\dot{M}_L} \frac{d\dot{M}_L}{dz} = \frac{-\dot{m} Y^* D}{\dot{M}_L} + \frac{\pi D \dot{m}}{\dot{M}_L} X_B \text{ from (7B-2)}$$

so, rearranging the last equation

$$\frac{M_L}{\pi D} = \dot{m}(X_B - Y^*) \frac{dz}{dX_B} \quad (7B-4)$$

Substituting (7B-4) into (7B-1b)

$$\dot{Q}_{sens_L} = \dot{m}C_{PL}(X_B - Y^*) \frac{dT_{bub}}{dX_B}$$

and (7B-1c) becomes

$$\dot{Q} = \dot{m}\Delta h_v + \dot{m}C_{PL}(X_B - Y^*) \frac{dT_{bub}}{dX_B} = \dot{m}\Delta h_{eff}$$

or

$$\Delta h_{v_{eff}} = \Delta h_v - C_{PL}(Y^* - X_B) \frac{dT_{bub}}{dX_B}$$

where again X_B and y are in terms of more volatile component. Bennett and Chen used less volatile so for their equation:

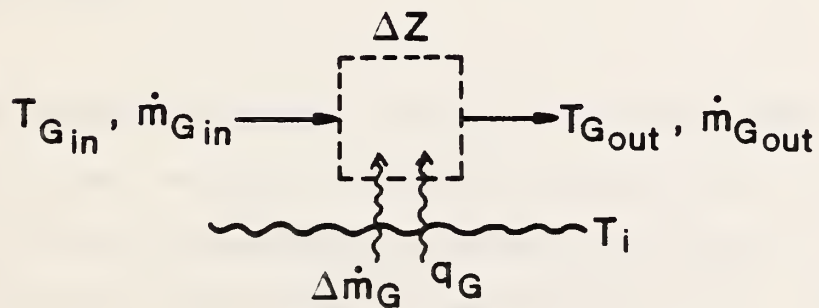
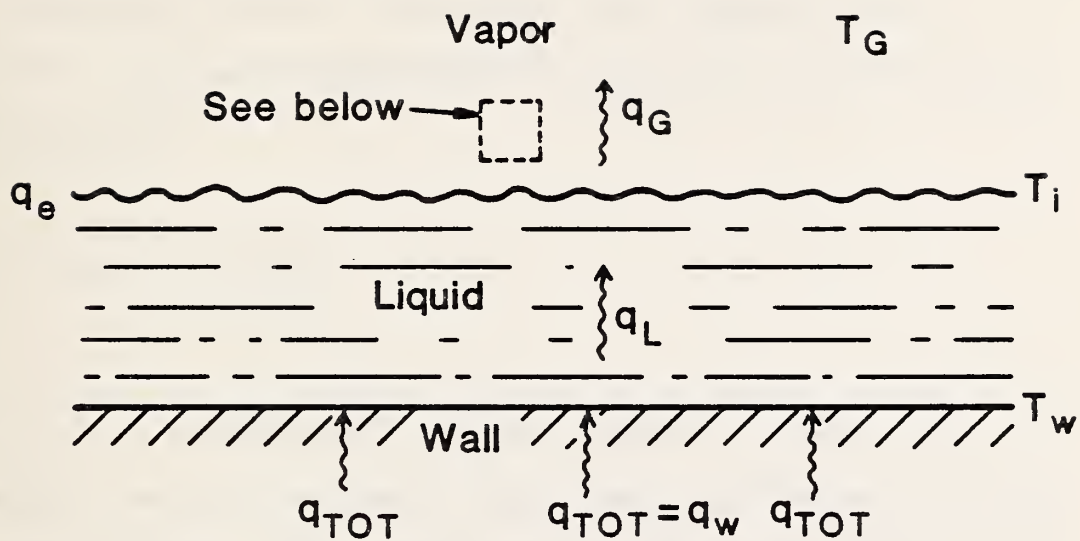
$$\Delta h_{v_{eff}} = \Delta h_v + C_{PL}(X_{LV} - Y_{LV}) \frac{dT_{bub}}{dX_{LV}}$$

APPENDIX 7C: MICROLAYER EVAPORATION MODELS

Van Ouwerkerk [Va72] analyzed a hemispherical bubble with a thin microlayer of liquid under it (see Figure 7C-1). The assumed physical properties were independent of both composition and temperature. The transient analysis of bubble growth showed that bubble growth rates were greatly reduced over an EPF fluid due to the depletion of the more volatile component in the microlayer. The depletion caused the usual rise in bubble point temperature reducing the evaporation rate. He noted that the Marangoni effect (i.e., surface tension gradient around a bubble influencing the growth rate) could theoretically assist evaporation by drawing the more volatile component from the bubble cap region to the microlayer. Upon calculation, he noted the effect is negligible for realistic bubble sizes.

Toral [To79] examined microlayer evaporation, but allowed thermal properties to vary with composition. His numerical analysis treated the microlayer as a 1-D transport problem (see Figure 7C-1). His conclusions are similar to Van Ouwerkerk. He further noted that all evaporation may cease, so that a dryout condition might never be reached. In this situation, much higher critical heat fluxes would be possible with a mixture. Recently, Stephan and Preuber [St82] developed a model which suggests that, while microlayer evaporation occurs, condensation might occur simultaneously at the bubble cap. They assume the microlayer has a lower liquid composition than the bulk liquid (see figure 7C-2). However, vapor is produced in this region due to its proximity to the heated wall surface. The vapor produced in microlayer evaporation is in equilibrium

with the liquid in this region, and once produced mixes completely with the vapor in the bubble (assumed). The vapor therefore has a composition no longer in equilibrium with the liquid at the bubble cap. To move toward equilibrium, the less volatile component condenses out at the same time the more volatile component evaporates. They note that, if this modelled process indeed is accurate, the mass transfer resistance between the bulk and microlayer increases, i.e., the boundary layer has more difficulty in finding available more volatile component.



$$q_G = \alpha_G (T_i - T_G) = \bar{\dot{m}}_G C_{pG} \Delta T_G$$

Figure 7E-1: The Bell and Ghaly Method

APPENDIX 7D: FURTHER COMMENTS ON SHOCK'S ANALYSIS

There are some concerns regarding the analysis. Turbulence damping near the interface was neglected (this might affect finding (a) in particular); eddy mass diffusivities are generally related to thermal diffusivities by

$$\varepsilon_D = \varepsilon_H^n, \quad n = \frac{1}{4} \text{ to } \frac{1}{2}$$

not $\varepsilon_D = \varepsilon_H$ as assumed in the analysis. However, finding (a) is supported by analytic modelling of multicomponent condensation by Webb and Sardesai [We82]. They examined two limiting cases: one in which the rate of mass transfer in the condensate film was assumed to be infinitely slow, and the other infinitely fast. Condensation rates of individual components agreed to within 15% of each other and within 10% of experimental results.

Shock's initial condition, selected to maximize the vapor-liquid composition difference, was only 7°C from the boiling point of water. This suggests that with the maximum mass transfer resistance, the interfacial temperature could differ from equilibrium by 7°C. Since the total temperature drop across the liquid film was calculated 40-70°C, the largest possible reduction in heat transfer coefficient was 10-15%. Shock does note that the findings may vary for mixtures with a wider boiling range than the considered 20°C of ethanol-water (R152a/R13B1 at 4.75 have about a 30°C boiling range). In a related problem Price and Bell [Pr74] compared a simplified condensation model which neglects mass

transfer resistance to a more exact model. Agreement was good for a mixture of methanol-water (small boiling range), but not for an n-butane/n-octane mixture (wide boiling range).

APPENDIX 7E: THE BELL AND GHALY MODEL

Figure 7E-1 shows simple heat transfer across a film and to a vapor core.

Neglecting any sensible heating of the liquid ($Q_{sL} = 0$ in equation 1-1),

$$q_{TOT} \approx q_L = \alpha_L (T_W - T_i) \quad (7E-1)$$

Similarly on the vapor side,

$$q_G = \alpha_G (T_i - T_G) \quad (7E-2)$$

Combining the previous equations, and eliminating T_i yields

$$q_{TOT} = \alpha_L (T_W - T_G \frac{q_G}{\alpha_G})$$

and dividing both sides by q_{TOT}

$$1 = \frac{\alpha_L}{q_{TOT}} (T_W - T_G) - \frac{\alpha_L}{\alpha_G} \frac{q_G}{q_{TOT}}$$

or

$$q_{TOT} = \frac{\alpha_L}{\frac{\alpha_L}{\alpha_G} \frac{q_G}{q_{TOT}}} \quad (7E-3 a)$$

so that defining an effective heat transfer coefficient,

$$a_{eff} = \frac{1}{\frac{1}{a_L} + \frac{q_G/q_{TOT}}{a_G}} \quad (7E-3b)$$

The ratio q_G/q_{TOT} represents the ratio of the heat gained by the vapor to the total heat. Over a length ΔZ ,

$$q_G = \dot{m}_G C_{PG} \Delta T_G \quad (7E-4a)$$

where the mass flow rate of vapor is a mean quantity over the interval. The total heat supplied is over this same length,

$$q_{TOT} = \dot{m}_{TOT} \Delta h \quad (7E-4b)$$

so that

$$\frac{q_G}{q_{TOT}} = \frac{\dot{m}_G}{\dot{m}_{TOT}} C_{PG} \frac{\Delta T}{\Delta h} \quad (7E-4c)$$

over an infinitesimal length ($\Delta Z \rightarrow 0$),

$$\frac{q_G}{q_{TOT}} = x C_{PG} \frac{dT_G}{dh} \quad (7E-4d)$$

To this point, the derivation is exact. The quantity dT_G is now approximated as

$$dT_G = dT_i = dT_{eqb} \quad (7E-5)$$

so that equation (7-4) becomes

$$\frac{q_G}{q_{TOT}} = x C_{PG} \frac{dT_{eqb}}{dH} \tag{7E-6}$$

The term dT_{eqb}/dh is referred to commonly as the 'condensation curve'. Typical curves for R13B1/R152a mixtures are shown on Figure 3-13. The effective heat transfer coefficient of equation (7E-3b) is then

$$a_{eff} = \frac{1}{\frac{1}{a_G} + \frac{x C_{PG} (dT_{eqb}/dh)}{a_G}} \tag{7E-7}$$

The problem remains to evaluate the heat transfer coefficients a_L and a_G . Bell and Ghaly recommended the classic single phase relations:

$$a_G = \left(\frac{G x D}{\mu_G} \right)^{.8} \left(Pr_G \right)^{.4} \frac{\lambda_G}{D} = a_{GO} \tag{7E-8}$$

and

$$a_L = \left(\frac{G(1-x)D}{\mu_G} \right)^{.8} \left(Pr_g \right)^{.4} \frac{\lambda_L}{D} = a_{LO} \tag{7E-9}$$

The stated philosophy behind their approach was to underestimate the heat transfer coefficients to compensate for the error of ignoring mass transfer resistance. There is however no assurance that the two errors (neglecting both two phase flow effects and most transfer resistance) are of the same magnitude.

In a later paper, Price and Bell [Pr74] suggest modifying equation (7-8) to include a two phase flow effect via the Martinelli parameter, tacitly assuming a Reynolds analogy:

$$\alpha_G = \alpha_{G0}(\rho_{Vtt}^2)^{.445} \quad (7E-10)$$

In a separate paper, Chisholm [Ch81] suggests using the two phase multiplier on the liquid phase as well:¹

$$\alpha_L = \alpha_{L0}(\rho_{Ltt}^2)^{.445} \quad (7E-11)$$

At this point, one can analyze the method in light of the previous section's discussion. First, Shock found little difference between T_i and T_G , and even less difference between dT_i and dT_G . Thus the assumption of (7-5) is minor for evaporation, though for condensation of a highly superheated vapor flow one might suspect problems.

Finding (c) of section 7.3 suggested that mass transfer resistance might be neglected without serious error. The basic philosophy of compensating errors with the original method is then undermined; it is not surprising that the modification suggested in equations (7E-10) and (7E-11) were required.

¹Chisholm credits Price and Bell, but no reference to this step could be found in their paper.

In still another paper, McNaught [Mc79] attempted to modify the whole approach to include a mass transfer effect on the vapor side. If, however, the finding (c) of section 7.3 is valid, this final change is unnecessary except for laminar flow.

Finding (f) of section 7.3 suggested that the sensible heating required on the vapor side is small when compared to the total heat (7-46).

Taking this to an extreme, equation (7-4d) yields

$$\frac{q_G}{q_{TOT}} \approx 0 \quad (7E-12)$$

or, on examining the condensation curves dT/dh is small. Equation (7-3b) becomes then

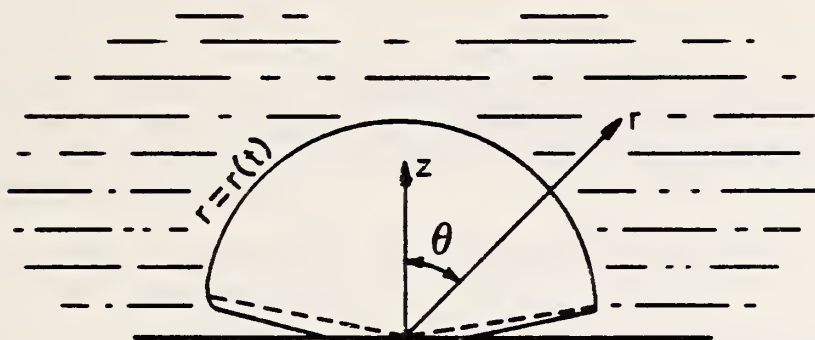
$$a_{eff} = a_{LO}(\delta^2_{L_{tt}})^{.445} \quad (7E-13)$$

or, the heat transfer coefficient is described completely by the liquid film! The suggestion by Chisholm to include a two phase effect is then well-placed. Equation (7-12) is only valid in the case of turbulent vapor flow. If the vapor heat transfer coefficient becomes small, as in stagelant or small laminar flow, then

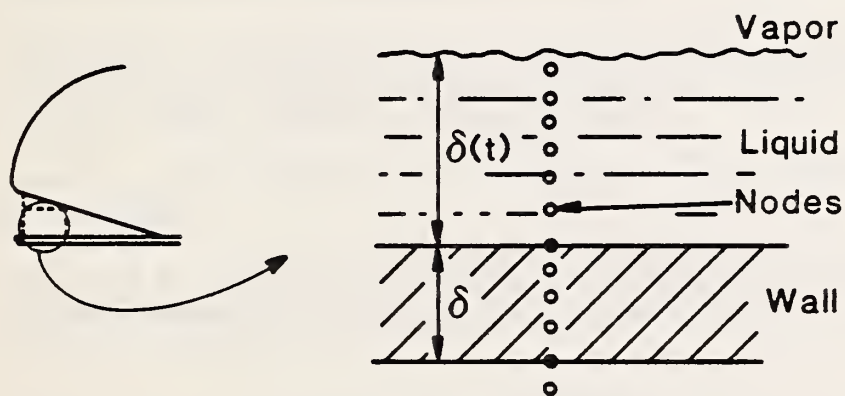
$$\frac{q_G/q_{TOT}}{a_G} \approx \frac{1}{a_L}$$

and the vapor side heat transfer must not be neglected. It is interesting to note that Price and Bell found the liquid side to control the process in several test cases. The implication of (7E-13) and in fact the findings of the previous section is that forced convection/evaporation of mixtures may be treated exactly as for pure fluids, requiring a good estimate, however, of the liquid properties.

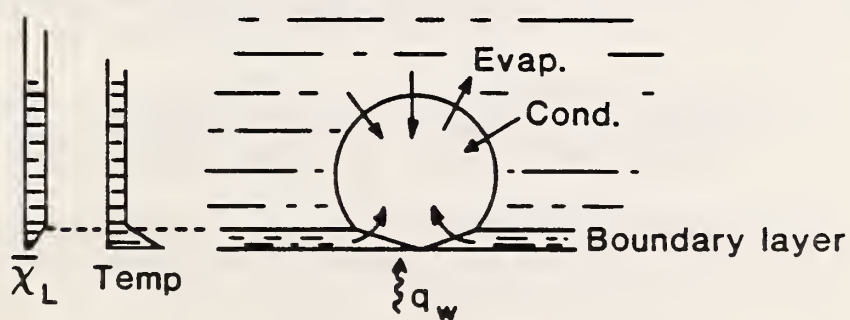
MICROLAYER EVAPORATION MODELS



a) Van Ouwkerk



b) Toral



c) Stephan and Preuber

Figure 7C-1: Microlayer Evaporation Models

REFERENCES

- Al60 Altman, M., Norris, R.H. and Staub, F.N., Local and Average Heat Transfer and Pressure Drop for Refrigerants Evaporating in Horizontal Tubes, J. Heat Transfer, 189-98, August 1960; ASME 59-A-278, November 1959.
- Al77 Aljarrah, M.S. and Duminil, M., Rev. Gen. Froid, vol. 68, No. 7, pp. 489-508, July/Aug. 1977.
- An66 Anderson, S.W., Rich, D.G., and Geary, D.F., Evaporation of Refrigerant 22 in a Horizontal 3/4 in. OD Tube, ASHRAE Transactions, Vol. 72, pp. 28-41.
- As81 ASHRAE Handbook of Fundamentals - 1981.
- Ao82 Aounallah, Y., Kenning, D.R.B., Whalley, P.B., and Hewitt, G.F., Boiling Heat Transfer in Annular Flow, Proc. 7th Int. Heat Transfer Conf., Munich, paper FB3 (1982).
- Al57 Aladiev, I.T., Dodonov, L.D. and Udalar, U.S., Teploenergetika 4, 9 (1957).
- Af66 Afgan, N.H., Boiling Heat Transfer and Burnout Heat Flux of Ethanol-Benzene Mixtures; 3rd Int'l Heat Transfer Conf. (Chicago) (1966).
- Bu79 Burkhardt, J. and Hahne, E., Influence of Oil on the Nucleate Boiling of R-11; Int'l. Congress of Refrigeration (Venice), pp. 539-544, Proceeding, Vol. 2; (1979).
- Bo51 Bonnet, W.E. and Gerster, J.A., Boiling Coefficients of Heat Transfer-C₄ Hydrocarbon/furfural Mixtures Inside Vertical Tubes, Chem. Engng. Prog., 77(3), 151-158 (1951).
- Be80 Bennett, D.L. and Chen, J.C., Forced Convective Boiling in Vertical Tubes for Saturated Pure Components and Binary Mixtures, AIChE Journal (Vol. 26, #3), pg. 454 (1980).
- Br55 Bryan, W.L. and Siegel, L.G., Heat Transfer Coefficients in Horizontal Tube Evaporators, Refrig. Eng. 63, #5, 36-45, 120, 1955.
- Ba53 Baker, M., Touloukian, Y.S. and Hawkins, G.A., Heat Transfer Film Coefficients for Refrigerants Boiling Inside Tubes, Ref. Eng., 986-91, september 1953.
- Br51 Bryan, W.L. and Quaint, G.W., Heat Transfer Coefficients in Horizontal Tube Evaporators, Ref. Eng., 67-73, January 1951.

- Ba74 Bandel, J. and Schlunder, E.U., Frictional Pressure Drop and Convective Heat Transfer of Gas Liquid Flow in Horizontal Tubes, Proceedings, Fifth International Heat Transfer Conference, 1974, pp. 190-194.
- Be82 Bejan, A., Entropy Generation
- Be75 Bennett, D.L., A study of Internal Forced Convective Boiling Heat Transfer for Binary Mixtures, Ph.D. Thesis, LeHigh University; 1975.
- Be72 Bell, K.J. and Ghaly, M.A., An Approximate Generalized Design Method, for Multicomponent/Partial Condensers, Chem. Eng. Prog. Symp. Series No. 131, 69, 72-79 (1972).
- Bo67 Bogdanov, S.N., Determination of Heat Transfer Coefficients for Boiling Halocarbon Inside Horizontal Tubes, English Translation in ASHRAE J., p. 59, July 1967.
- Be80a Bennett, D.L., David M.W. and Hertzler, B.L., AIChE Symp. Ser., Vol. 76, pp. 91-103, 1980.
- Be79 Beattie, D.R.H. Lawther, K.R., Letter to the Editor, AIChE J./25, 384 (1979).
- Be84 Beattie, D.R.H. and Green, The Existence of Nucleate Boiling in Diabatic Two Phase Annular Flow, Int. J. Heat Mass Transfer, Vol. 27, #2, pp. 315-317 (1984).
- Be63 Berenson and Stone, Chem. Eng. Progress, AIChE National Meeting, 1963, Paper #21.
- Be64 Bertoletti, S., Lombardi, C. and Silvesti, M., Heat Transfer to Steam-Water Mixture, CISE report R-78 (1964).
- Bu82 Butterworth, D., and Shock, R.A.W., Flow Boiling, Paper RK15, pg. 11, Proc. 7th Int. Heat Trans. Conf., Munich (1982); Hemisphere Publishing Corp.
- Ch79 Chaddock, J. and Mather, A.P., Heat Transfer to Oil-Refrigerant Mixtures Evaporating in Tubes; Multiphase Transport, Vol. 2, Hemisphere Publishing Corp, pg. 861ff.
- Ch67 Chawla, J.M., Wärmeübergang und Druckabfall in Waagrechten Rohren Bei Der Strömung Von Verdampfenden Kaltemitteln, VDI-Forschungsheft 523, 1967.
- Co64 Collier, J.G., Lacey, P.M.C. and Pulling, D.J., Heat Transfer to Two-Phase Gas-Liquid Mixtures in the Liquid Dispersed Region in an Annulus, AERE R-3809, 1964.

- Ch66a Chaddock, J. and Noerager, J.A., Evaporation of Refrigerant 12 in a Horizontal Tube with Constant Wall Heat Flux; ASHRAE Transactions, January 1966, pg. 90ff.
- Co37 Colburn, A.P. and Drew, T.B., The Condensation of Mixed Vapours, Trans. Am. Inst. Chem. Engng., 33, 197-215 (1937).
- Ca72 Calus, W.F. and Rice P., Pool Boiling-Binary Liquid Mixtures, Chem. Engng. Science, 27, 1687-1697 (1972).
- Ch67a Chisholm, D. A Theoretical Basis for the Lockhart-Martinelli Correlation for Two Phase Flow; Int'l J. Heat and Mass Transfer, Vol. 10, pp. 1767-1778.
- Ch66 Chen, J.C., A Correlation for Boiling Heat Transfer to Saturated Fluids in Convective Flow, Ind. Eng. Chem. Process Design Develop, 5, 322 (1966).
- Co80 Collier, J.G., Convective Boiling and Condensation, McGraw-Hill, 2nd Edition (1980).
- Ch81 Chisholm, D., Modern Developments in Marine Condenser: Non Condensable Gases: An Overview, pg. 95-142 in Power Condenser Heat Transfer Technology, ed. Marto, P.J. and Nunn, R.H., Hemisphere Publishing Corp., (1981).
- Da66 Davis, E.J., and Anderson, G.H., The Incipience of Nucleate Boiling in Forced Convection Flow; AIChE Journal, pp. 774-780, 1966.
- Di66 Dickson, A.J. and Gouse, S.W., Jr., Heat Transfer and Fluid Flow in a Horizontal Tube Evaporator-Phase III, MIT Eng. Proj. Lab. Report DSR 9649-3, August 15, 1966, Trans. ASHRAE 1967.
- De56 Dengler, C.E. and Addoms, J.N., Heat Transfer Mechanism for Vaporization of Water in Vertical Tube, Chemical Engineering Progress Symposium Series, Vol. 52, No. 18, 1956, pp. 95-103.
- De78 Dembi, N.J., Dhar, P.H., and Arora, C.P., Lett. Heat Mass Transfer, Vol. 5, pp. 287-296, 1978.
- Da69 Danilova, D.N., Heat Transfer to Boiling Refrigerants, pp. 107-130 of Problems of Heat Transfer and Hydraulics of Two Phase Media, Ed. S.S. Kutateladze, Pergamon Press, Oxford, 1969.
- Da66 David, E.J. and Anderson, G.H., AIChE J., Vol. 12, pp. 774-780, 1966.

- Di84 Didion, D.A. and Mulroy, W.J., The Performance of a Residential Heat Pump Operating with a Non-Azeotropic Binary Refrigerant Mixture—An Interim Report, DoE/ORNL Heat Pump Conference, December 11-12, 1984.
- Fo55 Forster, H.K. and Zuber, N., Dynamics of Vapor Bubbles and Boiling Heat Transfer; AIChE Journal, December 1955 (Vol. 1, #4), pg. 531-535.
- F170 Florschultz, L.W. and Rashid Khan, A., Growth Rates of Free Vapor Bubbles in Binary Liquid Mixtures at Uniform Superheta, 4th Int'l Heat Transfer Conference (Paris), Paper B.7.3. (1970).
- Go65 Gouse, S.W., Jr. and Coumou, K.G., Heat Transfer and Fluid Flow Inside a Horizontal Tube Evaporator, Phase I, MIT Eng. Proj. Lab. Report DSR 9649-1, June 1964; Tran ASHRAE Part II 71, 152-161, 1965.
- Go66 Gouse, S.W., Jr. and Dickson, A.J., Heat Transfer and Fluid Flow Inside a Horizontal Tube Evaporator, Trans of ASHRAE, Part I, 1966, See Discussion.
- Ha74 Happel, O. and Stephan, K., Heat Transfer from Nucleate Boiling to the Beginning of Film Boiling in Binary Mixtures, Paper B7.8 presented at 5th International Heat Transfer Conference, Tokyo, September (1974).
- He63 Hewitt, G.F., et al., Burnout and Nucleation in Climbing Film Flow, AERE-R4374 (1963).
- Ho63 Hosler, E.R., Visual Study of Boiling at High Pressure, Chem. Eng., Progress, AIChE National Meeting (1963).
- Hs76 Hsu, Y.Y. and Graham, R.W., Transport Processes in Boiling and Two Phase Systems, McGraw-Hill, Chapter 1, 1976.
- He84 Hewitt, G.F., Workshop on Two Phase Flow Processes, (1984).
- Ht83 Heat Transfer and Fluid Flow Service (HTFS), data base (subscription), as of 1983.
- Ja74 Jallouk, P.A., Two Phase Flow Pressure Drop and Heat Transfer Characteristics of Refrigerants in Vertical Tubes, Ph.D. Dissertation, University of Tennessee, 1974.
- Ka75 Kandlikar, S.G., Bijiani, C.A., and Sukhatme, S.P., Predicting the Properties of Mixtures of R22 and R12—Part II—Transport Properties, ASHRAE Transactions, Vol. 81, 1975, pg. 285ff.

- Ka84 Kandliker, S.G., An Improved Correlation for Predicting Two Phase Flow Boiling Heat Transfer Coefficient in Horizontal and Vertical Tubes; 21st National Heat Transfer Conference (Seattle) ASME 1983 (639-84-21).
- La66 Lavin, J.G. and Young, E.H., Heat Transfer to Evaporating Refrigerants in Two-Phase Flow, AIChE J. 11, #6, 1124-32, November 1966.
- Lo49 Lockhart, R.W. and Martinelli, R.C., Proposed Correlation of Data for Isothermal Two-Phase, Two Component Flow in Pipes, Chem. Eng. Progress, Vol. 45, #1, pp. 39-48 (1949).
- La62 Lacey, P.M.C., Hewitt, G.F., and Collier, J.G., Climbing Film Flow, AERE-R3962 (1962).
- Ma83 Mattingly, G., NBS Fluid Measurements Group, private communications.
- Mc42 McAdams, W.H., et al, Vaporization Inside Horizontal Tubes-II, Benzene-Oil Mixtures; Trans ASME, pp. 193-200 (1942).
- Ma76 Mathur, A.P., Heat Transfer to Oil-Refrigerant Mixtures Evaporating in Tubes; Duke University, (1976), (Ph.D. Thesis).
- Mi81 Mishra, M.P., Varma, H.K., and Sharma, C.P., Heat Transfer Coefficients in Forced Convection Evaporation of Refrigerant Mixtures; Letters in Heat and Mass Transfer, Vol. 8, pp. 127-136 (1981).
- Mo82 Morrison, G., (draft paper), An Equation of State for Refrigerant Mixtures,
- Mo84 Morrison, G., private communications.
- Mo85 Morrison, G., The Importance of Including the Liquid Phase in Equations of State for Non-Azeotropic Refrigerant Mixtures, ASHRAE Trans, Pt. 1 (1985).
- Me76 Mesler, R.B., A Mechanism Supported by Extensive Experimental Evidence to Explain High Heat Fluxes Observed During Nucleate Boiling, AIChE J/22, 246-252 (1976).
- Me77 Mesler, R.B., An Alternate to the Dengler and Addoms Convection Concept of Forced Convection Boiling Heat Transfer, AIChE, J/23, 448-453, (1977).
- Mc79 McNaught, J. Mass Transfer Correction Terms in Design Methods for Multi-Component Partial Condensers, 18th National Heat Transfer Conference, (San Diego), pp. 111-118 (1979).
- Mo78 Mori, S., Sakitani, K., and Isoaji, A., Reito, Vol. 50, pg. 1-6.

- Ma48 Martinelli, R.C. and Nelson, D.B., Prediction of Pressure Drop During Forced Circulation Boiling of Water, ASME Trans., pp. 695-702, August 1948.
- Mu72 Murphy, R.W. and Bergles, A.E., Proceedings of the 1972 Heat Transfer and Fluid Mechanics Institute, R.B. Landis and G.J. Hordemann, eds. Stanford University Press, pp. 400-416, 1972.
- Pi56 Pierre, B., Varmeovergangen vid Kokande Koldmedier Horizontella Rørtekn, Kylvtenick Tidakrift #3, 129, May 1957; also 12, 76, 1953; 16, #6, 225, December 1957. Warmei Bergangazahl Bei Verdampfenden F 12 in Horizontalen Röhren, Kältertechnik 7, heft 6, 163-66, 1955; also S.F. Review 2, #1, 55-68, 1955; The Coefficient of Heat Transfer for Boiling Freon 12 in Horizontal Tubes, Heating and Air Treatment Engineer, 302-310, December 1956.
- Pe70 Pethukov, B.S., Heat Transfer and Friction in Turbulent Pipe Flow; Advances in Heat Transfer, Pergamon Press, 1970, pg. 503ff.
- Pr74 Price, B.C. and Bell, K.J., Design of Binary Vapor Condensers using the Colburn-Drew Equations, AIChE Symp. Series, 70 (138) 163-171 (1974).
- Pu74 Purcupile, J.C., Riedle, K., and Schmidt, F.K., AIChE Symp. Ser., No. 138, Vol. 70, pp. 91-97, 1974.
- Po82 Polley, G., Application of the Chen Correlation to Water, (1982).
- Ra83 Radermacher, R., Ross, H., and Didion, D., Experimental Determination of Forced Convection Evaporative Heat Transfer Coefficients for Non-Azeotropic Refrigerant Mixtures, ASME National Heat Transfer Conference, ASME 83-WA/HT54 (1983).
- Ro78 Rohsenow, W.M. and Hartnett, J.P., Handbook of Heat Transfer, McGraw-Hill, New York, 1978.
- Ri73 Riedle, K. and Purcupile, J.C., ASHRAE Trans., Vol. 79, pp. 142-156, 1973.
- Rh74 Rhee, B.W. and Young, E.H., Int. J. Heat Mass Transfer, Vol. 23, pp. 73-87, 1980.
- Re79 Reid, Prausnitz and Sherwood, The Properties of Gases and Liquid, McGraw-Hill, (1979).
- Sh73 Shock, R.A.W., The Evaporation of Binary Mixtures in Forced Convection (Ph.D. Thesis), AERE-R7593 (1973).

- Sh82 Shock, R.A.W., Boiling in Multicomponent Fields, Multiphase Science and Technology - Vol. 1 by Hewitt, et al., Hemisphere Publishing Corp., 1982.
- Sh77 Shock, R.A.W., Nucleate Boiling in Binary Mixtures, Int'l. Journal of Heat Mass Transfer, Vol. 20, 701-709, (1977).
- Sh83 Shock, R.A.W., Workshop Notes, Multicomponent Boiling and Condensation, NBS. (1983).
- St78 Stephan, K. and Preuber, P., Heat Transfer in Natural Convection Boiling of Polynary Mixtures. Proceedings of 6th International Heat Transfer Conference, I, 187-192, Toronto, 7-11 August (1978).
- St69 Stephan, K. and Korner, M., Calculation of Heat Transfer in Evaporating Binary Liquid Mixtures, Chemie-Ingenieur Technik, 41(7), 409-417 (1969).
- St81 Stephan, K. and Auracher, H., Int. J. Heat Mass Transfer, Vol. 24, pp. 99-107, 1981.
- St80 Stephan, K. and Abdelsalam, M., Int. J. Heat Mass Transfer, Vol. 23, pp. 73-87, 1980.
- St82 Stephan K., Boiling of Mixtures, Vol. 1, Proceedings Seventh International Heat Transfer Conference, Munich (1982); Hemisphere Publishing Corp.
- Si83 Singal, L.C. Charma, C.P., and Varma, H.K., Experimental Heat Transfer Coefficient for Binary Refrigerant Mixtures of R13 and R12; ASHRAE Transactions, Pt. 1, p. 175, (No. 2747) (1983).
- Sa61 Sachs, P. and Long, R.A.K., A Correlation for Heat Transfer in Stratified Two-Phase Flow with Vaporization, Int. J. Heat and Mass Transfer 2, 223-30, 1961; NSA 15-19520.
- St66 Staub, F.W. and Zuber, N., Void Fraction Profiles, Flow Mechanisms and Heat Transfer Coefficients for R22 Evaporating in a Vertical Tube, ASHRAE Transactions, (1966), pg. 130ff.
- Sh76 Shah, M.M., A New Correlation for Heat Transfer During Boiling Flow Through Pipes, ASHRAE Transactions, Vol. 82, Part II, 1976, pp. 66-86.
- Sh82a Shah, M.M., Chart Correlation for Saturated Boiling Heat Transfer: Equations and Further Study, ASHRAE Transactions, Vol. 88, Part I, 1982.
- Sc62 Schrock, R.E. and Grossman, L.M., Forced Convection Boiling in Tubes, Nuclear Science Engineering, Vol. 12, 1962, pp. 474-481.

- Sc59 Scriven, L.D., On the Dynamics of Phase Growth, Chem. Engng. Science, 10 (1/2), 1-13 (1959).
- Sl70 Slipcevic, B., ASHRAE J., pp. 65-78, June 1970.
- St78 Standiford, F.C., Letter to the Editor, AIChE J/24, 750 (1978).
- St85 Stoecker, W.F., Condensing Coefficients for Refrigerant Mixtures, ASHRAE Trans., Part 2, (1985).
- Sa78 Sauer, H.J., et al., Influence of Oil on the Nucleate Boiling of Refrigerants, 6th Int'l Heat Transfer Conf., (Toronto), paper B.12, (1978).
- Si83a Singel, L.C., Sharma, C.P., and Varma, H.K., Pressure Drop During Forced Convection Boiling of Binary Refrigerant Mixtures, Int'l Journal Multiphase Flow, Vol. 9, #3, pp. 309-323 (1983).
- St81 Stoecker, W.F., Energy Characteristics of a Two Evaporator Refrigerator Using Refrigerant Mixture; ORNL/Sub/81-7762/2801 (1981).
- Sc85 Schulz, U.W., The Characteristics of Fluid Mixtures and their Utilization in Vapor Compression Refrigeration Systems; ASHRAE Transactions, Vol. 2, (1985).
- Sa82 Sardesai, Shock and Butterworth, Heat and Mass Transfer in Multicomponent Condensation and Boiling, Heat Transfer Engineering, Vol. 3, #3-4, Jan.-June 1982.
- Th82 Thome, J.R., Shakir, S., and Mercier, C., Effect of Composition on Boiling Incipient Superheats in Binary Liquid Mixtures; PB14, pp. 95-100; Proceedings 7th Int'l Heat Transfer Conference, Munich (1982).
- To79 Toral, H., Flow Boiling Heat Transfer in Mixtures (Ph.D. Thesis), University of Oxford, Department of Engineering Science, 1979.
- To73 Toda, S. and Uchida, H., Study of Liquid Film Cooling with Evaporation and Boiling, pg. 44-62, Heat Transfer - Japanese Research, (1973).
- Tr78 TRAC-Pla: An Advanced Best-Estimate Computer Program for PWR LOCA Analysis, Volume I: Los Alamos Scientific Laboratory, 1978; Los Alamos, New Mexico.
- Ti62 Tippetts, F.E., Am. Soc. Mech. Engrs. Paper No. 62-WA-162 (1962).

- Th70 Thorsen, R.S., Dobran, F., and Alcorta, J.A., A Comparative Study of Vertical Upflow and Downflow in a Uniformly Heated Boiling Fluid, paper B4.3, Int'l Heat Transfer Conference, (Toronto) (1970).
- Uc66 Uchida, H. and Yamaguchi, S., Heat Transfer in Two-Phase Flow of Refrigerant-12 Through Horizontal Tube, Proceeding 3rd International Heat Transfer Conference, Vol. V, 1966, p. 69.
- Va67 Van Stralen, S.T.D., Bubble Growth Rates in Boiling Binary Mixtures, Brit. Chem. Engng. 12(3), 390-394, March (1967).
- Va77 Vaihigen, D., The Influence of Nucleate Boiling Heat Transfer with Pressure; Heat Transfer in Boiling [ed. Hahne, E. and Grigill, U.](1977), Hemisphere Publishing Corp.
- Va72 Van Ouwerkerk, H.J., Hemispherical Bubble Growth in a Binary Mixture; Chem. Eng. Sci. vol. 27; pp. 1957-1967, (1972).
- Va79 Varma, H.K., Sharma, C.P., and Mirkra, M.P., International Congr. Refrig. Paper B1-46, Venice, 1979.
- Wo60 Worsoe-Schmidt, P., Some Characteristics of Flow Pattern and Heat Transfer of Freon 12 Evaporating in Horizontal Tubes, Ingenioren (Denmark) #3, September 1959; ref. Zh. Mekh. 11793, 1960.
- We80 Webb, R.L. and Wanniarachchi, A.S., The Effect of Noncondensable Gases in Water Chiller Condensers--Literature Survey and Theoretical Predictions, ASHRAE Trans. p. 142, (1980).
- We81 Webb, D.R. and Sardesai, R.G., Verification of Multicomponent Mass Transfer Models for Condensation Inside a Vertical Tube; Int'l Journal Multiphase Flow Vol. 7, #5, pp. 507-520, (1981).

U.S. DEPT. OF COMM. BIBLIOGRAPHIC DATA SHEET <i>(See instructions)</i>	1. PUBLICATION OR REPORT NO. NBSIR-86/3450	2. Performing Organ. Report No.	3. Publication Date NOVEMBER 1986
4. TITLE AND SUBTITLE An Investigation of Horizontal Flow Boiling of Pure and Mixed Refrigerants			
5. AUTHOR(S) Howard D. Ross			
6. PERFORMING ORGANIZATION <i>(If joint or other than NBS, see instructions)</i> NATIONAL BUREAU OF STANDARDS DEPARTMENT OF COMMERCE WASHINGTON, D.C. 20234		7. Contract/Grant No.	8. Type of Report & Period Covered
9. SPONSORING ORGANIZATION NAME AND COMPLETE ADDRESS <i>(Street, City, State, ZIP)</i> National Bureau of Standards U.S. Department of Energy Building Equipment Division, CBT (via Oak Ridge National Laboratory) <u>Thermal Machinery Group</u> Washington, D.C. 20585 Gaithersburg, MD 20899			
10. SUPPLEMENTARY NOTES <input type="checkbox"/> Document describes a computer program; SF-185, FIPS Software Summary, is attached.			
11. ABSTRACT <i>(A 200-word or less factual summary of most significant information. If document includes a significant bibliography or literature survey, mention it here)</i> The research involved determining experimental heat transfer coefficients (HTC), examining the phenomena involved in the physical process, and analyzing the predictive ability of available models and correlations. This work was done for pure R152a and R13B1 and for mixtures of these refrigerants. The mixtures yielded sharply lower heat transfer coefficients than either pure refrigerant. With pure refrigerants full suppression of nucleate boiling (FSNB) occurs only at rather low pressures. Correlative evidence suggests that suppression is easier to achieve with mixtures than pure fluids. In the evaporation-dominated heat transfer regime, Chen's correlation was successfully applied to our refrigerants with and without the occurrence of FSNB conditions. A Prandtl number correction is needed when some nucleation occurs. For mixtures, mass diffusion may not complicate the problem substantially under FSNB conditions, and the same correlation may be used with success. In the nucleate boiling dominated regime, the Stephan and Abdelsalam method was validated for pure fluids, and used successfully with Thome's method for mixtures. Pressure drop correlations for pure fluids were also extended to mixtures without modification.			
12. KEY WORDS <i>(Six to twelve entries; alphabetical order; capitalize only proper names; and separate key words by semicolons)</i> evaporative flow; flow boiling; nonazeotropic mixtures; refrigerants heat transfer; two phase flow			
13. AVAILABILITY <input checked="" type="checkbox"/> Unlimited <input type="checkbox"/> For Official Distribution. Do Not Release to NTIS <input type="checkbox"/> Order From Superintendent of Documents, U.S. Government Printing Office, Washington, D.C. 20402. <input checked="" type="checkbox"/> Order From National Technical Information Service (NTIS), Springfield, VA. 22161		14. NO. OF PRINTED PAGES 358	15. Price \$28.95

